University of Rzeszów
College of Natural Sciences
Institute of Physics

The Doctoral School
of University of Rzeszów

The impact of the system parameters on the entanglement in spin chains coupled to the bosonic reservoir

A doctoral thesis of
Michał Kaczor

Supervisor
dr hab. Paweł Jakubczyk, prof. UR

Rzeszów, 2024

Aknowledgement

I would hereby like to convey my heartfelt thanks to Prof. Paweł Jakubczyk for the many fruitful discussions, insightful comments, suggestions for solutions to the problems I have encountered, and endless patience for my specific work methods.

I would like to express my great gratitude to Prof. Igor Tralle, for his constant support in my scientific work, especially for the time spent critically reviewing this thesis, and for many smaller gestures and pieces of advice that helped me pursue my scientific goals.

Contents

I Theoretical Background for the Study of Entanglement in Spin Systems 13

1 Quantum Entanglement 15
1.1 Basic concepts of quantum mechanics 15
1.2 The phenomenon of quantum entanglement 19
1.3 EPR Paradox, Bell Inequality 21
1.4 Entanglement in pure states 24
1.5 Entanglement in mixed states 25
1.5.1 Separability criteria for mixed states. Measures of entanglement 26
1.6 Entanglement witnesses 29
1.7 Local Quantum Uncertainty. Local Quantum Fisher Information 31
1.8 Multipartite Entanglement 33
1.9 Quantum Discord 35

2 Open Quantum Systems 37
2.1 Dynamics of an open quantum systems 37
2.1.1 Liouville - von Neumann Equation 37
2.1.2 Intrinsic decoherence - Milburn Equation 39
2.2 Concept of open quantum systems 41
2.2.1 Composite quantum system 41
2.2.2 Open quantum systems 42
2.3 Markovian time evolution 42
2.3.1 Born - Markov equation 45
2.3.2 Lindblad master equation 47
2.4 Non-Markovian time evolution 51
2.4.1 Two-level system 52
2.4.2 Composite system in the non-Markovian environment . 55
2.5 Decoherence 57

3 Spin Systems in Quantum Computing 61
3.1 Spin chains 61
3.1.1 Spins in an external magnetic field - Zeeman effect . . 64
3.1.2 Dzyaloshinskii - Moriya interaction 64
3.1.3 Kaplan - Shethkman - Entin-Wohlman - Aharony interaction 66
3.1.4 Three spin interaction 66
3.2 Entanglement in the spin system - overview 67

II Study of the most common spin systems in terms of thermal entanglement and entanglement dynamics 79

4 81
4.1 Introduction 81
4.1.1 Remarks on dissipative time evolution in spin chains . 84
4.2 Study of the thermal and dynamic entanglement in most common spin systems 88
4.2.1 Exchange interaction only 88
4.2.2 External magnetic field 119
4.2.3 Dzyaloshinskii–Moriya interaction 133
4.2.4 Kaplan - Shekhtman - Entin-Wohlman - Aharony interaction 145
4.2.5 Three Spin Interaction 154

Abstract

The presented work covers a study of selected models of spin chains, conducted to quantify the bipartite quantum entanglement between the spins of the system. At first, the entanglement is investigated in isolated systems prepared in the thermal equilibrium state. The subsequent analysis focuses on the changes in entanglement within open systems with hybrid dynamics of interaction with the environment. The chain itself is placed in the bosonic reservoir of a Markovian type, characterized by irreversible information loss from the system to the environment which describes the Lindblad equation. The spins of the chain, between which the entanglement is not considered, are treated as a non-Markovian environment and "excluded" from the analysis by reducing the density matrix. The mean of expressing the entanglement strength in the considered systems is the concurrence, defined by Wooters and Hill. The calculations required to prepare the following dissertation are done numerically, using the authorial procedures settled on the Runge - Kutta method of the sixth order, used for iterative solving the Lindblad equation. Based on the preliminary analysis of the forms of Lindblad equation's solutions and obtained numerical results, the following conclusions are drawn: the most beneficial conditions for large entanglement in isolated spin chains are observed for shorter chains, possibly of even numbers of spins. In materials described by XXX Heisenberg model prepared in a thermal equilibrium state, negative exchange integral with high absolute value is preferable for the system to exhibit high entanglement; for XXZ exchange interaction model, the same fact holds for J_Z integral, for J_X integral, however, the sign does not matter, only its absolute value - the higher it is, the higher is the entanglement. For XYZ Heisenberg model, this relation is more complicated. Yet, it can be stated that for evenly numbered spin chains, the product of exchange integrals for all perpendicular directions should be negative. The uniform magnetic field mostly negatively impacts the entanglement, except for a small field for short spin chains of an odd number of spins. The non-uniform magnetic field can enhance the low entanglement; however, it reduces the entanglement in systems with its high initial value in a thermal state. Dzyaloshinskii - Moriya type of superexchange interaction has a slightly negative effect on the entanglement in most of the analysed systems; Kaplan - Shekhtman - Entin - Wohlman - Aharony exchange slightly enhances high entanglement in chains with an odd number of spins, but reduces low entanglement for the same chains. Finally, three-spin interactions prove to have a positive impact on the entanglement in chains with odd cardinality. Analysis of time evolution for spin chains in the Markovian bosonic environment led to the following observations. For only exchange interaction taken into

consideration, the most robust to decoherence turned out to be the states in which $|J_Z| < J_X$. A magnetic field constant in time has no impact on entanglement loss; a time-dependent field raises the entanglement only in shorter spin chains, and this effect can be benefitted only if one adapts the frequency of field changes to the number of spin excitations in the initial state. Dzyaloshinskii - Moriya and Kaplan - Shekhtman - Entin - Wohlman - Aharony interactions have almost only a negative impact on the entanglement, while three spin interaction is advantageous for short chains; in longer chains, its effect becomes negative.

Streszczenie

Niniejsza praca obejmuje analizę wybranych modeli łańcuchów spinowych pod kątem ilościowego określenia splątania pomiędzy dwoma spinami łańcucha. Splątanie zostało wyznaczone najpierw w układzie izolowanym znajdującym się w stanie równowagi termicznej z otoczeniem. Następnie przeprowadzono analizę splątania w czasie dla układu otwartego z hybrydową dynamiką oddziaływań z otoczeniem: sam łańcuch znajduje się w rezerwuarze bozonowym o charakterze markowiańskim (utrata informacji z łańcucha do otoczenia jest nieodwracalna), układ taki jest opisywany przy pomocy równania Lindblada. Spiny łańcucha, między którymi splątanie nie jest wyznaczane, traktowane są jako otoczenie niemarkowiańskie i "wyłącza" się je z analizy poprzez redukcję macierzy gęstości. Stosowaną miarą ilościowego splątania jest zgodność, określona przez Wootersa i Hilla. Obliczenia potrzebne do przygotowania niniejszej rozprawy zostały wykonane numerycznie, przy użyciu autorskich procedur opartych na algorytmie Rungego - Kutty szóstego rzędu, które zostały wykorzystane do iteracyjnego rozwiązania równania Lindblada. Na podstawie wstępnych analiz ogólnych rozwiązań równania Lindblada i uzyskanych rezultatów obliczeń numerycznych wyciągnięto następujące wnioski: najbardziej korzystne warunki dla splątania termalnego obserwuje się w łańcuchach możliwie krótkich, szczególnie takich o parzystej liczbie spinów. W materiałach opisywanych przez model Heisenberga typu XXX całka wymiany powinna być ujemna i o możliwie wysokiej wartości bezwzględnej, aby zapewnić wysokie splątanie w stanie równowagi termicznej; taką samą właściwość obserwuje się również w modelu typu XXZ dla całki J_Z, zaś dla całki J_X jej znak nie ma znaczenia z punktu widzenia splątania, a jedynie jej wartość bezwzględna - im jest ona większa, tym większe jest splątanie. Dla układów opisywanych modelem XYZ wpływ poszczególnych całek wymiany na wartość splątania jest bardziej skomplikowany, można natomiast stwierdzić, że dla łańcuchów o parzystej liczności w celu uzyskania wysokiego splątania, iloczyn trzech całek wymiany odpowiadających kierunkom

prostopadłym, powinien być ujemny. Jednorodne pole magnetyczne przejawia jednoznacznie negatywny wpływ na splątanie, wyjątkiem jest jedynie małe pole dla krótkich łańcuchów o nieparzystej liczbie spinów. Niejednorodne pole magnetyczne może wzmacniać splątanie w stanach o małej wartości splątania, jednak obniża jego wartość w układach o wysokim splątaniu wyjściowym. Oddziaływania nadwymienne Działoszyńskiego - Moriyi mają nieznacznie negatywny wpływ na splątanie w większości analizowanych układów. Oddziaływania Kaplana - Shekthkmana - Entina - Wohlmana - Aharony'ego nieznacznie podnoszą wartości splątania w układach silnie splątanych, natomiast w układach przygotowanych w stanie termalnym o niewielkim splątaniu obniżają to splątanie. Oddziaływania trójspinowe okazały się mieć pozytywny wpływ na splątanie w układach o nieparzystej liczbie spinów. Analiza ewolucji czasowej stanu układu spinowego w otoczeniu bozonowym o charakterze markowiańskim pozwoliła z kolei wyciągnąć następujące wnioski: dla układów, w których pod uwagę brane były tylko oddziaływania wymienne, najbardziej odporne na utratę splątania w procesie dekoherencji były łańcuchy, dla których $|J_Z| < J_X$. Stałe w czasie pole magnetyczne nie miało wpływu na proces dekoherencji. Pole czasowozależne powodowało wzrost splątania, jednak efekt ten można było wykorzystać jedynie dla krótkich łańcuchów, oraz wymagało to uzależnienia częstotliwości zmian pola od liczby wzbudzeń magnetycznych łańcucha w stanie początkowym układu. Oddziaływania Działoszyńskiego - Moriyi oraz Kaplana - Shekthkmana - Entina - Wohlmana - Aharony'ego w niemalże każdej rozważanej sytuacji okazywały się niekorzystne z punktu widzenia splątania, zaś oddziaływania trójspinowe mogą charakteryzować się pozytywnym wpływem na wielkość splątania w krótkich łańcuchach, w dłuższych jednak ich wpływ staje się niekorzystny.

Introduction

When the writing of this work started, one of the most popular topics in the scientific community was the rivalry between Google and IBM to create the most efficient quantum computer. I found this topic especially interesting due to the fact that I have always considered quantum mechanics an exceptionally absorbing topic and I was hoping to see this particular device, the peak achievement of this branch of science, as a fuse for the new technological evolution. Now, five years later, I still observe the development of quantum computing with curiosity, and this work here is my timid attempt to participate in this phenomenon, however small this contribution may be.

One of the most common physical realizations of qubits are the particles with spin $s = \frac{1}{2}$. Two distinguishable states, commonness (majority of ions qualify) and ease of manipulation, make these objects promising elements of potential quantum registers. They interact with each other by virtual electron exchange, which is a quantum effect, and therefore, allow for entanglement creation in multipartite systems. However, there is a pinch of salt in this observation – the mentioned entanglement is extremely fragile under external conditions, and many environmental effects prove to cause decoherence in spin systems.

The goal of this work is to provide a broad illustrative analysis of entanglement in spin systems, with various additional effects taken into account – be it different types of exchange interaction models, Dzyaloshinskii - Moriya or Kaplan-Shekhtman-Entin-Wohlman-Aharony interactions, constant and time-dependent magnetic field. This examination is carried out in two ways: first is the determination of entanglement and its dependence on the model parameters in the thermal state of an isolated system. This part has been prepared to estimate the quality of entanglement in systems for which interactions with the environment are negligible. The second is the calculation of the entanglement time behaviour in a non-Markovian chain coupled with a Markovian environment (this assumption would reflect the fact that, due to monogamy of entanglement, interactions between the spins of the register also cause loss of entanglement; however, this loss is reversible, as opposed to

the loss of entanglement to the environment). Two-, three-, four-, five-, and six-spin systems were analysed, and original procedures prepared in MATLAB and Python were used as computational tools. The calculations' results were then analyzed to search for system parameters that make decoherence, which is unavoidable in such systems, occur with the lowest possible loss of entanglement concurrence.

The work is organized as follows: the first three chapters provide a theoretical insight into entanglement examination in spin systems. Chapter I covers the mathematical formalism of quantum mechanics with particular emphasis on the algebraic tools used to determine the level of entanglement in pure and mixed states. Chapter II refers to techniques for analyzing the time evolution of quantum systems, especially the open systems, which are subjected to environmental influence. Chapter III describes the spin chains and various coupling effects that may occur in this type of system. This chapter ends with an overview of recent research done to determine the entanglement behaviour in spin structures. The final, IV chapter covers the catalogue of results obtained to analyse the impact of particular phenomena on the bipartite entanglement in spin chains – all the assumptions stated beforehand can be found in this section, alongside the initial conclusions from used models and equations, as well as the numerical results for particular parameters of the models. General conclusions are collected in the final summary of the work.

Part I

Theoretical Background for the Study of Entanglement in Spin Systems

Chapter 1

Quantum Entanglement

1.1 Basic concepts of quantum mechanics

Quantum Informatics originates from the combination of two most revolutionary theories of the XX century: quantum mechanics, which changes the way one describes the world on a subatomic scale, and information theory, formulated by Shannon in 1948 and underpinning the whole IT industry. The idea of applying the unusual properties of quantum systems to perform computational operations was proposed in the late seventies by Richard Feynmann. Yet, it has to wait until 1984 for its first application - the Bennett and Brassard quantum cryptography protocol. Quantum computers, the final products of this branch of science, are believed to be faster and more efficient than the classical Turing machines (like usual computers), partly because they have access to the resources impossible to utilize in classical computation protocols – superposition, uncertainty, and, probably most important, entanglement.

As it was hinted before, the most precise theoretical framework for discussing matter properties on a microscopic level is provided by quantum theory. This description is based on the notion of state space: for every isolated quantum system, one can assign some Hilbert space $\mathcal{H}_A$ (vector space with additional operations defined alongside the usual addition and multiplication of vectors by a scalar, namely the scalar product and the norm definition), which plays the role of **state space**. For every physical state of the system, there exists a vector $|\psi\rangle$ (state vector) belonging to the mentioned Hilbert space that represents this state. What is more, this relation can be reversed - every vector from the Hilbert space represents some achievable state of the system. This vector stores some knowledge about the state, the results of the measurements that are possible to conduct on the system, alongside the

probabilities of particular outcomes. This knowledge can then be extracted from the state vector, as a proper representation of the measurement can be found in terms of **operators**.

Hilbert space itself is a complex linear vector space, provided with a definition of scalar product, the norm of the vector, and with a set of **basis vectors**, $\{|e_i^A\rangle\}$. The space is complex and linear if, for any vectors $|\alpha_1\rangle$, $|\alpha_2\rangle$ that belong to the space, every linear combination of them with any complex coefficients c_1, c_2: $|\alpha\rangle = c_1|\alpha_1\rangle + c_2|\alpha_2\rangle$ also belongs to this space. The definitions of **scalar product** and **norm of the vector** are linked: the scalar product is an operation that assigns to two vectors, be it $|\psi\rangle$ and $|\theta\rangle$, a single complex number, denoted by $\langle\psi|\theta\rangle$, that satisfies the following conditions:

- $\langle\psi|\theta\rangle = \langle\theta|\psi\rangle^*$, where * denotes the complex conjugation;
- $\langle\theta|\theta\rangle \geq 0$, $\langle\theta|\theta\rangle$ is equal to zero only if the $|\theta\rangle$ is zero vector (a vector that can be added to any other vector and does not change it);
- if $|\psi\rangle = c_1|\phi_1\rangle + c_2|\phi_2\rangle$, then $\langle\theta|\psi\rangle = c_1\langle\theta|\phi_1\rangle + c_2\langle\theta|\phi_2\rangle$.

The norm of the vector is defined as $||\psi|| = \sqrt{\langle\psi|\psi\rangle}$. If the norm of the vector is equal to 1, the vector is called normalized or unit. It is worth mentioning here, that if two vectors differ only in the multiplicative factor, they represent the same physical state - therefore in quantum physics it is allowed and even recommended to normalize every state vector, as it allows to apply the Copenhagen interpretation of Quantum Physics, which will be discussed later. The vector $|\psi\rangle\langle\psi|\theta\rangle$ represents the projection of vector $|\theta\rangle$ on the direction of vector $|\psi\rangle$. Scalar product $\langle\psi|\theta\rangle$ can be seen as a measure of how much two vectors overlap - if it is equal to zero, then the vectors are perpendicular to each other - they are said to be **orthogonal**. Finally, the **basis** $\{|e_i^A\rangle\}$ is any set of vectors in Hilbert space that are **orthonormal** (orthogonal and normalized), $\langle e_i^A|e_j^A\rangle = \delta_{ij}$ and with a number of elements that are sufficient to express every vector that belongs to the space with a unique linear composition of basis vectors. This condition designates the **dimensionality** of Hilbert space $\dim(\mathcal{H}_A)$ - which is equal to the cardinality of the basis. As a consequence, every vector can be uniquely decomposed with respect to a particular basis:

$$|\psi^A\rangle = \sum_{i=1}^{\dim(\mathcal{H}_A)} a_i|e_i^A\rangle$$

with coefficients a_i that can be found by projecting the vector mentioned above on the basis directions:

$$a_i = \langle e_i^A | \psi^A \rangle.$$

As the state of the system changes due to external or internal factors, there must be a way of representing these changes in Hilbert space formalism. This role is played by **operators** - particular mappings in Hilbert space $\hat{A} : \mathcal{H}_A \mapsto \mathcal{H}_A$ - they assign to every state from the Hilbert state some other state but belonging to the same space (the set of all operators acting within the space $\mathcal{H}_A$ is denoted sometimes by $\mathcal{B}(\mathcal{H}_A)$). If the operator $\hat{A}$ represents the action that changes the state of the system from $|\psi_I\rangle$ to $|\psi_F\rangle$, this action can be written as:

$$\hat{A}|\psi_I\rangle = |\psi_F\rangle$$

To fully characterize the action of an operator, one has to formulate it with respect to some basis in the space. It can be done by determining the result of operator action for each basis vector - without loss of generality one may say, that operator $\hat{A}$ changes the i-th basis vector into some combination of the other basis elements, which translates to the following formula:

$$\hat{A}|e_i\rangle = \sum_j A_j^i |e_j\rangle.$$

Generally, the operator is expected to store all the results of its action - for all the basis elements. Therefore, one more summation is needed:

$$\hat{A} = \sum_{i,j}^{\dim(\mathcal{H}_A)} A_{i,j} |e_i\rangle\langle e_j|,$$

The coefficients $A_{i,j}$ might be seen as entries of matrix A, which can be calculated from equation $A_{ij} = \langle e_i | \hat{A} | e_j \rangle$.

Particularly important concept, related to the matrix representation of an operator, is **trace**. Trace of the operator $\hat{A}$ is defined by the formula:

$$\mathrm{Tr}(\hat{A}) \equiv \sum_i^{\dim(\mathcal{H}_A)} \langle e_i | \hat{A} | e_i \rangle = \sum_i^{\dim(\mathcal{H}_A)} A_{ii}$$

and in matrix representation can be seen simply as a sum of the diagonal elements of matrix $\hat{A}$. The trace is especially useful in the quantum mechanics of mixed systems and will be referred to further in the text.

Operator is said to be **linear** if for any $|\alpha_1\rangle$, $|\alpha_2\rangle \in \mathcal{H}_A$ and for any coefficients c_1, $c_2 \in \mathbb{C}$ the equation holds:

$$\hat{A}\left(c_1|\alpha_1\rangle + c_2|\alpha_2\rangle\right) = c_1 \cdot \hat{A}|\alpha_1\rangle + c_2 \cdot \hat{A}|\alpha_2\rangle$$

The **transposition** of the operator $\hat{A}$, $\hat{A}^T$, is given by definition:

$$\hat{A}^T = \sum_{i,j}^{\dim(\mathcal{H}_A)} \langle e_j|\hat{A}|e_i\rangle |e_i\rangle\langle e_j|$$

and in matrix representation is obtained by swapping the rows and columns of the original matrix. **Hermitian conjugate** of operator $\hat{A}$, $\hat{A}^\dagger$ is calculated by simultaneous transposition and complex conjugate of the elements from the original matrix:

$$\hat{A}^\dagger = \left(\hat{A}^T\right)^*$$

Operator $\hat{A}$ is **hermitian** if $\hat{A} = \hat{A}^\dagger$. Hermitian operators are also especially important in quantum mechanics, for they represent measurable physical quantities describing the system (so-called **observables**).

In general, the result of acting with operator $\hat{A}$ on some state, that has been previously affected by operator $\hat{B}$ is not identical to the result of applying the operator $\hat{B}$ on the system affected firstly by operator $\hat{A}$. In other words:

$$\hat{A}(\hat{B}|\psi\rangle) \neq \hat{B}(\hat{A}|\psi\rangle)$$

or, assuming the convention in which the order of operators runs from right to left, without the brackets:

$$\hat{A}\hat{B}|\psi\rangle \neq \hat{B}\hat{A}|\psi\rangle.$$

To determine, how much the sequence of operators differs depending on their order, one can recall the **commutator**, given as:

$$[\hat{A}, \hat{B}] \equiv \hat{A}\hat{B} - \hat{B}\hat{A}; \quad [\hat{A}, \hat{B}] = -[\hat{B}, \hat{A}].$$

When two operators **commute**, i.e. their commutator is zero, $[\hat{A}, \hat{B}] = 0$, the order of the operations they represent has no impact on the results. From the point of view of the uncertainty principle, which limits the precision of determining the results of simultaneous measurements in quantum mechanics, the commutator equals zero informs that the results of the operations under consideration can be measured with any accuracy.

The last, and yet extremely important from the point of view of quantum mechanics concept is **the eigenvalues problem of the operator**. Solving

the operator $\hat{A}$ eigenvalues problem means finding all the pairs consisting of scalar (a_j - eigenvalue) and vector ($|x_j\rangle$ - eigenvector) for which the following relation is satisfied:

$$\hat{A}|x_j\rangle = a_j|x_j\rangle.$$

The importance of the eigenvalues and eigenvectors in quantum mechanics is the consequence of representation: the measurement of some physical quantity associated with the operator $\hat{A}$ results in obtaining some value from a discrete set of all allowed outcomes - and this set is identical to the set of eigenvalues $\{a_j\}$. What is more, the measurement itself leads to the collapse of the state vector into a form that stores the obtained result and excludes the others - the set of eigenvectors $\{|x_j\rangle\}$ is the same as the set of all allowed vectors post-measurement with $\hat{A}$. Moreover, the outcome a_j allows to specify the state of the system after measurement as $|x_j\rangle$. One may notice however, that several eigenvectors may correspond to one eigenvalue - systems with this property are said to be **degenerated** with respect to operator $\hat{A}$ and it is impossible to uniquely determine the particular vector of the system after measurement resulting in degenerated eigenvalue [1–3].

1.2 The phenomenon of quantum entanglement

The description settled on the vectors from Hilbert space becomes even more nuanced in the case of composite quantum systems: the system consisting of n interacting subsystems will be described within the Hilbert space $\mathcal{H}$, resulting as the tensor product of the subsystem spaces $\mathcal{H} = \bigotimes_{l=1}^{n} \mathcal{H}_l$. Similarly, the basis of composite systems is the set of vectors, which originates from the tensor product of basis vectors from each subsystem (it is the most intuitive, however, not to only one allowed method of constructing the basis of a composite quantum system - in fact, every set of orthonormal vectors with cardinality equal to $\dim(\mathcal{H})$, can be treated as a basis). According to the superposition rule, the state of a composite system can therefore be written as:

$$|\Psi\rangle_{COMP.} = \sum_{\lambda=1}^{\Lambda} C_\lambda |\lambda\rangle \tag{1.1}$$

where the summation goes to $\Lambda = \dim(\mathcal{H}_1) \cdot \dim(\mathcal{H}_2) \cdot ... \cdot \dim(\mathcal{H}_n)$ and $|\lambda\rangle$ covers all composite basis vectors.

All the possible states of the composite system can be divided into two subgroups:

- separable states - states represented by vectors that can be decomposed into vectors from the individual subspaces:

$$|\Psi\rangle_{SEP.} = |\phi_1\rangle \in \mathcal{H}_1 \otimes |\phi_2\rangle \in \mathcal{H}_2 \otimes ... \otimes |\phi_n\rangle \in \mathcal{H}_n \tag{1.2}$$

  Such states are an equivalent of classical composite systems - one can fully characterize the system by describing the state of each individual particle separately.

- entangled states (quantum correlated states) - states that cannot be decomposed with respect to component subspaces; it is impossible to find the set of states $|\phi_i\rangle$ to satisfy equation (1.2). It implies that one cannot assign the particular state to each subsystem, and therefore, one cannot characterize the overall system by describing each subsystem individually. In this case, the composite system is described more precisely than the components [4–6].

As an example of quantum entanglement, one can refer to a composite system consisting of two particles with two quantum degrees of freedom. Let there be a particle A whose states belong to the Hilbert space $\mathcal{H}_A$ spanned by the basis $\{|0\rangle_A, |1\rangle_A\}$ and particle B with states from the Hilbert space $\mathcal{H}_B$ of basis $\{|0\rangle_B, |1\rangle_B\}$. The simplest basis of the composite system $\mathcal{H}_A \otimes \mathcal{H}_B$ is $\{|0\rangle_A \otimes |0\rangle_B, |0\rangle_A \otimes |1\rangle_B, |1\rangle_A \otimes |0\rangle_B, |1\rangle_A \otimes |1\rangle_B\}$, but more interesting case is so-called Bell (or EPR) basis, with vector defined as[1] [7]:

$$|\Psi^+\rangle = \frac{1}{\sqrt{2}}(|01\rangle + |10\rangle) \qquad |\Phi^+\rangle = \frac{1}{\sqrt{2}}(|00\rangle + |11\rangle)$$
$$|\Psi^-\rangle = \frac{1}{\sqrt{2}}(|01\rangle - |10\rangle) \qquad |\Phi^-\rangle = \frac{1}{\sqrt{2}}(|00\rangle - |11\rangle).$$

States of the Bell basis have a peculiar property: the measurement conducted on any subsystem can result in state $|0\rangle$ or $|1\rangle$ with equal probability, yet the measurement on the second subsystem will be perfectly correlated with the measurement on the first subsystem: measurements on the Φ states will always result in identical outcomes ($|00\rangle$ or $|11\rangle$), while measurements on Ψ will always return the opposite states ($|01\rangle$ or $|10\rangle$).

[1] In case of composite system vectors it is accustomed to omit the sign of tensor product; moreover, if the order of subsystem coupling is given in a context, also the lower index is neglected. The state is then written in a single ket-vector, so $|0\rangle_A \otimes |1\rangle_B$ becomes simply $|01\rangle$.

1.3 EPR Paradox, Bell Inequality

The most surprising features of quantum mechanics are its indeterminism and non-locality. The non-deterministic nature of quantum mechanics results from the fact, that in general, it is not possible to predict the result of a measurement conducted on a quantum system beforehand, regardless of the amount of information gathered about the system or experimental setup. One can at best provide a probability distribution of particular results. This stands in opposition to the paradigm of classical Physics where the results of experiment are supposed to be fully deterministic - one can precisely predict the outcome of random[2] classical experiment (tossing the coin, throwing the dice etc.), provided that the complete amount of information about the system is collected.

Entanglement raised another unique feature of quantum theory - the non-locality. Classical physics states that action performed in a point cannot result in a simultaneous response in a place spatially separated from the aforementioned place - this is the so-called locality of classical physics. As it is presently known, this is not the case in quantum mechanics. The counterintuitive behaviour of the entangled states was the source of the famous problem of physics in the XX century - the EPR paradox.

The paradox was first presented in a paper by Einstein, Podolsky, and Rosen (hence the name, EPR) [5] from 1935, but the most common formulation of it was provided by Bohm in 1952 [8]: the system in question contains two particles of spin $s = \frac{1}{2}$ interacting with each other. The system can be initially prepared in the singlet state (the lower index marks the axis, on which the spin component is measured):

$$|\Psi\rangle = \frac{1}{\sqrt{2}} \left(|\uparrow_Z \downarrow_Z\rangle - |\downarrow_Z \uparrow_Z\rangle \right).$$

What is worth mentioning here, there is no limitation on the distance between the particles - they can be spatially separated by any length. After the initial state preparation, the measurement is carried out: the spin of the first particle is measured with respect to the arbitrarily chosen axis containing the unit vector $\vec{u}_A$, spin of the second one is measured concerning the axis containing the unit vector $\vec{u}_B$. If both of the axes were set to be the z axis, $\vec{u}_A = \vec{u}_B = \hat{e}_Z$, the results would be in perfect (anti)correlation - measurement conducted on the first particle has the probability of 50% to be $\frac{\hbar}{2}$ (spin up) and 50% to be $-\frac{\hbar}{2}$ (spin down), but the spin of the second

[2]Given it can be predicted, a better term would be *pseudorandom*. The randomness comes not from an intrinsic property of the experiment, but from *unwillingness* of determining the outcome.

particle will always be in the opposite direction - it is impossible to get the same results in both measurements with this choice of axis. One can easily prove, that a similar result can be derived by measuring the spin projections for any axes as long as they are chosen to be the same for both spins - the result may be in perfect correlation for different axes, but this fact does not change the argument. For example, if the spin is measured with respect to x axis (transformation of the states results from the properties of Pauli matrices):

$$|\uparrow_X\rangle = \frac{1}{\sqrt{2}}\left(|\uparrow_Z\rangle + |\downarrow_Z\rangle\right) \qquad |\downarrow_X\rangle = \frac{1}{\sqrt{2}}\left(|\uparrow_Z\rangle - |\downarrow_Z\rangle\right)$$

$$|\Psi\rangle = \frac{1}{\sqrt{2}}\left(|\uparrow_X\uparrow_X\rangle - |\downarrow_X\downarrow_X\rangle\right).$$

Quantum mechanics states that the value of the observable is undetermined beforehand, and only the measurement can lead to the collapse of the quantum superposition, which results in a particular value of the observable as a result of the experiment. However, given that the distance between the spins in the situation described above can be arbitrarily long, one must take into consideration that some unexpected interaction acts immediately on the second particle during the measurement of the first. This conclusion stands in opposition to the special theory of relativity, which assumes that no interaction can be propagated faster than the speed of light.

The paradox mentioned above was the foundation of the opinion, that quantum physics is not complete: instead, Einstein was inclined towards the belief that outcomes of the quantum measurements are set before the measurement. Quantum theory can only provide the probability distribution, not the certain results, due to the existence of some hidden variables. The tools of quantum theory were considered to be insufficient to disclose these variables. This hypothesis therefore was called the local hidden variables model (LHVM).

This hypothesis was disproved by John Bell in 1964 [7]. His derivation was based on the parameter λ which was supposed to serve as a local variable proposed by Einstein. If it was meant to be, there would have to exist some functions $A(\vec{u}_A, \lambda)$ and $B(\vec{u}_B, \lambda)$ with the values taken from the set $\{\frac{\hbar}{2}, -\frac{\hbar}{2}\}$, that serves as a result of the measurement. The particular outcome would depend therefore only on λ - if $\lambda \in \Lambda^+_{u_A}$ the measurement will result in $A = \frac{\hbar}{2}$, if $\lambda \in \Lambda - \Lambda^+_{u_A}$, then the outcome will be $A = -\frac{\hbar}{2}$ (here, Λ is a set of all possible values of λ).

Bell introduces correlation function $E(\vec{u}_A, \vec{u}_B)$ defined as a product of expectation values of measurements in respect to the axes containing $\vec{u}_A$ and

$\vec{u}_B$, divided by $\frac{\hbar^2}{4}$ for convenience - therefore:

$$-1 \leq E(\vec{u}_A, \vec{u}_B) \leq 1$$

One can express this function as well as:

$$E(\vec{u}_A, \vec{u}_B) = \frac{4}{\hbar^2} \int_\Lambda P(\lambda) A(\vec{u}_A, \lambda) B(\vec{u}_B, \lambda) d\lambda$$

where $P(\lambda)$ describes probability distribution of λ values; or, in quantum mechanical interpretation:

$$E(\vec{u}_A, \vec{u}_B) = \frac{4}{\hbar^2} \langle \Psi | \hat{S}_A \cdot \vec{u}_A \otimes \hat{S}_B \cdot \vec{u}_B | \Psi \rangle$$

.

Bell's theorem. If the hypothesis of hidden local variables is true, then the inequality:

$$|E(\vec{u}_A, \vec{u}_B) + E(\vec{u}'_A, \vec{u}'_B) + E(\vec{u}_A, \vec{u}'_B) - E(\vec{u}'_A, \vec{u}_B)| \leq 2$$

will be satisfied for every $\vec{u}_A$, $\vec{u}_B$, $\vec{u}'_A$, $\vec{u}'_B$.

Bell's theorem proof. Let the function $S(\lambda)$ be defined as:

$$\begin{aligned} S(\lambda) &= A(\vec{u}_A, \lambda) B(\vec{u}_B, \lambda) + A(\vec{u}'_A, \lambda) B(\vec{u}'_B, \lambda) \\ &+ A(\vec{u}_A, \lambda) B(\vec{u}'_B, \lambda) - A(\vec{u}'_A, \lambda) B(\vec{u}_B, \lambda) \end{aligned}$$

therefore one can rewrite Bell's inequality as:

$$\left| \frac{4}{\hbar^2} \int_\Lambda P(\lambda) S(\lambda) d\lambda \right| \leq 2$$

It is easy to check by examining all the possibilities, that the function $S(\lambda)$ can be equal only to $\frac{\hbar^2}{2}$ or $-\frac{\hbar^2}{2}$. The $P(\lambda)$, as a distribution function, has to satisfy two conditions: $P(\lambda) \geq 0$ for all $\lambda \in \Lambda$ and $\int P(\lambda) d\lambda = 1$. Hence, the expression on the left-hand side of the inequality, putting aside the absolute value, can be either -2 or 2, which fulfills Bell's assumption.

However, if one assumes that the local hidden variables do not exist, and the result of the measurement depends only on the axes choice, it is sufficient to find a set of axes, for which the Bell's inequality will not be satisfied. These axes are for example:

$$\vec{u}_A = \hat{e}_Z \qquad \vec{u}_B = \frac{1}{\sqrt{2}} (\hat{e}_X + \hat{e}_Z)$$

$$\vec{u}'_A = \hat{e}_X \qquad \vec{u}'_B = \frac{1}{\sqrt{2}}(\hat{e}_X - \hat{e}_Z)$$

therefore:

$$\vec{u}_A \cdot \vec{u}_B = \vec{u}_A \cdot \vec{u}'_B = \vec{u}'_A \cdot \vec{u}'_B = -\vec{u}'_A \cdot \vec{u}_B = \frac{\sqrt{2}}{2}$$

which obviously violates the Bell inequality:

$$|E(\vec{u}_A, \vec{u}_B) + E(\vec{u}'_A, \vec{u}'_B) + E(\vec{u}_A, \vec{u}'_B) - E(\vec{u}'_A, \vec{u}_B)| = 2\sqrt{2}.$$

Bell therefore provided a recipe for experimental verification (or falsification) of Einstein's hypothesis: someone had to build an experimental setup allowing to measure the spin of a particle projected on the given axes. If the expected (mean) results violate the Bell inequality, the hypothesis of the local hidden variables would turn out to be false.

The first trials to verify the quantum mechanics accuracy in the context of Bell's inequality are dated to the seventies. Instead of the spin projections, they employed photon polarisation, as more convenient to implement. The $|\uparrow_Z\rangle$ and $|\downarrow_Z\rangle$ were substituted to vertical $|\updownarrow\rangle$ and horizontal polarization $|\leftrightarrow\rangle$, while $|\uparrow_X\rangle$ and $|\downarrow_X\rangle$ were substituted by diagonal polarizations perpendicular to each other, $|\nearrow\rangle$ and $|\nwarrow\rangle$. The experiments of Fry and Thomson [9] and Aspect's group [10, 11] managed to prove a violation of the Bell inequality in the correlation experiments. Their results clearly proved the correctness of the quantum theory formulations - with all its non-locality and nondeterminism - and disproved the hypothesis of local hidden variables [2].

1.4 Entanglement in pure states

Quantum state $|\psi\rangle$ is entangled if and only if it cannot be written as any tensor product of states belonging to component subspaces:

$$|\psi\rangle \neq |\alpha\rangle \in \mathcal{H}_A \otimes |\beta\rangle \in \mathcal{H}_B \tag{1.3}$$

However, the problem arises if one notices, that the vectors $|\alpha\rangle$ and $|\beta\rangle$ can be of any choice. Therefore the separability of state $|\psi\rangle$ requires careful examination. The method that allows one to relatively simple determination of state separability is to use **Schmidt decomposition**.

Let the subspace $\mathcal{H}_A$ be spanned by the basis $\{|e^i_A\rangle\}$ and $\mathcal{H}_B$ be spanned by $\{|e^j_B\rangle\}$. All the states belonging to the space $\mathcal{H}_{AB} = \mathcal{H}_A \otimes \mathcal{H}_B$ can be therefore written as:

$$|\psi\rangle = \sum_{i=1}^{dim(\mathcal{H}_A)} \sum_{j=1}^{dim(\mathcal{H}_B)} A_{ij}|e^i_A\rangle \otimes |e^j_B\rangle \tag{1.4}$$

One may interpret the factors A_{ij} as elements of a matrix. If the matrix is diagonalizable, namely if $dim(\mathcal{H}_A) = dim(\mathcal{H}_B)$, one can find the eigenvalues of this matrix and its eigenvectors, rewriting vector $|\psi\rangle$ as:

$$|\psi\rangle = \sum_{q=1} \Lambda_q |\epsilon_A^q\rangle \otimes |\epsilon_B^q\rangle \tag{1.5}$$

where Λ_q is q-th eigenvalue of the matrix $\{A_{ij}\}$ and $|\epsilon_A^q\rangle$, $|\epsilon_B^q\rangle$ are identical linear combination of vectors from the $\{|e_A^i\rangle\}$ and $\{|e_B^i\rangle\}$ basis, respectively. This transformation is called Schmidt decomposition, and it gives a clear answer, whether the pure state is separable or entangled. The Schmidt rank, the number (counted with multiplicity) of amplitudes Λ_q that have positive value, denotes the entangled states when it is greater than one. Schmidt rank equal to one corresponds then to the separable state. What is also noteworthy, if all the coefficients Λ_q are non-zero and equal, the state described by this decomposition is maximally entangled [12, 13].

1.5 Entanglement in mixed states

In the real implementations of quantum mechanics one usually works on many non-interfering, identical copies of selected system. In such situations, the more general description of the quantum state is provided by a density matrix (or density operator), in place of a state vector. The density matrix is defined as follows:

$$\hat{\rho} = \sum_{i=1} P(\psi_i) |\psi_i\rangle\langle\psi_i|, \tag{1.6}$$

where $P(\psi_i)$ is the statistical probability that the system will be in state $|\psi_i\rangle$, and $\{|\psi_i\rangle\}_i$ is a complete, orthonormal set of states of the aforementioned system. The density operator is self-adjoint, hermitian, and positive semi-definite, with trace equals to one. If there is a certainty that the system resides in one particular state $|\Psi\rangle$, then the system is in **the pure state**, and its density matrix for such state can be expressed simply as $\hat{\rho} = |\Psi\rangle\langle\Psi|$. If this isn't the case, then such a system is called to be in **the mixed state**. To definitely check, whether the system is pure or mixed, one can check the trace of the $\hat{\rho}^2$ - for the pure state $\mathrm{Tr}(\hat{\rho}^2) = 1$, while for the mixed ones: $\mathrm{Tr}(\hat{\rho}^2) < 1$ [4].

The mixed states can also exhibit entanglement. In general, the state $\hat{\rho}$ is entangled with respect to subsystems A and B, if it cannot be expressed as a Kronecker product of the density matrices describing the component subsystems:

$$\hat{\rho} = \sum_j P_j \cdot \rho_A^j \otimes \rho_B^j. \tag{1.7}$$

However, the basis of states regarded in definition (1.6) can be arbitrarily chosen, and the index j refers exactly to these multiple choices. Therefore, it is extremely difficult to judge the separability based solely on this definition. For this reason, there arose a need for more applicable **separability conditions** [14, 15].

1.5.1 Separability criteria for mixed states. Measures of entanglement

In the case of mixed states, the determination of separability turns out to be an exceptionally complicated issue - to use the Bell inequality or Schmidt decomposition one should know the statistical probability distribution, as the mixed separable state can be composed of the entangled pure states. For this reason, there exist special separability criteria for mixed states, usually limited to some specific cases.

Peres - Horodecki criterion of positive partial transposition

The criterion of positive partial transposition was formulated by Peres [16] and Horodecki *et al.* [17] and it is a necessary and sufficient condition to prove separability of subspaces with dimensionality $2 \otimes 2$ and $2 \otimes 3$ [14]. The operation necessary to specify this condition is **partial transpose**. Let $\{|\alpha_i\rangle\}$ be a basis in $\mathcal{H}_A$ Hilbert space and $\{|\beta_i\rangle\}$ - basis in $\mathcal{H}_B$ Hilbert space. The partial transpose done on some density matrix $\rho \in \mathcal{H}_A \otimes \mathcal{H}_B$ returns matrix ρ^Γ with elements given by formula:

$$\langle \alpha_i \beta_j | \rho^\Gamma | \alpha_j \beta_i \rangle = \langle \alpha_i \beta_i | \rho | \alpha_j \beta_j \rangle \tag{1.8}$$

Peres - Horodecki criterion states that the state ρ is separable if and only if its partial transposition matrix ρ^Γ also fulfills the condition to be a density operator - in explicit, its eigenvalues have to be non-negative.

Positive but not completely positive maps

Let $\mathcal{B}(\mathcal{H})$ be the space of all bound operators that act on the elements of Hilbert space $\mathcal{H}$. Operator $A \in \mathcal{B}(\mathcal{H})$ is positive if is hermitian and its eigenvalues are non-negative; and completely positive, if $\hat{I} \otimes A$ is positive for any dimensionality of identity operator $\hat{I}$. It has been proven [17] that positive, but not completely positive map $\Lambda : \mathcal{B}(\mathcal{H}_B) \mapsto \mathcal{B}(\mathcal{H}_A)$ generates a necessary and sufficient condition of separability of states - state ρ_{AB} is separable if and only if the inequality:

$$\left(\hat{I}_A \otimes \Lambda\right) \rho_{AB} \geq 0$$

is satisfied for all positive but not completely positive maps Λ. This concept lies at the core of the idea of **entanglement witnesses** - see sect. 1.6.

Entanglement monotone

There are several ways to associate a quantitative measurement as a means to express the amount of entanglement in a particular state ρ. One of them is to define the appropriate **entanglement monotone**, which is a function of non-negative values, which does not increase under local transformations. Such a function μ, $\mu(\rho) \to \mathcal{R}_+ \cup \{0\}$ has to have following properties:

1. $\mu(\rho) = 0$ for separable states;
2. (optionally) $\mu(\rho) = 1$ for maximally entangled states;
3. $\mu(\rho)$ decreases monotonically under local operations (action on only one part of the composite system) and classical commutations.

The examples of entanglement monotones involve **negativity** and **concurrence**, among others [18].

Negativity. The negativity is a measure of entanglement resulting from the Peres - Horodecki criterion, defined as [17]:

$$\mathcal{N}(\rho) = \frac{\mathrm{Tr}[(\rho^\Gamma)^\dagger \rho^\Gamma] - 1}{2}. \tag{1.9}$$

The above definition is equivalent to the absolute value of the sum of all negative eigenvalues of partially transposed matrix ρ^Γ:

$$\mathcal{N}(\rho) = \left| \sum_{\lambda_j < 0} \lambda_j \right|. \tag{1.10}$$

Concurrence. In aim to determine the concurrence C of the entanglement for a two-qubit system in state ρ one needs to perform a transformation of the state to obtain matrix R:

$$R = \rho(\sigma^Y \otimes \sigma^Y)\rho^\dagger(\sigma^Y \otimes \sigma^Y) \tag{1.11}$$

and then diagonalize it. Concurrence is defined as:

$$\mathcal{C}(\rho) = max\{0, \sqrt{\lambda_4} - \sqrt{\lambda_3} - \sqrt{\lambda_2} - \sqrt{\lambda_1}\} \tag{1.12}$$

where λ_1, λ_2, λ_3, λ_4 are eigenvalues of the R matrix, ordered increasingly [19, 20].

Entropic measures of entanglement

In quantum informatics the entanglement can manifest itself not only by the non-classical correlations but also by the unexpected behaviour of the quantum information. As it turns out, the von Neumann entropy, defined as [4]:

$$S(\rho) = -\mathrm{Tr}\left[\rho \cdot \log(\rho)\right] \tag{1.13}$$

which was established as a means to distinguish the mixed and pure states ($S = 0$ for pure states and $S = dim(\mathcal{H})$ for maximally mixed state) can also be interpreted as a number of qubits necessary to transmit the state generated by the statistical source [21]. It is the equivalent of Shannon entropy, defined as $H(X) = \sum_j p_j(x) \cdot \log\left(p_j(x)\right)$, which is the number of classical bits needed to send a message associated with the random variable X, of probability distribution $p_j(x)$ [22].

As it was pointed out by Schrödinger [6], the information of the whole entangled system is more complete than the information of the subsystems, therefore one can conclude, that the entropy of the whole system is smaller than the entropy of the subsystems. In the classical information theory, the following inequalities have to be satisfied:

$$H(X,Y) \geq H(X), \qquad H(X,Y) \geq H(Y)$$

The same holds for the pure, separable quantum states, in terms of von Neumann entropy; what is more, these inequalities can be extended to the α-Renyi entropies:

$$S_\alpha(\rho_{AB}) \geq S_\alpha(\rho_A), \qquad S_\alpha(\rho_{AB}) \geq S_\alpha(\rho_B). \tag{1.14}$$

α-Renyi entropy (a generalization of the entropies used in the information theory to quantify the randomness, uncertainty, unpredictability, and so on of a set random experiment outcomes) is defined as:

$$S_\alpha(\rho) = \begin{cases} \frac{1}{1-\alpha} \cdot \log\left(\mathrm{Tr}[\rho^\alpha]\right) & \text{for} \quad \alpha \neq 1 \\ \\ -\mathrm{Tr}\left[\rho \cdot \log(\rho)\right] & \text{for} \quad \alpha = 1 \end{cases} \tag{1.15}$$

If the inequalities (1.14) are not satisfied in the case of the pure state, then the state is entangled [23–25].

Entanglement of formation. For the pure state ρ_{AB} von Neumann entropies of reduced density matrices are equal, which can be proven based on Schmidt decomposition. One can define the measure, which can be

viewed as a number of Bell states necessary to copy the state ρ_{AB} using the local operations and classical commutations - entanglement of formation. Therefore, for pure state entanglement of formation is defined as $E_F(\rho_{AB}) = S(\rho_A) = S(\rho_B)$. In the case of mixed state, this measurement is, minimized after all the decompositions of the statistical mixture into pure states, the weighted average of pure states entanglements [20]:

$$E_F(\rho_{AB}) = min\left(\sum_i P(\psi_i)E_F(\psi_i)\right) \tag{1.16}$$

where $E_F(\psi_i) = E_F(P(\psi_i)|\psi_i\rangle\langle\psi_i|)$.

Entanglement of formation is connected to the concurrence C by the relation:

$$\begin{aligned} E_F(\rho) &= -\left[\frac{1+\sqrt{1-\mathcal{C}^2}}{2}\log_2\left(\frac{1+\sqrt{1-\mathcal{C}^2}}{2}\right)\right. \\ &\left. +\frac{1-\sqrt{1-\mathcal{C}^2}}{2}\log_2\left(\frac{1-\sqrt{1-\mathcal{C}^2}}{2}\right)\right] \end{aligned} \tag{1.17}$$

Relative entropy of entanglement. Let ρ and σ be some quantum states. One can define the function of relative entropy as [26]:

$$S_R(\rho|\sigma) = \mathrm{Tr}\left[\rho\cdot\log_2(\rho) - \rho\cdot\log_2(\sigma)\right] \tag{1.18}$$

Relative entropy of entanglement is defined as:

$$E_R(\rho) = \min_{\sigma_S\in\mathcal{D}} S_R(\rho|\sigma_S) \tag{1.19}$$

where $\mathcal{D}$ is a set of all separable states, which can be determined based on Peres - Horodecki criterion [27].

1.6 Entanglement witnesses

There is also a purely experimental way of detecting entanglement, by using the so-called **entanglement witnesses**. In the mathematical formalism of quantum systems, all the possible measurements are represented by hermitian operators (observables). The operator is hermitian if simultaneous transposition and complex conjugation of its elements (hermitian conjugate) results in an identical operator:

$$A^\dagger = \left(A^T\right)^* = A$$

By the **spectral theorem**, every observable can be written in diagonal form:

$$A = \sum_k a_k |\alpha_k\rangle\langle\alpha_k| \tag{1.20}$$

where a_k are the eigenvalues of the operator and possible measurement results of the observable, while $|\alpha_k\rangle$ are eigenvectors of the corresponding operator - if the measurement results in outcome equal to a_k. It will also lead to the collapse of the measured state, whatever it would be before measurement, to the final state $|\alpha_k\rangle$. The probability of a particular outcome, while acting with observable A on state $|\psi\rangle$, can be calculated using the formula:

$$P(a_k) = |\langle\alpha_k|\psi\rangle|^2. \tag{1.21}$$

The most likely result of the measurement, **expected value** $\langle A\rangle$, of observable A acting on state $|\psi\rangle$ reads:

$$\langle A\rangle = \langle\psi|A|\psi\rangle. \tag{1.22}$$

The same quantities can be written for mixed state ρ as:

$$P(a_k) = \mathrm{Tr}(|\alpha_k\rangle\langle\alpha_k| \cdot \rho)$$

$$\langle A\rangle = \sum_i P(\psi_i) \cdot \langle\psi_i|A|\psi_i\rangle = \langle A\rangle = \mathrm{Tr}(A \cdot \rho). \tag{1.23}$$

The observable W can play the role of an entanglement witness, if it has at least one non-zero eigenvalue and the expected value for this operator on any separable state is non-negative (so-called block-positive map):

$$\langle\psi|\langle\phi|W|\psi\rangle|\phi\rangle \geq 0 \qquad \text{for any } \ |\psi\rangle \in \mathcal{H}_A \ \text{ and } \ |\phi\rangle \in \mathcal{H}_B$$

An example of such an operator is a state swap operator, defined as:

$$\hat{V} = \sum_{i\neq j}^{\dim(\mathcal{H}_A),\dim(\mathcal{H}_B)} |i\rangle\langle j| \otimes |j\rangle\langle i|.$$

If this operator acts on the entangled state, the result will yield a negative value. Therefore, the measurement gives a clear answer as to whether the examined state is separable or entangled [28, 29].

There is a method of generating the entanglement witnesses using positive but not completely positive maps. The map Λ is positive if for every vector $|\psi\rangle \in \mathcal{H}$ the following condition is met:

$$\langle\psi|\Lambda|\psi\rangle \geq 0,$$

and completely positive if positive is every direct product of this map with the identity operator $\Lambda \otimes \hat{I}$, regardless of the dimensionality of the latter. Then, given that Λ is indeed the positive, but not completely positive map, the entanglement witness associated with it can be obtained by the formula:

$$W = (\hat{I} \otimes \Lambda)\hat{P}^{+} \tag{1.24}$$

where $\hat{P}^{+}$ is a projection operator on the maximally entangled state $|\Phi^{+}\rangle$ defined as:

$$|\Phi^{+}\rangle = \frac{1}{\sqrt{d}} \sum_{i=1} |i\rangle \otimes |i\rangle$$

$$\hat{P}^{+} = |\Phi^{+}\rangle\langle\Phi^{+}|.$$

1.7 Local Quantum Uncertainty. Local Quantum Fisher Information

Another method of quantifying the entanglement (and, by extension, any other non-classical correlations, see 1.9 for exemplification) in a quantum system is an applying the **local quantum uncertainty** - the minimal uncertainty introduced by acting with the local operators on only one part of the joint quantum system [30]. This method is based on the fact, that every measurement conducted on a composite system locally would lead to an increase in the uncertainty of the result (only the non-correlated in quantum sense states will not exhibit this increase) and on the notion of skew information. This quantity, defined by Wigner and Yanase [31], was introduced as a means of expressing the amount of information stored by the quantum state of a system with respect to some observable defined on this system.

Let there exist some conserved, additive observable labeled by $\hat{K}$. Skew information, stored in state ρ in relation to $\hat{K}$ is given by the formula:

$$\begin{aligned} I_{WY}(\rho, \hat{K}) &= -\frac{1}{2}\mathrm{Tr}\left([\sqrt{\rho}, \hat{K}]^2\right) \\ &= \mathrm{Tr}(\rho\hat{K}^2) - \mathrm{Tr}(\sqrt{\rho}\hat{K}\sqrt{\rho}\hat{K}). \end{aligned} \tag{1.25}$$

It can be easily seen that for pure states ($\rho^2 = \rho$) this expression reduces to the variance of this state:

$$I_{WY}(\rho, \hat{K}) = \mathrm{Tr}(\rho\hat{K}^2) - \left(\mathrm{Tr}(\rho\hat{K})\right)^2 \equiv \mathrm{Var}(\rho, \hat{K}).$$

which expresses the uncertainty of pure state ρ^P. For the mixed states, the uncertainty is the sum of variances resulting from the statistical mixture of

states that create the ensemble. As it has been proven [32], skew information indeed allows for a reliable estimation of uncertainty in mixed states. The definition (1.25) was later extended by Dyson and Lieb [33], to the form:

$$\begin{aligned} I^{\alpha}_{WYDL}(\rho,\hat{K}) &= -\frac{1}{2}\mathrm{Tr}\left([\rho^{\alpha},\hat{K}]\cdot[\rho^{1-\alpha},\hat{K}]\right) \\ &= \mathrm{Tr}(\rho\hat{K}^2)-\mathrm{Tr}(\rho^{\alpha}\hat{K}\rho^{1-\alpha}\hat{K}). \end{aligned} \tag{1.26}$$

where α takes any value from the range $(0;1)$. This extension, depending on the particular α serves as a symmetry monotone [34].

Local Quantum Uncertainty (LQU) is defined as a minimal skew information that can be achieved by local operations on the particular subsystem of a composite quantum system:

$$LQU = \min_{\hat{K}_A} I_{WY}(\rho,\hat{K}_A\otimes\hat{I}_B), \tag{1.27}$$

where the minimization goes over all the conserved and additive operators existing in the bound operator space of $\mathcal{H}_A$. However, for systems being the conjunction of the qubit with some larger subsystem ($\mathcal{H}=\mathcal{H}_2\otimes\mathcal{H}_B$) this minimization is done by the formula [30]:

$$LQU = 1-\max\{\lambda_1,\lambda_2,\lambda_3\}, \tag{1.28}$$

where $\lambda_1,\lambda_2,\lambda_3$ are the eigenvalues of matrix M, defined element-by-element as:

$$\langle i|M|j\rangle = \mathrm{Tr}\left(\sqrt{\rho}(\sigma^i\otimes\hat{I}_B)\sqrt{\rho}(\sigma^j\otimes\hat{I}_B)\right) \tag{1.29}$$

with σ^i,σ^j being the Pauli matrices, $\sigma^X,\sigma^Y\sigma^Z$ for the system of dimensionality 2.

Local Quantum Fisher Information (LQFI) is yet another technique to express the amount of non-classical correlation in the system. Let this system undergo a unitary time evolution:

$$\rho(\tau) = e^{-i\hat{H}\tau}\rho(0)e^{-i\hat{H}\tau}.$$

Quantum Fisher Information is defined as [35, 36]:

$$F^2(\rho(\tau)) = \frac{1}{4}\mathrm{Tr}\left(\rho(\tau)L^2(\tau)\right) \tag{1.30}$$

where $L(\tau)$ is operator satisfying the equation:

$$\frac{d}{d\tau}\rho = \frac{1}{2}\left(L(\tau)\rho(\tau)-\rho(\tau)L(\tau)\right).$$

For a state $\rho = \sum_m p_m |m\rangle\langle m|$, $p_m \geq 0$ for any m and $\sum_m p_m = 1$, Quantum Fisher Information simplifies to the form:

$$F^2(\rho, \hat{H}) = \frac{1}{2} \sum_{m \neq n} \frac{p_m - p_n}{p_m + p_n} |\langle m|\hat{H}|n\rangle|^2 \tag{1.31}$$

If the system in question is composite, $\mathcal{H} = \mathcal{H}_A \otimes \mathcal{H}_B$, where the dynamics of the first subsystem is described by Hamiltonian $\hat{H}_A \otimes \hat{I}_B$ and the second by $\hat{I}_A \otimes \hat{H}_B$, one can define Local Quantum Fisher Information as [37]:

$$F^2(\rho, \hat{H}_A) = \mathrm{Tr}(\rho \hat{H}_A^2) - \sum_{m \neq n} \frac{2p_m \cdot p_n}{p_m + p_n} |\langle m|\hat{H}_A|n\rangle|^2 \tag{1.32}$$

by minimization over all local Hamiltonians, one obtains the measure Q_A^2:

$$Q_A^2 = \min_{\hat{H}_A} F^2(\rho, \hat{H}_A) \tag{1.33}$$

which vanishes for all states that are non-correlated in the quantum sense - therefore may serve as an entanglement measure.

If the minimization is over the two-level subsystems (qubits), the formula above may be simplified to:

$$Q_A^2 = 1 - \max\{\lambda_1, \lambda_2, \lambda_3\}$$

where λ_1, λ_2, λ_3 are the eigenvalues of a matrix defined as [30]:

$$\langle i|M|j\rangle = \sum_{m,n} \frac{2p_m \cdot p_n}{p_m + p_n} \langle m|\sigma^i \otimes \hat{I}|n\rangle\langle n|\sigma^j \otimes \hat{I}|m\rangle. \tag{1.34}$$

1.8 Multipartite Entanglement

The composite quantum system consisting of only two smaller parts is only a simplification - in many cases, the systems designed to be used in quantum technologies consist of three or more interacting subsystems. Each of the subsystems has quantum degrees of freedom that form the most natural basis for describing the physical phenomena behind its actions. Also, the entanglement, besides its bipartite aspect (which, after all, is best understood and most commonly used quantum correlations even in multipartite systems) has a more global nature.

The simplest multipartite system is the tripartite one; however, the way the generalization proceeds provides a clear recipe to expand this consideration further. Let the system in consideration be described in the product

Hilbert space, $\mathcal{H}_A \otimes \mathcal{H}_B \otimes \mathcal{H}_C$. If the state of the system can be written as:

$$\rho = \sum_i P_i \cdot \rho_A^i \otimes \rho_B^i \otimes \rho_C^i; \qquad \rho_X^i \in \mathcal{H}_X \tag{1.35}$$

the system is in a separable state, the state of each subsystem is perfectly known. If this is not the case, the system exhibits some degree of entanglement. This entanglement may be bipartite (the state of one subsystem is clearly specified, and the two remaining systems are entangled):

$$\rho_{BE} = \sum_i P_i \cdot \rho_{AB}^i \otimes \rho_C^i; \qquad \exists_i \ : \ \rho_{AB}^i \neq \sum_j P_j \cdot \rho_A^j \otimes \rho_B^j$$

or in **genuine tripartite entangled** state [38] - the state of the entire system is more precisely defined than the state of any component subsystem [39].

From the perspective of the pure states of tripartite systems consisting of two-level subsystems, the maximally entangled tripartite states are:

- GHZ (Greenberg - Horne - Zeilinger) state [40, 41]:

  $$|GHZ\rangle = \frac{1}{\sqrt{2}} \left(|\downarrow\downarrow\downarrow\rangle + |\uparrow\uparrow\uparrow\rangle \right)$$

  The tripartite entanglement in the GHZ state can be accused of some competitiveness regarding bipartite entanglement - tracing out any of the subspace results in a bipartite separable state. Despite that, the GHZ is widely applied in photonic protocols [42–46] - the component states represent the situation in which all the photons have the same polarization.

- W state [47]:

  $$|W\rangle = \frac{1}{\sqrt{3}} \left(|\uparrow\uparrow\downarrow\rangle + |\uparrow\downarrow\uparrow\rangle + |\downarrow\uparrow\uparrow\rangle \right)$$

  The W state, while also genuine tripartite entangled, is more resilient than GHZ - tracing out any subspace results in a mixed entangled state. This state gained popularity in quantum devices based on spin structures [48–52] - all component states have identical magnetization, which makes them easy to prepare.

These states can be easily generalized for any size of the composite system:

$$|GHZ_M\rangle = \frac{1}{\sqrt{2}} \left(|\uparrow_1\uparrow_2 \ldots \uparrow_M\rangle + |\downarrow_1\downarrow_2 \ldots \downarrow_M\rangle \right)$$

$$|W_M\rangle = \frac{1}{\sqrt{M}} \left(|\downarrow_1\uparrow_2 ... \uparrow_M\rangle + |\uparrow_1\downarrow_2 ... \uparrow_M\rangle + ... + |\uparrow_1\uparrow_2 ... \downarrow_M\rangle \right)$$

with all properties mentioned above.

In terms of separability criterion, any **positive but not completely positive** map still can serve as a base of the necessary condition of separability: if the map $\hat{\Lambda} : \mathcal{B}(\mathcal{H}_2 \otimes ... \otimes \mathcal{H}_M) \mapsto \mathcal{B}(\mathcal{H}_1)$ is positive, but not completely positive, the separable states satisfies the equation:

$$\left[\hat{I}_1 \otimes \hat{\Lambda}\right] \rho \geq 0.$$

Similarly, the notion of **entanglement witness** can be expanded - there exists operator W, which has expectation value $\mathrm{Tr}(W\rho) \geq 0$ for separable states ρ, and $\mathrm{Tr}(W\rho) < 0$ for entangled states - such operator plays the role of entanglement witness in multipartite systems.

1.9 Quantum Discord

Quantum entanglement is not the only non-classical correlation that can be detected in composite quantum systems; the other is quantum discord, also widely used in Quantum Information Theory. The uniqueness of this resource results from the fact, that it can be present in mixed states, that are separable in the sense of quantum entanglement - quantum discord arises as a consequence of the non-commutativity of quantum operators, which is in general not related to entanglement.

The measure of quantum discord is closely connected to the informational entropy (average level of uncertainty of particular outcome when a measurement is conducted upon the mixed state) of composite system state. Let us define two measures of mutual information stored in the state of the bipartite system, $\rho_{AB} \in \mathcal{H}_A \otimes \mathcal{H}_B$:

$$\begin{aligned} I(\rho_{AB}) &= S(\rho_A) + S(\rho_B) - S(\rho_{AB}) \\ J_A(\rho_{AB}) &= S(\rho_B) - S(\rho_B|\rho_A) \end{aligned} \tag{1.36}$$

where: $\rho_A = \mathrm{Tr}_B(\rho_{AB})$, $\rho_B = \mathrm{Tr}_A(\rho_{AB})$, $S(\rho) = -\mathrm{Tr}\left(\rho \cdot \log\rho\right)$ - von Neumann entropy, and $S(\rho_B|\rho_A) = S(\rho_{AB}) - S(\rho_A)$ - conditional entropy. Quantum discord is then given as a difference between these measures [53–55]:

$$\tilde{QD}_A(\rho_{AB}) = I(\rho) - J_A(\rho) = S(\rho_A) - S(\rho_{AB}) + S(\rho_A|\rho_B). \tag{1.37}$$

It is noteworthy, that this discord definition is asymmetric; generally, $\tilde{QD}_A \neq \tilde{QD}_B$ [56], and basis-dependent. To remove the basis impact on the discord,

one may apply the extended definition, with maximization over all the projection operators on the eigenbasis of $\mathcal{H}_A$:

$$QD_A(\rho_{AB}) = I(\rho_{AB}) - \max_{\hat{\Pi}_j^A} J_{\hat{\Pi}_j^A}(\rho). \tag{1.38}$$

where $\Pi_j^A = |\alpha_j\rangle\langle\alpha_j|$ is projection operator.

Also the problem of non-symmetry in quantum discord can be solved by application of von Neumann projection operators, $\hat{\Pi}_j^A \otimes \hat{\Pi}_k^B$. To define the symmetric quantum discord, $SQD_A = SQD_B$, one needs to refer to auxiliary measures from (1.36) in terms of relative entropies (definition of which is identical to (1.18)):

$$I(\rho_{AB}) = S_R(\rho_{AB}|\rho_A \otimes \rho_B) = -\mathrm{Tr}\left(\rho_{AB} \cdot \log\rho_{AB} - \rho_{AB} \cdot \log(\rho_A \otimes \rho_B)\right).$$

$$J_A(\rho_{AB}) = \max_{\Phi_A} S_R(\Phi_A(\rho_{AB})|\Phi_A(\rho_A) \otimes \rho_B),$$

where the maximization goes over the Φ_A - projective valued measures (PVM) of rank 1. The symmetric form of discord is then:

$$SQD(\rho_{AB}) = \min_{\hat{\Pi}_j^A \otimes \hat{\Pi}_k^B} \left[S_R(\rho_{AB}|\rho_A \otimes \rho_B) - S_R\Phi_{AB}(\rho_{AB})|\Phi_A(\rho_A) \otimes \Phi_B(\rho_B))\right], \tag{1.39}$$

where:

$$\Phi_{AB}(\rho_{AB}) = \sum_{j,k} (\hat{\Pi}_j^A \otimes \hat{\Pi}_k^B)\rho_{AB}\hat{\Pi}_j^A \otimes \hat{\Pi}_k^B$$

$$\Phi_A(\rho_A) = \sum_j \hat{\Pi}_j^A \rho_A \hat{\Pi}_j^A.$$

The same definition can be written shortly as:

$$SQD(\rho_{AB}) = \min_{\hat{\Pi}_j^A \otimes \hat{\Pi}_k^B} \left[I(\rho_A B) - I(\Phi_{AB}(\rho_{AB}))\right].$$

Such discord can be interpreted as a minimal amount of correlation that is lost during the measurement [57, 58].

In recent years quantum discord has proven to be another important resource in Quantum Computing, with lesser vulnerability to dissipative environment and temperature increase than the entanglement [59–61].

Chapter 2

Open Quantum Systems

2.1 Dynamics of an open quantum systems

2.1.1 Liouville - von Neumann Equation

It is beyond question that the quantum system, to be useful in practical applications, has to be analysed as open - interaction with the environment is inevitable and therefore must be taken into account. However, the description of open quantum system dynamics is paradoxically worth starting with the characterization of dynamics for closed systems, to be able to develop it further by analogy. The time evolution of pure state $|\psi(t)\rangle$ is governed by Schrödinger equation:

$$\frac{d}{dt}|\psi(t)\rangle = -i\hat{H}|\psi(t)\rangle \tag{2.1}$$

where $\hat{H}$ is the Hamiltonian of closed system. One can define unitary evolution operator, $U(t, t_0)$, which translates system from some initial state $|\psi(t_0)\rangle$ into state of the system in a time t:

$$|\psi(t)\rangle = U(t, t_0)|\psi(t_0)\rangle \tag{2.2}$$

This operator has to satisfy the following properties:

$$1) \quad U(t, t_0)U^\dagger(t, t_0) = U^\dagger(t, t_0)U(t, t_0) = \hat{I}$$

$$2) \quad U(t_0, t_0) = \hat{I}$$

Substituting (2.2) in (2.1) one can obtain:

$$\frac{d}{dt}U(t, t_0)|\psi(t_0)\rangle = -i\hat{H}U(t, t_0)|\psi(t_0)\rangle.$$

The initial state of the system is independent of time and, therefore can be neglected:

$$\frac{d}{dt}U(t,t_0) = -i\hat{H}U(t,t_0) \tag{2.3}$$

so the solution of the differential equation above reads:

$$U(t,t_0) = e^{-i\int_{t_0}^{t}\hat{H}(\tau)d\tau}.$$

This can be simplified further if the Hamiltonian is time-independent:

$$U(t,t_0) = e^{-i\hat{H}\cdot(t-t_0)}.$$

Hence, the explicit form of vector $|\psi(t)\rangle$ reads:

$$|\psi(t)\rangle = e^{-i\hat{H}\cdot(t-t_0)}|\psi(t_0)\rangle.$$

However, if the system is in a mixed state, it must be characterized in terms of density matrix - its initial form can be assumed as:

$$\rho(t_0) = \sum_j p_j|\psi_j(t_0)\rangle\langle\psi_j(t_0)|,$$

where p_j indicates the probability that the system selected to measure will be in state $|\psi_j(t_0)\rangle$. The time evolution of the density operator will be a result of every component vector evolution that is governed by the Schrödinger equation:

$$\rho(t) = \sum_j p_j|\psi_j(t)\rangle\langle\psi_j(t)| = \sum_j p_j U(t,t_0)|\psi_j(t_0)\rangle\langle\psi_j(t_0)|U^\dagger(t,t_0)$$

$$\rho(t) = U(t,t_0)\rho(t_0)U^\dagger(t,t_0).$$

The differentiation over t turns this equation into the **Liouville - von Neumann equation**:

$$\begin{aligned}\frac{d}{dt}\rho(t) &= \sum_j p_j\frac{dU(t,t_0)}{dt}|\psi_j(t_0)\rangle\langle\psi_j(t_0)|U^\dagger(t,t_0)\\ &\quad + \sum_j p_j U(t,t_0)|\psi_j(t_0)\rangle\langle\psi_j(t_0)|\frac{dU^\dagger(t,t_0)}{dt}\end{aligned}$$

substituting the derivative of the unitary operator in accordance with (2.3) results in:

$$\begin{aligned}\frac{d}{dt}\rho(t) &= -i\hat{H}\sum_j p_j U(t,t_0)|\psi_j(t_0)\rangle\langle\psi_j(t_0)|U^\dagger(t,t_0) \\ &\quad +i\sum_j p_j U(t,t_0)|\psi_j(t_0)\rangle\langle\psi_j(t_0)|U^\dagger(t,t_0)\hat{H}\end{aligned}$$

It is worth emphasizing here, that one can omit the hermitian conjugation in Hamiltonian without additional assumptions - Hamiltonian represents real, physical quantity, total energy of the system, and therefore has to be self-adjoint. Thus,

$$\begin{aligned}\frac{d}{dt}\rho(t) &= -i\left(\hat{H}\rho(t) - \rho(t)\hat{H}\right) \\ \frac{d}{dt}\rho(t) &= -i\left[\hat{H},\rho(t)\right], \end{aligned} \tag{2.4}$$

which describes the time evolution of a density matrix in an isolated system [4].

2.1.2 Intrinsic decoherence - Milburn Equation

The previous derivation assumes that the time evolution of a closed quantum system is unitary - however, aiming to explain the fact that macroscopic systems are not able to exhibit the quantum correlated states, Milburn [62] assumed the opposite. His investigation was to introduce decoherence (loss of quantum correlation; the decoherence itself will be further discussed later on) in closed system formalism. He hypothesized that in macroscopic systems the decoherence coefficient is so large that correlated states are immediately destroyed. The transformation of state during a short time interval τ can be calculated from the formula:

$$\rho(t+\tau) = e^{-i\hat{H}\tau}\rho(t)e^{i\hat{H}\tau},$$

Milburn however postulated otherwise:

- for sufficiently short τ the change of state may not even happen - let the probability of change be denoted by $p(\tau)$;
- if the change of state occurs, the new state can be described by formula:

  $$\rho(t+\tau) = e^{-i\hat{H}\theta(\tau)}\rho(t)e^{i\hat{H}\theta(\tau)} \equiv \delta\tau\rho(t)$$

  where $\theta(\tau)$ describes the change of phase - it can be postulated to be, for example, $\theta(\tau) = \frac{\tau}{p(\tau)}$;

– there exist some minimal change of phase:

$$\lim_{\tau \to 0} \theta(\tau) = \theta_0.$$

In regards to these assumptions, one can divide the time t into K identical intervals, each lasting τ, $t = K \cdot \tau$, and write the state $\rho(t)$ as a result of time evolution:

$$\begin{aligned} \rho(t) &= \sum_{k=0}^{K} \binom{K}{k} p(\tau)^k (1 - p(\tau))^{K-k} e^{-ik\hat{H}\theta(\tau)} \rho(0) e^{ik\hat{H}\theta(\tau)} \\ &= (1 + p(\tau) \cdot U(\tau))^K \rho(0) \end{aligned}$$

where

$$U(\tau) = \delta(\tau) - 1$$

Milburn noted, that this result is similar to the description of a sub-Poissonian pumped laser [63] and used the rate of change from that model to formulate the equation:

$$\frac{d}{dt}\rho(t) = \frac{1}{\theta(\tau)p(\tau)} \ln\left((1 + p(\tau)U(\tau))\rho(t)\right)$$

which, for infinitesimally short time interval τ takes the form:

$$\frac{d}{dt}\rho(t) = \frac{1}{\theta_0 p_0} \ln\left((1 + p_0 U_0)\rho(t)\right).$$

By setting the probability of change $p_0 \equiv 0$ one can expand the equation above:

$$\frac{d}{dt}\rho(t) = \frac{1}{\theta_0} e^{-i\hat{H}\theta_0} \rho(t) e^{i\hat{H}\theta_0}$$

and, by expanding it further to the first order of θ_0 one can get the **Milburn equation**, describing the closed system with intrinsic decoherence:

$$\frac{d}{dt}\rho(t) = -i[\hat{H}, \rho(t)] + \gamma \left[\hat{H}, [\hat{H}, \rho(t)]\right],$$

where $\gamma = \frac{\theta_0}{2}$ is a decoherence factor for a closed system. This result is somehow surprising - in general, a loss of correlation in a closed system is not expected. However, from the mathematical point of view, it is easy to see that both unitary and Milburn time evolution lead finally to the eigenstate of the Hamiltonian. In the Milburn equation decoherence occurs in the relaxation process [64], while most commonly the decoherence is associated with the influence of the environment - this aspect will be discussed in section 2.5.

2.2 Concept of open quantum systems

2.2.1 Composite quantum system

To extend the description of time evolution in quantum mechanics to open systems, it is advantageous to recall the concept of a composite quantum system. As mentioned, when two quantum subsystems, A, B, described in corresponding Hilbert spaces $\mathcal{H}_A$ and $\mathcal{H}_B$, come into interaction, they will create a composite quantum system. The system in question will be spanned over the Hilbert space $\mathcal{H}_{AB}$, being the tensor product of component subspaces $\mathcal{H}_{AB} = \mathcal{H}_A \otimes \mathcal{H}_B$. If we choose the basis $\{|\phi_i^A\rangle\}$ in the subspace $\mathcal{H}_A$ and $\{|\phi_j^B\rangle\}$ to be the basis in the subspace $\mathcal{H}_B$, then we can write down the general formula on a state vector in system $A + B$ as:

$$|\Psi\rangle_{AB} = \sum_i \sum_j a_{i,j} |\phi_i^A\rangle \otimes |\phi_j^B\rangle.$$

The interaction and correlation between the quantum systems do not rule out the acting on or analyzing only one of the subsystems; let the $\hat{S}^A$ be an operator acting on subsystem A. Its action on a state of a composite system can be written as:

$$\left(\hat{S}^A \otimes \hat{I}^B\right) |\Psi\rangle_{AB} = \sum_i \sum_j a_{i,j} \cdot \hat{S}^A |\phi_i^A\rangle \otimes |\phi_j^B\rangle$$

where $\hat{I}^B$ is the identity operator in the subspace $\mathcal{H}_B$. Analogously, the action of the operator $\hat{S}^B$ defined for subsystem B can be written as:

$$\left(\hat{I}^A \otimes \hat{S}^B\right) |\Psi\rangle_{AB} = \sum_i \sum_j a_{i,j} |\phi_i^A\rangle \otimes \hat{S}^B |\phi_j^B\rangle$$

Therefore, if the operator acts on both subsystems simultaneously, it is a tensor product of operators from corresponding subspaces. As a matter of fact, every operator defined on the composite subspace can be decomposed as a sum of operators from the component subspaces:

$$\hat{S}^{AB} = \sum_\alpha \hat{S}_\alpha^A \otimes \hat{S}_\alpha^B$$

Analysis of the parameters describing only one of the subsystems may force one to reduce the overall density matrix in accordance with the formula:

$$\rho_A = \mathrm{Tr}_B(\rho_{AB}) = \sum_{j=1}^{\dim(\mathcal{H}_B)} \left(\hat{I}_A \otimes \langle\phi_j^B|\right) \rho_{AB} \left(\hat{I}_A \otimes |\phi_j^B\rangle\right)$$

so the expectation value of some parameter S^A can be calculated as:

$$\langle S^A \rangle = \mathrm{Tr}_A[\hat{S}^A \cdot \mathrm{Tr}_B(\rho_{AB})]$$

2.2.2 Open quantum systems

The term **open quantum system** relates to the composite system, consisting of the smaller quantum system, described in terms of canonical operators (so-called **reduced system**), and the bigger one, described in statistical terms, called **environment**. The dynamics of the reduced system is changed due to interaction with the environment, so it can be no longer characterized by the unitary time evolution operators.

The general form of a Hamiltonian describing the open quantum system reads:

$$\hat{H}(t) = \hat{H}_S + \hat{H}_E + \hat{H}_I(t) \tag{2.5}$$

where $\hat{H}_S$ is the Hamiltonian of the reduced system, taken as if it was isolated, $\hat{H}_E$ is a free Hamiltonian of an environment, and $\hat{H}_I(t)$ is the operator of the interactions between the reduced system and the environment. In most cases, the environment acts only as a surrounding, and all of the physical quantities of interest refer to the reduced system. Therefore it is a common practice to reduce the overall density matrix to a form describing only the system of interest:

$$\rho_S = \mathrm{Tr}_E(\rho).$$

For example, the time evolution of a density matrix describing the reduced system is simply:

$$\frac{d}{dt}\rho_S(t) = -i \cdot \mathrm{Tr}_E \left[H(t), \rho(t)\right].$$

However, due to the interaction term in Hamiltonian (2.5), the attempts to analyse the behaviour of the open system using the equation above are far from trivial, some simplifying assumptions are therefore necessary.

2.3 Markovian time evolution

Markovian process belongs to a class of stochastic processes in which the memory effect of the system is very short. This allows for the assumption, that only the present state of the system has an impact on its future behaviour; its future is statistically independent from its history. Markovian processes are rather simple in mathematical analysis, given that all the hierarchy of joint probabilities can be effectively simplified - one can consider some random variable $X(t)$. Its probability distribution can be written generally as:

$$p_X(X(t) = x | X(t_n) = x_n; X(t_{n-1}) = x_{n-1}; \ldots X(t_1) = x_1; X(t_0) = x_0)$$

$$t > t_n > t_{n-1} > \ldots > t_1 > t_0$$

which expresses the probability that the mentioned variable will take value x in time t, if it was equal to x_n in time t_n, x_{n-1} in time t_{n-1}, and so on. However, if for this variable the Markovian assumption is applicable, this distribution simplifies to the form:

$$p_X(X(t) = x|X(t_n) = x_n; ... \; X(t_0) = x_0) = p_X(X(t) = x|X(t_n) = x_n).$$

In practice, the Markovian processes are some idealization of the real system behaviour. However, if the evolution of the system is characterized by the clear difference in time of relaxation of the reduced system and the environment in favor of the former, one can assume that the memory effect in the environment is negligible and approximate the process to the Markovian evolution.

Analysing the open systems that interact with the Markovian environment, we assume that for some initial time $t = 0$, the state of the reduced system and the environment can be described independently from each other:

$$\rho(t = 0) = \rho_S(0) \otimes \rho_E.$$

Markovian assumption allows also for treating the state of the environment as fixed, so the time dependency was omitted. The Liouville - von Neumann equation and mathematical formalism behind the composite quantum systems leads to the formula for reduced system state after some time t, which reads:

$$\rho_S(t) = \mathrm{Tr}_E \left[U(t,0)(\rho_S(0) \otimes \rho_E)U^\dagger(t,0) \right] \tag{2.6}$$

According to the spectral theorem, the density matrix of the environment can be decomposed into form:

$$\rho_E = \sum_j \lambda_j |\phi_j^E\rangle\langle\phi_j^E|.$$

This, and the definition of the partial trace, leads to following form of equation (2.6):

$$\rho_S(t) = \sum_i \langle\phi_i^E|U(t,0)\rho_S(0) \cdot \sum_j \lambda_j |\phi_j^E\rangle\langle\phi_j^E|U^\dagger(t,0)|\phi_i\rangle$$

$$\rho_S(t) = \sum_i \sum_j \left[\sqrt{\lambda_j}\langle\phi_i^E|U(t,0)|\phi_j^E\rangle\rho_S(0)\sqrt{\lambda_j}\langle\phi_j^E|U^\dagger(t,0)|\phi_i\rangle \right].$$

One can then introduce the operators W_{ij}:

$$W_{ij}(t) = \sqrt{\lambda_j}\langle\phi_i^E|U(t,0)|\phi_j^E\rangle$$

which reduces the above equation to the following form:

$$\rho_S(t) = \sum_i \sum_j W_{ij}(t)\rho_S(0)W_{ij}^\dagger(t).$$

The action of the operators $W_{ij}(t)$ transforms the initial state of the reduced system into its form after the fixed time; so in the notation above the operators can be replaced by the **dynamical map** $V(t)$ - the operator that acts in the Hilbert space according to the formula t:

$$V(t) : \mathcal{H}_S \mapsto \mathcal{H}_S$$

$$\rho_S(t) = \sum_i \sum_j W_{ij}(t)\rho_S(0)W_{ij}^\dagger(t) = V(t)\rho(0)$$

Dynamical map $V(t)$ is convex linear, positive (maps one density matrix into another, both positive by definition), and trace-preserving operator, since:

$$\sum_{i,j} W_{ij}(t)W_{ij}^\dagger(t) = \hat{I}_E$$

$$\mathrm{Tr}_S V(t)\rho(0) = \mathrm{Tr}_S \rho_S(0) = 1$$

and has, rather obvious, semigroup property:

$$V(t_1)V(t_2) = V(t_1 + t_2)$$

- the left-hand side of the formula above corresponds to the sequence of operators transforming the initial state firstly to state after t_2 and then to state after t_1, right-hand side corresponds to the operator which transforms the initial state into its form after time $t_1 + t_2$ at once [65–67].

Completely positive, trace preserving operators (CPT)

The equation for the time evolution of the density matrix which properly describe its evolution in time, has to be associated with observable (previously mentioned dynamical map $V(t)$), that transforms the density matrix into the density matrix. In other words, the result of $V(t)$ action on the initial density matrix has to be positive and with a trace equal to one. This implies, that $V(t)$ has to be:

1. **trace - preserving.** Operator V is trace-preserving if $\mathrm{Tr}(V\rho) = \mathrm{Tr}(\rho)$ for every $\rho \in \rho(\mathcal{H})$, where $\rho(\mathcal{H})$ is a set of all density matrices defined in the Hilbert space $\mathcal{H}$.

2. **completely positive.** Operator V is positive if all its eigenvalues are positive. The operator V is k positive if the operator $V \otimes \hat{I}_k$ is positive, where $\hat{I}_k$ is the identity operator of dimensionality $k \times k$. The operator V is completely positive if the operator $V \otimes \hat{I}_k$ is positive for every k.

Operators fulfilling the conditions listed above are called CPT (completely positive and trace-preserving) maps.

2.3.1 Born - Markov equation

If the open system is described by Hamiltonian (2.5), its overall time evolution will result from Liouville - von Neumann equation:

$$\frac{d}{dt}\rho(t) = -i\left[\hat{H}(t), \rho(t)\right]. \tag{2.7}$$

However our main interest is an evolution of the reduced system labeled with S, so the density matrix will be then traced over the environmental degrees of freedom:

$$\rho_S = \mathrm{Tr}_E \rho(t).$$

Having made these preliminary observations, one can assume (without loss of generality) that the term describing the interactions between the reduced system and its environment in (2.5) can be written as:

$$\hat{H}_I(t) = \alpha \cdot \hat{h}_I(t),$$

where α works only as a scaling factor of energy - it carries the information of the magnitude of the interacting part. The Liouville - von Neumann equation can be therefore expanded as:

$$\frac{d}{dt}\rho(t) = -i\left[\hat{H}_S + \hat{H}_E + \alpha\hat{h}_I(t), \rho(t)\right], \tag{2.8}$$

and, given that only the interacting part is time-dependent, such an equation is more convenient to analyse in **the interaction picture**. In quantum mechanics, there are three leading formulations: **Schrödinger picture**, which assumes that the time evolution concerns solely the state vector (and, in the bigger picture, also the density matrices), while the operators are constant in time (with the exception being the time-dependent potential in the Hamiltonian, as it is in the case of open systems - $\hat{h}_I(t)$ plays its role); **the Heisenberg picture** is based on state vectors that are constant in time, and the evolution results from time-dependent operators; and **interaction picture** mentioned before, where both operators and state vectors carry out

the time evolution. Given that neither the vectors nor the operators are available for direct observation (only the values of individual observables can be extracted from the system), these three formalisms are not contradictory, they need only a specific theoretical approach. Up to this point, all the equations were written in Schrödinger picture, to convert the Hamiltonian and the density matrix to the interaction picture (indicated by a tilde over the entry) one has to perform the following operations:

$$\tilde{h}_I(t) = e^{i(H_S+H_E)t} \cdot \hat{h}_I(t) \cdot e^{-i(H_S+H_E)t}, \tag{2.9}$$

$$\tilde{\rho}(t) = e^{i(H_S+H_E)t} \cdot \rho(t) \cdot e^{-i(H_S+H_E)t}. \tag{2.10}$$

These transformations appear in the Liouville - von Neumann equation as:

$$\frac{d}{dt}\tilde{\rho}(t) = -i\alpha \left[\tilde{h}_I(t), \tilde{\rho}(t)\right], \tag{2.11}$$

so it can be solved "forcefully":

$$\tilde{\rho}(t) = \tilde{\rho}(0) - i\alpha \int_0^t \left[\tilde{h}_I(s), \tilde{\rho}(s)\right] ds. \tag{2.12}$$

To use some simplifications related to this equation, the solution should be implanted back into (2.11), to get:

$$\frac{d}{dt}\tilde{\rho}(t) = -i\alpha \left[\tilde{h}_I(t), \tilde{\rho}(0)\right] - \alpha^2 \int_0^t \left[\tilde{h}_I(t), [\tilde{h}_I(s), \tilde{\rho}(s)]\right] ds. \tag{2.13}$$

The robust method from above can be applied once again, resulting in:

$$\tilde{\rho}(t) = \tilde{\rho}(0) - i\alpha \int_0^t \left[\tilde{h}_I(s), \tilde{\rho}(0)\right] ds - \alpha^2 \int_0^t \int_0^{t'} \left[\tilde{h}_I(t')[\tilde{h}_I(s), \tilde{\rho}(s)]\right] dt' ds, \tag{2.14}$$

$$\begin{aligned} \frac{d}{dt}\tilde{\rho}(t) &= -i\alpha[\tilde{h}_I(t), \tilde{\rho}(0)] - \alpha^2 \int_0^t \left[\tilde{h}_I(t)[\tilde{h}_I(s), \tilde{\rho}(s)]\right] ds \\ &\quad + i\alpha^3 \int_0^t \int_0^{t'} \int_0^{t''} \left[\tilde{h}_I(t')[\tilde{h}_I(t''), [\tilde{h}_I(s), \tilde{\rho}(s)]]\right] dt'' dt' ds. \end{aligned} \tag{2.15}$$

Of course, these actions can be iterated indefinitely, so it's worth applying at this point a simplification - **Born assumption**: for weak coupling between the system and the environment, the terms with higher powers of α are negligible. What is more, it is common to assume the initial state as a separable combination of reduced system and environment states, $\tilde{\rho}(0) = \rho_S \otimes \rho_E$; therefore the first term (commutator) vanishes. Applying this observation to the equation above results in the **Born - Markov equation**:

$$\frac{d}{dt}\tilde{\rho}(t) = -\alpha^2 \int_0^t \left[\tilde{h}_I(t)[\tilde{h}_I(s), \tilde{\rho}(s)]\right] ds. \tag{2.16}$$

To complete the search for the time evolution of reduced system state, one needs to return to Schrödinger picture and trace out the environment - the result is:

$$\frac{d}{dt}\rho_S(t) = -\mathrm{Tr}_E \int_0^t \left[\hat{H}(t), [\hat{H}(s), \rho(s)]\right] ds. \tag{2.17}$$

2.3.2 Lindblad master equation

The derivation of the Lindblad equation is based on the assumption, that one can write the interaction part of Hamiltonian (2.5) as a sum of operators in a form:

$$\hat{H}_I = \hat{S} \otimes \hat{B}^\dagger + \hat{S}^\dagger \otimes \hat{B} \tag{2.18}$$

where $\hat{S}$ acts in the Hilbert space of the reduced system and $\hat{B}$ in the space of the environment. Let the $\hat{S}$ commute with the reduced system Hamiltonian - this implies that its interaction picture representation will be identical to its Schrödinger picture form:

$$\left[\hat{H}_S, \hat{S}\right] = 0, \qquad \tilde{S}(t) = \hat{S}.$$

The Hamiltonian of the environment can be written in its statistical form as:

$$\hat{H}_E = \sum_k \omega_k \hat{a}_k^\dagger \hat{a}_k \tag{2.19}$$

where $\hat{a}_k^\dagger$ and $\hat{a}_k$ are respectively: creation and annihilation operators of boson with energy equal to ω_k. This approach allows for defining the $\hat{B}$ as:

$$\hat{B} = \sum_k g_k^* \hat{a}_k. \tag{2.20}$$

In the equation above g_k is a complex constant factor acting as a coupling coefficient. In the interaction picture, the formula for the $\hat{B}$ operator reads:

$$\tilde{B}(t) = e^{-iH_B t}\hat{B}e^{iH_B t} = \sum_k g_k^* \hat{a}_k e^{-i\omega_k t}. \tag{2.21}$$

Applying this form of $B(t)$ to (2.18) makes it similar to Jaynes - Cummings model of interaction between the optical cavity and two-level atom [68] (the direct product sign has been omitted for brevity):

$$\tilde{h}_I(t) = \tilde{S}\sum_k g_k \hat{a}_k^\dagger e^{i\omega_k t} + \tilde{S}^\dagger \sum_k g_k^* \hat{a}_k e^{-i\omega_k t}. \tag{2.22}$$

However, the aim here is to express the integrand from (2.16) in terms of $\tilde{S}$ and $\tilde{B}(t)$:

$$\begin{aligned}
\Big[\tilde{h}_I(t), [\tilde{h}_I(s), \tilde{\rho}(t)]\Big] &= \Big[\tilde{S}^\dagger\tilde{B}(t) + \tilde{S}\tilde{B}^\dagger(t), [\tilde{S}^\dagger\tilde{B}(s) + \tilde{S}\tilde{B}^\dagger(s), \tilde{\rho}(t)]\Big] \\
&= \tilde{S}^\dagger\tilde{B}(t)\tilde{S}^\dagger\tilde{B}(s)\tilde{\rho}(t) + \tilde{S}^\dagger\tilde{B}(t)\tilde{B}^\dagger(s)\tilde{S}\tilde{\rho}(t) \\
&- \tilde{S}^\dagger\tilde{B}(t)\tilde{\rho}(t)\tilde{S}^\dagger\tilde{B}(s) - \tilde{S}^\dagger\tilde{B}(t)\tilde{\rho}(t)\tilde{B}^\dagger(s)\tilde{S} \\
&- \tilde{S}^\dagger\tilde{B}(s)\tilde{\rho}(t)\tilde{S}^\dagger\tilde{B}(t) - \tilde{B}^\dagger(s)\tilde{S}\tilde{\rho}(t)\tilde{S}^\dagger\tilde{B}(t) \\
&+ \tilde{\rho}(t)\tilde{S}^\dagger\tilde{B}(s)\tilde{S}^\dagger\tilde{B}(t) + \tilde{\rho}(t)\tilde{B}^\dagger(s)\tilde{S}\tilde{S}^\dagger\tilde{B}(t) \\
&+ \tilde{S}\tilde{B}^\dagger(t)\tilde{S}^\dagger\tilde{B}(s)\tilde{\rho}(t) + \tilde{S}\tilde{B}^\dagger(t)\tilde{B}^\dagger(s)\tilde{S}\tilde{\rho}(t) \\
&- \tilde{S}\tilde{B}^\dagger(t)\tilde{\rho}(t)\tilde{S}^\dagger\tilde{B}(s) - \tilde{S}\tilde{B}^\dagger(t)\tilde{\rho}(t)\tilde{B}^\dagger(s)\tilde{S} \\
&- \tilde{S}^\dagger\tilde{B}(s)\tilde{\rho}(t)\tilde{S}\tilde{B}^\dagger(t) - \tilde{B}^\dagger(s)\tilde{S}\tilde{\rho}(t)\tilde{S}\tilde{B}^\dagger(t) \\
&+ \tilde{\rho}(t)\tilde{S}^\dagger\tilde{B}(s)\tilde{S}\tilde{B}^\dagger(t) + \tilde{\rho}(t)\tilde{B}^\dagger(s)\tilde{S}\tilde{S}\tilde{B}^\dagger(t)
\end{aligned} \tag{2.23}$$

The next step is to trace out the environment from the equation. To do this, one can refer to the following simplification: let the state of the environment not be affected by the presence of the reduced system - from the point of view of Markov's assumption it can be said that all the excitations outside the system relax so quickly, that it can be neglected in comparison with the timescale of reduced system evolution. Such environment is therefore effectively in a thermal state:

$$\rho_E = \frac{e^{-\beta\hat{H}_E}}{\mathrm{Tr}[e^{-\beta\hat{H}_E}]} \qquad \beta = \frac{1}{k_B T} \tag{2.24}$$

and the whole open system is described by the separable (with respect to environment and reduced system) state:

$$\tilde{\rho}(t) = \rho_S(t) \otimes \rho_E. \tag{2.25}$$

Moreover, it is easy to verify with (2.21) that the following relation holds:

$$\mathrm{Tr}_E\left[\tilde{B}(t)\tilde{B}(s)\rho_E\right] = \mathrm{Tr}_E\left[\tilde{B}^\dagger(t)\tilde{B}^\dagger(s)\rho_E\right] = 0 \quad \text{for } t \neq s. \tag{2.26}$$

This fact, and the cyclic property of the trace ($\mathrm{Tr}[ABC] = \mathrm{Tr}[BCA] = \mathrm{Tr}[CAB]$) allows to simplify the equation (2.23) term by term:

$$\begin{aligned}
\mathrm{Tr}_E\left[\tilde{h}_I(t),[\tilde{h}_I(s),\tilde{\rho}(t)]\right] &= \\
&= \hat{S}^\dagger\hat{S}^\dagger\rho_S(t)\cdot\mathrm{Tr}_E\left[\tilde{B}(t)\tilde{B}(s)\rho_E\right] \quad (\to 0)\\
&+ \hat{S}^\dagger\hat{S}\rho_S(t)\cdot\mathrm{Tr}_E\left[\tilde{B}(t)\tilde{B}^\dagger(s)\rho_E\right]\\
&- \hat{S}^\dagger\rho_S(t)\hat{S}^\dagger\cdot\mathrm{Tr}_E\left[\tilde{B}(s)\tilde{B}(t)\rho_E\right] \quad (\to 0)\\
&- \hat{S}^\dagger\rho_S(t)\hat{S}\cdot\mathrm{Tr}_E\left[\tilde{B}^\dagger(s)\tilde{B}(t)\rho_E\right]\\
&- \hat{S}^\dagger\rho_S(t)\hat{S}^\dagger\cdot\mathrm{Tr}_E\left[\tilde{B}(t)\tilde{B}(s)\rho_E\right] \quad (\to 0)\\
&- \hat{S}\rho_S(t)\hat{S}^\dagger\cdot\mathrm{Tr}_E\left[\tilde{B}(t)\tilde{B}^\dagger(s)\rho_E\right]\\
&+ \rho_S(t)\hat{S}^\dagger\hat{S}^\dagger\cdot\mathrm{Tr}_E\left[\tilde{B}(s)\tilde{B}(t)\rho_E\right] \quad (\to 0)\\
&+ \rho_S(t)\hat{S}\hat{S}^\dagger\cdot\mathrm{Tr}_E\left[\tilde{B}(t)\tilde{B}^\dagger(s)\rho_E\right] \qquad (2.27)\\
&+ \hat{S}\hat{S}^\dagger\rho_S(t)\cdot\mathrm{Tr}_E\left[\tilde{B}^\dagger(t)\tilde{B}(s)\rho_E\right]\\
&+ \hat{S}\hat{S}\rho_S(t)\cdot\mathrm{Tr}_E\left[\tilde{B}^\dagger(t)\tilde{B}^\dagger(s)\rho_E\right] \quad (\to 0)\\
&- \hat{S}\rho_S(t)\hat{S}^\dagger\cdot\mathrm{Tr}_E\left[\tilde{B}^\dagger(t)\tilde{B}(s)\rho_E\right]\\
&- \hat{S}\rho_S(t)\hat{S}\cdot\mathrm{Tr}_E\left[\tilde{B}^\dagger(s)\tilde{B}^\dagger(t)\rho_E\right] \quad (\to 0)\\
&- \hat{S}^\dagger\rho_S(t)\hat{S}\cdot\mathrm{Tr}_E\left[\tilde{B}^\dagger(t)\tilde{B}(s)\rho_E\right]\\
&- \hat{S}\rho_S(t)\hat{S}\cdot\mathrm{Tr}_E\left[\tilde{B}^\dagger(t)\tilde{B}^\dagger(s)\rho_E\right] \quad (\to 0)\\
&+ \rho_S(t)\hat{S}^\dagger\hat{S}\cdot\mathrm{Tr}_E\left[\tilde{B}(s)\tilde{B}^\dagger(t)\rho_E\right]\\
&+ \rho_S(t)\hat{S}\hat{S}\cdot\mathrm{Tr}_E\left[\tilde{B}^\dagger(s)\tilde{B}^\dagger(t)\rho_E\right] \quad (\to 0).
\end{aligned}$$

At this point, it is preferable to adopt the following notations:

$$f(t,s) = \mathrm{Tr}_E\left[\tilde{B}(t)\tilde{B}^\dagger(s)\rho_E\right]$$

$$g(t,s) = \mathrm{Tr}_E \left[\tilde{B}^\dagger(t) \tilde{B}(s) \rho_E \right]$$

and rearrange the equation (2.27) into:

$$\begin{aligned} \mathrm{Tr}_E \left[\tilde{h}_I(t), [\tilde{h}_I(s), \tilde{\rho}(t)] \right] &= (\hat{S}^\dagger \hat{S} \rho_S(t) - \hat{S} \rho_S(t) \hat{S}^\dagger) \cdot f(t,s) \\ &+ (\hat{S}^\dagger \hat{S} \rho_S(t) - \hat{S}^\dagger \rho_S(t) \hat{S}) \cdot g(t,s) \\ &+ (\rho_S(t) \hat{S}^\dagger \hat{S} - \hat{S} \rho_S(t) \hat{S}^\dagger) \cdot f^*(t,s) \\ &+ (\rho_S(t) \hat{S}^\dagger \hat{S} - \hat{S}^\dagger \rho_S(t) \hat{S}) \cdot g^*(t,s). \end{aligned} \tag{2.28}$$

Lindblad equation arises after applying this derivation into formula (2.16) and assuming that:

$$\int_0^t g(t,s) ds = \int_0^t g^*(t,s) ds = 0$$

$$-\int_0^t f(t,s) ds = -\int_0^t f^*(t,s) ds \equiv \gamma$$

which results in:

$$\frac{d}{dt} \rho_S(t) = \gamma \left(2 \hat{S} \rho_S(t) \hat{S}^\dagger - \hat{S}^\dagger \hat{S} \rho_S(t) - \rho_S(t) \hat{S}^\dagger \hat{S} \right). \tag{2.29}$$

The usual form of the Lindblad equation however takes into account two more factors: firstly, it disregards the assumption that the commutator in (2.13) vanishes; secondly, it allows more than one channel of interaction between the environment and system - the interaction term is therefore:

$$\hat{H}_I = \sum_q \hat{S}_q \otimes \hat{B}^\dagger + \hat{S}_q^\dagger \hat{B} \tag{2.30}$$

so finally, the full form of the Lindblad equation reads:

$$\frac{d}{dt} \rho_S(t) = -i \left[\hat{H}_S(t), \rho_S(t) \right] + \sum_q \gamma_q \left(2 \hat{S}_q \rho_S(t) \hat{S}_q^\dagger - \hat{S}_q^\dagger \hat{S}_q \rho_S(t) - \rho_S(t) \hat{S}_q^\dagger \hat{S}_q \right). \tag{2.31}$$

where q is the index that runs through all the operators describing the influence of the environment on reduced system. The role of γ_q is a decoherence rate for each of these operators [66, 69–72].

2.4 Non-Markovian time evolution

In general, the Markov assumption cannot be applied to every quantum system - if the relaxation rates of the system itself and its environment are of similar magnitude, there is a backflow of information from the environment to the reduced system, which has to be taken into account. The proper way to analyse such open systems is to consider them in a non-Markovian regime - tracing not only the system of consideration's past but the environment as well. The master equation of a system coupled to the environment, without distinction between the Markovian and non-Markovian system-environment dynamics, can be written in the form:

$$\frac{d}{dt}\rho(t) = -i\left[H(t), \rho(t)\right] + \int_0^t K_{t,u}(\rho(u))du \tag{2.32}$$

where $H(t)$ - open system Hamiltonian in interaction picture, and $K_{t,u}$ - memory kernel of the system, linear map describing the history of environment impact on the system. In the Born - Markov approximation, this kernel is assumed in the form $K_{t,u}(\rho(u)) = K \cdot \delta(t-u)\rho(u)$, which, with the additional assumption that the interaction between the system and environment is weak and the memory effect does not occur, allows to write the master equation in Lindblad form (2.31).

However, referring to the fact that the time evolution of a system must be described by some *completely positive map* ϕ_t, such that:

$$\rho(t) = \phi_t(\rho(0)) = \sum_k \hat{A}_k(t)\rho(0)\hat{A}_k^\dagger(t). \tag{2.33}$$

Then, one may obtain the time-local version of the Lindblad equation, suitable also for systems with non-Markovian dynamics. In the equation above, $\hat{A}_k(t)$ is some time-dependent Kraus operator, whose characteristic feature is to satisfy the condition of preserving the trace of the density matrix. In other words, $\sum_k \hat{A}_k(t)\hat{A}_k^\dagger(t) = \hat{I}$. Omitting the obviously local-in-time part of the master equation, $-i\left[H(t), \rho(t)\right]$, and transforming the remaining part in the following way:

$$\begin{aligned}
\frac{d}{dt}\rho(t) &= \int_0^t K_{t,u}(\rho(u))du \\
&= \int_0^t K_{t,u}\phi_u(\rho(0))du \\
&= \int_0^t K_{t,u}\phi_u\phi_t^{-1}(\rho(t))du
\end{aligned} \tag{2.34}$$

one can notice that under the condition that operator ϕ_t^{-1} exists - which denotes that the time evolution is invertible - the master equation can be written in local form, which by no means excludes the systems with non-Markovian dynamics. Such a master equation translates to the expanded form of the Lindblad equation:

$$\begin{aligned} \frac{d}{dt}\rho(t) &= -i\left[\hat{H}(t),\rho(t)\right] \\ &\quad -\sum_k \frac{\gamma_k(t)}{2}\left(\hat{S}_k^\dagger(t)\hat{S}_k(t)\rho(t)+\rho(t)\hat{S}_k^\dagger(t)\hat{S}_k(t)-2\hat{S}_k(t)\rho(t)\hat{S}_k^\dagger(t)\right). \end{aligned} \tag{2.35}$$

The time dependency in decoherence rates $\gamma_k(t)$ and environment interaction parameters $\hat{S}_k(t)$ stores information about the past of the system [73].

2.4.1 Two-level system

A similar result can be achieved by analyzing the simplest non-Markovian system: a two-level atom (described by Hamiltonian $\hat{H}_S$) coupled to the bosonic reservoir ($\hat{H}_B$). The total Hamiltonian of the problem reads:

$$\begin{aligned} \hat{H} &= \hat{H}_S + \hat{H}_B + \hat{V} \\ \hat{H}_S &= \omega_0 \hat{\sigma}^+\hat{\sigma}^- \\ \hat{H}_B &= \sum_k \omega_k \hat{b}_k^\dagger \hat{b}_k \\ \hat{V} &= \sum_k g_k\left(\hat{\sigma}^+\hat{b}_k + \hat{\sigma}^-\hat{b}_k^\dagger\right) \end{aligned} \tag{2.36}$$

In the equations above, the $\hat{\sigma}^+$, $\hat{\sigma}^-$ denote respectively raising and lowering operators in the system of interest's Hilbert space, and $\hat{b}_k^\dagger$, $\hat{b}_k$ are creation and annihilation operators of a boson with energy ω_k.

Determination of a time evolution can be done in a framework defined by [74]. Let us assume the following state notation:

$$\begin{aligned} \psi_0 &= |0\rangle_S \otimes |0\rangle_B \\ \psi_1 &= |1\rangle_S \otimes |0\rangle_B \\ \psi^k &= |0\rangle_S \otimes |1_k\rangle_B \end{aligned}$$

and initial state in a form:

$$\Phi(0) = c_0\psi_0 + c_1(0)\psi_1 + \sum_k c_k(0)\psi^k.$$

This state will evolve into state $\Phi(t)$:

$$\Phi(t) = c_0\psi_0 + c_1(t)\psi_1 + \sum_k c_k(t)\psi^k,$$

and the equation describing this evolution in the interaction picture can be written as:

$$\frac{d}{dt}\Phi(t) = -i\hat{V}(t)\Phi(t). \tag{2.37}$$

The time-dependent form of the interaction Hamiltonian can be derived by transforming all the component operators into their interaction picture forms, namely:

$$\hat{V}(t) = \sum_k g_k \left(\hat{\sigma}^+(t)\hat{b}_k(t) + \hat{\sigma}^-(t)\hat{b}_k^\dagger(t)\right) \tag{2.38}$$

$$\hat{\sigma}^\pm(t) = \sigma^\pm e^{\pm i\omega_0 t}$$

$$\hat{b}_k(t) = \hat{b}_k e^{-i\omega_k t}$$

$$\hat{b}_k^\dagger(t) = \hat{b}_k^\dagger e^{i\omega_k t}.$$

In this place, it is important to explain, why the amplitude c_0 remains constant in time. The particle number operator is defined as:

$$\hat{N} = \hat{\sigma}^+\hat{\sigma}^- + \sum_k \hat{b}_k^\dagger\hat{b}_k \tag{2.39}$$

and it commutes with Hamiltonian - in other words, remains constant in time. In the state associated with amplitude c_0, $|0\rangle_S \otimes |0\rangle_B$ there are no particles - it is so so-called *vacuum state* - therefore no particle exchange can occur, for there is no place for these particles to come from.

The equation (2.37) can be expanded into a set of interconnected differential equations for particular amplitudes:

$$\frac{d}{dt}c_1(t) = -i\sum_k g_k e^{i(\omega_0-\omega_k)t}c_k(t) \tag{2.40}$$

$$\frac{d}{dt}c_k(t) = -ig_k e^{-i(\omega_0-\omega_k)t}c_1(t). \tag{2.41}$$

The procedure of solving such a set of equations requires a "forceful" solution of the second equation [75]:

$$c_k(t) = -ig_k\int_0^t c_1(\tau)e^{-i(\omega_0-\omega_k)\tau}d\tau \tag{2.42}$$

and inserting this form into the first equation results in:

$$\frac{d}{dt}c_1(t) = -i\sum_k g_k^2 e^{i(\omega_0-\omega_k)t}\int_0^t c_1(\tau)e^{-i(\omega_0-\omega_k)\tau}d\tau. \tag{2.43}$$

This outcome can be differently expressed with reservoir correlation function $f(t_2 - t_1)$:

$$\frac{d}{dt}c_1(t) = -\int_0^t f(t-\tau)c_1(\tau)d\tau, \tag{2.44}$$

which can be given as:

$$f(t_2 - t_1) = \mathrm{Tr}_b\left[\sum_k g_k^2 \hat{b}_k(t_2)\hat{b}_k^\dagger(t_1)|0_B\rangle\langle 0_B|\right]e^{i\omega_0(t_2-t_1)} \tag{2.45}$$

or, by using $J(\omega)$, **the spectral density of reservoir**:

$$f(t_2 - t_1) = \int J(\omega)e^{i(\omega_0-\omega)(t_2-t_1)}d\omega. \tag{2.46}$$

The open system analysis aims to determine the time-dependent form of the density matrix describing only the reduced system. This matrix, in its implicit form, reads:

$$\rho_S(t) = \begin{bmatrix} 1-|c_1(t)|^2 & c_0c_1^*(t) \\ c_0^*c_1(t) & |c_1(t)|^2 \end{bmatrix}, \tag{2.47}$$

which can be differentiated over time, to describe its evolution. As the amplitude c_0 is constant in time, its derivative equals zero, $\frac{d}{dt}c_0 = 0$. With this fact taken into account, one can formulate this matrix derivative as:

$$\frac{d}{dt}\rho_S(t) = \begin{bmatrix} -\frac{d}{dt}|c_1(t)|^2 & c_0 \cdot \frac{d}{dt}c_1^*(t) \\ c_0^* \cdot \frac{d}{dt}c_1(t) & \frac{d}{dt}|c_1(t)|^2 \end{bmatrix}. \tag{2.48}$$

Then, by introducing the following parameters:

$$S(t) \equiv -2 \cdot \mathrm{Im}\left(\frac{\frac{d}{dt}c_1(t)}{c_1(t)}\right)$$

$$\gamma(t) \equiv -2 \cdot \mathrm{Re}\left(\frac{\frac{d}{dt}c_1(t)}{c_1(t)}\right)$$

and applying some calculations, one can represent the equation (2.48) in a form similar to the Lindblad equation:

$$\begin{aligned}\frac{d}{dt}\rho_S(t) &= -i\frac{S(t)}{2}[\hat{\sigma}^+\hat{\sigma}^-, \rho_S(t)] + \\ &+\gamma(t)\left(\hat{\sigma}^-\rho_S(t)\hat{\sigma}^+ - \frac{1}{2}(\hat{\sigma}^+\hat{\sigma}^-\rho_S(t) + \rho_S(t)\hat{\sigma}^+\hat{\sigma}^-)\right)\end{aligned} \tag{2.49}$$

where $S(t)$ plays the role of time-dependent Lamb shift parameter, and $\gamma(t)$ describes the decoherence rate.

2.4.2 Composite system in the non-Markovian environment

Let us analyse the composite quantum system in the non-Markovian environment in the context of spin chains, composed of spins $s = \frac{1}{2}$. A chain containing N spins can be described in a 2^N-dimensional Hilbert space, spanned by the basis:

$$\{|1\rangle, |2\rangle, |3\rangle ..., |2^N - 1\rangle, |2^N\rangle\}$$

where:

$$|1\rangle \equiv |\uparrow\uparrow ... \uparrow\uparrow\rangle \equiv |s_1^Z = \frac{1}{2}, s_2^Z = \frac{1}{2}, ..., s_{N-1}^Z = \frac{1}{2}, s_N^Z = \frac{1}{2}\rangle$$

$$|2\rangle = |\uparrow\uparrow ... \uparrow\downarrow\rangle \equiv |s_1^Z = \frac{1}{2}, s_2^Z = \frac{1}{2}, ..., s_{N-1}^Z = \frac{1}{2}, s_N^Z = -\frac{1}{2}\rangle$$

$$\vdots$$

$$|2^N\rangle \equiv |\downarrow\downarrow ... \downarrow\downarrow\rangle \equiv |s_1^Z = -\frac{1}{2}, s_2^Z = -\frac{1}{2}, ..., s_{N-1}^Z = -\frac{1}{2}, s_N^Z = -\frac{1}{2}\rangle.$$

The Hamiltonians of the spin system and its environment can be written as:

$$\hat{H}_S = \sum_{i,j}^{2^N} E_{i,j}|i\rangle\langle j| \tag{2.50}$$

$$\hat{H}_B = \sum_k \omega_k \hat{b}_k^\dagger \hat{b}_k \tag{2.51}$$

and interaction as:

$$\hat{V} = \sum_n^N \left(\sigma_n^+ \hat{B} + \sigma_n^- \hat{B}^\dagger\right) \tag{2.52}$$

where $\hat{B} = \sum_k g_k \hat{b}_k$. Therefore, the total Hamiltonian of the open system reads:

$$\hat{H} = \hat{H}_S + \hat{H}_B + \hat{V}.$$

Since the transformation to the interaction picture is cumbersome and requires complicated calculations, it is customary to apply some simplifications while considering this kind of problem. One of the possible approaches is to utilize the **low excitation approximation** [76,77]. This method is settled on the reduction of Hilbert space of the spin system to the subspace spanned by ground state, $|g\rangle$ (usually state $|1\rangle$ from the list above) and set of all states with one excitation, $\{|n\rangle\}$, where:

$$|n\rangle = \frac{1}{\sqrt{N}} \sum_{l=1}^{N} e^{-inl} |1_l\rangle$$

$$|1_l\rangle = |\uparrow_1 \uparrow_2 ... \downarrow_l ... \uparrow_N\rangle.$$

This reduces the Hamiltonian of the system and the interaction between the system and environment to the form:

$$\hat{H}_{S0} = E_0 |g\rangle\langle g| + E_n |n\rangle\langle n|$$

$$\hat{V}_0 = \sum_n^N \left(|g\rangle\langle n|\hat{B} + |n\rangle\langle g|\hat{B}^\dagger \right).$$

The general state of the system reads:

$$|\Phi(t)\rangle = \left(c_0|g\rangle + \sum_{n=1}^{N} c_n(t)|n\rangle \right) |0_k\rangle + \sum_k f_k(t)|g\rangle|1_k\rangle$$

where the state $|0_k\rangle$ represents empty reservoir, and the state $|1_k\rangle$ collects different modes ω_k of the reservoir. The time evolution of such system is again described by the system of interconnected equations:

$$\begin{cases} \frac{d}{dt}c_n(t) = -i\left(\omega_n c_n(t) + \sum\limits_k g_k f_k(t)\right) \\ \frac{d}{dt}f_k(t) = -i\left(\omega_k f_k(t) + \sum\limits_{m=1}^{N} g_k c_m(t)\right) \end{cases}.$$

By assuming that energy of ground state $E_g = 0$ and switching to the interaction picture, one may rewrite these equations as:

$$\begin{cases} \frac{d}{dt}c_n(t) = -i\sum\limits_k g_k e^{i(\omega_n - \omega_k)t} f_k(t) \\ \frac{d}{dt}f_k(t) = -i\sum\limits_{m=1}^{N} g_k e^{-i(\omega_m - \omega_k)t} c_m(t) \end{cases}.$$

From now on, the solution, supported with the normalization condition:

$$\frac{d}{dt}\left(\sum_{n=1}^{N}|c_n(t)|^2+\sum_k|f_k(t)|^2\right)=0$$
$$\sum_{n=1}^{N}|c_n(t)|^2+\sum_k|f_k(t)|^2=1-c_0^2$$

follows the same path as in the case of a two-level system - firstly, the formal solution for the second equation is postulated to be:

$$f_k(t)=-i\sum_{m=1}^{N}\int_0^t g_k c_m(\tau)e^{-i(\omega_m-\omega_k)\tau}d\tau$$

and being inserted into the first equation it gives:

$$\frac{d}{dt}c_n(t)=-\sum_{m=1}^{N}\int_0^t c_m(\tau)\sum_k g_k^2 e^{-i(\omega_m-\omega_k)(t-\tau)}d\tau.$$

This formula can be then supplemented with the spectral density of the reservoir, as in (2.46):

$$\frac{d}{dt}c_n(t)=-\sum_{m\neq n}^{N}\int_0^t c_m(\tau)f(t-\tau)d\tau.$$

Further considerations are highly dependent on the frequency distribution of modes in the reservoir and may require a numerical approach. However, the final step is to determine the time-dependent form of the reduced density matrix.

2.5 Decoherence

Quantum coherence is a property of quantum systems that allows them to be in the superposition state. It is a source of correlations that are impossible to create in classical physics. Quantum coherence is crucial in the formation of entangled states, therefore in technological quantum applications, no distinction is made between coherence and entanglement in terms of quantum resources. However, the interaction between the system and the environment leads to an inevitable loss of coherence - some correlation between the system's and environmental degrees of freedom arises, and it comes at the cost

of correlation loss within the system itself. One way of visualizing it is to look at the environment as the measuring factor: during the study of the open system at one point, the environment's degrees of freedom are traced out, and one can notice that some states exhibit a certain stability over time; yet, information of the superpositions of these states is gradually lost, to the point of no correlations in the system of interest. This phenomenon is called **decoherence**.

To express this phenomenon both qualitatively and quantitatively one may refer to **the decoherence function**. Once again, the description of the open system is done by the Hamiltonian consisting of three parts, respectively, for the system of interest, environment, and interaction between these two:

$$\hat{H} = \hat{H}_S + \hat{H}_E + \hat{V}_{SE} = \hat{H}_0 + \hat{V}_{SE}.$$

The interaction term $\hat{V}_{SE}$ is defined by some specific set of vectors $|n\rangle \in \mathcal{H}_S$ coupled to the operator acting in Hilbert space of environment:

$$\hat{V}_{SE} = \sum_n |n\rangle\langle n| \otimes \hat{B}_n \equiv \sum_n \hat{A}_n \otimes \hat{B}_n$$

with the requirement that $\hat{B}_n = \hat{B}_n^\dagger$. The operators $\hat{A}_n$ are examples of projections, and can be defined in a way that they commute with the Hamiltonian of the system of interest, and in consequence, with the total Hamiltonian of a whole open system, as they are only specified for $\mathcal{H}_S$:

$$\left[\hat{H}_S, \hat{A}_n\right] = \left[\hat{H}_0, \hat{A}_n\right] = \left[\hat{H}_0 + \hat{V}_{SE}, \hat{A}_n\right] = 0.$$

This mirrors the fact that these operators are the representations of conserved quantities, and result in mean system energy, constant in time:

$$\frac{d}{dt}\langle \hat{H}_S \rangle = 0.$$

By switching to the interaction picture, one can express the interaction Hamiltonian as:

$$\tilde{V}(t) = e^{i\hat{H}_0 t}\hat{V}_{SE}e^{-i\hat{H}_0 t} = \sum_n \hat{A}_n \otimes \tilde{B}_n(t),$$

$$\tilde{B}_n(t) = e^{i\hat{H}_0 t}\hat{B}_n e^{-i\hat{H}_0 t},$$

and time evolution unitary operator as:

$$U(t) = \exp\left(-i\int_0^t \sum_n \hat{A}_n \otimes \tilde{B}_n(s)ds\right).$$

The initial state can be assumed in the form:

$$|\psi(0)\rangle = \sum_n c_n |n\rangle \otimes |\beta_0\rangle,$$

where $|\beta_0\rangle$ is some arbitrary initial state of the environment. This state evolves according to the formula:

$$|\psi(t)\rangle = U(t)|\psi(0)\rangle = \sum_n c_n |n\rangle \otimes |\beta_n(t)\rangle, \tag{2.53}$$

where

$$|\beta_n(t)\rangle = \exp\left(-i\int_0^t \tilde{B}_n(s)ds\right)|\beta_0\rangle \equiv V_n(t)|\beta_0\rangle. \tag{2.54}$$

The state $|\psi(t)\rangle$ in (2.53) is clearly an entangled one - there are interactions present between the n-th eigenstate of a system and some specific state of the environment - $|\beta_n\rangle$. As a result, the environment captures and stores some information about the system of interest. This fact is also reflected in the form of a reduced density matrix, as shown below:

$$\rho_S(t) = \mathrm{Tr}_E|\psi(t)\rangle\langle\psi(t)| = \sum_{n,m} c_n c_m^* |n\rangle\langle m| \cdot \langle\beta_m(t)|\beta_n(t)\rangle.$$

Properties of a state vector indicate that $\langle\beta_n(t)|\beta_n(t)\rangle = 1$ for all times t and possible indices n - therefore the diagonal elements of density matrix $\rho_S(t)$, associated with the populations of particular states $|n\rangle$, remain constant in time. In general, however, this cannot be said for the off-diagonal elements of this matrix, related to correlations between individual states. Time variability of elements $\langle n|\rho_S(t)|m\rangle$ is characterized by the overlap of environmental state vectors $|\beta_n(t)$ and $|\beta_m(t)$, expressed by formula:

$$\langle\beta_n(t)|\beta_m(t)\rangle = e^{\Gamma_{n,m}(t)}.$$

The function $\Gamma_{m,n}(t), \Gamma_{m,n}(t) \geq 0$ for all $m \neq n$, describes the behaviour of the off-diagonal elements of the density matrix and is called **the decoherence function**. An alternative way to define this function is to use the expressions derived from (2.54):

$$\Gamma_{n,m}(t) = \ln|V_m^{-1}(t) \cdot V_n(t)|.$$

The explicit form of a decoherence function is strongly dependent on the coupling model of system-environment interaction, intrinsic properties of system and environment, and initial state. However, in general, it is expected

that $\Gamma_{m,n}(t)$ rapidly decreases in time. This results from the irreversible dynamics of system-environment interactions and the dissipation of quantum correlations specific to the system of interest. Therefore, for a sufficiently long time (namely for times longer than the characteristic time of the system, $\tau_D = \frac{1}{\hbar}[E_{max} - E_{min}]$), the density matrix evolves into the diagonal form:

$$\rho_S(t) \to \sum_n |c_n(t)|^2 |n\rangle\langle n|,$$

that indicates the lack of quantum correlations, and entanglement among the others [66, 78].

Chapter 3

Spin Systems in Quantum Computing

3.1 Spin chains

Just like in the classical information theory the bit is the most fundamental unit of information, the qubit is the most fundamental unit in Quantum Information Science. Qubit - which is short for "quantum bit" - is a quantum system spanned on two orthogonal states. There are numerous ways to realize the qubit - one can use a light polarization (horizontal or vertical), Rydberg atom (in ground or excited state), or the direction of a spin magnetic momentum for a particle with $s = \frac{1}{2}$ spin - so-called "spin up" ($m_S = \frac{\hbar}{2}$) and "spin down" ($m_S = -\frac{\hbar}{2}$) states. Especially the latest way is gaining popularity, as the spins can be connected into larger chains, which increases their computational utility and allows one to make use of the bonding exchange interactions in quantum informatics procedures. Spin chains have proven to be the means for successful implementation the state transfer [79–81], quantum computation [82, 83] and quantum cryptography protocols [84]. The relatively low complexity of manufacturing the spin systems devices, their compactness, and low cost also contribute to the growing interest in these structures. From the point of view of quantum computing based on open systems, a big advantage of spin systems is their long decoherence and relaxation time [48, 85, 86].

Spin chains are the one-dimensional systems of particles with non-zero spin, held together by the exchange interactions. Spin itself is a physical property of quantum objects, which provides them with intrinsic magnetic moments. Exchange interactions result equally from the Pauli exclusion principle and from the electrical repulsion of particles with the same charge.

Such interactions are relatively strong (of the order of several dozen milielectronovolts), yet short-ranged; in the macroscopic structures of ferromagnetic nature they cause the formation of areas of homogeneous magnetization (so-called magnetic domains). The energy of exchange interaction between two spins can be described by the equation:

$$\hat{H} = -J\vec{S}_1 \cdot \vec{S}_2 \tag{3.1}$$

where J is the so-called exchange integral, the energy of coupling between the spins, and its sign determines the magnetic ordering in the ground state. Pairs with negative exchange integral will prefer anti-parallel (antiferromagnetic) ordering, for the positive sign of the integral one should expect parallel (ferromagnetic) ordering in the state with the lowest energy. The operator $\vec{S}$ consists of three components, corresponding to spin projections on three mutually perpendicular axes, $\vec{S} = \left[\hat{S}^X, \hat{S}^Y, \hat{S}^Z\right]$, which can be constructed employing the Pauli matrices $\sigma^X, \sigma^Y, \sigma^Z$:

$$\hat{S}^j = \frac{\hbar}{2}\sigma^j \qquad j = X, Y, Z.$$

Pauli matrices for spin $s = \frac{1}{2}$ are:

$$\sigma^X = \begin{bmatrix} 0 & 1 \\ 1 & 0 \end{bmatrix} \quad \sigma^Y = \begin{bmatrix} 0 & -i \\ i & 0 \end{bmatrix} \quad \sigma^Z = \begin{bmatrix} 1 & 0 \\ 0 & -1 \end{bmatrix},$$

and for spin $S = 1$:

$$\sigma^X = \begin{bmatrix} 0 & 1 & 0 \\ 1 & 0 & 1 \\ 0 & 1 & 0 \end{bmatrix} \quad \sigma^Y = \begin{bmatrix} 0 & -i & 0 \\ i & 0 & -i \\ 0 & i & 0 \end{bmatrix} \quad \sigma^Z = \begin{bmatrix} 1 & 0 & 0 \\ 0 & 0 & 0 \\ 0 & 0 & -1 \end{bmatrix}.$$

The general formula for elements of the Pauli matrix for arbitrary spin S:

$$\langle m'_S|\sigma^X|m_S\rangle = \sqrt{S(S+1) - m'_S m_S} \cdot (\delta_{m'_S, m_S+1} + \delta_{m'_S+1, m_S})$$

$$\langle m'_S|\sigma^Y|m_S\rangle = -i \cdot \sqrt{S(S+1) - m'_S m_S} \cdot (\delta_{m'_S, m_S+1} - \delta_{m'_S+1, m_S})$$

$$\langle m'_S|\sigma^Z|m_S\rangle = 2 \cdot m_S \cdot \delta_{m'_S, m_S}$$

where m_S is the value of Z-projection of the spin vector, from the set $m_S \in \{-S, -S+1, ..., S-1, S\}$. Construction of the operators for many-body quantum systems is done using the direct product with unity operators of appropriate dimensionality (2×2 for spin $s = \frac{1}{2}$, 3×3 for $S = 1$, and so on),

for example, to obtain X-projection of spins in the two-spin system, one has to calculate the following operators:

$$\hat{S}_1^X = \hat{S}^X \otimes \hat{I}, \qquad \hat{S}_2^X = \hat{I} \otimes \hat{S}^X.$$

There are several models of Hamiltonians for spin chains, depending on the degree of anisotropy between the exchange interaction (in all the models below, one can also exceed the upper limit of summation to N and adapt the following boundary condition $N + i \equiv i$ to obtain the closed (circular) spin chain):

a) **Ising model:**

$$\hat{H}_I = -J \sum_{i=1}^{N-1} \hat{S}_i^Z \hat{S}_{i+1}^Z$$

Semiclassical model of exchange interaction, suitable for material with high anisotropy, where one direction of spin angular moment interacts much stronger than the remaining two, or when the strong crystal field forces spins to align with a particular direction. This model, due to its classical nature, does not allow entangled states to form without additional effects, therefore, it will not be further elaborated here.

b) **XXX Heisenberg model:**

$$\hat{H}_{XXX} = -J \sum_{i=1}^{N-1} \left(\hat{S}_i^X \hat{S}_{i+1}^X + \hat{S}_i^Y \hat{S}_{i+1}^Y + \hat{S}_i^Z \hat{S}_{i+1}^Z \right)$$

Fully isotropic model, in which all the spin components interact with equal strength.

c) **XXZ Heisenberg model:**

$$\hat{H}_{XXZ} = -J_X \sum_{i=1}^{N-1} \left(\hat{S}_i^X \hat{S}_{i+1}^X + \hat{S}_i^Y \hat{S}_{i+1}^Y \right) - J_Z \sum_{i=1}^{N-1} \hat{S}_i^Z \hat{S}_{i+1}^Z$$

Model for materials, in which one component (usually parallel to the external field) interacts differently than the other two.

d) **XYZ Heisenberg model:**

$$\hat{H}_{XYZ} = -J_X \sum_{i=1}^{N-1} \hat{S}_i^X \hat{S}_{i+1}^X - J_Y \sum_{i=1}^{N-1} \hat{S}_i^Y \hat{S}_{i+1}^Y - J_Z \sum_{i=1}^{N-1} \hat{S}_i^Z \hat{S}_{i+1}^Z$$

Model for materials with fully anisotropic exchange interactions.

Here is worth emphasizing that restricting interactions to only nearest neighbours in the spin chain is an explicit approximation - it is obvious that spin in the chain senses also the presence of the magnetic momenta of further neighbours, and this fact contributes to the total energy of chain; however, the exchange interaction decreases with increasing distance, therefore interactions with further neighbours can be neglected to some extent.

3.1.1 Spins in an external magnetic field - Zeeman effect

If the particle with non-zero spin is located in an external magnetic field, additional energy arises, coming from the interaction between spin (which makes the particle a specific magnetic dipole) and the field. The presence of these interactions manifests itself as the shift of the particle's energy levels. Such an occurrence is called **the Zeeman effect** [88]. In physics, it is accustomed that the direction of the external magnetic field is aligned with the z-direction of the coordinate system. Therefore, to reach the energy minimum for the parallel arrangement of magnetic field and spin (serving as a vector of a magnetic dipole, in analogy to the similar, classical situation) it is assumed that only the z-component of spin interacts with the field. Additional energy is then expressed by the formula:

$$\hat{H}_Z = -\sum_{i=1}^{N} \gamma \mu_B \cdot B \cdot \hat{S}_i^Z. \tag{3.2}$$

In the equation above, γ is the gyromagnetic ratio and μ_B is Bohr magneton. However, the problems considered in Quantum Computation regarding the interactions between spins and external magnetic field are treated using a special unit system in which $\gamma = \mu_B = 1$. Therefore the formula from (3.2) is reduced to:

$$\hat{H}_Z = -\sum_{i=1}^{N} B \cdot \hat{S}_i^Z. \tag{3.3}$$

Index i enumerates the spins in a chain [3].

3.1.2 Dzyaloshinskii - Moriya interaction

The Dzyaloshinskii - Moriya (DM) interaction constitutes an additional contribution to the exchange energy, resulting from the spin-orbit coupling in structures with broken inversion symmetry. It is an additional exchange interaction between the excited state of one ion and the ground state of the

second - the first ion is excited by spin-orbit interaction. The formula describing such effect can be derived as a second-order correction in the perturbative analysis of spin-orbit interaction, and expressed as [89, 90]:

$$\hat{H}_{DM} = \sum_{i=1}^{N-1} \Big(D_X(\hat{S}_i^Y \hat{S}_{i+1}^Z - \hat{S}_i^Z \hat{S}_{i+1}^Y) + D_Y(\hat{S}_i^Z \hat{S}_{i+1}^X - \hat{S}_i^X \hat{S}_{i+1}^Z) + D_Z(\hat{S}_i^X \hat{S}_{i+1}^Y - \hat{S}_i^Y \hat{S}_{i+1}^X) \Big) \tag{3.4}$$

The DM interaction exhibits itself in so-called spin canting - a non-zero net magnetic moment of an antiferromagnet in temperature close to absolute zero. This effect originates in slight tilts of magnetic momenta from the direction of the antiparallel ordering, provided by antiferromagnetic exchange interactions (which should lead to zero net magnetic moment alone) - these tilts are caused exactly by DM contribution and result in a change of ground state energy [91]. Moreover, DM interactions are suspected to be the source of skyrmions - statically stable vortex-like magnetization regions in ferromagnetics and thin magnetic films [92,93]. They are also crucial in the emergence of the magnetoelectric effect in multiferroics [94].

The Dzyaloshinskii - Moriya parameters can be arranged in the form of a vector, $\vec{D} = [D_X, D_Y, D_Z]$. Such vector is closely connected to the symmetry of a spin structure:

a) if there is an inversion center exactly in the middle between two interacting nodes of spin structure (spin chain), Dzyaloshinskii - Moriya interaction does not occur, $\vec{D} = 0$;

b) if there is a mirror plane exactly in the middle between two nodes, perpendicular to the line connecting the nodes, the vector $\vec{D}$ will be parallel to this plane;

c) if there is a mirror plane that contains both interacting nodes, the vector $\vec{D}$ will be perpendicular to this plane [95, 96].

d) if the line between two interacting nodes in a crystal lies along the [110] lattice direction, $\vec{D}$ must be aligned with the $[1\bar{1}0]$ lattice vector, which translates to its form equal to $\left[\frac{D}{\sqrt{2}}, -\frac{D}{\sqrt{2}}, 0\right]$ - such an interaction occurs in materials which crystallize in pyrochlore structure [97].

Dzyaloshinskii - Moriya effect is commonly found in chiral magnets, such as α-Fe_2O_3, $MnCO_3$, $CoCO_3$, or $CdCr_2O_4$.

3.1.3 Kaplan - Shethkman - Entin-Wohlman - Aharony interaction

In the materials, in which the Dzyaloshinskii - Moriya interaction appears, there can be observed also additional symmetrical helical interaction. Since this interaction is usually of one order of magnitude smaller than DM it was difficult to observe and often neglected in theoretical analysis. This interaction was first described in Kaplan's seminal paper [98] and then explained by Shetkhman, Entin-Wohlman, and Aharony [99]. This effect was then named Kaplan - Shetkhman - Entin-Wohlman - Aharony interaction (KSEA). It was confirmed to occur for the materials such as $Ba_2CuGe_2O_7$, [100], La_2CuO_4 [101] or Yb_4As_3 [102]. Hamiltonian of KSEA interaction can be written in the form:

$$\hat{H}_{KSEA} = \sum_{j=1}^{N-1} \vec{S}_j \cdot \hat{\Gamma} \cdot \vec{S}_{j+1} \tag{3.5}$$

where $\hat{\Gamma}$ is a symmetric KSEA tensor, given as:

$$\hat{\Gamma} = \begin{bmatrix} \Gamma_{XX} & \Gamma_{XY} & \Gamma_{XZ} \\ \Gamma_{XY} & \Gamma_{YY} & \Gamma_{YZ} \\ \Gamma_{XZ} & \Gamma_{YZ} & \Gamma_{ZZ} \end{bmatrix}$$

so the explicit formula for KSEA energy reads:

$$\begin{aligned} \hat{H}_{KSEA} &= \sum_{j=1}^{N-1} \Big(\Gamma_{XY}(\hat{S}_j^X \hat{S}_{j+1}^Y + \hat{S}_j^Y \hat{S}_{j+1}^X) + \Gamma_{XZ}(\hat{S}_j^X \hat{S}_{j+1}^Z + \hat{S}_j^Z \hat{S}_{j+1}^X) \\ &+ \Gamma_{YZ}(\hat{S}_j^Y \hat{S}_{j+1}^Z + \hat{S}_j^Z \hat{S}_{j+1}^Y) + \Gamma_{XX} \hat{S}_j^X \hat{S}_{j+1}^X + \Gamma_{YY} \hat{S}_j^Y \hat{S}_{j+1}^Y + \Gamma_{ZZ} \hat{S}_j^Z \hat{S}_{j+1}^Z \Big) \end{aligned} \tag{3.6}$$

However, in most cases the terms associated with Γ_{XX}, Γ_{YY}, and Γ_{ZZ} can be incorporated in exchange integral, and therefore are neglected; the KSEA takes a simplified form:

$$\begin{aligned} \hat{H}_{KSEA} &= \sum_{j=1}^{N-1} \Big(\Gamma_{XY}(\hat{S}_j^X \hat{S}_{j+1}^Y + \hat{S}_j^Y \hat{S}_{j+1}^X) + \Gamma_{XZ}(\hat{S}_j^X \hat{S}_{j+1}^Z + \hat{S}_j^Z \hat{S}_{j+1}^X) \\ &+ \Gamma_{YZ}(\hat{S}_j^Y \hat{S}_{j+1}^Z + \hat{S}_j^Z \hat{S}_{j+1}^Y) \Big) \end{aligned} \tag{3.7}$$

3.1.4 Three spin interaction

The assumption commonly accepted when describing the interaction of magnetic momenta, that only two spins interact at the same time is only an

approximation - in the case of some phenomena it is necessary to refer to multipartite spin interactions [103, 104]. One of the most common models in the literature regarding multipartite magnetic interaction is the three spin interactions (TSI) model, given by Hamiltonian:

$$\hat{H}_{TSI} = k \sum_{j=2}^{N-1} \left(\hat{S}_{j-1}^{X} \hat{S}_{j}^{Z} \hat{S}_{j+1}^{X} + \hat{S}_{j-1}^{Y} \hat{S}_{j}^{Z} \hat{S}_{j+1}^{Y} \right)$$

and are common in complex magnetic structures, especially containing transition metal ions, for example, $CsMn_{0.28}Mg_{0.72}Br_3$ [104], $Eu_xSr_{1-x}S$ [105], $Eu_xSr_{1-x}Te$ [106].

3.2 Entanglement in the spin system - overview

This section serves as a concise review of the works regarding quantum entanglement in spin systems. The papers referred to here were published in the last fourteen years (2010 - 2024) and constitute the currently recognized level of knowledge about quantum correlations in these systems.

The most often discussed type of entanglement in the thermal, stationary state of the quantum spin system. Łuczak and Bułka [107] investigated the impact of electric field and magnetic flux on entanglement between spins $s = \frac{1}{2}$ of quantum dots, arranged at the corners of an equilateral triangle. This system was described by the Hubbard model, which was then simplified to the XXX Heisenberg model with antisymmetric exchange interactions, resulting from the presence of the external electric field. As an entanglement measure, the concurrence was used. The authors proved that the electric field can serve in such a system as a means to control the entanglement. The spin coupling due to antisymmetric exchange interactions may be linear (in weak field) or quadratic (in strong field) function of the field - it is the consequence of the Stark effect. What is more, for the particular field orientation one may achieve the state, in which two spins are maximally entangled, while the third remains separable (entanglement monogamy) - for small fields this orientation coincides with the direction pointing forward the separable spin, which does not hold for bigger fields. Moreover, the impact of the magnetic flux was determined - it forces even distribution of the bipartite entanglement between the spins. Furman *et al.* [108] analysed the appearance of entangled states in finite, one-dimensional chains of spins interacting by dipolar coupling in the external magnetic field. The concurrence was employed as an entanglement measure. It was found out that for a magnetic field noticeably larger than dipolar coupling in terms of interaction energy, the thermal

state is separable - entanglement occurs when these two types of interaction are similar in magnitude (Zeeman energy can be also one or two orders of magnitude smaller to obtain this effect, however, the entanglement will be lower). The authors considered the relation between the temperature of entanglement loss and applied magnetic field and found out that the relation between the heat capacity, temperature, and magnetic field is visibly different for entangled and separable states, and therefore may serve as an entanglement witness. Sadiek and Kais [109] compared two seven spins systems - a two-dimensional section of triangular lattice and a one-dimensional linear spin chain, in terms of thermal bipartite and multipartite entanglement under the influence of temperature range close to absolute zero. Both systems were described by the XY Heisenberg model with an external magnetic field. Bipartite entanglement was expressed by concurrence and entanglement of formation, multipartite entanglement was measured by the so-called robustness of entanglement and with a geometrical method. In both cases, one- and two-dimensional structures, authors managed to find non-zero entanglement in the high magnetic field, however with relatively small magnitude and susceptibility to a decrease in value with increasing temperature. What is more, the authors determined the critical temperatures - temperature, in which entanglement rapidly decreases to zero - for bipartite entanglement of nearest, next-nearest, and third-order neighbours, as well as for multipartite entanglement in both of the compared systems. In the special case, XX model ($J_X = J_Y$), both types of entanglement vanish at the same temperature, yet for anisotropic models ($J_X \neq J_Y$), multipartite entanglement decreases faster as the temperature increases. In general, the closer to each other the two spins are, the higher their critical temperature is, it may be however slightly increased with the strong external magnetic field. The authors also proposed supplementation of structure with a magnetic dopant (one of the spins was replaced with a similar particle with a different type of interaction), which, according to their calculation, may have the potential to noticeably raise the temperature of entanglement decay. This effect, alongside the strong magnetic field, could allow for manufacturing a quantum information system resistant to temperature increase. Del Cima *et al.* [110] considered the antiferromagnetic chain described by the XXX Heisenberg model, expressing the entanglement quantitatively by the minimal distance (counted according to Hilbert - Schmidt norm) between the analysed state and subspace of separable states, defined utilizing Peres - Horodecki criterion. Their analysis resulted in finding a relation between the decoherence temperature and the value of exchange integral describing the model. Najarbashi *et al.* [111] analysed the thermal entanglement in a triangular system of $S = \frac{1}{2}$ and $S = 1$ spins. Four different systems were investigated and compared, all described

by the XXZ Heisenberg model with an external magnetic field. The authors described the entanglement using concurrence and carried out their research to obtain the following dependencies: concurrence vs. temperature and concurrence vs. magnetic field. Their result was that the sign of magnetic field has no importance for the entanglement, only the magnitude of said field. They also found a correlation between the anisotropy parameter $\frac{J_X}{J_Z}$, magnetic field, and type of spins in structure and temperature of total entanglement decay. Milivojević [112] analysed three spin systems, described by XXX Heisenberg model with different types of three-spin interactions and external magnetic field. By applying entanglement fidelity, the author analysed the states in terms of the creation of the states of maximal entanglement, GHZ, and W states. The paper shows the possibility of exploiting the magnetic field as a detector of W-type entanglement. Park [113] investigated thermal entanglement and thermal discord in a two-spin XYZ Heisenberg system with Dzyaloshinskii-Moriya (DM) interactions. The author managed to determine the temperature of sudden entanglement loss (T_C), which suggests, that this temperature may also indicate the phase transition. The study was divided into two parts: one focused on antiferromagnetic ($J_{x,y,z} < 0$) and the other on ferromagnetic ($J_{x,y,z} > 0$) systems. In antiferromagnetic systems, the entanglement decreases exponentially with temperature, and quantum discord is characterized by exponentially damped behaviour, however, discord does not reach zero. The temperature of total entanglement loss increases along the DM exchange coefficient. In the ferromagnetic system, both entanglement and quantum discord are equal to zero even for small temperatures (close to absolute zero). This observation suggests that in this class of materials investigated quantum resources cannot be utilized. Redwan *et al.* [114] studied the impact of exchange interaction of Calogero-Moser type (interactions in the systems where their components oscillate around equilibrium positions, so the exchange interaction tends to depend on the distance between the spins; in this paper, this relation was assumed to be $J(R) = \frac{J_0}{R^2}$) in a two-spin system with non-uniform magnetic field and unidirectional DM interaction on entanglement in thermal state and possibilities of quantum teleportation. The entanglement was characterized by the negativity while the quality of quantum teleportation was by the fidelity - the quantity that expresses the similarity between the initial (ρ_I) and final (ρ_F) state of quantum teleportation protocol. Fidelity is given by the formula:

$$F(\rho_I, \rho_F) = \left(\sqrt{\sqrt{\rho_I} \rho_F \sqrt{\rho_I}} \right)^2$$

and takes its value in the range of 0 to 1: the fidelity equal 1 indicates that the final state perfectly reproduces the initial state, while 0 means that the

final state is orthogonal to the initial state, therefore all the information about it was lost during teleportation and protocol failed. Authors managed to find the critical value of spin distance, above which the entanglement in the thermal state rapidly decreases; moreover, the DM interaction was shown to be a positive factor in terms of entanglement; also anisotropy of magnetic field can be used as an entanglement enhancer in some set of parameters. In terms of quantum teleportation fidelity, there were certain sets of parameters, that ensured the teleportation with maximal fidelity; as it turns out, the appropriately low temperature and short distance between spins is crucial to provide the effective teleportation medium. Lima [27] examined the one and two-dimensional arrangement of spins, described by XXZ Heisenberg model with DM interactions. Analysis of entanglement was supported by von Neumann entropy. The author concluded that entanglement entropy tends to zero as the temperature declines; additionally, the paper contains a comparison between two formalisms used in the analysis of such structures: Modified Spin Wave (MSW) and Schwinger Boson Theory (SBW). The same author, in a different paper [115] approached the analysis of entanglement in two systems: triangular and honeycomb lattice of spins. The exchange interaction was described by the XXZ Heisenberg model, and as an entanglement measure, von Neumann entropy and relative entropy of entanglement were applied. By using spin wave approximation, determination of the relation between temperature or exchange integral and entanglement was achieved, and results showed the impact the frustration occurring for antiferromagnetic exchange has on the entanglement. Niezgoda *et al.* [116] analysed the ground and thermal state of various spin chains (long-range Ising interactions, XXZ Heisenberg model, and Majumdar - Ghosh model) as a means to prove the original approach to obtaining the information from a single element of density matrix. The entanglement was expressed by the correlator, resulting from Bell inequality. As the paper was not focused on entanglement, the results were not interpreted in depth, however, the effectiveness of the proposed approach was confirmed. Li *et al.* [117] studied the XXZ model of two spins, $s = \frac{1}{2}$ and $S = 1$, in terms of entropic uncertainty and its behaviour under the increasing temperature or external, inhomogeneous magnetic field. The analysis was conducted on the thermal state. Besides the uncertainty, also entanglement was investigated, and measured by negativity. In general, quantum entanglement, as a quantum correlation, increases while the entropic uncertainty decreases, and a thorough examination of this phenomenon in the considered model was the purpose of the authors. Their results confirmed that external magnetic field and temperature have a degrading effect on the entanglement, and exchange integral effectively reduces the entropic uncertainty, and can to some extent prevent

the loss of entanglement due to temperature or magnetic field. Fedorova and Yurischev [118] analysed the two spin XYZ Heisenberg model, with three components Dzyaloshinskii-Moriya (DM) and Kaplan - Shekhtman - Entin - Wohlmann - Aharony (KSEA) interaction, in the external magnetic field. Their work was settled on the division of states due to symmetry, and analysis of entanglement in each symmetry family. The amount of entanglement was described by concurrence and entanglement of formation. Besides developing a formula to calculate the entanglement in a particular symmetric group, they also described the impact of DM and KSEA factors on the entanglement. Gálisová and Kaczor [119] conducted an investigation of magnetic properties in a hybrid model - planar Ising lattice with interconnected trigonal pyramids of Ising/Heisenberg XXZ spins; one of the analysed parameters being the thermal entanglement between spin in pyramids, expressed in entanglement concurrence. Their analytic approach and numerical simulations resulted in determining the concurrence for particular sets of parameters. Huang [120] described the two-spin Ising model, with DM interaction and a non-uniform magnetic field. The measure of entanglement adopted in the paper was the concurrence. Investigation on thermal entanglement in this case revealed that the magnetic field has a destructive impact on the entanglement, and its anisotropy only enhances this effect. DM interaction changes the temperature of entanglement loss. Khedif *et al.* [121] investigated the two spin system described with XYZ model and z-oriented DM interaction, to determine the impact of model parameters such as temperature, exchange interaction, and DM coupling factor on the non-classical correlations, entanglement, and quantum discord, in state of thermal equilibrium. The former was described by negativity, the latter with local quantum uncertainty (LQU) and uncertainty-induced nonlocality (UIN). The research results allowed the authors to deduce that increasing the DM factor corresponds to the increase of LQU and UIN and that the total entanglement loss does not translate to loss of all quantum correlations - quantum discord remains even above the temperature of entanglement decoherence. Elghaayda *et al.* [122] described the thermal entanglement in a pair of spins coupled not by exchange interaction, but by dipolar magnetic coupling, with the inclusion of DM and KSEA interaction, in the external magnetic field. Besides the logarithmic negativity, applied to evaluate the entanglement, researchers used also local quantum uncertainty (LQU) and uncertainty-induced nonlocality (UIN) to examine the correlations beyond the entanglement. The most important conclusion derived from their investigation is that the KSEA interaction may, to some extent, reduce the loss of entanglement due to thermal decoherence. Tae-Hung *et al.* [123] considered the four-qubit chain of spins interacting by XY Heisenberg model, with DM interaction taken into account, in terms

of preserving the non-classical correlations in thermal state and under the impact of some quantum communication channels. As a measure of these correlations, Local Quantum Uncertainty (LQU) was applied. The authors found out that temperature has a negative impact on the correlations, however, this effect can be overcome with sufficiently high exchange interactions or DM coefficients. The following decoherence channels were investigated: phase damping channel, depolarizing channel, and phase flip channel. Two former turned out to decrease the LQU with the increase of decoherence factor γ, while the latest one reaches minimal LQU for $\gamma = 0.5$, and for higher decoherence parameters one can witness the growth in quantum correlations.

In recent years, the research focused on the time evolution and dissipation of entanglement in quantum spin systems is gaining popularity. Given that the actual layouts for Quantum Informatics purposes cannot be separated from the environment, the approach of open quantum systems theory is common - there are plenty of analyses for spin systems coupled to Markovian or non-Markovian reservoirs. Xu *et al* [124] analysed the time evolution of entanglement in a system of seven Ising spins arranged on a triangular lattice in the presence of various, time-dependent magnetic fields (of step, exponential, hyperbolic, and periodic type of time dependence). As the external magnetic field impacts the thermal equilibrium state, also evolution of thermal state entanglement was also considered. The authors investigated the bipartite entanglement between the nearest and next-nearest neighbours in their model, treating the rest of the spins as a non-Markovian reservoir. Authors found that the behaviour of the entanglement in such a model is ergodic; the system exhibits some controllability for some types of time-dependent magnetic fields, however, it holds only for fields of small magnitude. A high magnetic field introduces disturbances in the time evolution of entanglement. Entanglement also adjusts the frequency of its changes to the frequency of the external field in temperatures close to zero, nevertheless the higher the temperature is, the lower the amplitude of entanglement. Mahmoudi *et al.* [125] prepared an analysis of entanglement, mutual information, and quantum discord dynamics in closed spin chains of spins $\frac{1}{2}$, interacting in accordance with XX Heisenberg model and in the presence of three-spin interactions. As the research was focused on bipartite quantum correlations, two neighbouring spins from the chain were selected, and the rest played the role of a supposedly non-Markovian environment. The model in question can be exactly solvable using the fermionization technique - joint Jordan-Wigner and Fourier transformation, that maps the problem onto the momentum space. As the solution depends on the initial state, the maximally entangled state of two considered spins was selected as such $(\frac{1}{\sqrt{2}}\left(|\uparrow\downarrow\rangle + e^{i\theta}|\downarrow\uparrow\rangle\right))$, com-

plemented with the ferromagnetic state of the remaining spins (all of them were pointing in the same direction). As the entanglement measure, the concurrence was chosen; the authors investigated also the mutual information, $\mathcal{I}(\rho_{AB}) = S(\rho_A) + S(\rho_B) + \sum_{\alpha=1}^{4} \lambda_\alpha \log_2 \lambda_\alpha$, where $S(\rho)$ indicates von Neumann entropy of state ρ, and λ_α are the eigenvalues of the ρ_{AB} density matrix; and the behaviour of quantum discord. They managed to find a point, where the non-Markovian dynamics (periodic losses and recoveries of quantum correlations) turn into Markovian (exponential loss of quantum correlations) - the limiting point is when the three spin interaction factor reaches the half of exchange interaction, $J_{TSI} = 0.5 J_{HEIS}$: J_{TSI} below this value results in non-Markovian behaviour, J_{TSI} above - in Markovian. The authors also proved that quantum correlations in the environment are also sensitive to the Markovianity of the problem. Sivkov et al. [126] conducted ab initio calculations and spin Hamiltonian analysis on antiferromagnetic chains of Co deposited on $Cu_3N/Cu(110)$ substrate. These particular materials were chosen due to the fact, that they exhibit quantum correlations, entanglement included, in relatively high temperatures (20K - 100K). Moreover, the insulating properties of the substrate limit the decoherence to the environment. The analysed spin chains were up to seven spins in length and the first spins was subject to a switchable magnetic field along Z axis and magnetic pulses along X axis of a few teslas magnitude and 2 - 4 picosecond duration time. Von Neumann entropies of singular spins indicated that the expected total magnetization of the chain during spin-flip (caused by magnetic field switching) is equal to zero, $\langle S_Z \rangle = 0$, which is a premise for non-zero entanglement. The research reveals the substantial difference in time scales of spin switching in chains with even and odd numbers of spins. Strong quantum entanglement appears during spin switching and decays during relaxation. Hama *et al.* [127] proposed a model of two spin ensembles, connected to the common bosonic reservoir, to investigate the relation between the number of spins in such an ensembles and the time behaviour of quantum entanglement. The spin domains were described separately by the Ising Hamiltonian, and the interaction between them was realized through the reservoir - the absorption of boson from the reservoir was associated with the raising of down-spin in one of the domains, while the change from spin-up to spin-down was related to the creation of boson in the reservoir. Time evolution was calculated by the Lindblad equation. The initial state was an antiparallel polarization of domains - all spins in the first domain were in the up state, while all spins of the second were in the down state; the reservoir was initialized in a state of thermal equilibrium. The entanglement was expressed by logarithmic negativity. Analysis of obtained results allowed authors to formulate the following conclusions: despite initializing the second domain in the ground state (all

spins down), the interaction with the reservoir and the first ensemble results in some excitations in its spins, with the rate of such excitation depending on the difference between the numbers of spins in domains. This leads to the creation of a new equilibrium state for the entire system; the entanglement between the domains in the thermal state turned to be a function of spin number in the first domain: it increases for n from 1 to 5, and for the larger number of spins decreases monotonically. The authors also indicated potential materials, for which such a model can be applied experimentally, GaAs among others. Kuzmak [128] analysed the entanglement dynamics of the N-spin $\frac{1}{2}$ system described by Ising Hamiltonian with all ranges of interaction. The system was initially assumed in state $\psi(0) = |++...+\rangle$, where $|+\rangle = \cos\frac{\theta}{2}|\uparrow\rangle + e^{i\phi}\sin\frac{\theta}{2}|\downarrow\rangle$ and its dynamics resulted from unitary evolution, which was postulated in accordance with the proposed Hamiltonian. The entanglement between the selected spin and the rest of the chain was examined, and in the end, to express this feature quantitatively, the geometrical measure was applied, using the average value of spin, $E = \frac{1}{2}(1 - |\langle\sigma_Z\rangle|)$. In the further part of the paper, the analysis was supplemented with the impact of an external, transverse magnetic field. The dynamics of the problem turned out to strongly depend on the initial state geometry - the author determined the range of polar angle θ, for which the extended period of maximal entanglement can be observed, and proved that the number of spins in the chain also has a significant impact of entanglement value; however, the entanglement showed to be independent on azimuth angle ϕ. To investigate this independence, the manifold of entangled states was explored; the research revealed that the entanglement drops, when the curvature of the manifold increases - therefore, in aim to preserve the system in a highly entangled state, the mentioned manifold should have possibly the smallest curvature. Kolovsky [129], to test the validity of Born-Markov approximation for different than the usual type of environment, analysed the quantum two-level system coupled to the Bose-Hubbard chain, which served in this analysis as an environment. This model was chosen due to the fact, that in opposition to the commonly assumed bosonic reservoir, which can be seen as an ensemble of linear quantum oscillators, the Bose-Hubbard chain has strong ergodic properties. These properties manifest as a tendency to create the entanglement not only between the modes of the chain but also between the states of chain and coupled system of interest. This entanglement was inspected by analysis of the time behaviour of von Neumann entropy. The author proved that the Born - Markov approximation can be indeed applied also to the proposed model, and pointed out an additional advantage of the ergodic environment in terms of open system analysis - it is relatively easy to modify the assumptions to reach the non-Markovian model. Mahmoudi [130]

researched the entanglement dynamics in a one-dimensional XX Heisenberg spin chain with three-spin interaction (TSI) and DM superexchange also taken into consideration. The whole system underwent the unitary interaction and then was reduced to two spins, between which the entanglement was determined - therefore the dynamics of the system were non-Markovian in initial assumptions. The initial state was the maximally entangled state of the two first spins of the chain, coupled with the separable, ferromagnetic state of the rest of the system. The author observed the expected decrease of entanglement due to decoherence (entanglement sudden death), however, the non-Markovian nature of the problem results in periodic increases in entanglement. The amplitudes of subsequent peaks decrease exponentially, which is expected, nevertheless, the rate of amplitude decrease may serve as an indicator of how non-Markovian the dynamics really are. Using this tool, the author managed to determine, that DM interactions enhance the entanglement regain, which leads to the conclusion, that materials with sufficiently high DM interactions may be characterized by low decoherence. Also, TSI contributes to the preservation of non-Markovian behaviour in the system, however, they must satisfy two conditions: TSI cannot exceed DM and half of the exchange integral for closest neighbour interactions. Otherwise, the TSI would contribute to the Markovian type of dynamics. Tchoffo and Tene [131] considered the entanglement dynamics in a two-qubit system, described by XXZ exchange interaction, with anisotropic magnetic field and DM interactions. All the parameters of the Hamiltonian were time-dependent and of a harmonic nature. The environment was assumed to be Markovian, by modeling the time evolution of a system with the Lindblad equation. The paper covers both analytical solutions and numerical investigations; the conclusions from the two approaches are as follows: due to the dependence of the parameters of the Hamiltonian on time there was observed a slight enhancement of the entanglement during the decoherence. Moreover, the manipulation of the magnetic field anisotropy allows for the introduction of periods of sudden increases of entanglement concurrence during the time evolution of the system. Hashem *et al.* [132] investigated a system of two spins, connected by exchange interaction described by XYZ Heisenberg model, with external magnetic field and KSEA and DM antisymmetric exchange taken also into consideration. The system evolved under the intrinsic decoherence - its time evolution was described by the Milburn equation. The research aimed to compare the behaviour of three entanglement measures, Bell nonlocality, concurrence, and entropic uncertainty during such an evolution. The initial states were $|\uparrow\uparrow\rangle\langle\downarrow\downarrow|$ and $\frac{1}{2}|\Phi^+\rangle\langle\Phi^+|$ (see Bell basis in sect. 1.2). Both initial states exhibit the oscillatory changes in entanglement; moreover, the DM and KSEA interaction proven to be the crucial factor influencing

the period of the change. By controlling the magnetic field, DM and KSEA interaction one may reach the high entanglement value and slow down its decay due to decoherence, which, according to the authors' assumptions, may increase the precision of measurements on entangled systems. Noorinejad *et al.* [133] investigated the time evolution of entanglement in a system of three spins interacting in accordance with the XX Heisenberg model, taking into account also the three-spin interaction. The bipartite entanglement was analysed, between the first and second and first and third spin, while the remaining spin acted as a non-Markovian environment. The authors applied concurrence to express the amount of entanglement, and used the W state, $|W\rangle = \frac{1}{\sqrt{3}}(|\uparrow\uparrow\downarrow\rangle + |\uparrow\downarrow\uparrow\rangle + |\downarrow\uparrow\uparrow\rangle)$, as an initial state. Their investigations revealed that with the adopted assumptions the evolution of the entanglement is periodic, and the W state is perfectly revived - there are no quantum correlations loss in such an evolution. Sadiek and AlQasimi [134] analysed the time evolution of entanglement in a two-dimensional, triangular finite lattice of seven spins. Their idea was to treat the central spin of such an arrangement as an impurity; six remaining spins interacted in accordance to XYZ Heisenberg model with particular exchange interaction coefficients (however, by using certain values, the authors tested also XXX Heisenberg and Ising model), while the impurity interacted with the rest by adjustable, different exchange integral. Researchers assumed Markovian interaction between the system and environment and modeled the evolution using the Lindblad equation. The considered initial states consist of maximally entangled, partially entangled and separable, pure states. Entanglement was expressed by the concurrence. Based on the results of numerical simulation authors deduced that the introduction of impurity and increasing its exchange interaction parameter leads to entanglement formation between the impurity and surrounding spins, however, it comes at the cost of entanglement between the original spins (so-called monogamy of entanglement). Moreover, by changing the anisotropy parameter (namely, going from XXX to XYZ model) one can make the entanglement between the impurity and original spin stronger and more stable. Kaczor and Jakubczyk [135] examined the entanglement evolution in the following model - one cell of simple cubic with spins $s = \frac{1}{2}$ on the corners, doped with additional spin $S = 1$ in the center. The rest of the lattice serves as a bosonic (magnonic) reservoir. As a consequence of focusing on bipartite entanglement (between two spins $s = \frac{1}{2}$ and between spins $s = \frac{1}{2}$ and $S = 1$), the dynamics of the system as a whole was hybrid - the remaining spins of the cell constituted the non-Markovian surrounding, while the rest of the lattice serves as a Markovian environment. The exchange interaction was described using the XXX Heisenberg model, the external magnetic field was also included in the description. The initial state

of a system was proposed as an equivalent of W state for corner spins - uniform superposition of states with one magnetic excitation in each corner - expanded with state $|S_Z = 0\rangle$ for central spin $S = 1$. Change of the system in time was calculated based on the Lindblad equation, the concurrence served as an entanglement measure. The investigation revealed that the evolution of entanglement in a dissipative environment will have a dumped (due to decoherence) periodic course, in which peaks can be decomposed on three Gaussian modes. This holds also for non-dissipative time evolution and is probably a result of internal magnon exchange, in a cell isolated from the rest of the lattice. The magnetic field turns out to not have any influence on the entanglement evolution, while exchange interaction between the spins $s = \frac{1}{2}$ and $S = 1$ is a factor that increases the frequency of entanglement changes. Appropriate manipulation of this parameter allows one to obtain two types of entanglement and, depending on the needs, maximize one or the other.

Part II

Study of the most common spin systems in terms of thermal entanglement and entanglement dynamics

Chapter 4

4.1 Introduction

The following section contains an analysis of the entanglement between two spins for the most common models of interactions in spin chains of varied lengths - in other words, it may serve as a catalogue of entanglement in specific spin structures, under particular environmental conditions. The analysis proceeds in two ways: firstly, the thermal entanglement is determined - the stationary solution for a state in thermal equilibrium with the environment. In general, the outcome determination method begins with formulating an appropriate Hamiltonian and finding its eigenvalues $E_1, E_2, \ldots E_{2^N}$, where N is the number of spins in the chains, and eigenvectors $|\phi_1\rangle, |\phi_2\rangle, \ldots, |\phi_{2^N}\rangle$. Based on them, the density matrix is defined by the formula:

$$\rho_T = \sum_{i=1}^{2^N} p(E_j) \cdot |\phi_j\rangle\langle\phi_j| \tag{4.1}$$

where $p(E_j)$ is the probability that the system is in the state with energy E_j. Such a probability for the thermal equilibrium results from the Boltzmann distribution:

$$p(E_j) = \frac{1}{Z} \cdot \exp\left(-\frac{E_j}{k_B T}\right), \qquad Z = \sum_{i=1}^{2^N} \exp\left(-\frac{E_i}{k_B T}\right).$$

As a quantitative means to express the entanglement, the concurrence is applied. It is given by the formula:

$$C = \max\{0, \sqrt{\lambda_4} - \sqrt{\lambda_3} - \sqrt{\lambda_2} - \sqrt{\lambda_1}\}$$

where the $\lambda_4 \geq \lambda_3 \geq \lambda_2 \geq \lambda_1$ are the eigenvalues of the following matrix R :

$$R = \rho \left(\sigma^Y \otimes \sigma^Y\right) \rho^\dagger \left(\sigma^Y \otimes \sigma^Y\right)$$

where the σ^Y is Pauli Y-matrix and ρ is a reduced density matrix covering only those two spins between which the entanglement concurrence is determined - Hilbert space A in the equation below contains all the remaining spins:

$$\rho = \mathrm{Tr}_A \left(\rho_T\right).$$

The concurrence will often be calculated for nearest neighbours unless stated otherwise. As the models in question are characterized by translational symmetry, it does not matter between which spins the entanglement is calculated, as long as they are next to each other in the chain. Nevertheless, for the sake of clarity, the calculations are carried out for entanglement between the first and second spin in the chain.

The second part of the analysis is conducted to determine the time behaviour of the entanglement when the system in question is located in a Markovian, dissipative environment. Time evolution, appropriate for such condition, is governed by the master Lindblad equation:

$$\frac{d}{dt}\rho(t) = -i\left[\hat{H}, \rho(t)\right] + \mathcal{D}(\rho(t)) \tag{4.2}$$

where $\mathcal{D}(\rho)$ is a dissipator. This dissipator can be defined as:

$$\mathcal{D}(\rho) = \gamma_1 \sum_{j=1}^{N} \mathcal{L}(\hat{s}_j^+) + \gamma_2 \sum_{j=1}^{N} \mathcal{L}(\hat{s}_j^-)$$

which translates to the following situation: the system can receive the energy for raising any of the spins from the environment with ratio γ_1, or lower any of the spins and release excess energy to the environment with ratio γ_2 - and Markovian assumption allows to neglect the tracking of the environment state, so the equation above refers only to the density matrix of the system itself. Superoperator (as it depends not solely on the operator in argument, but also on the density matrix) $\mathcal{L}(A)$ is called Lindblad operator and defined as:

$$\mathcal{L}(A) = A\rho A^\dagger - \frac{1}{2}A^\dagger A\rho - \rho A^\dagger A.$$

As the time behaviour of the system strongly depends on the initial state, the following initial states are analysed:

- for $N = 2$:

$$|\psi_A\rangle = |\uparrow\uparrow\rangle, \quad |\psi_B\rangle = \frac{1}{\sqrt{2}}\left(|\uparrow\downarrow\rangle + |\downarrow\uparrow\rangle\right)$$

- for $N = 3$:

$$|\psi_A\rangle = |\uparrow\uparrow\uparrow\rangle, \quad |\psi_B\rangle = \frac{1}{\sqrt{3}}\left(|\uparrow\uparrow\downarrow\rangle + |\uparrow\downarrow\uparrow\rangle + |\downarrow\uparrow\uparrow\rangle\right)$$

- for $N = 4$:

$$|\psi_A\rangle = |\uparrow\uparrow\uparrow\uparrow\rangle,$$

$$|\psi_B\rangle = \frac{1}{2}\left(|\uparrow\uparrow\uparrow\downarrow\rangle + |\uparrow\uparrow\downarrow\uparrow\rangle + |\uparrow\downarrow\uparrow\uparrow\rangle + |\downarrow\uparrow\uparrow\uparrow\rangle\right)$$

$$|\psi_C\rangle = \frac{1}{\sqrt{6}}\left(|\uparrow\uparrow\downarrow\downarrow\rangle + |\uparrow\downarrow\uparrow\downarrow\rangle + |\uparrow\downarrow\downarrow\uparrow\rangle + |\downarrow\uparrow\uparrow\downarrow\rangle + |\downarrow\uparrow\downarrow\uparrow\rangle + |\downarrow\downarrow\uparrow\uparrow\rangle\right)$$

- for $N = 5$:

$$|\psi_A\rangle = |\uparrow\uparrow\uparrow\uparrow\uparrow\rangle,$$

$$|\psi_B\rangle = \frac{1}{\sqrt{5}}\left(|\uparrow\uparrow\uparrow\uparrow\downarrow\rangle + |\uparrow\uparrow\uparrow\downarrow\uparrow\rangle + |\uparrow\uparrow\downarrow\uparrow\uparrow\rangle + |\uparrow\downarrow\uparrow\uparrow\uparrow\rangle + |\downarrow\uparrow\uparrow\uparrow\uparrow\rangle\right)$$

$$\begin{aligned}|\psi_C\rangle \;=\; & \frac{1}{\sqrt{10}}\left(|\uparrow\uparrow\uparrow\downarrow\downarrow\rangle + |\uparrow\uparrow\downarrow\uparrow\downarrow\rangle + |\uparrow\uparrow\downarrow\downarrow\uparrow\rangle + |\uparrow\downarrow\uparrow\uparrow\downarrow\rangle + |\uparrow\downarrow\uparrow\downarrow\uparrow\rangle\right.\\ & \left. + |\uparrow\downarrow\downarrow\uparrow\uparrow\rangle + |\downarrow\uparrow\uparrow\uparrow\downarrow\rangle + |\downarrow\uparrow\uparrow\downarrow\uparrow\rangle + |\downarrow\uparrow\downarrow\uparrow\uparrow\rangle + |\downarrow\downarrow\uparrow\uparrow\uparrow\rangle\right)\end{aligned}$$

- for $N = 6$:

$$|\psi_A\rangle = |\uparrow\uparrow\uparrow\uparrow\uparrow\uparrow\rangle,$$

$$\begin{aligned}|\psi_B\rangle \;=\; & \frac{1}{\sqrt{6}}\left(|\uparrow\uparrow\uparrow\uparrow\uparrow\downarrow\rangle + |\uparrow\uparrow\uparrow\uparrow\downarrow\uparrow\rangle + |\uparrow\uparrow\uparrow\downarrow\uparrow\uparrow\rangle\right.\\ & \left. + |\uparrow\uparrow\downarrow\uparrow\uparrow\uparrow\rangle + |\uparrow\downarrow\uparrow\uparrow\uparrow\uparrow\rangle + |\downarrow\uparrow\uparrow\uparrow\uparrow\uparrow\rangle\right)\end{aligned}$$

$$\begin{aligned}|\psi_C\rangle \;=\; & \frac{1}{\sqrt{15}}\left(|\uparrow\uparrow\uparrow\uparrow\downarrow\downarrow\rangle + |\uparrow\uparrow\uparrow\downarrow\uparrow\downarrow\rangle + |\uparrow\uparrow\uparrow\downarrow\downarrow\uparrow\rangle + |\uparrow\uparrow\downarrow\uparrow\uparrow\downarrow\rangle + |\uparrow\uparrow\downarrow\uparrow\downarrow\uparrow\rangle\right.\\ & + |\uparrow\uparrow\downarrow\downarrow\uparrow\uparrow\rangle + |\uparrow\downarrow\uparrow\uparrow\uparrow\downarrow\rangle + |\uparrow\downarrow\uparrow\uparrow\downarrow\uparrow\rangle + |\uparrow\downarrow\uparrow\downarrow\uparrow\uparrow\rangle + |\uparrow\downarrow\downarrow\uparrow\uparrow\uparrow\rangle\\ & \left. + |\downarrow\uparrow\uparrow\uparrow\uparrow\downarrow\rangle + |\downarrow\uparrow\uparrow\uparrow\downarrow\uparrow\rangle + |\downarrow\uparrow\uparrow\downarrow\uparrow\uparrow\rangle + |\downarrow\uparrow\downarrow\uparrow\uparrow\uparrow\rangle + |\downarrow\downarrow\uparrow\uparrow\uparrow\uparrow\rangle\right)\end{aligned}$$

$$\begin{aligned}|\psi_D\rangle \;=\; & \frac{1}{2\sqrt{5}}\left(|\uparrow\uparrow\uparrow\downarrow\downarrow\downarrow\rangle + |\uparrow\uparrow\downarrow\uparrow\downarrow\downarrow\rangle + |\uparrow\uparrow\downarrow\downarrow\uparrow\downarrow\rangle + |\uparrow\uparrow\downarrow\downarrow\downarrow\uparrow\rangle + |\uparrow\downarrow\uparrow\uparrow\downarrow\downarrow\rangle\right.\\ & + |\uparrow\downarrow\uparrow\downarrow\uparrow\downarrow\rangle + |\uparrow\downarrow\uparrow\downarrow\downarrow\uparrow\rangle + |\uparrow\downarrow\downarrow\uparrow\uparrow\downarrow\rangle + |\uparrow\downarrow\downarrow\uparrow\downarrow\uparrow\rangle + |\uparrow\downarrow\downarrow\downarrow\uparrow\uparrow\rangle\\ & + |\downarrow\uparrow\uparrow\uparrow\downarrow\downarrow\rangle + |\downarrow\uparrow\uparrow\downarrow\uparrow\downarrow\rangle + |\downarrow\uparrow\uparrow\downarrow\downarrow\uparrow\rangle + |\downarrow\uparrow\downarrow\uparrow\uparrow\downarrow\rangle + |\downarrow\uparrow\downarrow\uparrow\downarrow\uparrow\rangle\\ & \left. + |\downarrow\uparrow\downarrow\downarrow\uparrow\uparrow\rangle + |\downarrow\downarrow\uparrow\uparrow\uparrow\downarrow\rangle + |\downarrow\downarrow\uparrow\uparrow\downarrow\uparrow\rangle + |\downarrow\downarrow\uparrow\downarrow\uparrow\uparrow\rangle + |\downarrow\downarrow\downarrow\uparrow\uparrow\uparrow\rangle\right)\end{aligned}$$

These states are selected for their accessibility. All components of the final states possess the same magnetization, and each contributes an identical component to the superposition. Consequently, their preparation involves applying suitable magnetic excitation to the ferromagnetic state. Moreover, all the initial states are chosen to be pure states, i.e. $\rho(t=0) \in \{|\psi_A\rangle\langle\psi_A|, |\psi_B\rangle\langle\psi_B|...\}$.

4.1.1 Remarks on dissipative time evolution in spin chains

Let us assume, that the state in question ρ is an eigenstate, so $\left[\hat{H}, \rho\right] = 0$; therefore the first term in (4.2) vanishes, and overall time evolution is governed solely by the dissipator:

$$\frac{d}{dt}\rho(t) = \mathcal{D}(\rho) = \sum_{j=1}^{N} \left[\gamma_1 \mathcal{L}(\hat{S}_j^+) + \gamma_2 \mathcal{L}(\hat{S}_j^-)\right]. \tag{4.3}$$

To simplify the problem, yet still derive some interesting conclusions, one can restrict the consideration to a single component of the sum from (4.3):

$$\mathcal{D}^q(\rho) = \gamma_1 \mathcal{L}(\hat{S}_q^+) + \gamma_2 \mathcal{L}(\hat{S}_q^-)$$

From this point we allow ourselves to omit the index q in $\hat{S}^{\pm}$ operators for the sake of clarity, so the explicit form of the above equation with this convention will be then:

$$\mathcal{D}^q(\rho) = 2\gamma_1 \hat{S}^+ \rho \hat{S}^- - \gamma_1(\hat{S}^-\hat{S}^+\rho + \rho\hat{S}^-\hat{S}^+) + 2\gamma_2 \hat{S}^+\rho\hat{S}^- - \gamma_2(\hat{S}^+\hat{S}^-\rho + \rho\hat{S}^+\hat{S}^-).$$

The j,k-the element of the dissipator matrix (the derivation is done in a calculational basis) is given by the formula:

$$\begin{aligned}
\langle j|\mathcal{D}^q|k\rangle = \sum_{l,m,n,p,s,q} \big(&2\gamma_1 \langle j|S^+_{l,m}|l\rangle\langle m|p_{n,p}|n\rangle\langle p|S^-_{s,q}|s\rangle\langle q|k\rangle \\
&-\gamma_1\langle j|S^-_{l,m}|l\rangle\langle m|S^+_{n,p}|n\rangle\langle p|p_{s,q}|s\rangle\langle q|k\rangle - \gamma_1\langle j|p_{l,m}|l\rangle\langle m|S^-_{n,p}|n\rangle\langle p|S^+_{s,q}|s\rangle\langle q|k\rangle \\
&+ 2\gamma_2\langle j|S^-_{l,m}|l\rangle\langle m|p_{n,p}|n\rangle\langle p|S^+_{s,q}|s\rangle\langle q|k\rangle \\
&-\gamma_2\langle j|S^+_{l,m}|l\rangle\langle m|S^-_{n,p}|n\rangle\langle p|p_{s,q}|s\rangle\langle q|k\rangle \ - \gamma_2\langle j|p_{l,m}|l\rangle\langle m|S^+_{n,p}|n\rangle\langle p|S^-_{s,q}|s\rangle\langle q|k\rangle\big)
\end{aligned}$$

where $p_{a,b}$ is a,b-th element of the density matrix ρ, and $S^{\pm}_{a,b}$ - the element for spin raising/lowering operator. Appealing to the property of scalar product for basis vectors, $\langle a|b\rangle = \delta_{a,b}$, one can simplify the formula above to the form:

$$\begin{aligned}
\mathcal{D}^q_{j,k} \ = \ \sum_{m,n} \big(&2\gamma_1 S^+_{j,m} p_{m,n} S^-_{n,k} - \gamma_1 S^-_{j,m} S^+_{m,n} p_{n,k} - \gamma_1 p_{j,m} S^-_{m,n} S^+_{n,k} \\
&+2\gamma_2 S^-_{j,m} p_{m,n} S^+_{n,k} - \gamma_2 S^+_{j,m} S^-_{m,n} p_{n,k} - \gamma_2 p_{j,m} S^+_{m,n} S^-_{n,k}\big).
\end{aligned}$$

Moreover, $\left(\hat{S}^{+}\right)^{\dagger} = \hat{S}^{-}$ for any spin in the chain (and their elements are real, so the hermitian conjugate reduces only to transposition), therefore the notation can be simplified further, by marking $S^{-}_{a,b} \equiv S_{a,b}$:

$$\begin{aligned}\mathcal{D}^{q}_{j,k} &= \sum_{m,n} (2\gamma_1 S_{m,j} p_{m,n} S_{n,k} - \gamma_1 S_{j,m} S_{n,m} p_{n,k} - \gamma_1 p_{j,m} S_{m,n} S_{k,n} \\ &\quad +2\gamma_2 S_{j,m} p_{m,n} S_{k,n} - \gamma_2 S_{m,j} S_{m,n} p_{n,k} - \gamma_2 p_{j,m} S_{n,m} S_{n,k}) \,.\end{aligned}$$

In a calculational basis, acting with the operator S^{-}_{q} on a state results in zero, if the spin in the q site of the chain was in the $\downarrow$ state. If the mentioned spin was in the $\uparrow$ state, it changes the spin into the $\downarrow$ state, while the other spins remain unchanged. In matrix representation, this observation translates to the fact that in each column and each row, only one element is equal to one, and all the others to zeros. It allows then to rewrite the equation above as:

$$\begin{aligned}\mathcal{D}^{q}_{j,k} &= \sum_{m,n} (2\gamma_1 S_{m,j} p_{m,n} S_{n,k} - \gamma_1 S_{j,m} S_{j,m} p_{j,k} - \gamma_1 p_{j,k} S_{k,n} S_{k,n} \\ &\quad +2\gamma_2 S_{j,m} p_{m,n} S_{k,n} - \gamma_2 S_{m,j} S_{m,j} p_{j,k} - \gamma_2 p_{j,k} S_{n,k} S_{n,k}) \,.\end{aligned}$$

Here, one needs to consider four cases:

1. both spins in q site in the states $|j\rangle$ and $|k\rangle$ are in $\uparrow$ state:

$$\begin{aligned} S_{j,m} = 1 &\iff m = j - 2^{q-1} \\ S_{k,n} = 1 &\iff n = k - 2^{q-1} \\ S_{m,j} = S_{n,k} = 0 &\text{ for all } m, n \\ \mathcal{D}^{q}_{j,k} &= 2\gamma_2 \rho_{m,n} - 2\gamma_1 \rho_{j,k} \end{aligned} \tag{4.4}$$

2. spin in q site in state $|j\rangle$ is in $\uparrow$ state, spin in $|k\rangle$ is in $\downarrow$:

$$\begin{aligned} S_{j,m} = 1 &\iff m = j - 2^{q-1} \\ S_{n,k} = 1 &\iff n = k + 2^{q-1} \\ S_{m,j} = S_{k,n} = 0 &\text{ for all } m, n \\ \mathcal{D}^{q}_{j,k} &= -(\gamma_1 + \gamma_2) \cdot \rho_{j,k} \end{aligned} \tag{4.5}$$

3. spin in q site in state $|j\rangle$ is in $\downarrow$ state, spin in $|k\rangle$ is in $\uparrow$:

$$\begin{aligned} S_{m,j} = 1 &\iff m = j + 2^{q-1} \\ S_{k,n} = 1 &\iff n = k - 2^{q-1} \\ S_{j,m} = S_{n,k} = 0 &\text{ for all } m, n \\ \mathcal{D}^{q}_{j,k} &= -(\gamma_1 + \gamma_2) \cdot \rho_{j,k} \end{aligned} \tag{4.6}$$

4. both spins in q site in the states $|j\rangle$ and $|k\rangle$ are in $\downarrow$ state:

$$S_{m,j} = 1 \iff m = j + 2^{q-1}$$
$$S_{n,k} = 1 \iff n = k + 2^{q-1}$$
$$S_{j,m} = S_{k,n} = 0 \text{ for all } m, n$$
$$\mathcal{D}^q_{j,k} = 2\gamma_1\rho_{m,n} - 2\gamma_2\rho_{j,k} \tag{4.7}$$

This reasoning allows us to simplify the expression for dissipator in the case of spin systems interacting with the Markovian environment via magnon exchange:

EXAMPLE: Let us assume that we are dealing with a spin chain of four spins. We number the states from $|0\rangle = |\downarrow\downarrow\downarrow\downarrow\rangle$ to $|15\rangle = |\uparrow\uparrow\uparrow\uparrow\rangle$. One can easily check that there is a perfect correspondence between the number of states represented in a binary system and the state form in the calculational basis - $\uparrow$ corresponds to the binary digit 1 and $\downarrow$ to the binary digit 0. We would like to know the time evolution of the $\rho_{5,7}$ element on a calculational basis. Using the previously obtained results, we must convert the „coordinates" of this element to binary format:

$$5_{10} = 0101_2$$
$$7_{10} = 0111_2$$

As we assumed that $|0\rangle = |\downarrow\downarrow\downarrow\downarrow\rangle$, we need to rewrite these states in $\uparrow$,$\downarrow$ notation. Hence:

$$|5\rangle = |\downarrow\uparrow\downarrow\uparrow\rangle$$
$$|7\rangle = |\downarrow\uparrow\uparrow\uparrow\rangle$$

The order of position runs from the right to the left:

1. first spins - both in $\uparrow$ state:

$$\mathcal{D}^1_{5,7} = 2\gamma_2\rho_{4,6} - 2\gamma_1\rho_{5,7}$$

2. seconds spins - different states:

$$\mathcal{D}^2_{5,7}(t) = -(\gamma_1 + \gamma_2) \cdot \rho_{5,7}$$

3. third spins - both in $\uparrow$ state:

$$\mathcal{D}^3_{5,7} = 2\gamma_2\rho_{1,3} - 2\gamma_1\rho_{5,7}$$

4. and fourth spins - both in $\downarrow$ state:

$$\mathcal{D}^4_{5,7} = 2\gamma_1\rho_{13,15} - 2\gamma_2\rho_{5,7}$$

The final result:

$$\mathcal{D}_{5,7}(t) = \mathcal{D}^1_{5,7}(t) + \mathcal{D}^2_{5,7}(t) + \mathcal{D}^3_{5,7}(t) + \mathcal{D}^4_{5,7}(t)$$

$$\frac{d}{dt}\rho_{5,7}(t) = 2\gamma_2\rho_{4,6}(t) + 2\gamma_2\rho_{1,3}(t) + 2\gamma_1\rho_{13,15}(t) - (5\gamma_1 + 3\gamma_2)\rho_{5,7}(t) \quad (4.8)$$

To complete the picture, it should be noted that the unitary evolution of the non-eigenstate is governed by the first component of the Lindblad equation, the commutator $\left[\hat{H}, \rho\right]$. To solve the equation of unitary evolution, the best strategy is to represent the density matrix in the basis of Hamiltonian eigenstates - this convention assures us that only diagonal elements of Hamiltonian are non-zero. Without loss of generality, one can write:

$$\frac{d}{dt}\rho(t) = -i\left[\hat{H}, \rho\right]$$

$$\frac{d}{dt}\rho_{x,y} = -i(\langle x|\hat{H}\rho|y\rangle - \langle x|\rho\hat{H}|y\rangle)$$

$$\frac{d}{dt}\rho_{x,y} = -i(H_{x,x}\rho_{x,y} - \rho_{x,y}H_{y,y})$$

$$\rho_{x,y}(t) = \rho_{x,y}(0)\cdot e^{-i(H_{xx}-H_{yy})t}$$

which illustrates harmonic (wavelike) evolution for elements of non-eigenstates (of course, this result holds only in Hamiltonian eigenbasis; to examine the behaviour of density matrix elements in a calculational basis, additional transformation is necessary - however, translation of this transformation onto the outcome is that the wavelike behaviour of density matrix elements does not result from one, but from the combination of harmonic functions).

To summarize the consideration above, one may notice that the Markovian time evolution governed by the Lindblad equation may proceed in two ways: in the case of a non-eigenstate as an initial state, the change of the entanglement concurrence will include the wavelike behaviour due to system attempts to reach the eigenstate, coupled to the exponential decay of entanglement resulting from the interaction with the environment. Although the initial state is an eigenstate from the start, its concurrence will decrease with the rate of combined exponents, a solution of the Lindblad equation, similar to (4.8).

4.2 Study of the thermal and dynamic entanglement in most common spin systems

4.2.1 Exchange interaction only

XXX Heisenberg model

The simplest spin chain of N spins is XXX Heisenberg model (one may also encounter the simpler, XX model, which excludes the interaction of one, usually S^Y, component), described by the Hamiltonian:

$$\hat{H} = -J \sum_{i=1}^{N} \left(\hat{S}_i^X \hat{S}_{i+1}^X + \hat{S}_i^Y \hat{S}_{i+1}^Y + \hat{S}_i^Z \hat{S}_{i+1}^Z \right)$$

with boundary conditions, which will be applied in the following considerations, that $N+1 \equiv 1$. The matrix form of this Hamiltonian for two spins in calculational basis reads ($\frac{\hbar}{2} \equiv 1$):

$$\hat{H} = \begin{bmatrix} -J & 0 & 0 & 0 \\ 0 & J & -2J & 0 \\ 0 & -2J & J & 0 \\ 0 & 0 & 0 & -J \end{bmatrix}$$

which translates to the following eigenvalues and eigenvectors:

$$E_1 = -J \qquad |\alpha_1\rangle = |\uparrow\uparrow\rangle$$

$$E_2 = -J \qquad |\alpha_2\rangle = |\downarrow\downarrow\rangle$$

$$E_3 = -J \qquad |\alpha_3\rangle = \frac{1}{\sqrt{2}} \left(|\uparrow\downarrow\rangle + |\downarrow\uparrow\rangle \right)$$

$$E_4 = 3J \qquad |\alpha_4\rangle = \frac{1}{\sqrt{2}} \left(|\uparrow\downarrow\rangle - |\downarrow\uparrow\rangle \right).$$

Using these eigenvalues and eigenvectors, the thermal state was prepared for numerical calculations; similar calculations were carried out for systems with a larger number of spins. The results of numerical calculations of the concurrence entanglement dependence on the exchange integrals and temperature are presented below, starting from a two- to eight-spin system. The calculations have been done for the nearest neighbours, next-nearest neighbours, and for next-next-nearest neighbours (the lower index of C in the chart title indicates the order of neighbours).

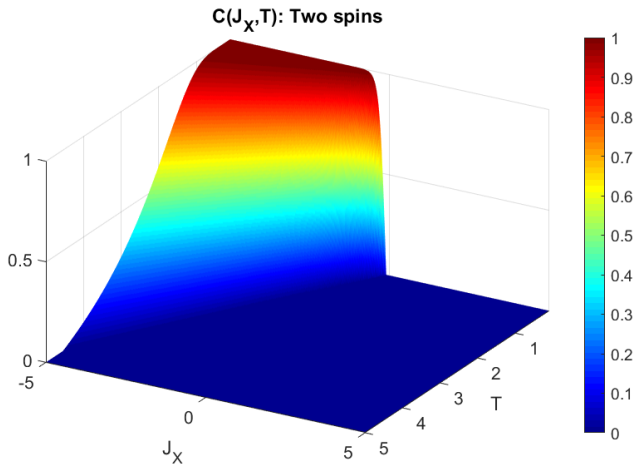

Figure 1: Entanglement concurrence as a function of exchange interaction and temperature in two-spin chain described by XXX Heisenberg model.

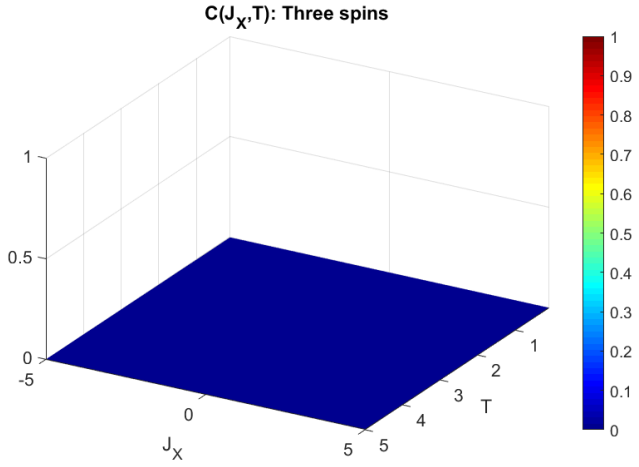

Figure 2: Entanglement concurrence between the nearest neighbours as a function of exchange interaction and temperature in a three-spin chain described by XXX Heisenberg model.

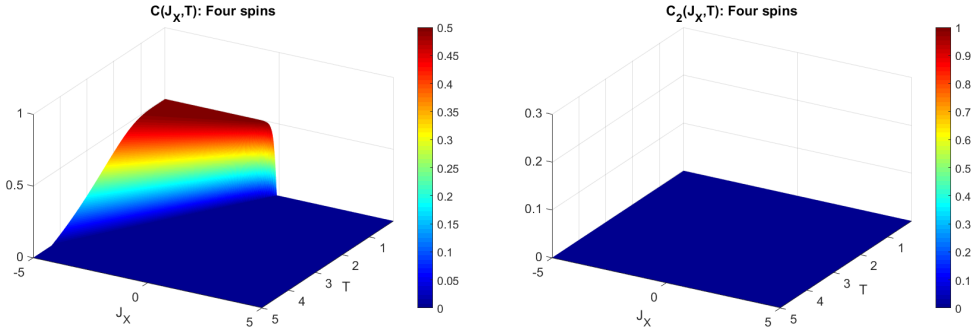

Figure 3: Entanglement concurrence between the nearest neighbours (left) and next-nearest neighbours (right) as a function of the exchange interaction and temperature in the four-spin chain.

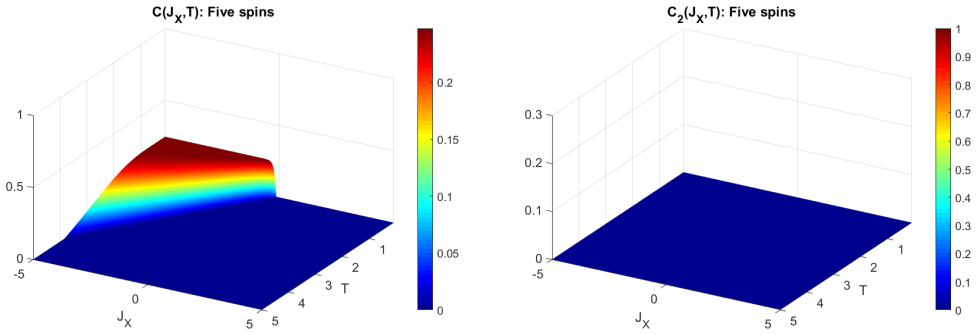

Figure 4: Entanglement concurrence between the nearest neighbours (left) and next-nearest neighbours (right) as a function of the exchange interaction and temperature in a five-spin chain.

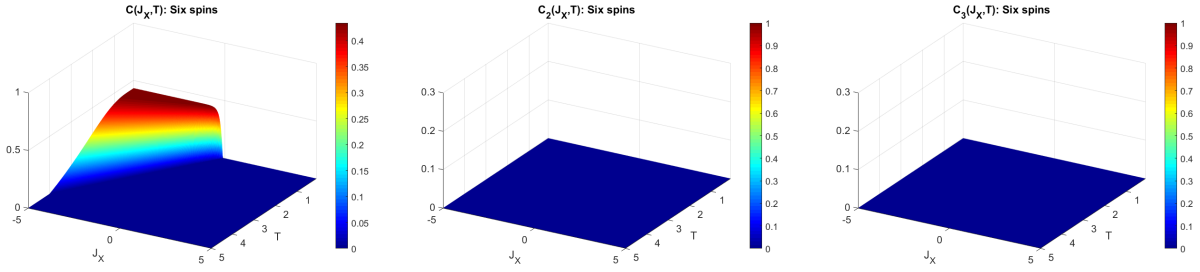

Figure 5: Entanglement concurrence between the nearest neighbours (left), next-nearest neighbours (center), and next-next-nearest neighbours (right) as a function of the exchange interaction and temperature in a six-spin chain.

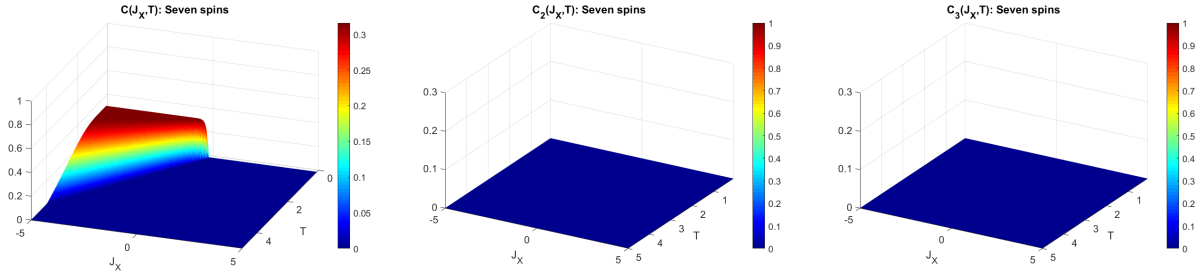

Figure 6: Entanglement concurrence between the nearest neighbours (left), next-nearest neighbours (center), and next-next-nearest neighbours (right) as a function of the exchange interaction and temperature in a seven-spin chain.

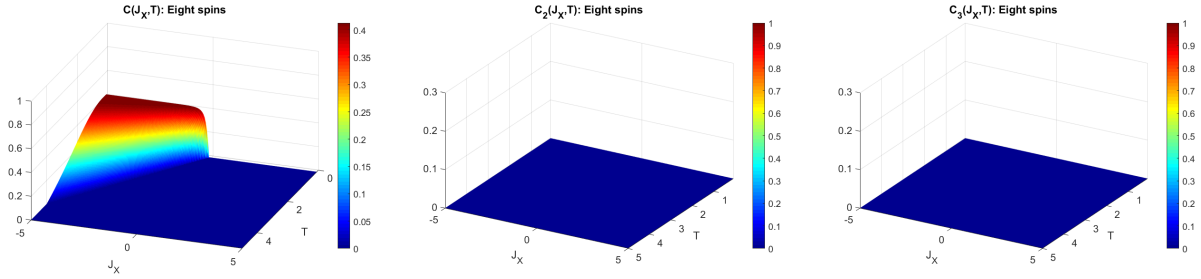

Figure 7: Entanglement concurrence between the nearest neighbours (left), next-nearest neighbours (center), and next-next-nearest neighbours (right) as a function of the exchange interaction and temperature in an eight-spin chain.

CONCLUSION: In the XXX model, the entanglement occurs only between the closest neighbours, and only for negative values of the exchange integral, which can be proven by applying the PPT condition to two spin case - for brevity, the following notation is used:

$$Z = 3 \cdot \exp\left(\frac{J}{k_B T}\right) + \exp\left(\frac{-3J}{k_B T}\right)$$

$$p_1 = \frac{1}{Z} \cdot \exp\left(\frac{J}{k_B T}\right) \qquad p_2 = \frac{1}{Z} \cdot \exp\left(\frac{-3J}{k_B T}\right)$$

so the thermal state can be simply expressed as:

$$\rho_T = \begin{bmatrix} p_1 & 0 & 0 & 0 \\ 0 & \frac{p_1+p_2}{2} & \frac{p_1-p_2}{2} & 0 \\ 0 & \frac{p_1+p_2}{2} & \frac{p_1-p_2}{2} & 0 \\ 0 & 0 & 0 & p_1 \end{bmatrix}.$$

The same matrix, after a partial transposition, reads:

$$\rho_T^{\Gamma} = \begin{bmatrix} p_1 & 0 & 0 & 0 \\ 0 & \frac{p_1+p_2}{2} & \frac{p_1-p_2}{2} & 0 \\ 0 & \frac{p_1+p_2}{2} & \frac{p_1-p_2}{2} & 0 \\ 0 & 0 & 0 & p_1 \end{bmatrix}.$$

Its partially transposed (with respect to the second subsystem) form reads:

$$\rho_T^{\Gamma} = \begin{bmatrix} p_1 & 0 & 0 & \frac{p_1-p_2}{2} \\ 0 & \frac{p_1+p_2}{2} & 0 & 0 \\ 0 & 0 & \frac{p_1+p_2}{2} & 0 \\ \frac{p_1-p_2}{2} & 0 & 0 & p_1 \end{bmatrix}$$

and will represent a separable state if and only if all its eigenvalues are positive. They are as follows - three of them are $\frac{p_1+p_2}{2}$, which are by definition positive, and $\frac{3p_1-p_2}{2}$ which is positive only when $p_1 > \frac{p_2}{3}$. This condition translates into the following inequality for the exchange integrals:

$$-\frac{1}{4}k_B T \cdot \ln(3) < J$$

which is satisfied for all positive J, and that corresponds to the ferromagnetic alignment of the spins. However, as we seek for nonseparable states, we need values that violate this statement - so the condition for entanglement reads:

$$J < -\frac{1}{4}k_B T \cdot \ln(3)$$

and holds only for antiferromagnetic materials, whose exchange interactions are strong enough to compensate for the entanglement decay due to temperature. Similar calculations can be repeated for other cases, leading to analogous conclusions.

For the even number of spins in the chain, the maximal entanglement decreases with the attachment of additional spins - see Figs. 1, 3, 5; for odd number, this entanglement increases (Figs. 2, 4), and both entanglements converge to a certain value for larger numbers of spin in the chain (Figs. 6, 7) - the explanation of this effect may be attributed to magnetic frustrations[1]. In antiferromagnetic spin chains with the odd number of spins (as its contribution will be larger in shorter spin chains and negligible in longer ones) and the parity effect, the phenomenon discussed in article [126], among others.

[1] In antiferromagnetic chain spins force on their neighbours the anti-parallel orientation - frustration occurs, when left neighbour of particular spin forces different orientation that the right one. It is a common phenomenon in spin chains with an odd number of nodes.

XXX HEISENBERG INTERACTIONS OF HIGHER ORDER:
To examine the effect of higher order exchange interaction in XXX Heisenberg model, the following Hamiltonian was postulated ($n > 1$):

$$\hat{H} = -J \sum_{i=1}^{N} \left(\hat{S}_i^X (\hat{S}_{i+1}^X - \frac{1}{n} \hat{S}_{i+2}^X) + \hat{S}_i^Y (\hat{S}_{i+1}^Y - \frac{1}{n} \hat{S}_{i+2}^Y) + \hat{S}_i^Z (\hat{S}_{i+1}^Z - \frac{1}{n} \hat{S}_{i+2}^Z) \right)$$

for 4 and 5 spins in the chain, and

$$\hat{H} = -J \sum_{i=1}^{N} \left(\hat{S}_i^X (\hat{S}_{i+1}^X - \frac{1}{n} \hat{S}_{i+2}^X + \frac{1}{n^2} \hat{S}_{i+3}^X) + \hat{S}_i^Y (\hat{S}_{i+1}^Y - \frac{1}{n} \hat{S}_{i+2}^Y + \frac{1}{n^2} \hat{S}_{i+3}^Y) \right.$$
$$\left. + \hat{S}_i^Z (\hat{S}_{i+1}^Z - \frac{1}{n} \hat{S}_{i+2}^Z + \frac{1}{n^2} \hat{S}_{i+3}^Z) \right)$$

for 6, 7 and 8. The parameter n scales the force of exchange interaction between neighbors of higher order, since the farther the spins are, the weaker they interact. The following results were obtained for $n = 2$ and $n = 4$:

- for n = 2:

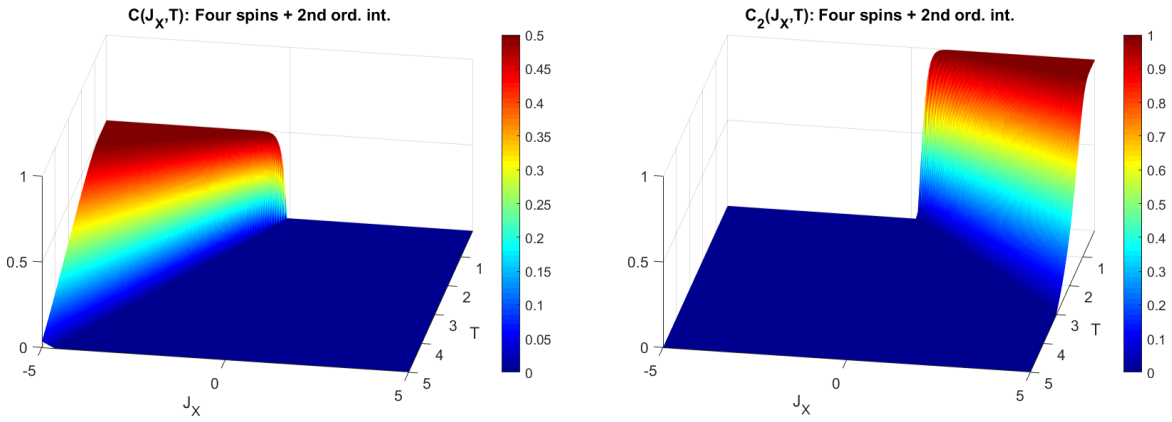

Figure 8: Entanglement concurrence between the nearest neighbours (left) and next-nearest neighbours (right) as a function of the exchange interaction and temperature in a four-spin chain described by XXX Heisenberg model with higher-order exchange interaction.

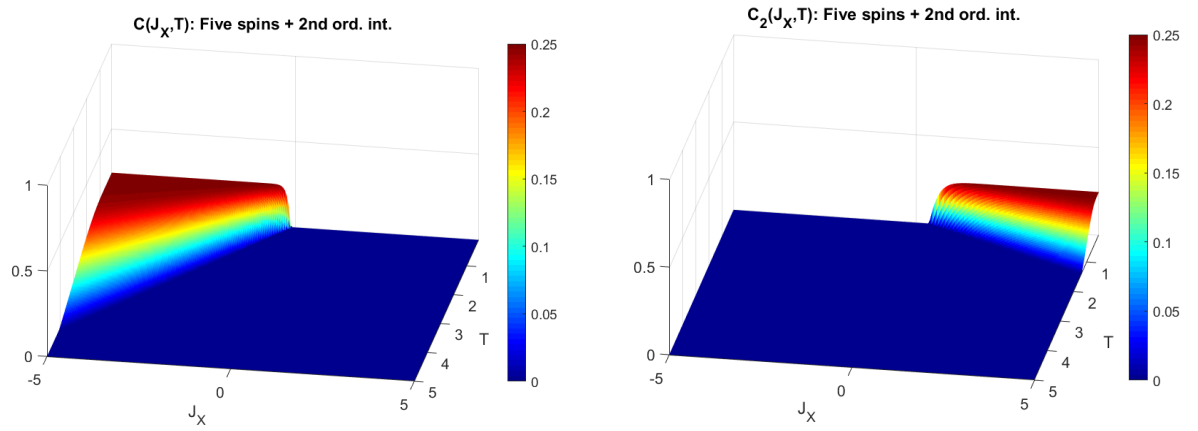

Figure 9: Entanglement concurrence between the nearest neighbours (left) and next-nearest neighbours (right) as a function of the exchange interaction and temperature in a five-spin chain described by XXX Heisenberg model with higher-order exchange interaction.

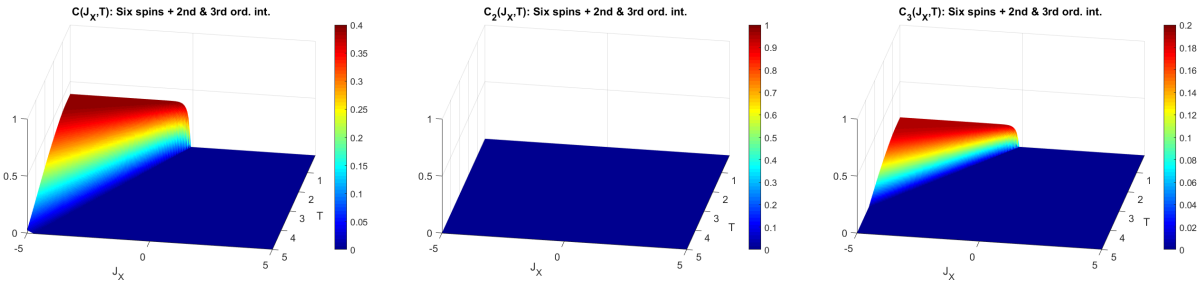

Figure 10: Entanglement concurrence between the nearest neighbours (left), next-nearest neighbours (center), and next-next nearest neighbours (right) as a function of the exchange interaction and temperature in a six-spin chain described by XXX Heisenberg model with higher-order exchange interaction.

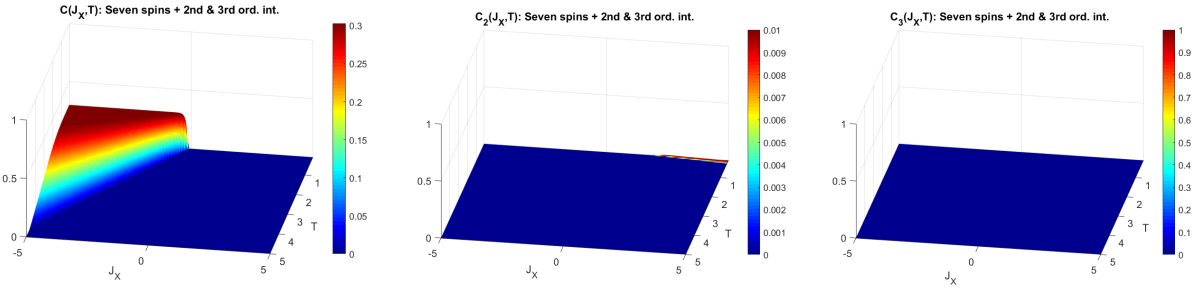

Figure 11: Entanglement concurrence between the nearest neighbours (left), next-nearest neighbours (center), and next-next nearest neighbours (right) as a function of the exchange interaction and temperature in a seven-spin chain described by XXX Heisenberg model with higher-order exchange interaction.

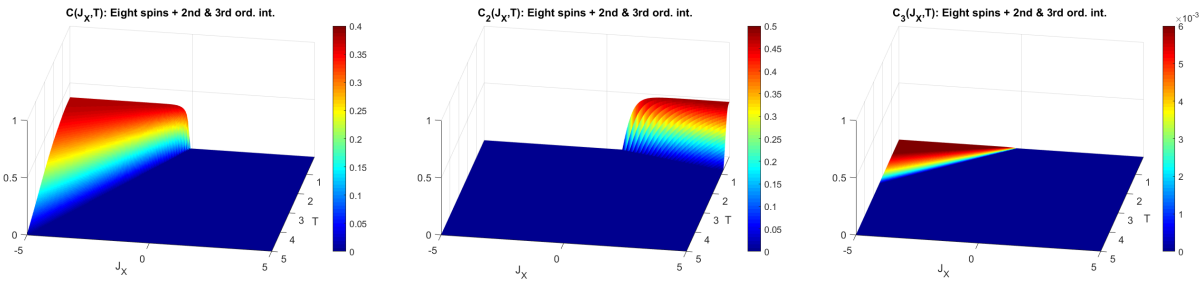

Figure 12: Entanglement concurrence between the nearest neighbours (left), next-nearest neighbours (center) and next-next nearest neighbours (right) as a function of exchange interaction and temperature in eight-spin chain described by XXX Heisenberg model with higher-order exchange interaction.

- for n = 4:

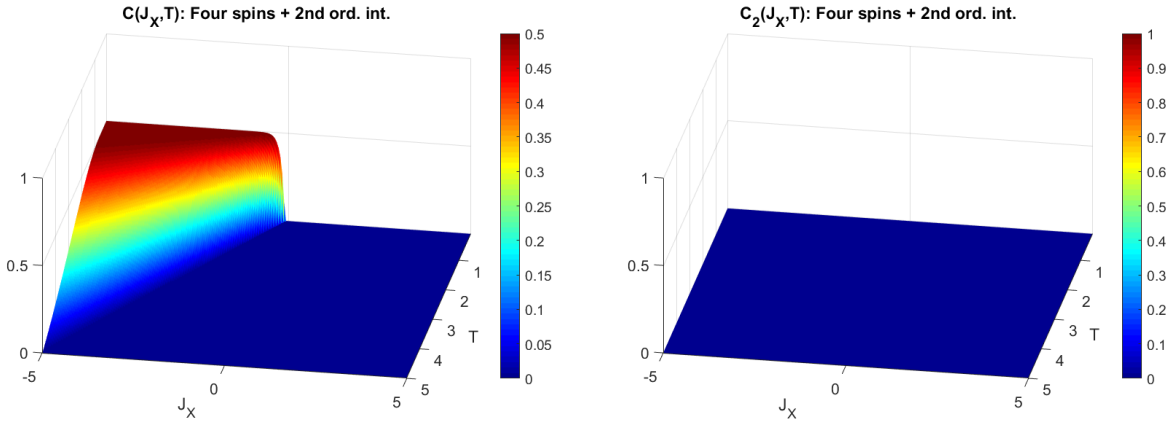

Figure 13: Entanglement concurrence between the nearest neighbours (left) and next-nearest neighbours (right) as a function of the exchange interaction and temperature in a four-spin chain described by XXX Heisenberg model with higher-order exchange interaction.

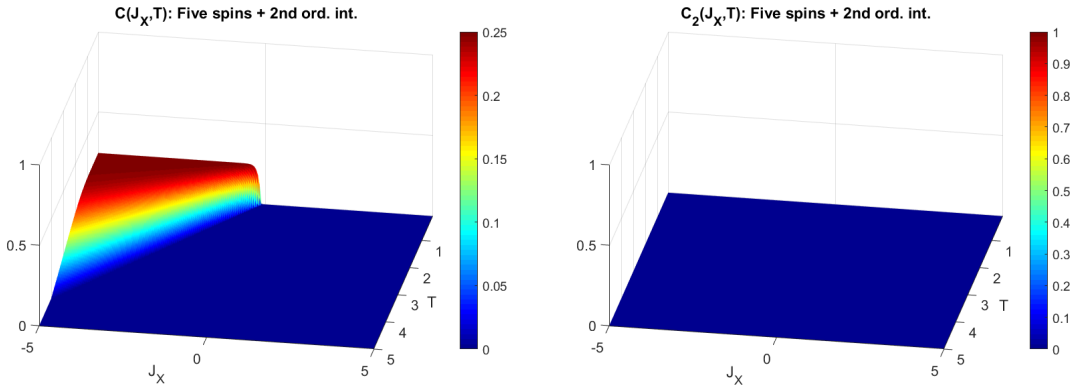

Figure 14: Entanglement concurrence between the nearest neighbours (left) and next-nearest neighbours (right) as a function of the exchange interaction and temperature in a five-spin chain described by XXX Heisenberg model with higher-order exchange interaction.

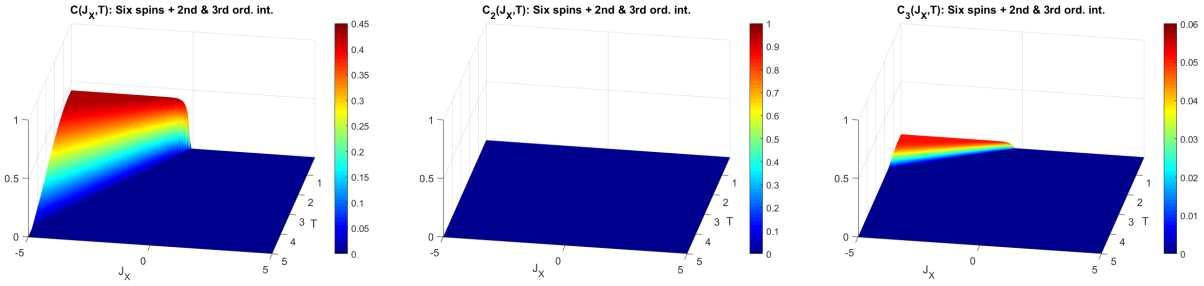

Figure 15: Entanglement concurrence between the nearest neighbours (left), next-nearest neighbours (center), and next-next nearest neighbours (right) as a function of the exchange interaction and temperature in a six-spin chain described by XXX Heisenberg model with higher-order exchange interaction.

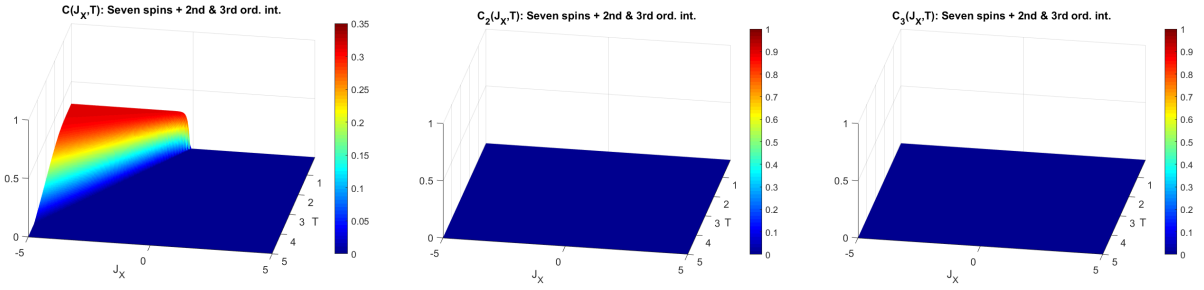

Figure 16: Entanglement concurrence between the nearest neighbours (left), next-nearest neighbours (center), and next-next nearest neighbours (right) as a function of the exchange interaction and temperature in a seven-spin chain described by XXX Heisenberg model with higher-order exchange interaction.

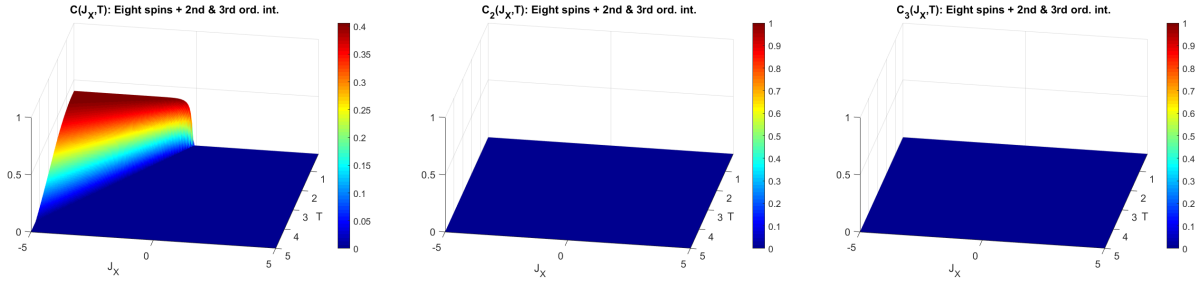

Figure 17: Entanglement concurrence between the nearest neighbours (left), next-nearest neighbours (center), and next-next nearest neighbours (right) as a function of the exchange interaction and temperature in an eight-spin chain described by XXX Heisenberg model with higher-order exchange interaction.

CONCLUSION: The introduction of higher-order exchange interaction has no impact on the entanglement between the nearest neighbors in the spin chain; however, it may lead to entanglement arising between next-nearest or further spins. For the next-nearest neighbours and small factor n, the entanglement occurs only for ferromagnetic ordering (positive exchange integral) (Figs. 8, 9, 12) - however, this entanglement is not present in a six-spin chain (Fig 10) and very weak in seven-spin (Fig. 11). For the next-next-nearest neighbors, once again the antiferromagnetic exchange integral provides the entanglement (Figs. 10, 12); however, this quantum correlation does not appear in the seven-spin chain. For a larger n factor, the entanglement between the next-nearest neighbors completely vanishes (Figs. 13 - 17) and between the next-next-nearest neighbors occurs only in a six-spin chain (Fig. 15) and is relatively low compared to its counterpart for smaller n.

DYNAMICS OF ENTANGLEMENT IN THE DISSIPATIVE ENVIRONMENT:

The results of numerical calculations of the loss of entanglement due to the interaction with the Markovian-type environment are presented in Figs. 18 - 20. State labeling follows the convention adopted in Section 4.1. As the chosen states are all eigenstates of XXX Hamiltonian, individual plots are not specified by the Hamiltonian parameters but by the dissipation rates. This is because Hamiltonian parameters are not significant for the evolution described by the Lindblad equation in this particular case.

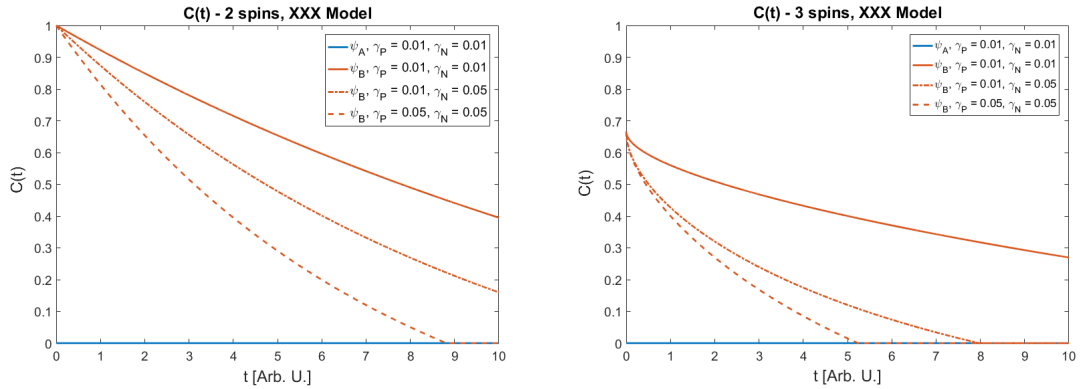

Figure 18: Time evolution of entanglement in two- (left) and three- (right) spin chains described by XXX Heisenberg model.

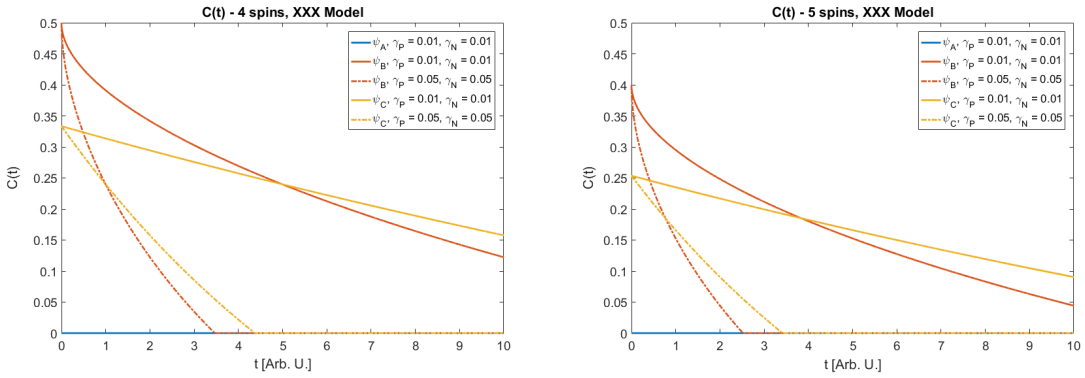

Figure 19: Time evolution of entanglement in four- (left) and five- (right) spin chains described by XXX Heisenberg model.

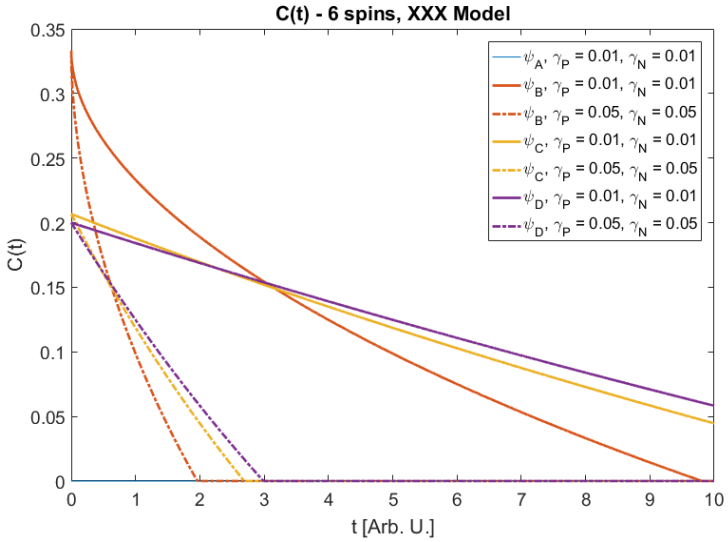

Figure 20: Time evolution of entanglement in six-spin chain described by XXX Heisenberg model.

CONCLUSION: As the states ψ_A represent the ferromagnetic ordering of the spins in the chain, all of them are characterized by zero entanglement and do not appear as a result of interactions with the environment. Analysis of the other states reveals that the highest initial entanglement is obtained for a single nonlocalized magnetic excitation in a chain; however, the closer the number of excitations is to the half of the whole chain number of spins, the slower the loss of entanglement is (Figs. 19, 20). This suggests that with a sufficiently long timescale of environment interaction, states with a large number of excitations will show a higher entanglement despite the initial entanglement being lower.

XXZ Heisenberg model

To carry out the analysis further, the next considered Hamiltonian is the one describing the anisotropic XXZ Heisenberg model:

$$\hat{H} = -J_X \sum_{i=1}^{N} \left(\hat{S}_i^X \hat{S}_{i+1}^X + \hat{S}_i^Y \hat{S}_{i+1}^Y \right) - J_Z \hat{S}_i^Z \hat{S}_{i+1}^Z,$$

which for two spins has the following matrix representation:

$$\hat{H} = \begin{bmatrix} -J_Z & 0 & 0 & 0 \\ 0 & J_Z & -2J_X & 0 \\ 0 & -2J_X & J_Z & 0 \\ 0 & 0 & 0 & -J_Z \end{bmatrix}$$

with the eigenvalues and eigenvectors shown below:

$$E_1 = -J_Z \qquad |\alpha_1\rangle = |\uparrow\uparrow\rangle$$

$$E_2 = -J_Z \qquad |\alpha_2\rangle = |\downarrow\downarrow\rangle$$

$$E_3 = J_Z - 2J_X \qquad |\alpha_3\rangle = \frac{1}{\sqrt{2}}\left(|\uparrow\downarrow\rangle + |\downarrow\uparrow\rangle\right)$$

$$E_4 = J_Z + 2J_X \qquad |\alpha_4\rangle = \frac{1}{\sqrt{2}}\left(|\uparrow\downarrow\rangle - |\downarrow\uparrow\rangle\right).$$

The results of numerical calculations of the entanglement concurrence for the spin chains containing different number of spins are shown by colour maps below:

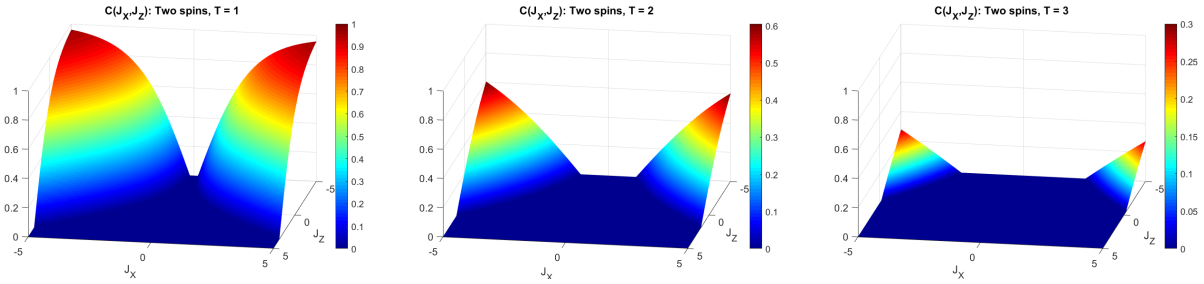

Figure 21: Entanglement concurrence as a function of J_X and J_Z integrals of XXZ Heisenberg model in two-spin chain, for various temperatures.

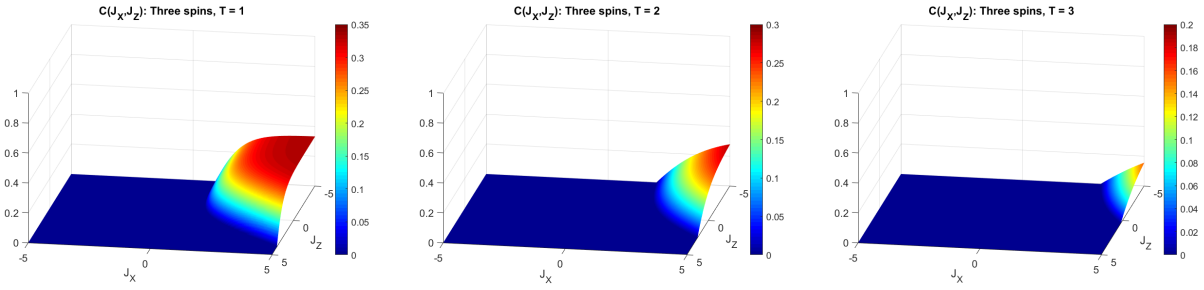

Figure 22: Entanglement concurrence as a function of J_X and J_Z integrals of XXZ Heisenberg model in a three-spin chain, for various temperatures.

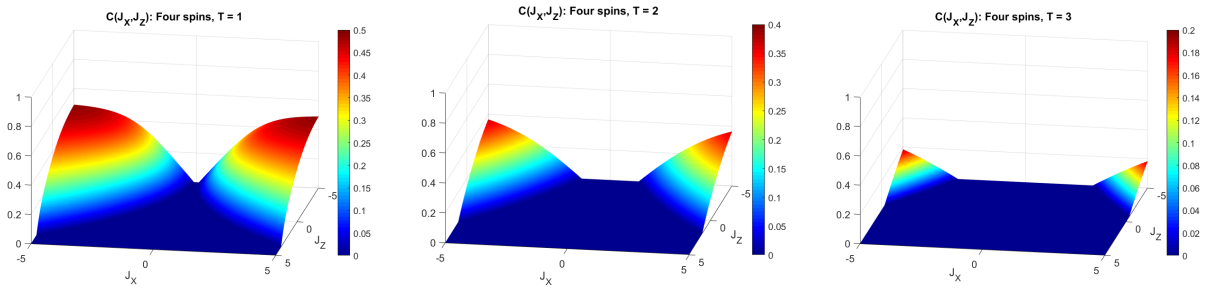

Figure 23: Entanglement concurrence as a function of J_X and J_Z integrals of XXZ Heisenberg model in a four-spin chain, for various temperatures.

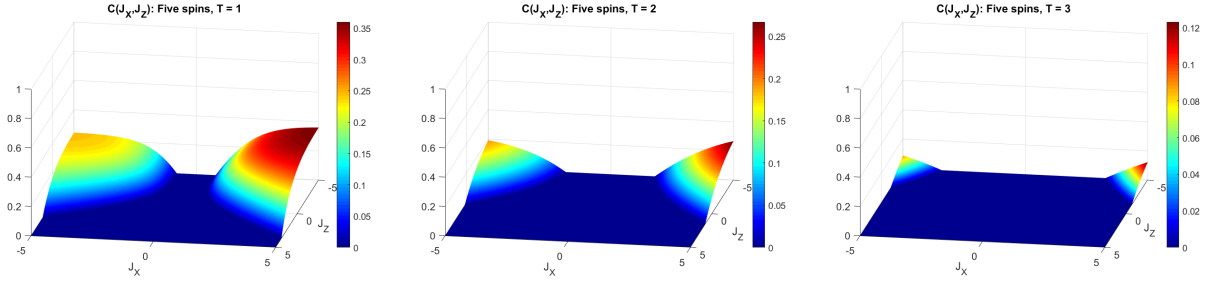

Figure 24: Entanglement concurrence as a function of J_X and J_Z integrals of XXZ Heisenberg model in a five-spin chain, for various temperatures.

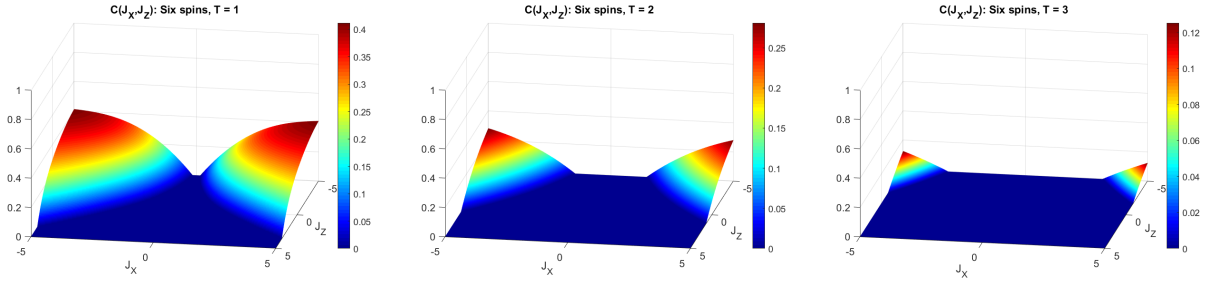

Figure 25: Entanglement concurrence as a function of J_X and J_Z integrals of XXZ Heisenberg model in a six-spin chain, for various temperatures.

CONCLUSION: As it was stated before, the temperature has a negative effect on the entanglement and this trend will continue throughout the catalog. For the even number of spins in the chain described by the XXZ Heisenberg model (Figs. 21, 23, 25), the J_X sign has no impact on the entanglement - only its magnitude has, so the higher this parameter is, the higher the entanglement concurrence. However, for the odd number of spins (Figs. 22 and 24), the preferable sign of the J_X integral is positive - the chains with the positive J_X factor, in general, are characterized by higher entanglement degree than systems with negative J_X - this feature nevertheless disappears for longer spin chains and the disproportion between the entanglement for the positive and negative exchange integrals J_X vanishes. Higher entanglement in the thermal state occurs for the systems with a negative J_Z sign; it may however still be non-zero for the systems with a small positive J_Z, depending on temperature and J_X value.

DYNAMICS OF ENTANGLEMENT IN THE DISSIPATIVE ENVIRONMENT:

The figures below illustrate the time evolution of the nearest-neighbors entanglement in spin chains interacting with the Markovian environment:

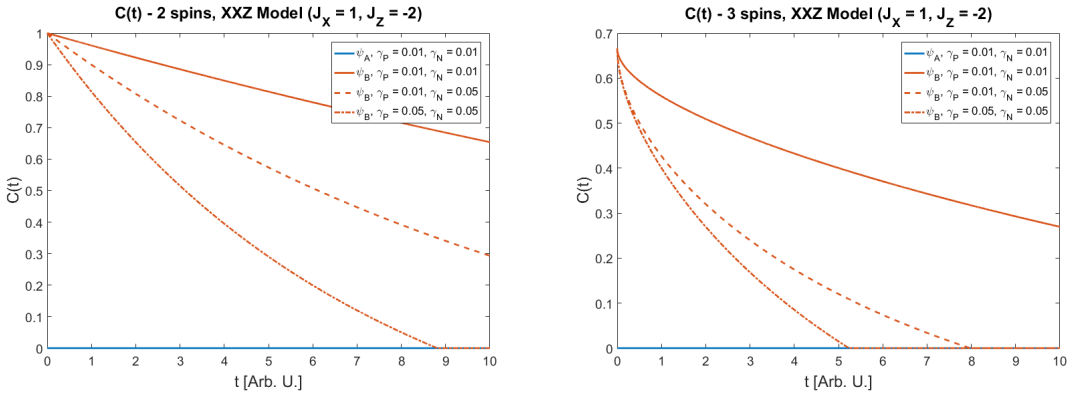

Figure 26: Time evolution of entanglement in two- (left) and three- (right) spin chains described by XXZ Heisenberg model.

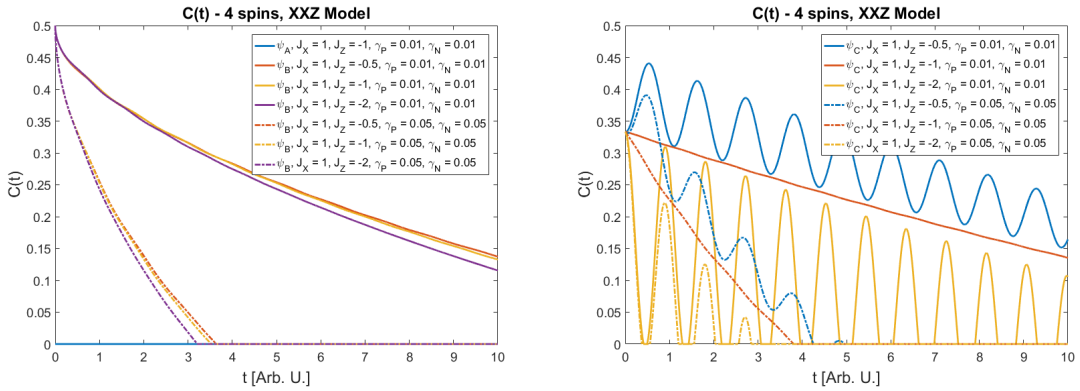

Figure 27: Time evolution of entanglement in four-spin chain described by XXZ Heisenberg model.

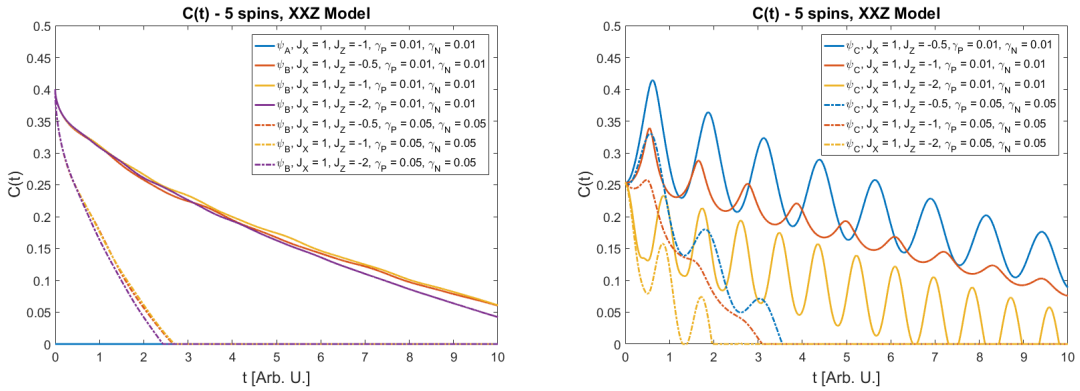

Figure 28: Time evolution of entanglement in five-spin chain described by XXZ Heisenberg model.

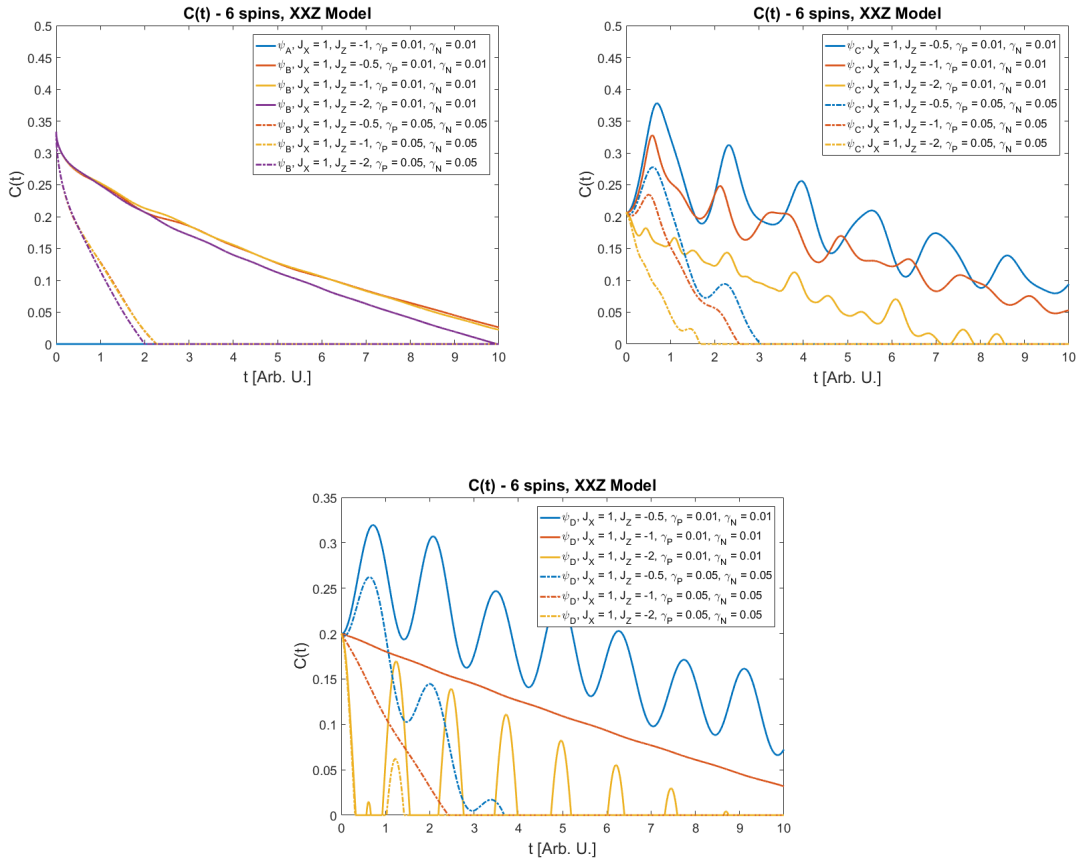

Figure 29: Time evolution of entanglement in six-spin chain described by XXZ Heisenberg model.

CONCLUSION: The plots above clearly indicate that the most decoherence resistant layout for the spin chain occurs when the J_Z exchange integral is lower in magnitude than its X-direction counterpart J_X (previous investigation imposed a sign of the exchange integrals - the highest entanglement occurs for systems with positive J_X and negative J_Z values). However, this property reveals itself fully for the initial state with more than one magnetic excitation (Figs. 27 - 29) - while it is present in states with one flipped spin, the difference between the individual values of J_Z is insignificant. In states with two or three flipped spins for J_Z/J_X = -0.5 higher values of entanglement are observed during its decay in comparison to, for example, J_Z/J_X = -1; although it is worth noticing that in this case the entanglement decays more stably.

XYZ Heisenberg model

In the most general case, all spin components interact with their counterparts with different exchange integrals. This is the idea behind the XYZ Heisenberg model - Hamiltonian in question is:

$$\hat{H} = \sum_{i=1}^{N} \left(-J_X \hat{S}_i^X \hat{S}_{i+1}^X - J_Y \hat{S}_i^Y \hat{S}_{i+1}^Y - J_Z \hat{S}_i^Z \hat{S}_{i+1}^Z \right),$$

which, in the case of two spins, can be represented by the following matrix:

$$\hat{H} = \begin{bmatrix} -J_Z & 0 & 0 & J_Y - J_X \\ 0 & J_Z & -J_X - J_Y & 0 \\ 0 & -J_X - J_Y & J_Z & 0 \\ J_Y - J_X & 0 & 0 & J_Z \end{bmatrix}.$$

As one can see below, all the eigenvectors are maximally entangled - however, the thermal state in general is a mixed one, so it may not be entangled:

$$E_1 = J_Y - J_X - J_Z \qquad |\alpha_1\rangle = \frac{1}{\sqrt{2}} \left(|\uparrow\uparrow\rangle + |\downarrow\downarrow\rangle \right)$$

$$E_2 = J_X - J_Y - J_Z \qquad |\alpha_2\rangle = \frac{1}{\sqrt{2}} \left(|\uparrow\uparrow\rangle - |\downarrow\downarrow\rangle \right)$$

$$E_3 = J_Z - J_X - J_Y \qquad |\alpha_3\rangle = \frac{1}{\sqrt{2}} \left(|\uparrow\downarrow\rangle + |\downarrow\uparrow\rangle \right)$$

$$E_4 = J_Z + J_X + J_Y \qquad |\alpha_4\rangle = \frac{1}{\sqrt{2}} \left(|\uparrow\downarrow\rangle - |\downarrow\uparrow\rangle \right).$$

The results of the numerical calculations of entanglement concurrence in the thermal state vary for different sets of exchange integrals. In the form of the colormaps, they are presented in Figs. 30 - 39. Since it is already established that temperature has a negative impact on entanglement, from now on it will be set to 1 in an arbitrarily unit system:

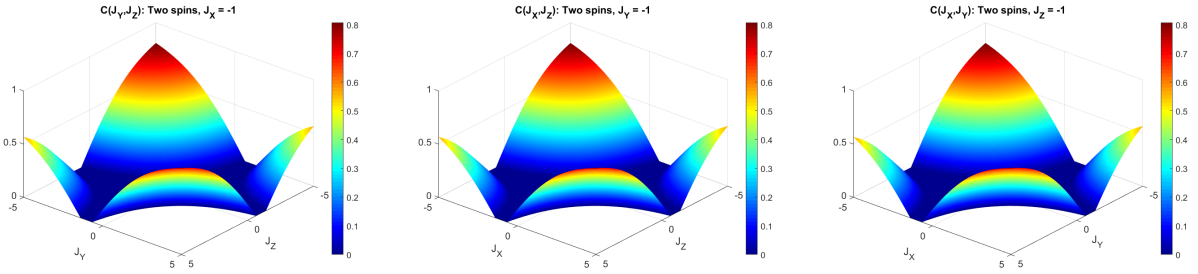

Figure 30: Entanglement concurrence as a function of: J_Y and J_Z exchange integral at $J_X = -1$ (left), J_X and J_Z exchange integral at $J_Y = -1$ (center) and J_X and J_Y exchange integral at $J_Z = -1$ (right), all for two-spin chain.

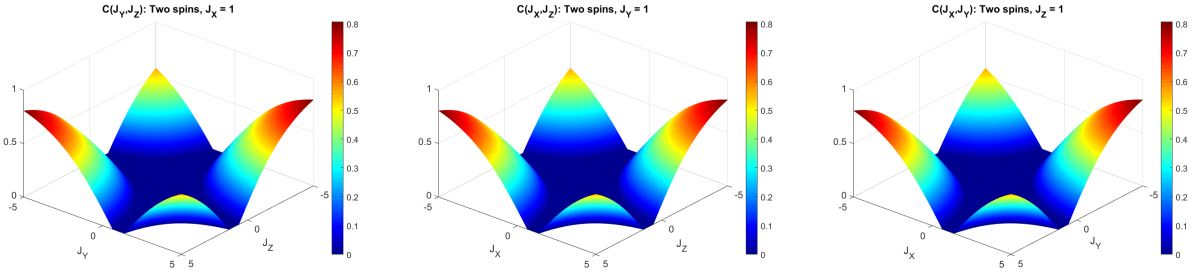

Figure 31: Entanglement concurrence as a function of: J_Y and J_Z exchange integral at $J_X = 1$ (left), J_X and J_Z exchange integral at $J_Y = 1$ (center) and J_X and J_Y exchange integral at $J_Z = 1$ (right), all for two-spin chain.

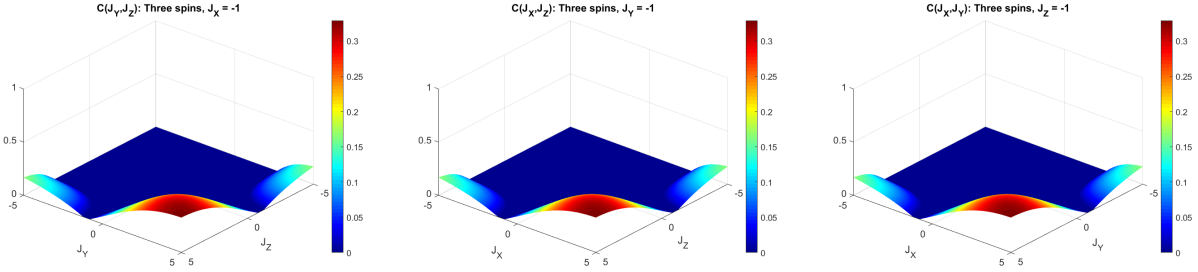

Figure 32: Entanglement concurrence as a function of: J_Y and J_Z exchange integral at $J_X = -1$ (left), J_X and J_Z exchange integral at $J_Y = -1$ (center) and J_X and J_Y exchange integral at $J_Z = -1$ (right), all for three-spin chain.

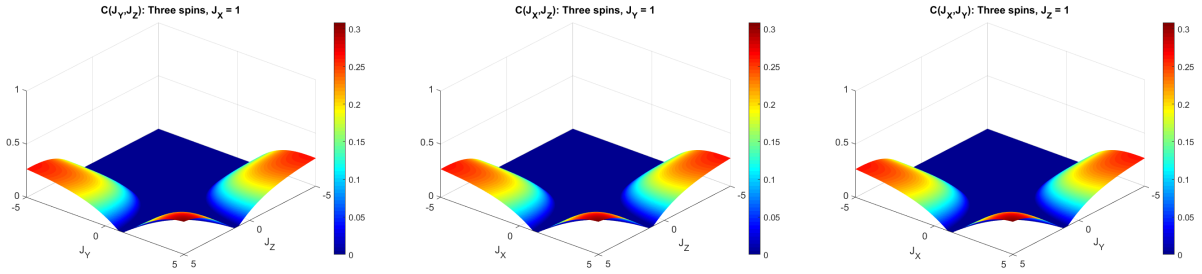

Figure 33: Entanglement concurrence as a function of: J_Y and J_Z exchange integral at $J_X = 1$ (left), J_X and J_Z exchange integral at $J_Y = 1$ (center) and J_X and J_Y exchange integral at $J_Z = 1$ (right), all for three-spin chain.

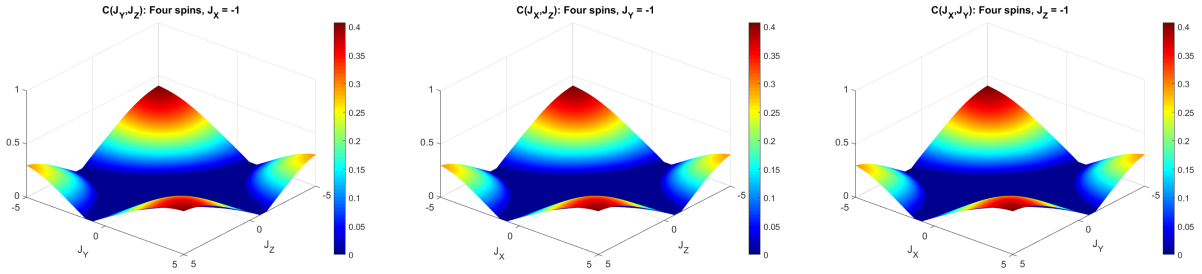

Figure 34: Entanglement concurrence as a function of: J_Y and J_Z exchange integral at $J_X = -1$ (left), J_X and J_Z exchange integral at $J_Y = -1$ (center) and J_X and J_Y exchange integral at $J_Z = -1$ (right), all for four-spin chain.

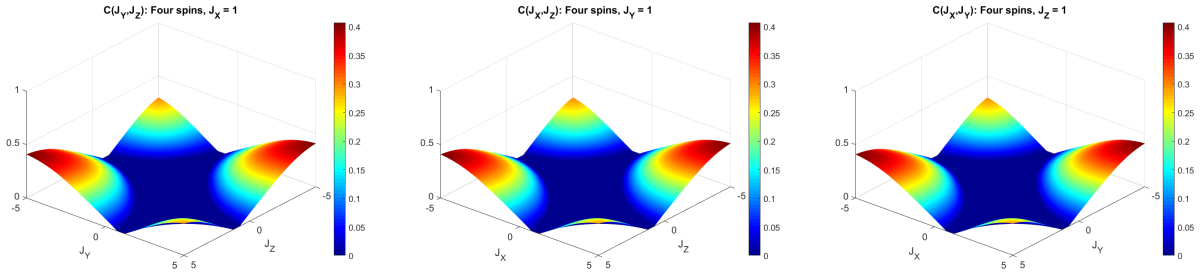

Figure 35: Entanglement concurrence as a function of: J_Y and J_Z exchange integral at $J_X = 1$ (left), J_X and J_Z exchange integral at $J_Y = 1$ (center) and J_X and J_Y exchange integral at $J_Z = 1$ (right), all for four-spin chain.

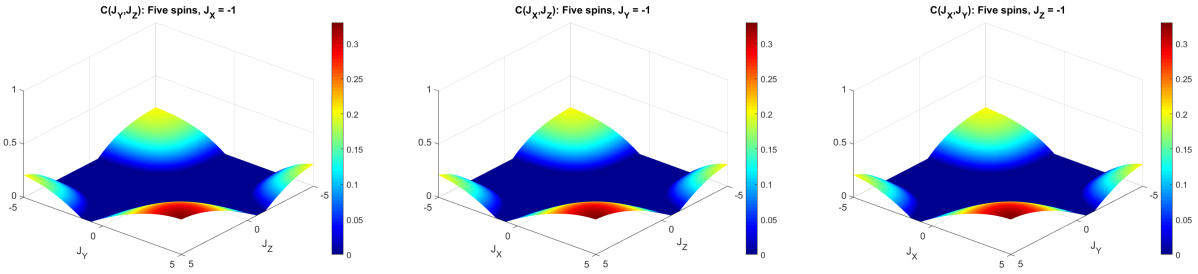

Figure 36: Entanglement concurrence as a function of: J_Y and J_Z exchange integral at $J_X = -1$ (left), J_X and J_Z exchange integral at $J_Y = -1$ (center) and J_X and J_Y exchange integral at $J_Z = -1$ (right), all for five-spin chain.

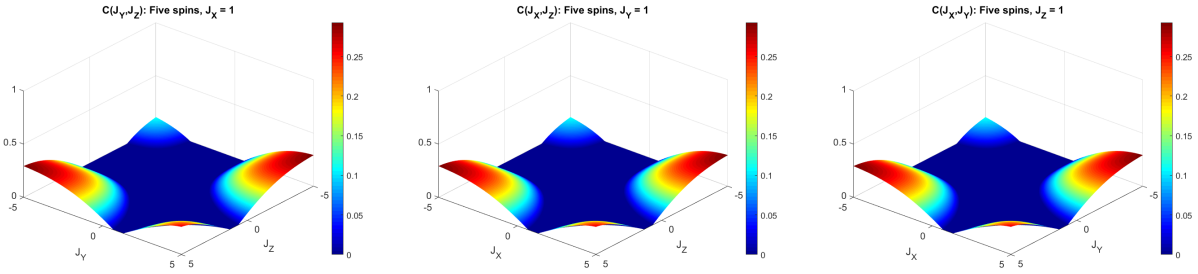

Figure 37: Entanglement concurrence as a function of: J_Y and J_Z exchange integral at $J_X = 1$ (left), J_X and J_Z exchange integral at $J_Y = 1$ (center) and J_X and J_Y exchange integral at $J_Z = 1$ (right), all for five-spin chain.

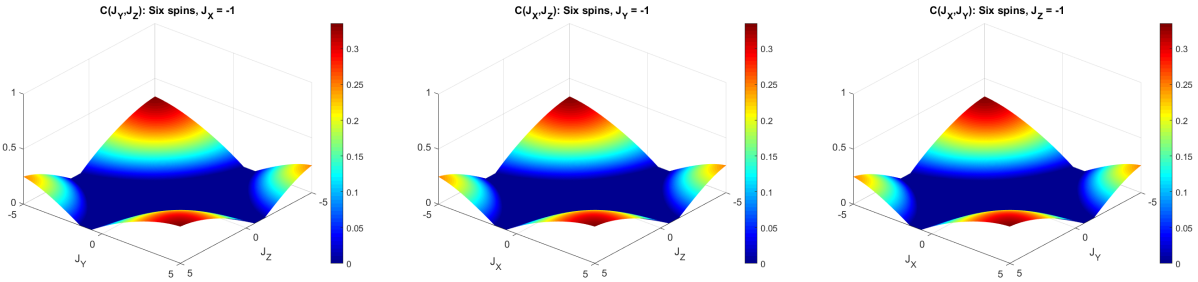

Figure 38: Entanglement concurrence as a function of: J_Y and J_Z exchange integral at $J_X = -1$ (left), J_X and J_Z exchange integral at $J_Y = -1$ (center) and J_X and J_Y exchange integral at $J_Z = -1$ (right), all for six-spin chain.

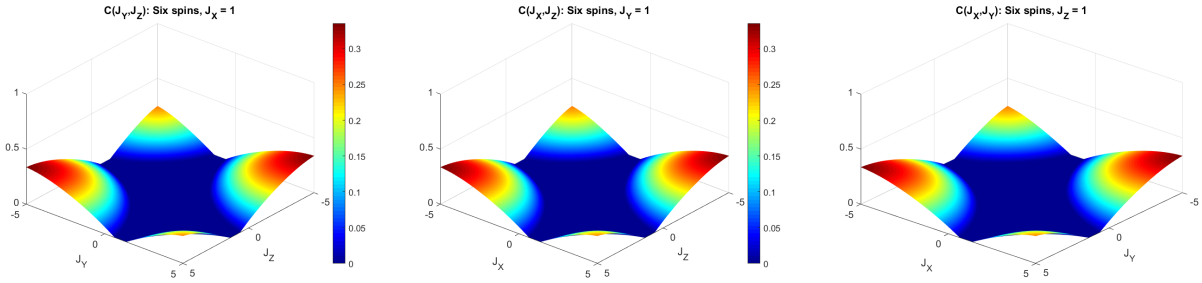

Figure 39: Entanglement concurrence as a function of: J_Y and J_Z exchange integral at $J_X = 1$ (left), J_X and J_Z exchange integral at $J_Y = 1$ (center) and J_X and J_Y exchange integral at $J_Z = 1$ (right), all for six-spin chain.

CONCLUSION: In the case of the XYZ model and the even number of spins in the chain, it can be found that the most favorable situation in terms of high entanglement occurs when the product of all directional exchange integrals is negative, $J_X \cdot J_Y \cdot J_Z < 0$ (compare Figs. 30, 31, 34 and so on). However, for a positive product of integrals, the entanglement is considerably lower but still present. As expected, the entanglement favors higher values of the exchange integrals. For the odd number of spins slightly different effects can be observed: the highest entanglement occurs for the system with all exchange integrals positive (see, for example, Fig. 32), one negative integral and two positive results in lower entanglement, and the lowest appears in systems with two or three negative exchange integrals (Figs. 36, 37). An increase in number of spins eliminates this discrepancy and causes similar entanglement to occur in systems with high exchange integrals, regardless of their signs (compare Figs. 36 and 38 or 37 with 39).

DYNAMICS OF ENTANGLEMENT IN THE DISSIPATIVE ENVIRONMENT:
In order to study the entanglement dynamics in a dissipative environment, several different Hamiltonians were used. However, as a compromise between the conciseness of the thesis and results diversity, only the following three generic, characterized by the corresponding parameters were selected to represent the most characteristic features of entanglement dynamics:

$$H_A: \ J_X = 0.5; \ J_Y = -2; \ J_Z = 1$$

$$H_B: \ J_X = 1; \ J_Y = 0.5; \ J_Z = -2$$

$$H_C: \ J_X = -0.5; \ J_Y = 1; \ J_Z = 2$$

There are two technicalities to note:

- plots for H_B and H_C for $\gamma_P = \gamma_N$ are not shown in Figure 40 - they overlap the plot for H_A;
- timescale on the upper left plot in Fig. 44 is shortened - after total decay of entanglement it never appears again, so the decision was made to clearly show the divergence of the plots for different decoherence parameters - similarly, the times were shortened in figures 46 and in the lower part of 47.

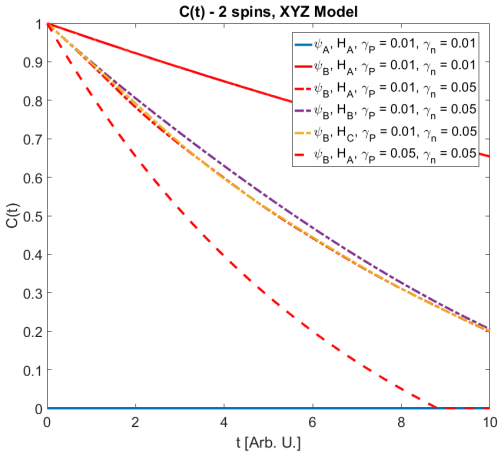

Figure 40: Time evolution of entanglement in two-spin chain described by XYZ Heisenberg model, for various exchange parameters.

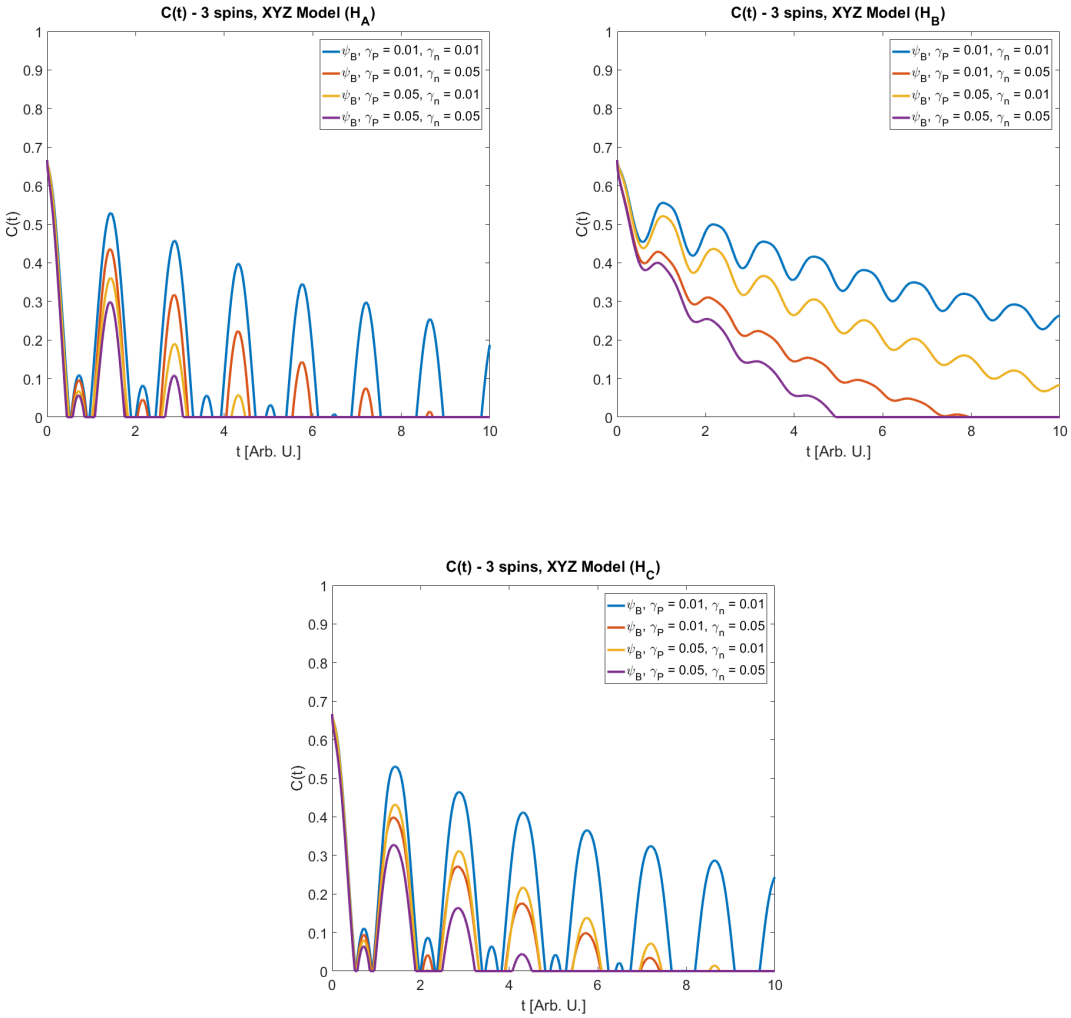

Figure 41: Time evolution of entanglement in three-spin chain described by XYZ Heisenberg model, for Hamiltonian H_A (left upper plot), Hamiltonian H_B (right upper plot) and Hamiltonian H_C (lower plot).

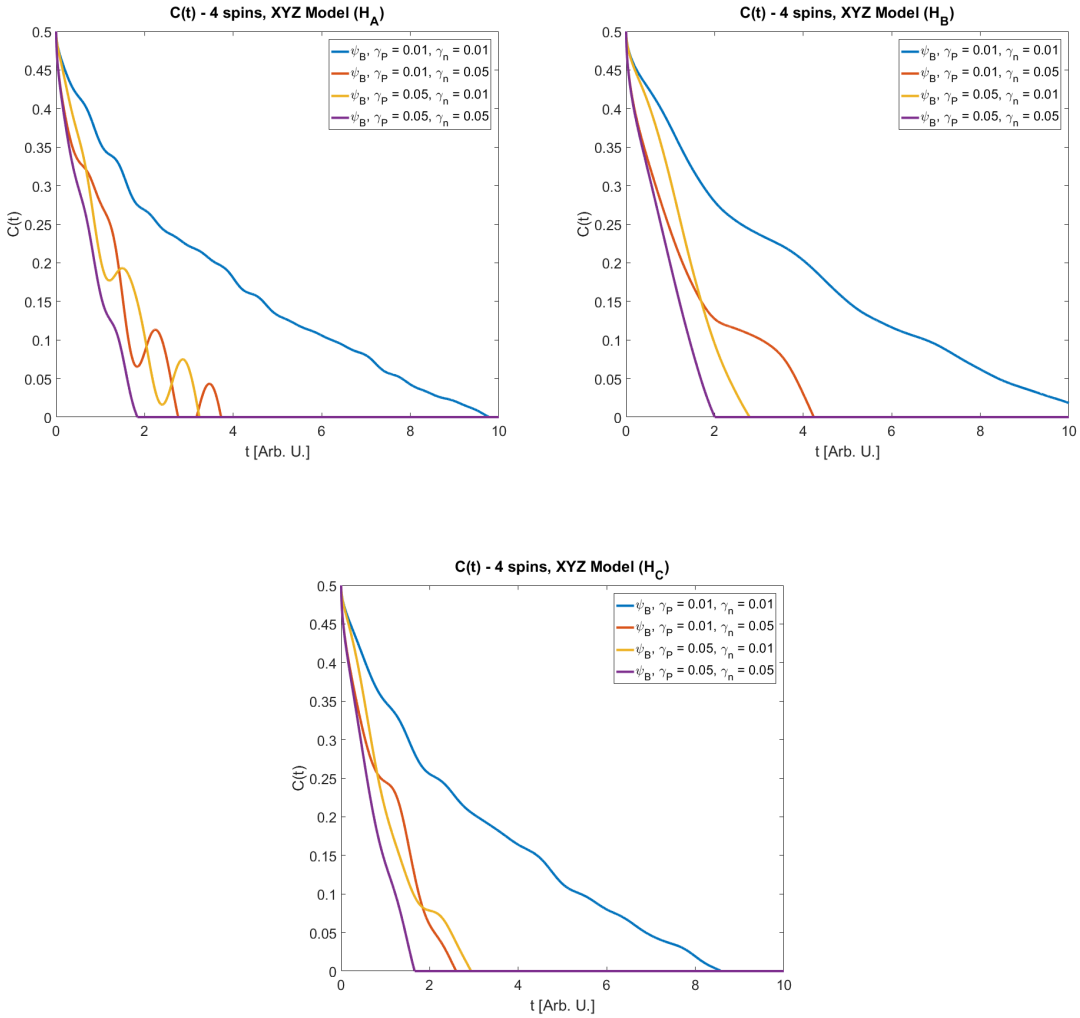

Figure 42: Time evolution of entanglement in four-spin chain described by XYZ Heisenberg model, for Hamiltonian H_A (left upper plot), Hamiltonian H_B (right upper plot) and Hamiltonian H_C (lower plot) for initial state ψ_B.

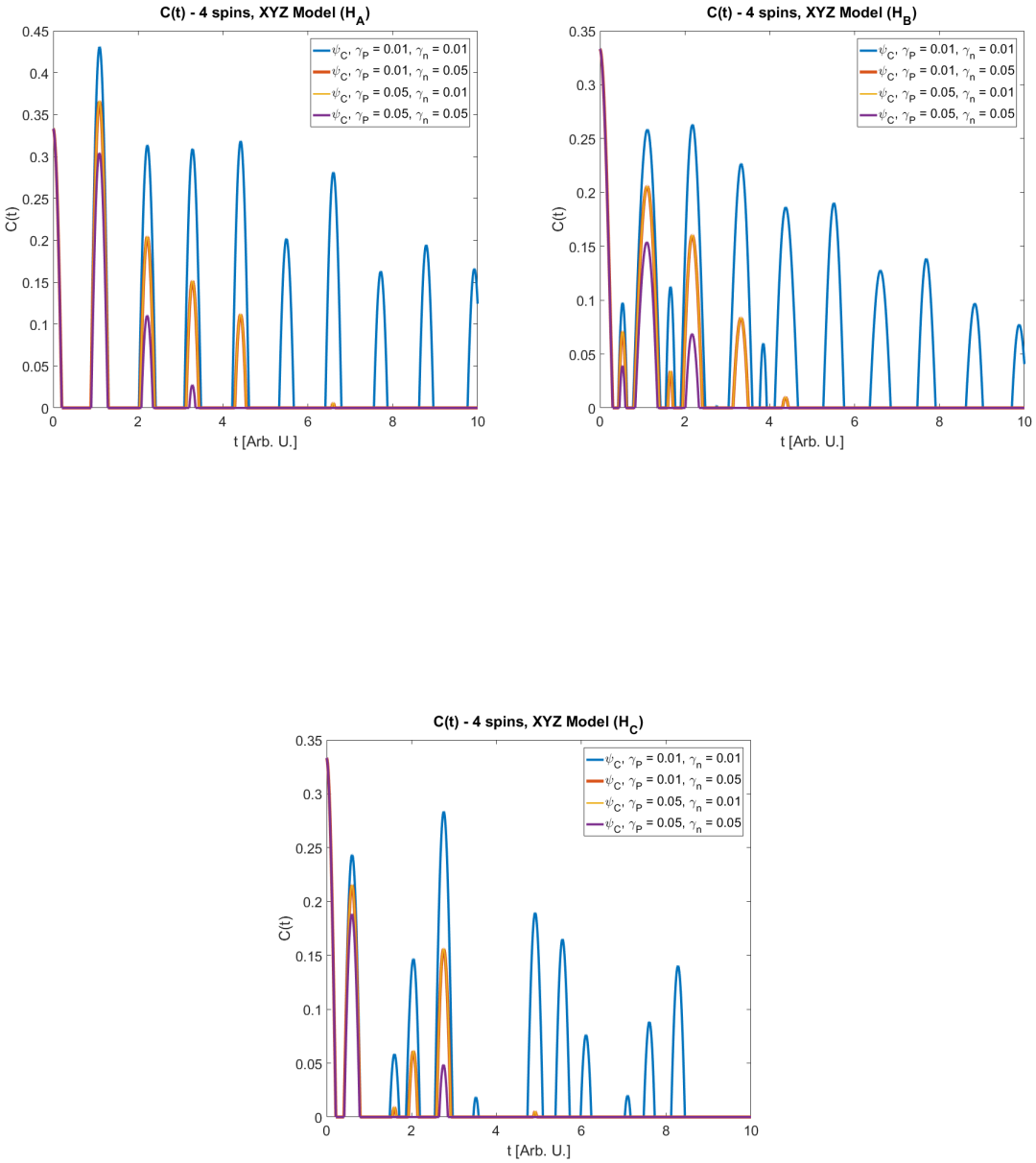

Figure 43: Time evolution of entanglement in four-spin chain described by XYZ Heisenberg model, for Hamiltonian H_A (left upper plot), Hamiltonian H_B (right upper plot) and Hamiltonian H_C (lower plot) for initial state ψ_C.

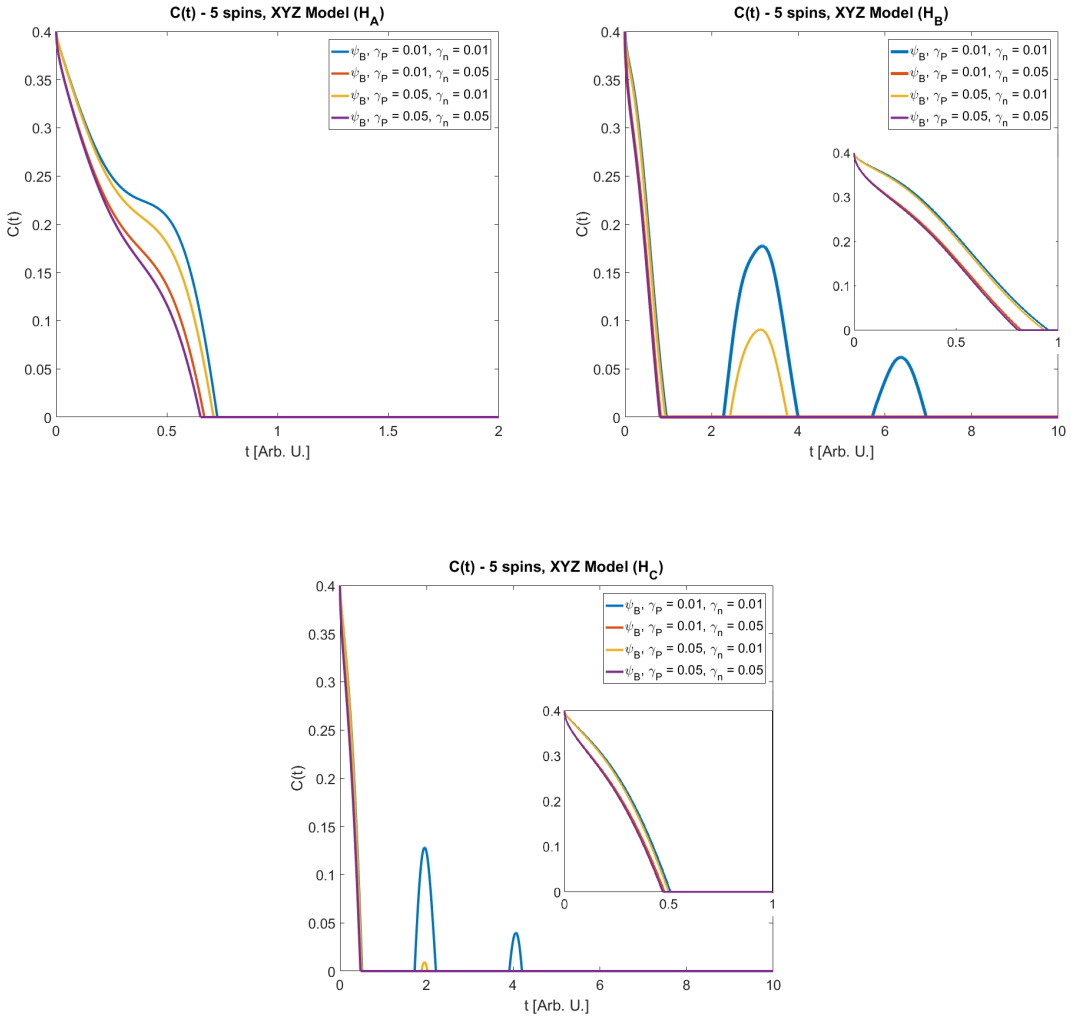

Figure 44: Time evolution of entanglement in five-spin chain described by XYZ Heisenberg model, for Hamiltonian H_A (left upper plot), Hamiltonian H_B (right upper plot) and Hamiltonian H_C (lower plot) for initial state ψ_B.

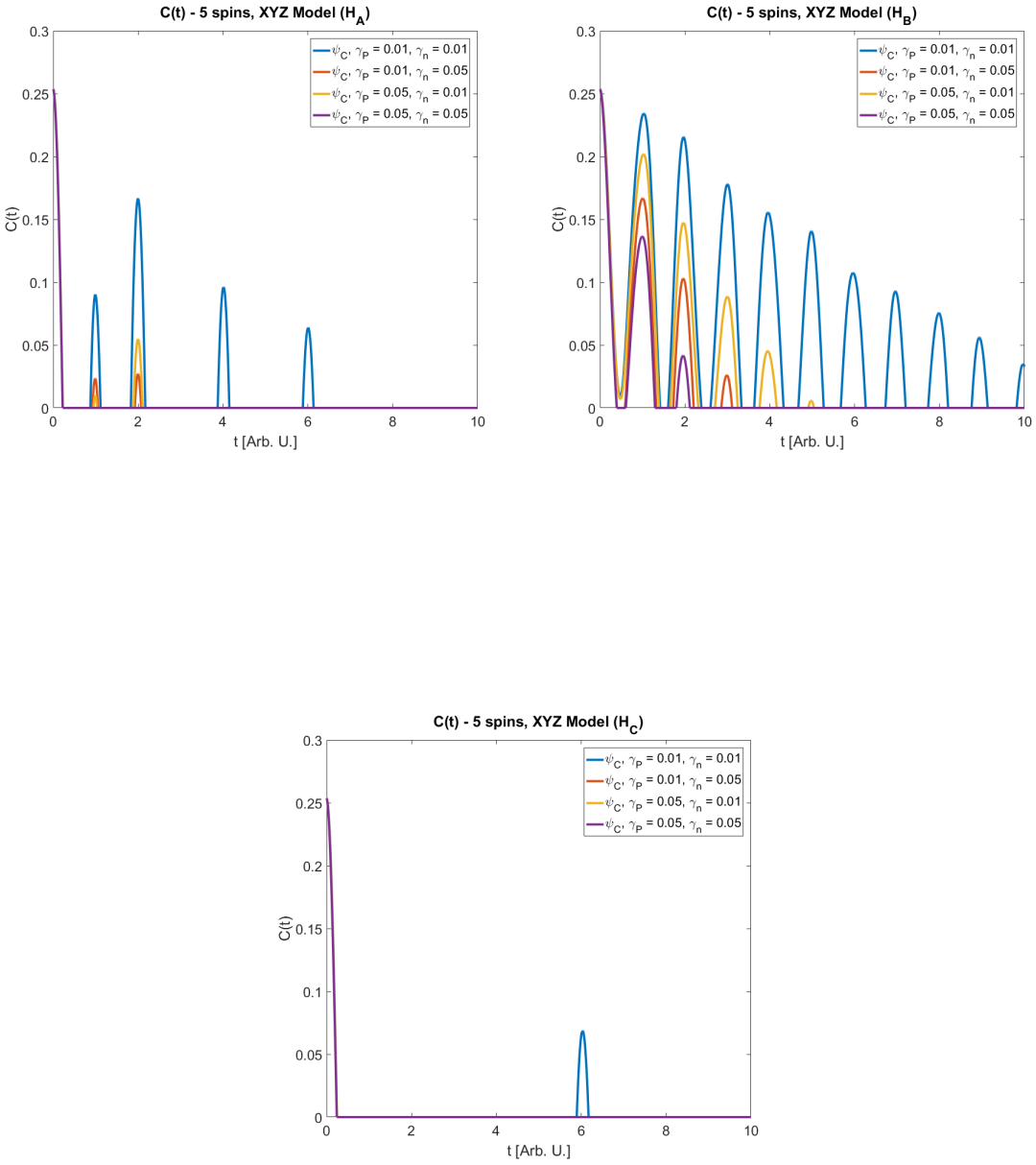

Figure 45: Time evolution of entanglement in five-spin chain described by XYZ Heisenberg model, for Hamiltonian H_A (left upper plot), Hamiltonian H_B (right upper plot) and Hamiltonian H_C (lower plot) for initial state ψ_C.

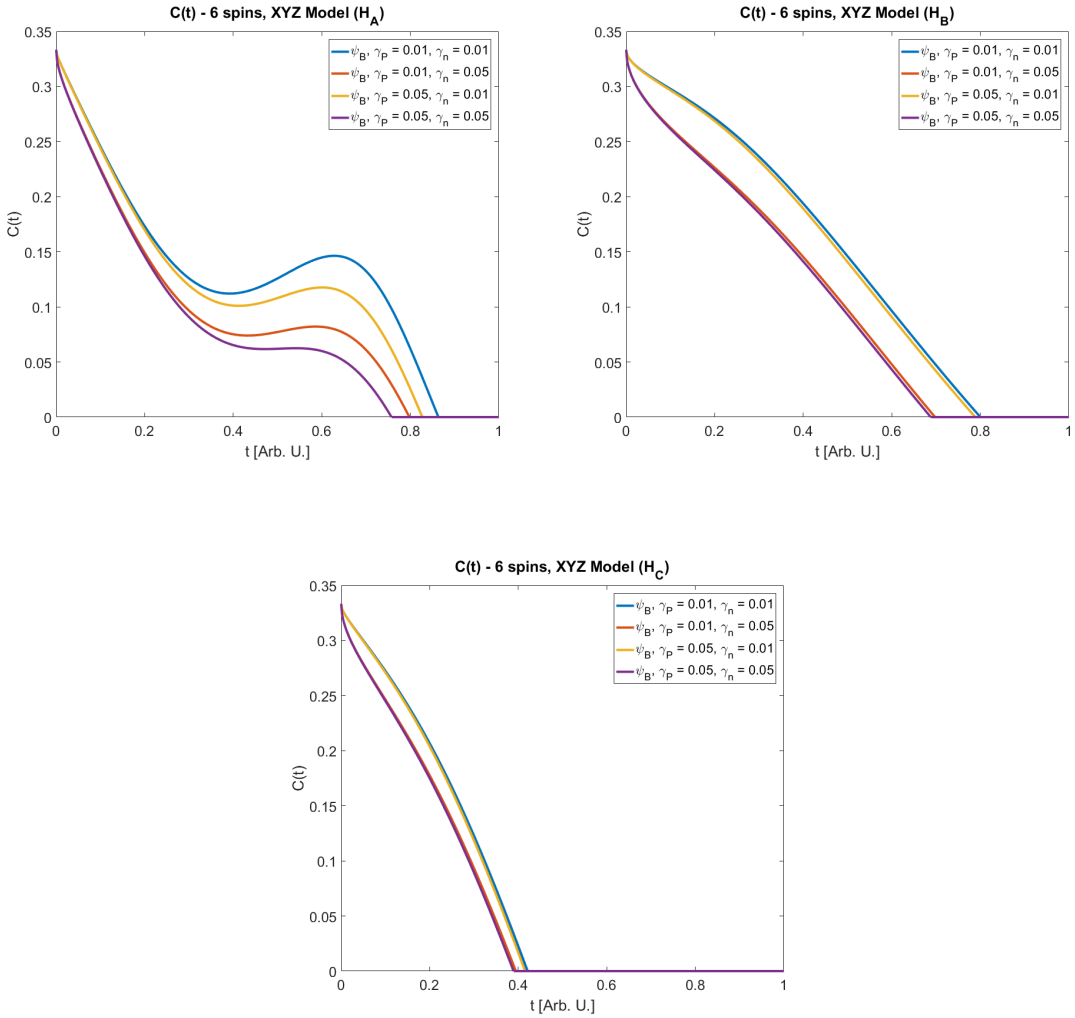

Figure 46: Time evolution of entanglement in six-spin chain described by XYZ Heisenberg model, for Hamiltonian H_A (left upper plot), Hamiltonian H_B (right upper plot) and Hamiltonian H_C (lower plot) for initial state ψ_B.

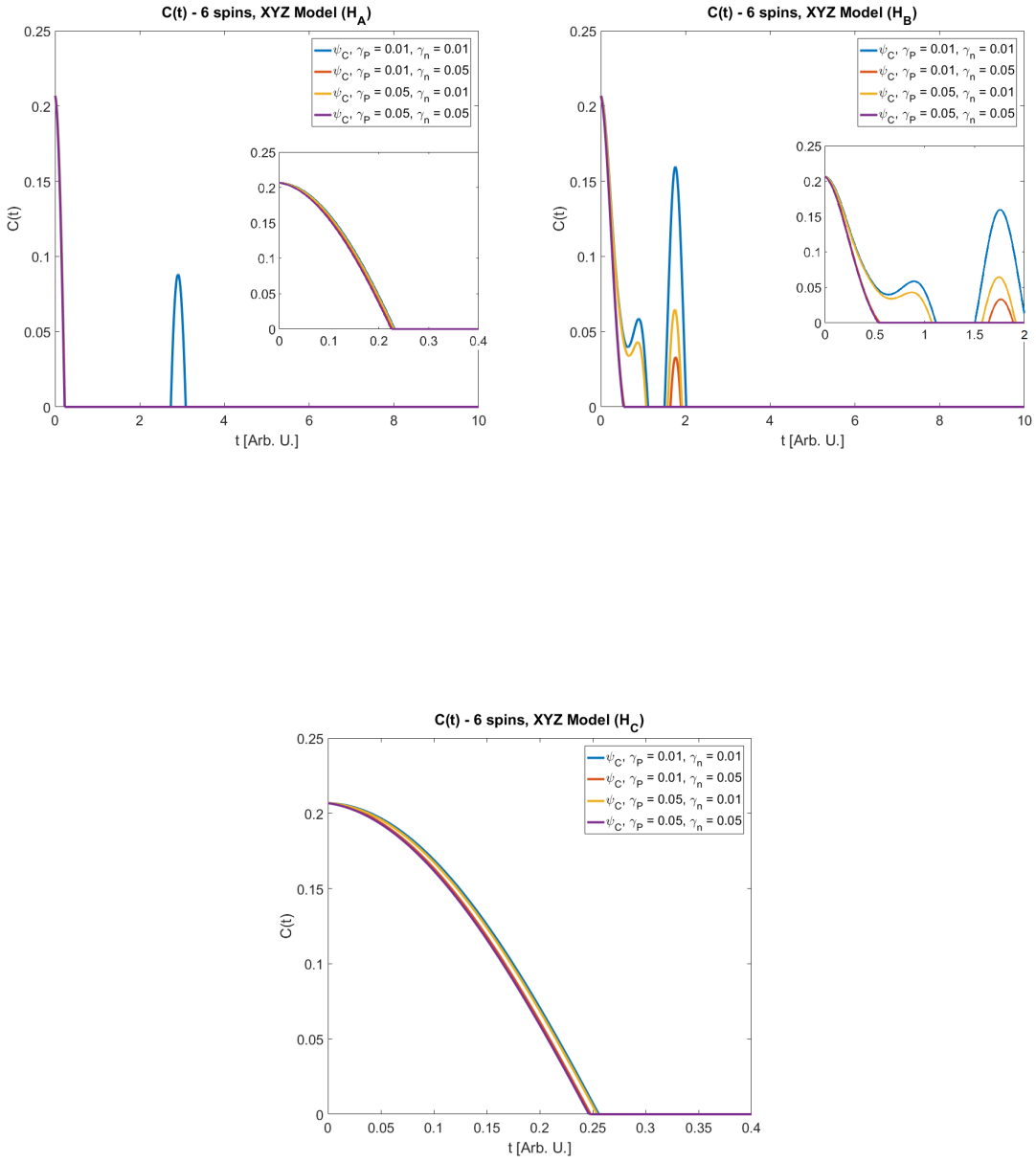

Figure 47: Time evolution of entanglement in five-spin chain described by XYZ Heisenberg model, for Hamiltonian H_A (left upper plot), Hamiltonian H_B (right upper plot) and Hamiltonian H_C (lower plot) for initial state ψ_C.

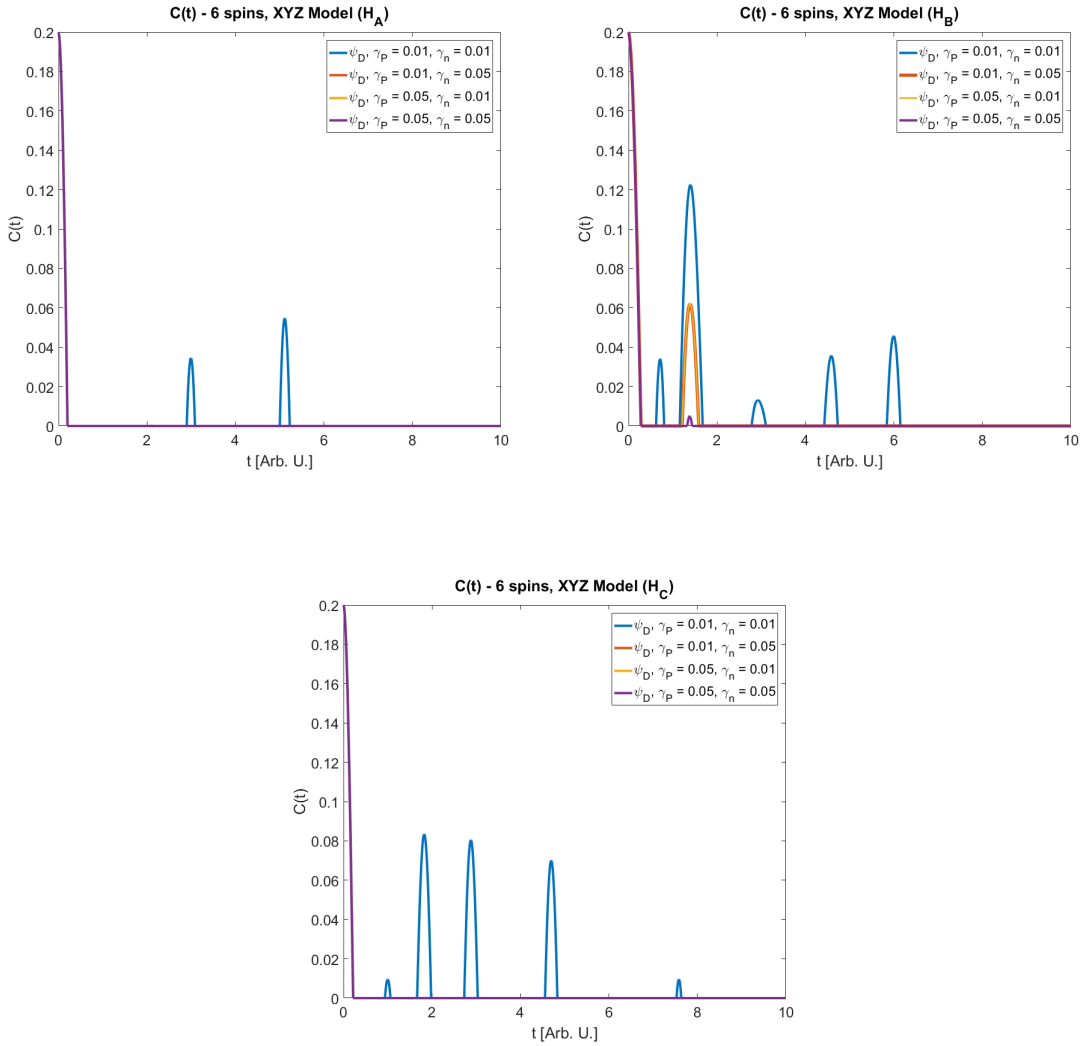

Figure 48: Time evolution of entanglement in six-spin chain described by XYZ Heisenberg model, for Hamiltonian H_A (left upper plot), Hamiltonian H_B (right upper plot) and Hamiltonian H_C (lower plot) for initial state ψ_D.

CONCLUSION: For two-spin chains (Fig. 40) the time evolution for different Hamiltonians differs only when the spin-raising and spin-lowering effects of interaction with the environment are taken into consideration with different decoherence coefficients, and even in this case this divergence is minimal. For three spins (Fig. 41) there is, however, a significant discrepancy between the time evolution with different Hamiltonians - both H_A and H_C result in complete decay and reconstructions of entanglement, while in the system described by the Hamiltonian H_B entanglement does not reach zero before its ultimate decay, even for high decoherence coefficients. This relates

to the conclusion of the XXZ model, as the H_B exchange integral J_Z is negative, while J_X and J_Y (counterparts of J_X in the XXZ model) are positive, as it was indicated to be favorable to obtain high entanglement in XXZ. In the case of four spins in the chain and one magnetic excitation (Fig. 42) similarly, the Hamiltonian H_B turned out to be the most beneficial, as all of the selected Hamiltonians result in a mostly exponential decay of entanglement, for H_B time of total decoherence is the longest. In the case of ψ_C state (two excitations) in a four-spin chain, all selected Hamiltonians result in mostly harmonic (fast alternating increases and decreases) evolution of entanglement (Fig. 43). The amplitudes of the entanglement peaks fall exponentially over time, yet, for significantly small decoherence factors, the total time of the loss of entanglement is relatively long - only in the case of Hamiltonian H_C does not exceed 10 arbitrary units. For five-spin chains with one excitation (Fig. 44) the evolution of the entanglement runs abruptly, with a sudden decrease at the beginning and small temporary increases in the case of H_B and, less effectively, in H_C. For two excitations (Fig. 45, only H_B provides a stable, mostly harmonic time evolution of entanglement; other Hamiltonians result only in single jumps of entanglement in seemingly random moments. In the case of six spins in the chain, both states with one, two and three excitations (Figs. 46, 47 and 48)) evolve with a sharp initial decrease of entanglement and sporadic entanglement increases. To summarize the results, one can note that the most favorable entanglement evolutions are obtained for the Hamiltonian H_B, which coincides with the conclusion drawn from the analysis of the XXZ model. The decay and rebirth of entanglement under specific environmental conditions is also noteworthy. We have demonstrated that it is feasible to select the parameters of the system and the environment in such a manner that the designated subsystem achieves entanglement, for instance, during specific time intervals (as depicted in Figs. 43-48).

4.2.2 External magnetic field

For further investigation, we restrict ourselves to the XXZ model, as the previous results provide a clear recipe for relatively high entanglement that is resistant to the environment: in this model, J_Z must be negative and smaller in magnitude than the integral J_X, which in turn should be as high as possible and positive.

Uniform magnetic field

The spin chain in the external, uniform magnetic field is described by following Hamiltonian (with an assumption of XXZ Heisenberg character of

exchange interaction):

$$\hat{H} = -J_X \sum_{i=1}^{N} \left(\hat{S}_i^X \hat{S}_{i+1}^X + \hat{S}_i^Y \hat{S}_{i+1}^Y \right) - J_Z \hat{S}_i^Z \hat{S}_{i+1}^Z + B \hat{S}_i^Z .$$

The representation of this Hamiltonian in computational basis for two spins reads:

$$\hat{H} = \begin{bmatrix} -J_Z + 2B & 0 & 0 & 0 \\ 0 & J_Z & -2J_X & 0 \\ 0 & -2J_X & J_Z & 0 \\ 0 & 0 & 0 & -J_Z - 2B \end{bmatrix}$$

with the following eigenvalues and eigenvectors:

$$\begin{aligned} E_1 &= -J_Z + 2B & |\alpha_1\rangle &= |\uparrow\uparrow\rangle \\ E_2 &= -J_Z - 2B & |\alpha_2\rangle &= |\downarrow\downarrow\rangle \\ E_3 &= J_Z - 2J_X & |\alpha_3\rangle &= \frac{1}{\sqrt{2}} \left(|\uparrow\downarrow\rangle + |\downarrow\uparrow\rangle \right) \\ E_4 &= J_Z + 2J_X & |\alpha_4\rangle &= \frac{1}{\sqrt{2}} \left(|\uparrow\downarrow\rangle - |\downarrow\uparrow\rangle \right) . \end{aligned}$$

Similarly, the eigenstates and eigenenergies can be calculated for longer chains and then used to prepare the thermal state of the system. The results of calculations of the dependence of the entanglement in this state on the system parameters are shown in Figs.49 - 53. The colormaps in Fig. 50 are presented as rotated through some angle to make it more readable):

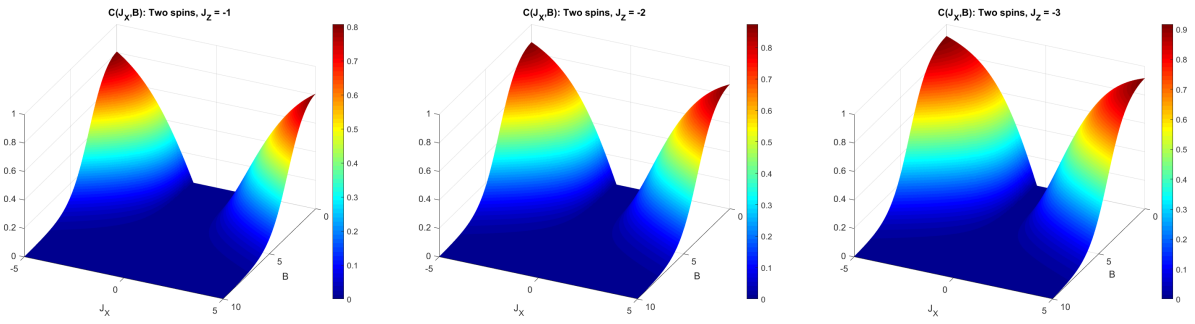

Figure 49: Entanglement as a function of external magnetic field and J_X exchange integral, for various values of J_Z integral, in two-spin system.

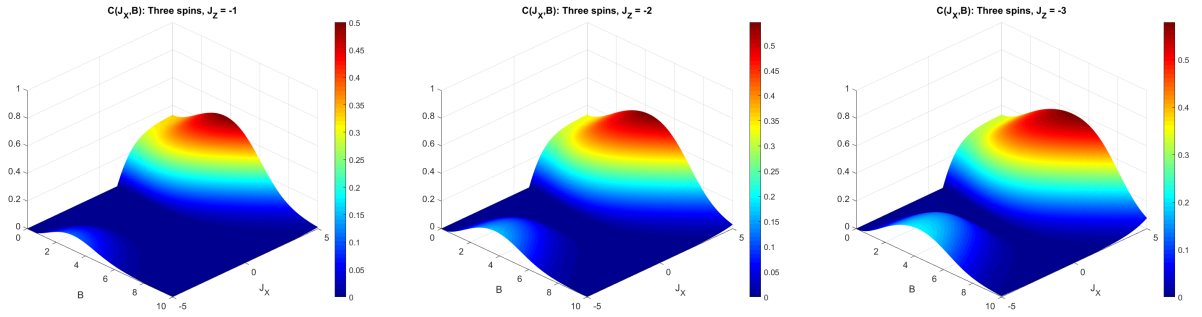

Figure 50: Entanglement as a function of external magnetic field and J_X exchange integral, for various values of J_Z integral, in three-spin system.

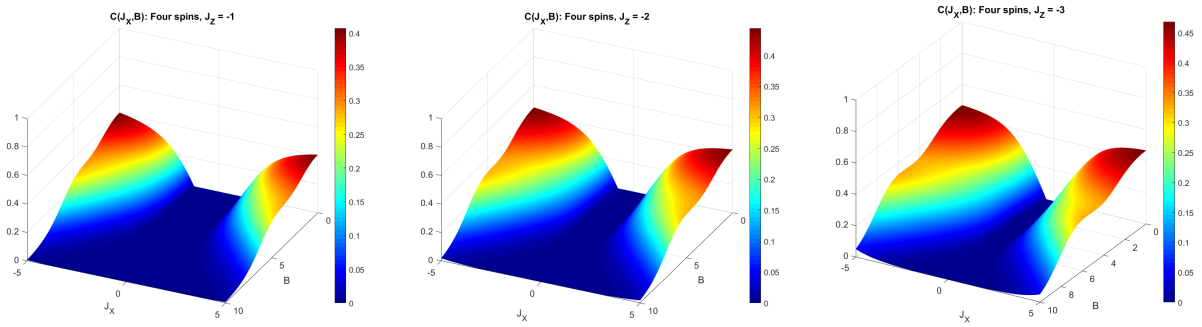

Figure 51: Entanglement as a function of external magnetic field and J_X exchange integral, for various values of J_Z integral, in four-spin system.

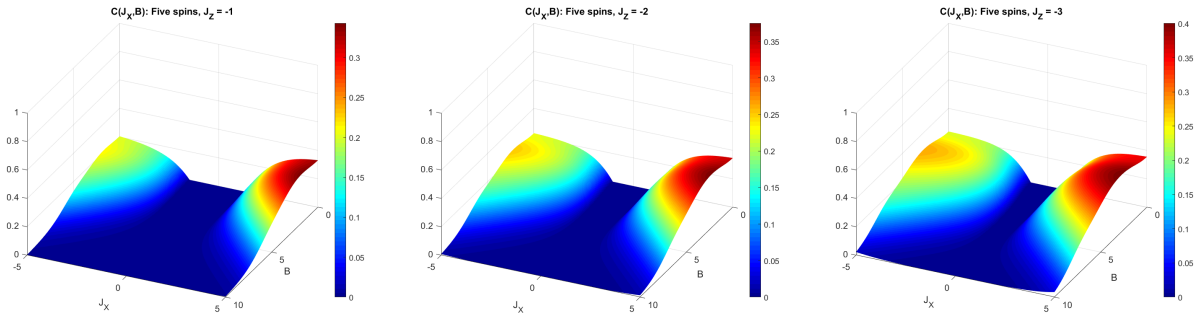

Figure 52: Entanglement as a function of external magnetic field and J_X exchange integral, for various values of J_Z integral, in five-spin system.

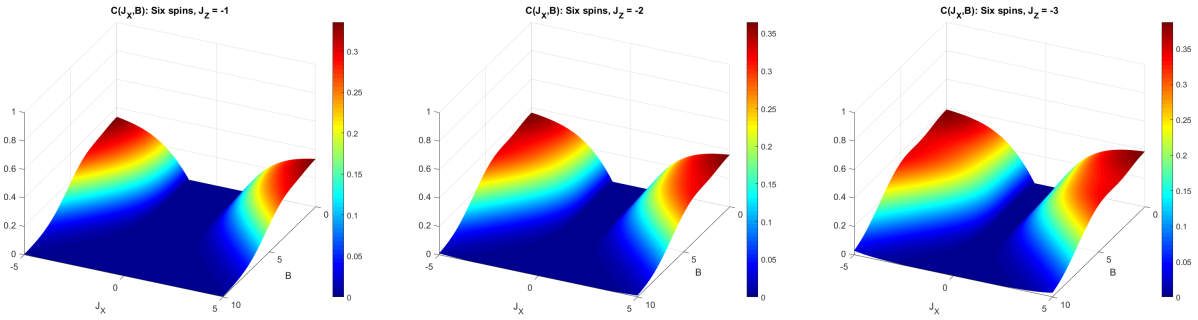

Figure 53: Entanglement as a function of external magnetic field and J_X exchange integral, for various values of J_Z integral, in six-spin system.

CONCLUSION: For the even number of spins in the chain (Figs. 49, 51 and 53), the external magnetic field clearly has a negative impact on entanglement, lowering the concurrence with its growth. A different situation occurs for odd-numbered spin chains - in these systems, maximal entanglement appears for some small, nonzero magnetic field, which is most visible for high J_Z exchange interaction.

DYNAMICS OF ENTANGLEMENT IN THE DISSIPATIVE ENVIRONMENT:

The following section covers the time evolution of spin systems in the uniform magnetic field, exposed to the influence of the Markovian environment:

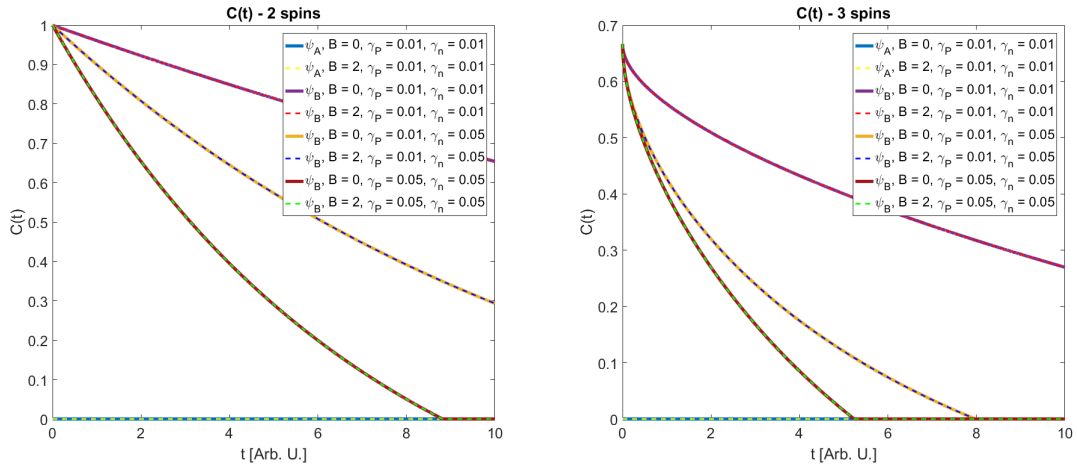

Figure 54: Time evolution of entanglement for two- (left) and three- (right) spin chain with and without external magnetic field. The dashed line indicates the presence of a magnetic field, solid line indicates its absence.

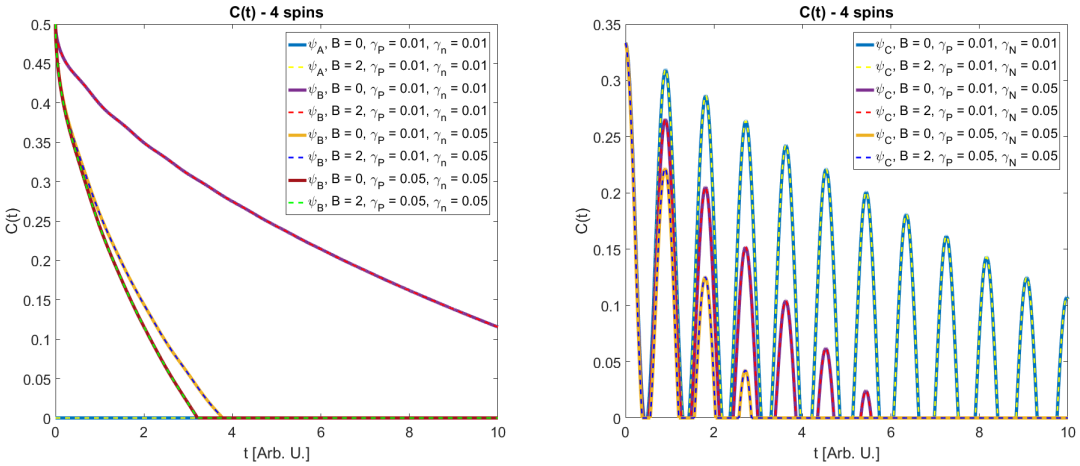

Figure 55: Time evolution of entanglement for four-spin chain with and without external magnetic field.

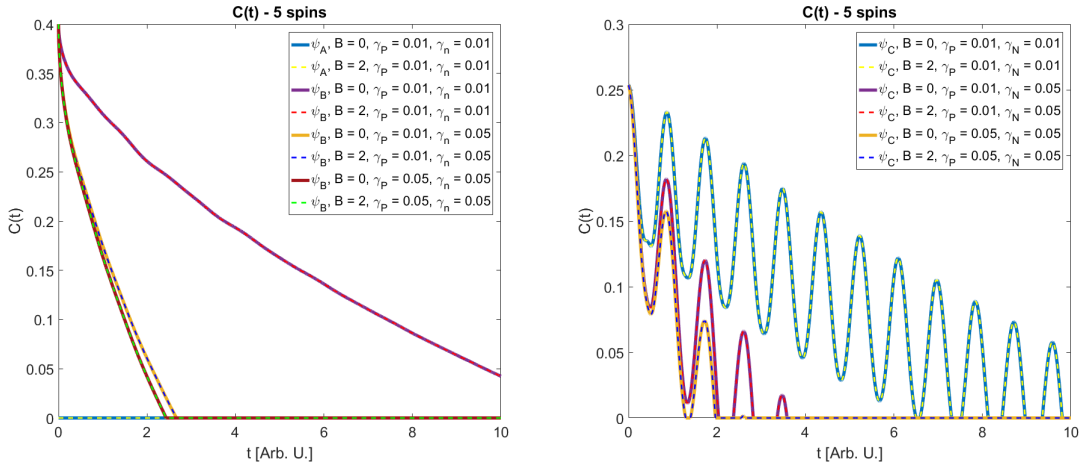

Figure 56: Time evolution of entanglement for five-spin chain with and without external magnetic field.

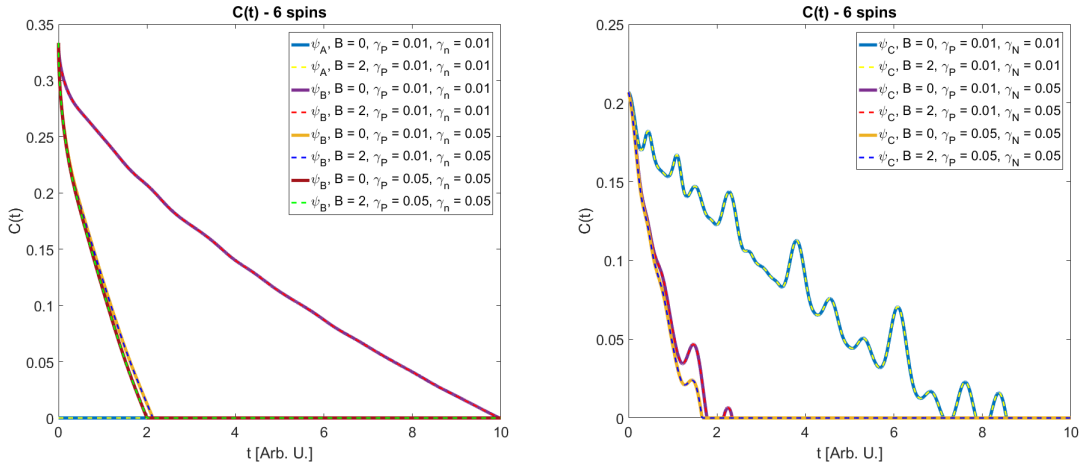

Figure 57: Time evolution of entanglement for a six-spin chain with and without external magnetic field.

CONCLUSION: The results presented above (Figs. 54 - 57) indicate that the magnetic field has no impact on the time evolution of the entanglement - solid lines (no field) exactly overlap dashed lines (nonzero magnetic field). Despite only presenting the singular value of a magnetic field in the analysis above, the investigation was repeated for various fields with identical results and only confirmed the conclusion. It should also be noted that periodic behavior in the evolution of entanglements emerges for the $|\Psi_C\rangle$ states, implying that the source of this periodicity could be an interaction between spin deviations.

Non-uniform magnetic field

In recent years, several articles have been published [120, 131, 136] in which spin systems with different magnetic fields applied to each spin were analyzed in terms of quantum entanglement. This non-uniformity was suspected to be a relevant factor in controlling the entanglement in the thermal state. The results of calculations done in the frame of a similar approach are presented below.
Hamiltonian in question (to avoid ambiguity, only chains with an even number of spins will be analysed):

$$\hat{H} = \sum_{i=1}^{N} \left(-J_X (S_i^X S_{i+1}^X + S_i^Y S_{i+1}^Y) - J_Z S_i^Z S_{i+1}^Z + B(1 + (-1)^{i+1} h) S_i^Z \right)$$

where $h \in (0, 1)$. In simpler terms, the odd spins are subjected to the field $B + hB$, while even spins are subjected to $B - hB$. As shown in the previous section, the static magnetic field has no impact on entanglement time evolution in a Markovian environment, and that is why only the thermal state was analysed in our study. The results of the calculations are presented in Figs. 58 - 60:

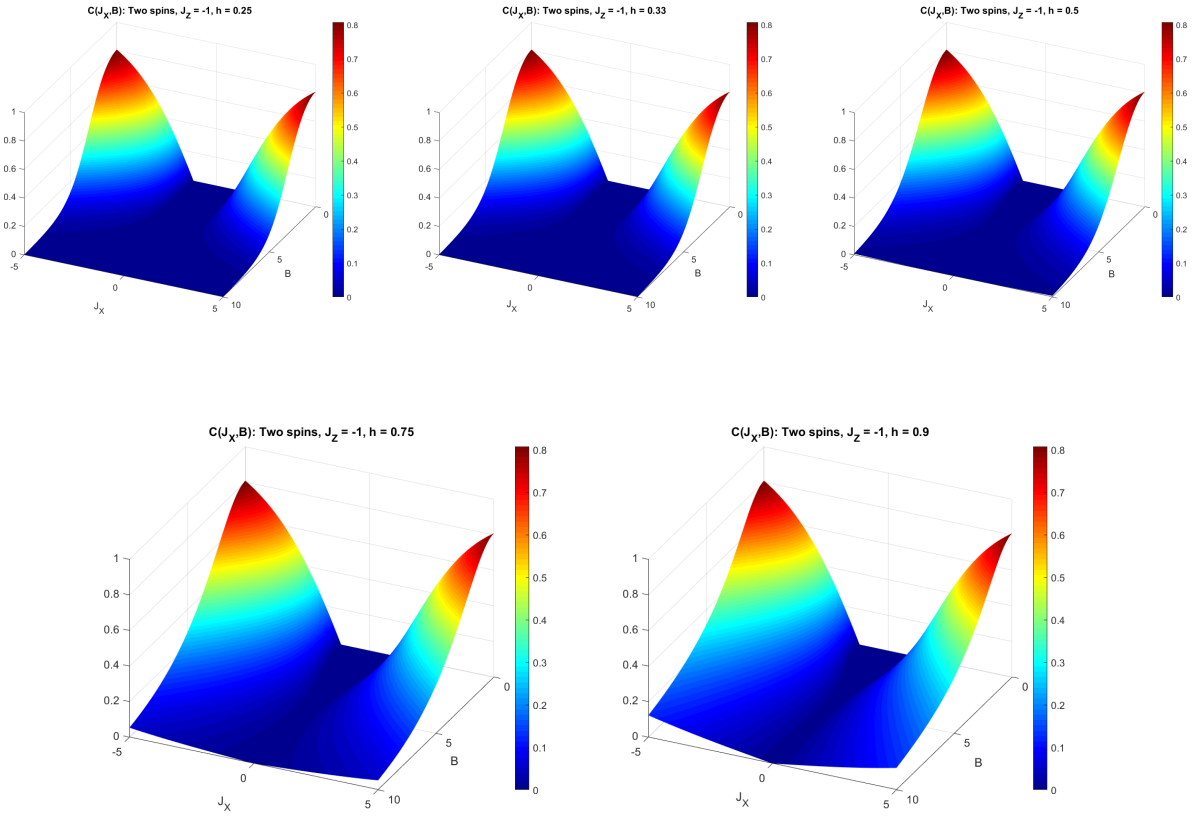

Figure 58: Entanglement concurrence as a function of magnetic field B and J_X exchange integral for different magnetic field non-uniformity coefficients h (see Hamiltonian above) - 0.25 (left upper plot), 0.33 (middle upper plot), 0.5 (right upper plot), 0.75 (left lower plot) and 0.9 (right lower plot). The model in question is two-spin chain described by XXZ model with exchange integral $J_Z = -1$.

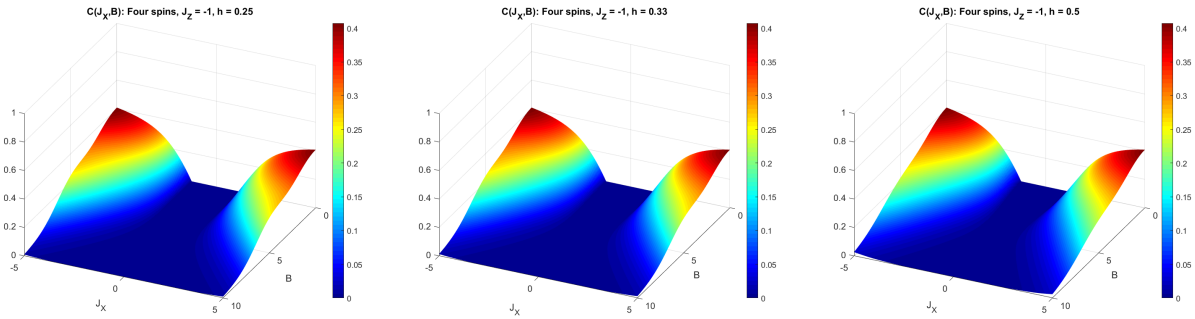

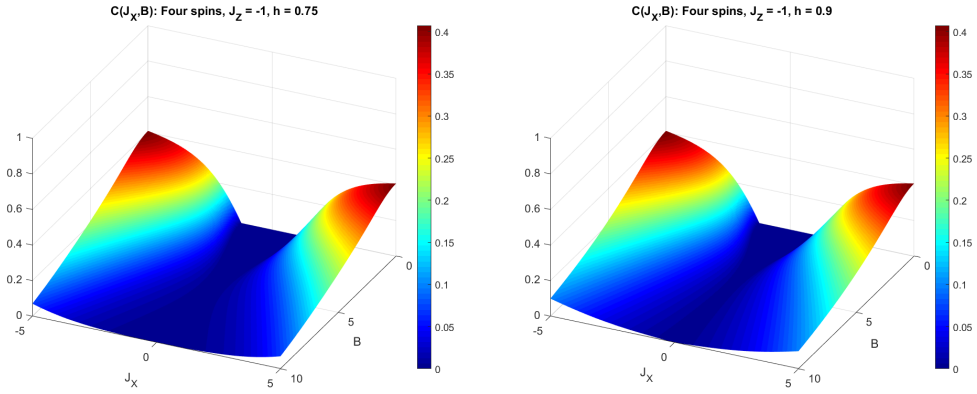

Figure 59: Entanglement concurrence as a function of magnetic field B and J_X exchange integral for different magnetic field non-uniformity coefficients h. The model in question is four-spin chain described by XXZ model with exchange integral $J_Z = -1$.

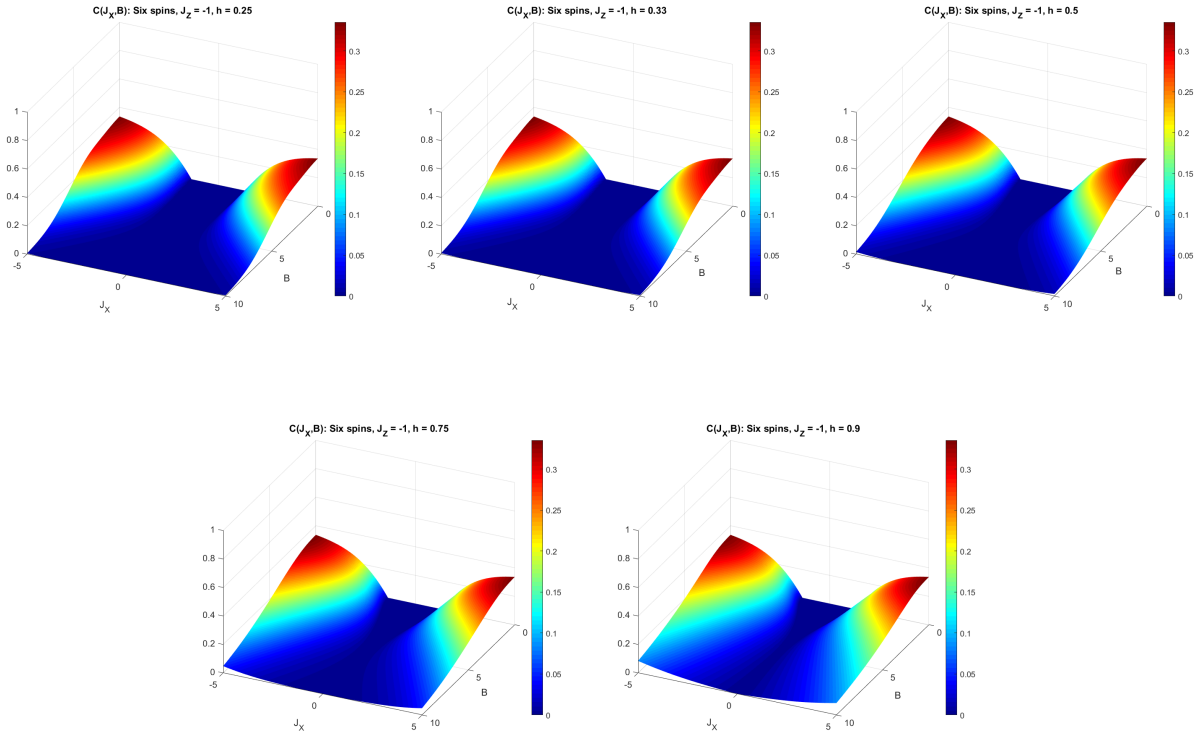

Figure 60: Entanglement concurrence as a function of magnetic field B and J_X exchange integral for different magnetic field non-uniformity coefficients h. The model in question is a six-spin chain described by XXZ model with exchange integral $J_Z = -1$.

CONCLUSION: As one can see (Figs. 58 - 60), non-uniformity of the magnetic field can enhance the quantum correlations in states of low entanglement ("lifting" of the entanglement alongside the increase in non-uniformity for high magnetic field B and larger in magnitude J_X), however, comparison of plots with corresponding results from the previous section (for example Fig. 51 with Fig. 59) clearly shows, that in the systems with high thermal entanglement, the non-uniformity of the magnetic field becomes less and less relevant - maximal entanglement is the same for uniform and non-uniform magnetic field.

Time-dependent magnetic field

Since the static magnetic field does not change the evolution of entanglement, the question arises of whether a time-dependent magnetic field does? To test this hypothesis, a model with two types of magnetic field was proposed: one static to determine the quantization axis, and another time-dependent, perpendicular to the first one. Hamiltonian in question is therefore:

$$\hat{H} = \sum_{i=1}^{N} \left(-J_X (S_i^X S_{i+1}^X + S_i^Y S_{i+1}^Y) - J_Z S_i^Z S_{i+1}^Z + B_0 S_i^Z + B_X \cdot sin(\omega t) \cdot S_i^X \right)$$

(based on a previous investigation, the following parameters' values are assumed: $J_X = 4$, $J_Z = -2$ and $B_0 = 1$). The results of calculating the time evolution of the entanglement in the Markovian-type environment are presented in Figs. 61 - 69:

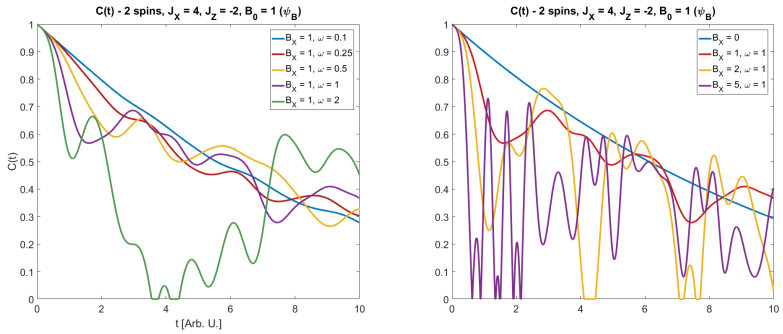

Figure 61: Time evolution of entanglement concurrence for a two-spin chain in the time-dependent magnetic field - the plots show entanglement behaviour for different angular frequencies (left) or magnetic field amplitudes (right). Initial state: ψ_B.

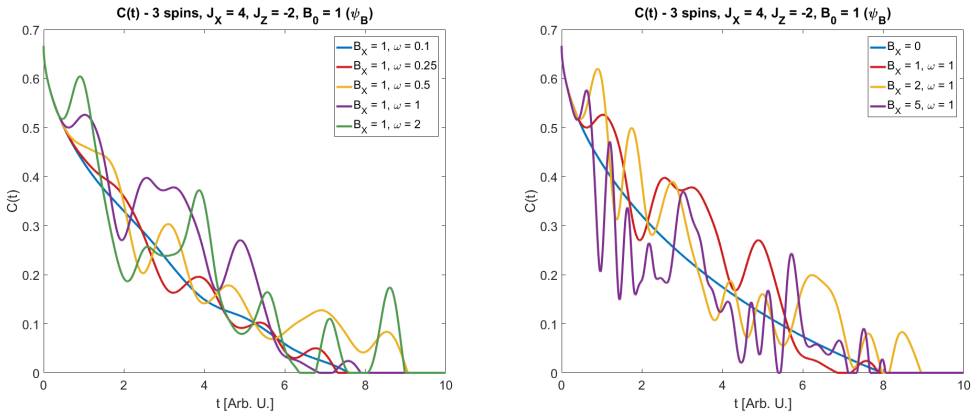

Figure 62: Time evolution of entanglement concurrence for a three-spin chain in the time-dependent magnetic field - the plots show entanglement behaviour for different angular frequencies (left) or magnetic field amplitudes (right). Initial state: ψ_B.

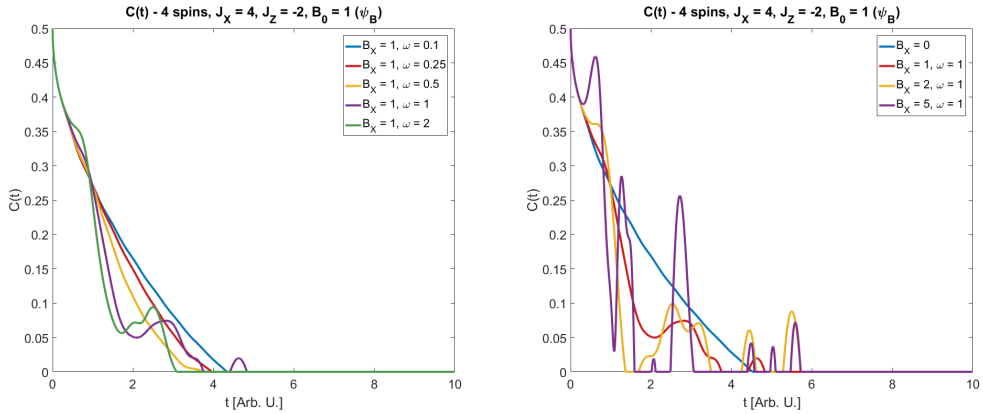

Figure 63: Time evolution of entanglement concurrence for a four-spin chain in the time-dependent magnetic field - the plots show entanglement behaviour for different angular frequencies (left) or magnetic field amplitudes (right). Initial state: ψ_B.

CONCLUSION: The general conclusion from the analysis of the right graphs of the figures 61 - 69 is that the higher the number of spins in the chain, the less beneficial it is to apply the time-dependent field. The blue plot, representing the system without this field, shows the evolution with the highest peaks of entanglement and the longest time of total entanglement decay, especially for the six spins (Figs. 67 - 69), but also for two spins with one excitation in the initial state (Fig. 61). The curves representing the systems with the time-dependent field may temporarily exceed it slightly, but they experience larger and more rapid declines as the field amplitude increases.

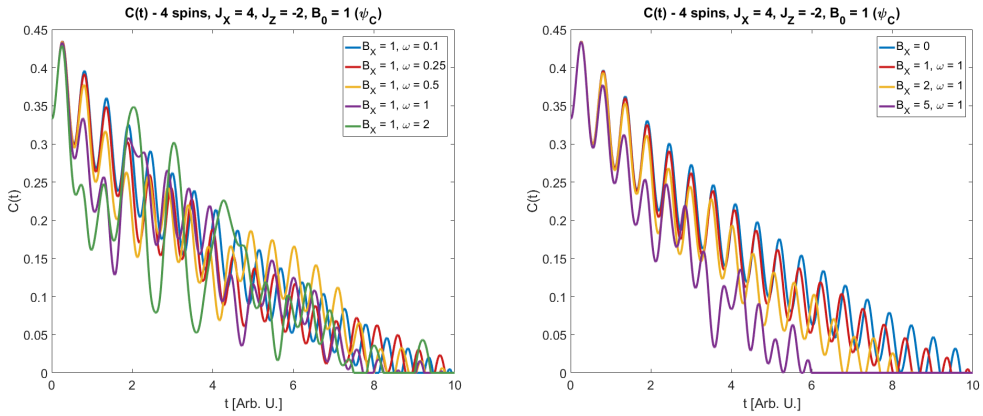

Figure 64: Time evolution of entanglement concurrence for a four-spin chain in the time-dependent magnetic field - the plots show entanglement behaviour for different angular frequencies (left) or magnetic field amplitudes (right). Initial state: ψ_C.

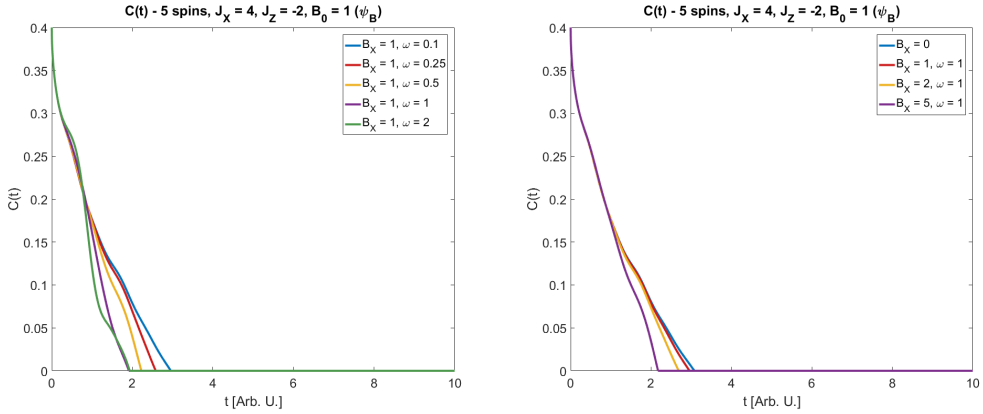

Figure 65: Time evolution of entanglement concurrence for a five-spin chain in the time-dependent magnetic field - the plots show entanglement behaviour for different angular frequencies (left) or magnetic field amplitudes (right). Initial state: ψ_B.

Similarly, for four spins with two excitations in the initial state (Fig. 64) the same fact is observed; however, it is noteworthy that in this case a high magnetic field initially provides a more favorable decrease of entanglement, which may find its use in applications with very short operation time). For shorter chains, the impact of the time-dependent field for the examined angular frequency ($\omega = 1$) is negligible, so it is worth observing whether the change in this parameter can affect the behavior of the entanglement or not.

Generally, the states can be divided into two groups - those for which a better result is obtained for small frequencies (i.e. $\omega = 0.1$) - those are ψ_B (single flipped spin) for two (Fig. 61), four (Fig. 63), five (Fig. 65 and six

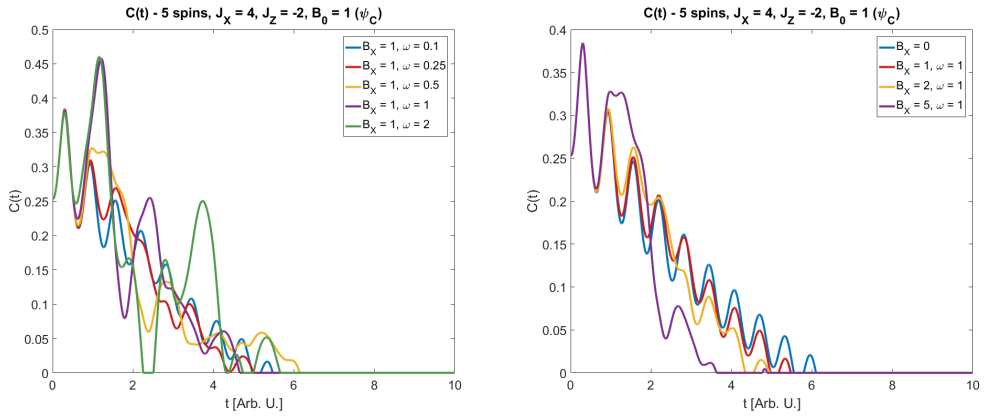

Figure 66: Time evolution of entanglement concurrence for a five-spin chain in the time-dependent magnetic field - the plots show entanglement behaviour for different angular frequencies (left) or magnetic field amplitudes (right). Initial state: ψ_C.

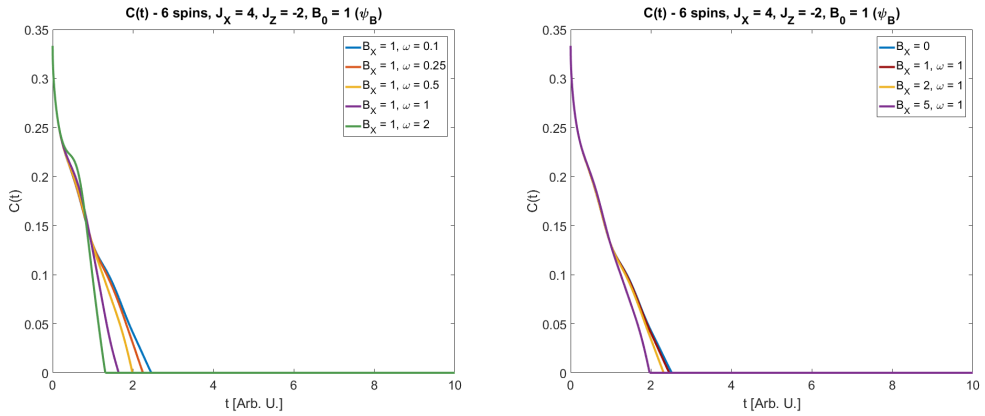

Figure 67: Time evolution of entanglement concurrence for a six-spin chain in the time-dependent magnetic field - the plots show entanglement behaviour for different angular frequencies (left) or magnetic field amplitudes (right). Initial state: ψ_B.

(Fig. 67) spins in the chain, and also for ψ_D (three excitations) in six-spin chain (Fig. 69); and those, for which the most favourable is to apply the field of high frequency ($\omega = 2$) - this effect is visible for example in state ψ_B in three-spin chain (Fig. 62) and states with two excitations, ψ_C, for chains with four (Fig. 64) and five (Fig. 66) spins in them. In the initial part of time evolution for ψ_C in the six-spin chain also this frequency provides better results, however, the field with low frequency in this particular case turned out to be characterized by longer decoherence time.

To summarize, the time-dependent magnetic field may enhance the entanglement only for short spin chains (except for two spin chains, this may

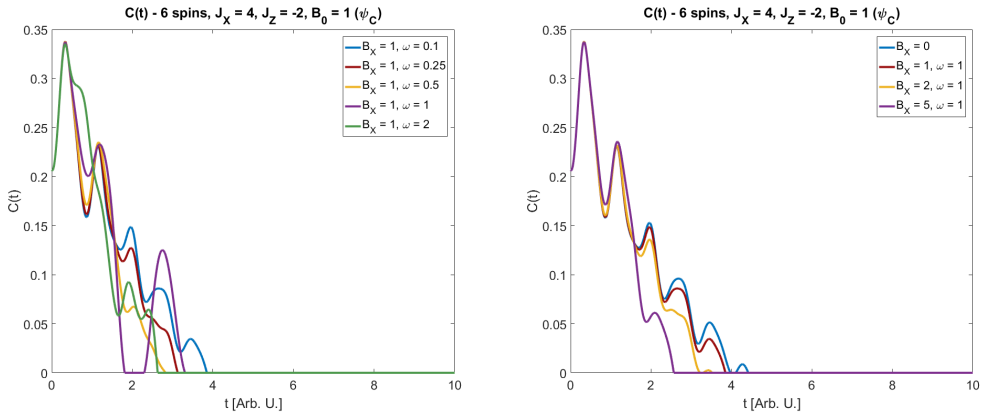

Figure 68: Time evolution of entanglement concurrence for a six-spin chain in the time-dependent magnetic field - the plots show entanglement behaviour for different angular frequencies (left) or magnetic field amplitudes (right). Initial state: ψ_C.

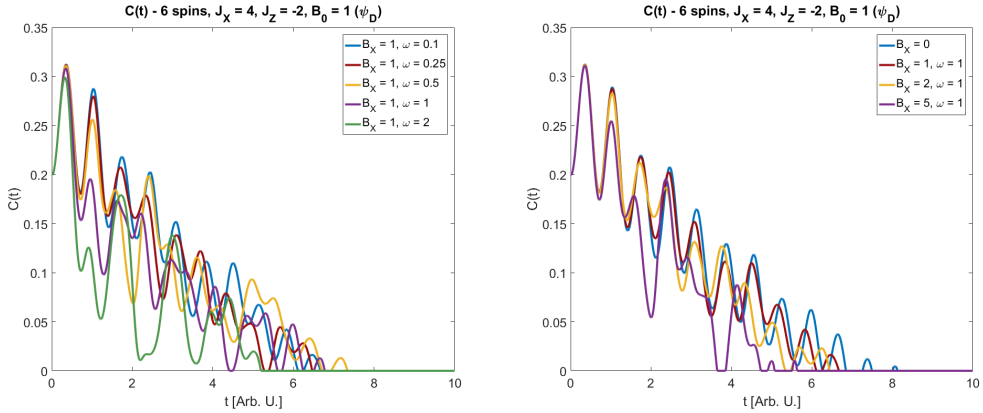

Figure 69: Time evolution of entanglement concurrence for a six-spin chain in the time-dependent magnetic field - the plots show entanglement behaviour for different angular frequencies (left) or magnetic field amplitudes (right). Initial state: ψ_D.

be related to boundary condition - interaction between the last and the first spin - imposed on all the longer chains), and the frequency of the field should be adapted to the number of excitation. An odd number of flipped spins required a field of low frequency, and for an even number of flipped spins one should aim at the higher-frequency field.

4.2.3 Dzyaloshinskii–Moriya interaction

Unidirectional DM interaction

To take into account antisymmetric exchange, we analyze the simplest and probably most common interaction of this type, namely the unidirectional Dzyaloshinskii-Moriya interaction. Hamiltonian of such model reads:

$$\hat{H} = \sum_{i=1}^{N} \left(-J_X (S_i^X S_{i+1}^X + S_i^Y S_{i+1}^Y) - J_Z S_i^Z S_{i+1}^Z + D_Z (S_i^X S_{i+1}^Y - S_i^Y S_{i+1}^X) \right).$$

In the computational basis of two spins, the matrix representation of the Hamiltonian presented above is:

$$\hat{H} = \begin{bmatrix} -J_Z & 0 & 0 & 0 \\ 0 & J_Z & -2J_X + 2iD_Z & 0 \\ 0 & -2J_X - 2iD_Z & J_Z & 0 \\ 0 & 0 & 0 & -J_Z \end{bmatrix}.$$

The eigenstates and corresponding energies, upon which the thermal states will be constructed, are:

$$E_1 = -J_Z \qquad |\alpha_1\rangle = |\uparrow\uparrow\rangle$$

$$E_2 = J_Z - 2\sqrt{J_X^2 + D_Z^2} \qquad |\alpha_2\rangle = \frac{J_X - iD_Z}{\sqrt{2(J_X^2 + D_Z^2)}} |\uparrow\downarrow\rangle + \frac{1}{\sqrt{2}} |\downarrow\uparrow\rangle$$

$$E_3 = J_Z + 2\sqrt{J_X^2 + D_Z^2} \qquad |\alpha_2\rangle = \frac{J_X + iD_Z}{\sqrt{2(J_X^2 + D_Z^2)}} |\uparrow\downarrow\rangle + \frac{1}{\sqrt{2}} |\downarrow\uparrow\rangle$$

$$E_4 = -J_Z \qquad |\alpha_4\rangle = |\downarrow\downarrow\rangle.$$

The numerical calculations of entanglement as a function of the DM coefficient D_Z and exchange integral J_X are presented in color maps in Figs. 70 - 74:

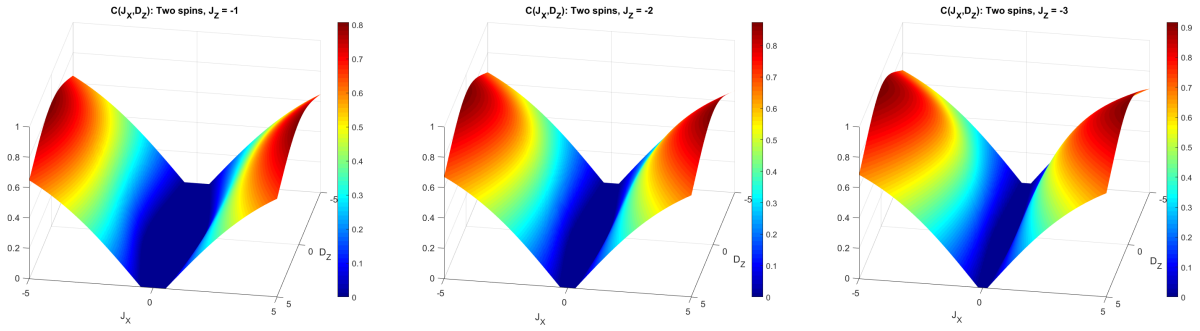

Figure 70: Entanglement as a function of Dzyaloshinskii - Moriya interaction coefficient D_Z and J_X exchange integral, for various values of J_Z integral, in two-spin system.

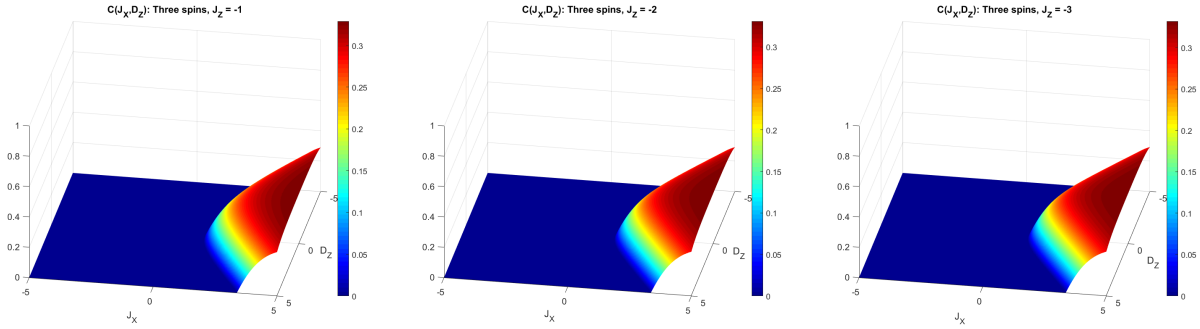

Figure 71: Entanglement as a function of Dzyaloshinskii - Moriya interaction coefficient D_Z and J_X exchange integral, for various values of J_Z integral, in three-spin system.

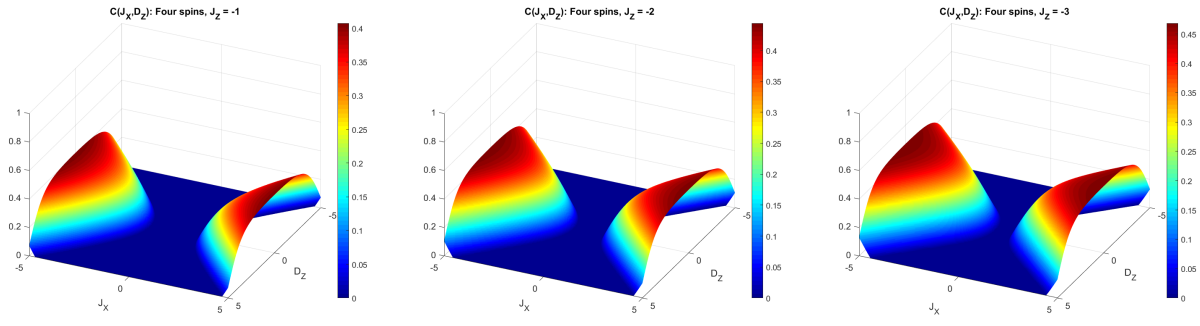

Figure 72: Entanglement as a function of Dzyaloshinskii - Moriya interaction coefficient D_Z and J_X exchange integral, for various values of J_Z integral, in four-spin system.

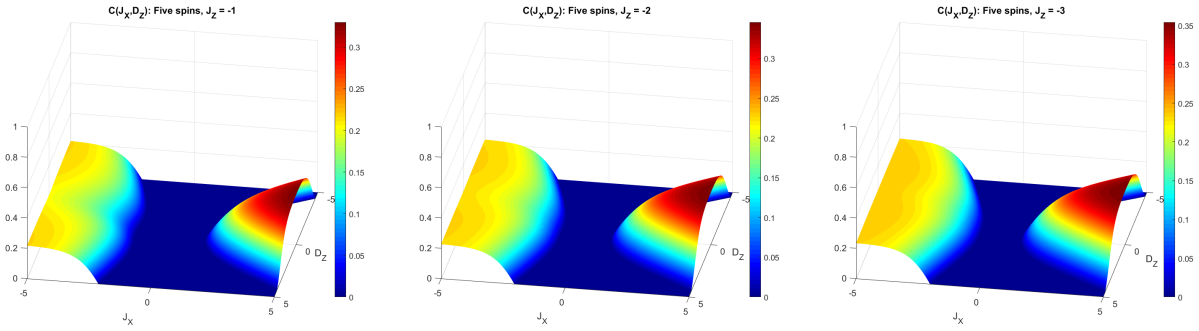

Figure 73: Entanglement as a function of Dzyaloshinskii - Moriya interaction coefficient D_Z and J_X exchange integral, for various values of J_Z integral, in five-spin system.

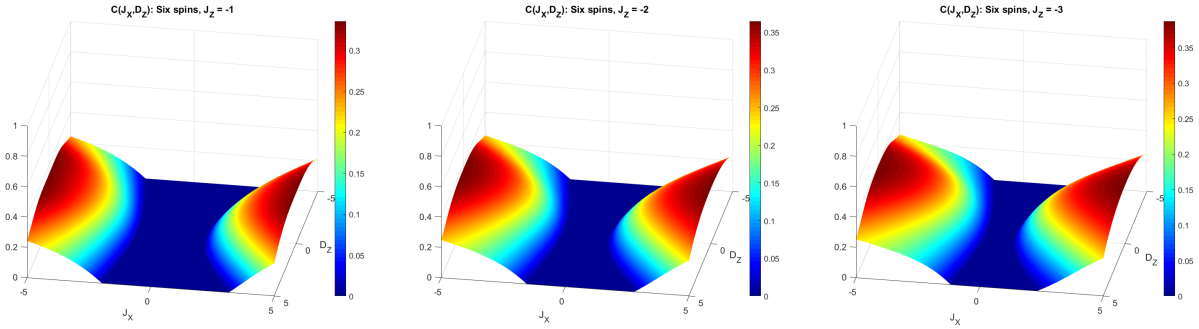

Figure 74: Entanglement as a function of Dzyaloshinskii - Moriya interaction coefficient D_Z and J_X exchange integral, for various values of J_Z integral, in six-spin system.

CONCLUSION: All of the above plots, Figs. 70 - 74 indicate that as the absolute value of the Z-component of DM interactions increases, the entanglement in the thermal state drops. The maximum entanglement is obtained for $D_Z = 0$.

DYNAMICS OF ENTANGLEMENT IN THE DISSIPATIVE ENVIRONMENT:

This section covers the time evolution of spin systems that, in addition to exchange interactions, also exhibit unidirectional antisymmetric superexchange interactions of DM type, located in the Markovian environment. The results of numerical simulations are shown in Figs. 75 - 78:

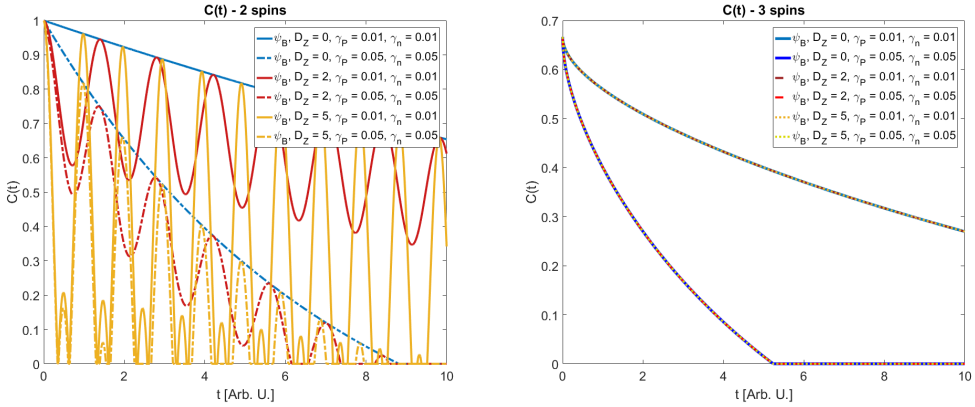

Figure 75: Time evolution of entanglement concurrence for two-spin (left) and three-spin chain (right) in the presence of unidirectional DM interaction of Z-type. Both initial states are characterized by single-flipped spin (ψ_B).

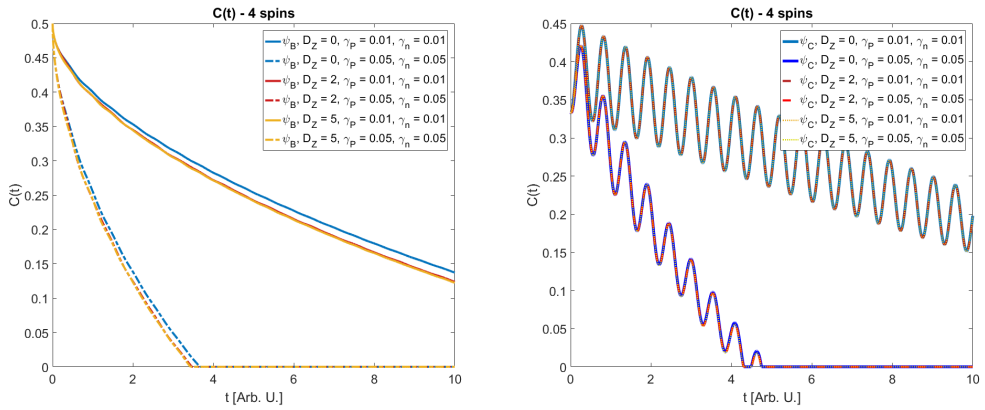

Figure 76: Time evolution of entanglement concurrence for a four-spin chain in the presence of unidirectional DM interaction of Z-type. The left plot depicts the time evolution of the state with one magnetic excitation in a chain and the right - the state with two excitations.

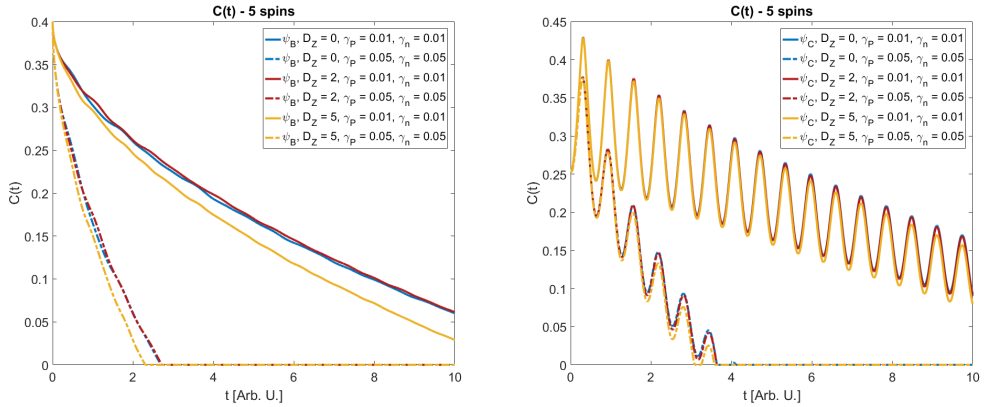

Figure 77: Time evolution of entanglement concurrence for a five-spin chain in the presence of unidirectional DM interaction of Z-type. The left plot depicts the time evolution of the state with one magnetic excitation in a chain, and the right - state with two excitations.

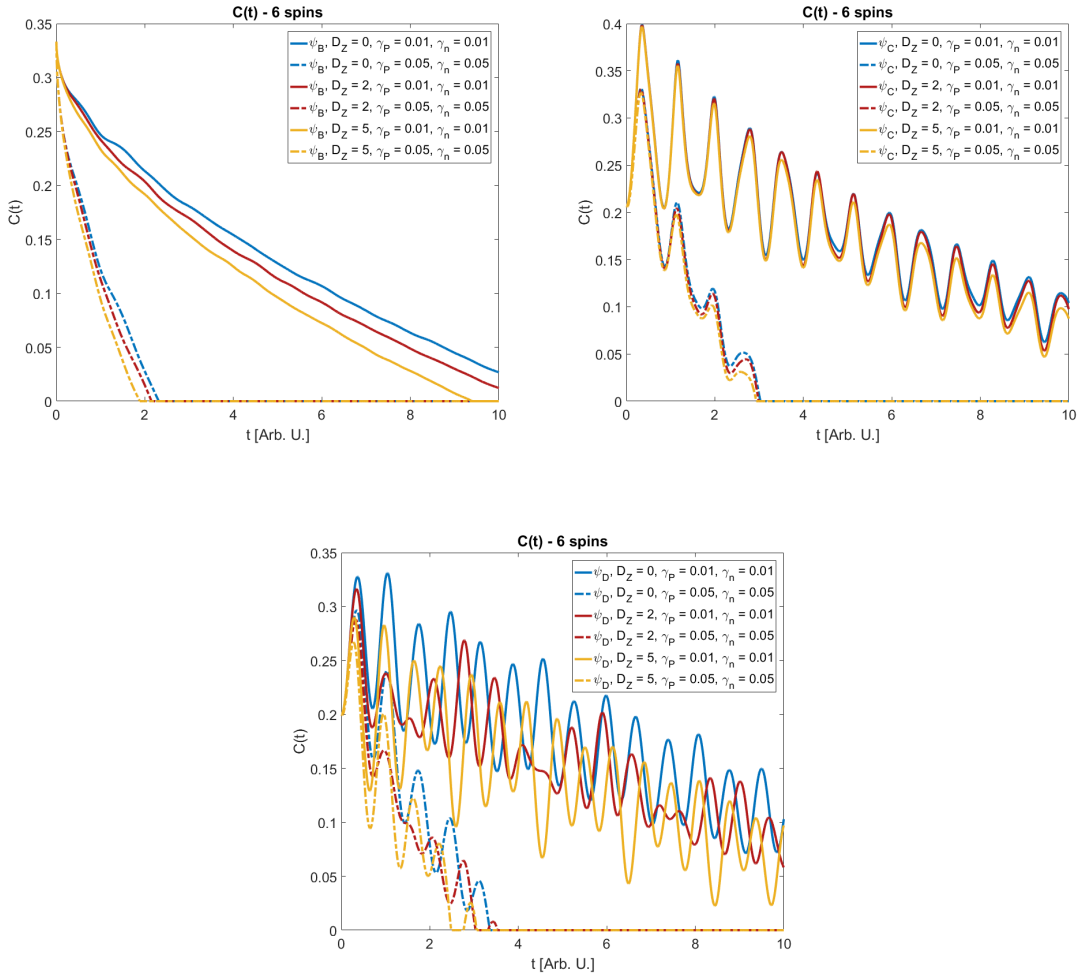

Figure 78: Time evolution of entanglement concurrence for a six-spin chain in the presence of unidirectional DM interaction of Z-type. The left upper plot depicts the time evolution of the state with one magnetic excitation in the chain, the right upper plot - with two excitations, and the lower - with three.

CONCLUSION: In the majority of situations considered, the DM interaction along the Z axis has a negative impact on the system's entanglement. In some states, however, this type of interaction does not affect the decoherence. For example, in the case of three spins and the initial state with one excitation (Fig. 75, right plot), a four-spin chain and two excitations (Fig. 76, right plot), and, to some extent, in the case of five and six spins in the chain, for initial state with two flipped spins (Figs. 77, right and 78, upper right plot). However, in some cases, the time evolution of the entanglement exhibits an unusual behavior: the initial state with three excitations for the six-spin chain (Fig. 78, lower plot) is characterized by evolution with periodic increases and decreases of entanglement for various values of the DM

D_Z component. However, the highest entanglement peaks occur for a system without this interaction and are lower for higher coefficients of D_Z. The most interesting behaviour can be seen for five spins and one flipped spin in the initial state. As it turns out, some non-zero D_Z factor can improve the entanglement evolution, extending the decoherence time of the system. To better illustrate this effect, the additional plots are shown below (Fig. 79). Although the effect may not be significant, the fact that the plots for $D_Z = 1$ and $D_Z = 2$ for this particular state exceed the plot for $D_Z = 0$ may prove to be a beneficial phenomenon in quantum computing.

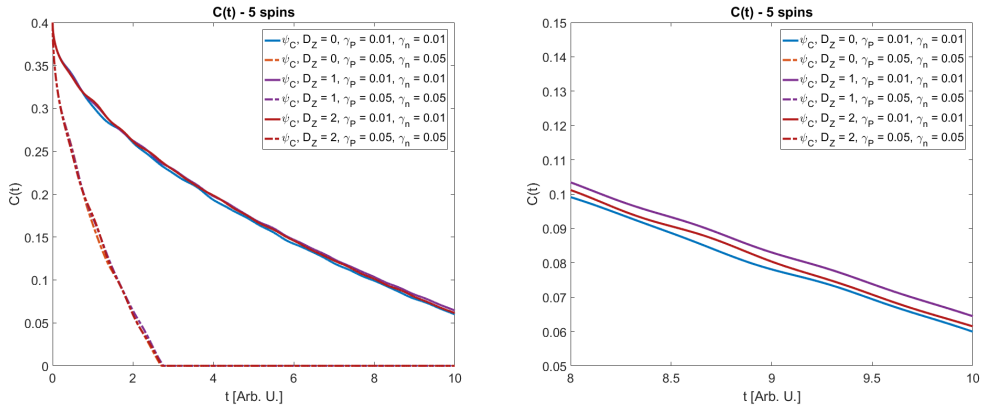

Figure 79: Time evolution of entanglement concurrence for the five-spin chain in the presence of unidirectional DM interaction of Z-type, for different values of D_Z that in Fig. 77 (left). Close up on the plots to illustrate that the non-zero D_Z coefficient in this case results in raising the entanglement plot above the one corresponding to $D_Z = 0$ (right).

Multidirectional DM interaction

To generalize the analysis of the impact of the DM interaction on entanglement in the spin system, all three components should be taken into account. The Hamiltonian corresponding to such case reads:

$$\hat{H} = \sum_{i=1}^{N}(-J_X(S_i^X S_{i+1}^X + S_i^Y S_{i+1}^Y) - J_Z S_i^Z S_{i+1}^Z$$

$$+D_X(S_i^Y S_{i+1}^Z - S_i^Z S_{i+1}^Y) + D_Y(S_i^Z S_{i+1}^X - S_i^X S_{i+1}^Z) + D_Z(S_i^X S_{i+1}^Y - S_i^Y S_{i+1}^X)).$$

For example, this Hamiltonian for two spins in matrix representation corresponding to calculational basis is of the form:

$$\hat{H} = \begin{bmatrix} -J_Z & D_Y + iD_X & -D_Y - iD_X & 0 \\ D_Y - iD_X & J_Z & -2J_X + 2iD_Z & D_Y + iD_X \\ iD_X - D_Y & -2J_X - 2iD_Z & J_Z & -D_Y - iD_X \\ 0 & D_Y - iD_X & iD_X - D_Y & -J_Z \end{bmatrix}.$$

As the eigenvalues and components of eigenvectors of such matrix, in general, are rather complicated functions of all the five parameters appearing in Hamiltonian, they are not listed here. Nevertheless, the computational tools give the possibility to determine them without any problem, as well as the thermal state density matrix. The analysis is based on the results obtained in this way. The numerical simulations of concurrence as a function of the DM coefficients D_X, D_Y, D_Z are presented below, in the form of colormaps:

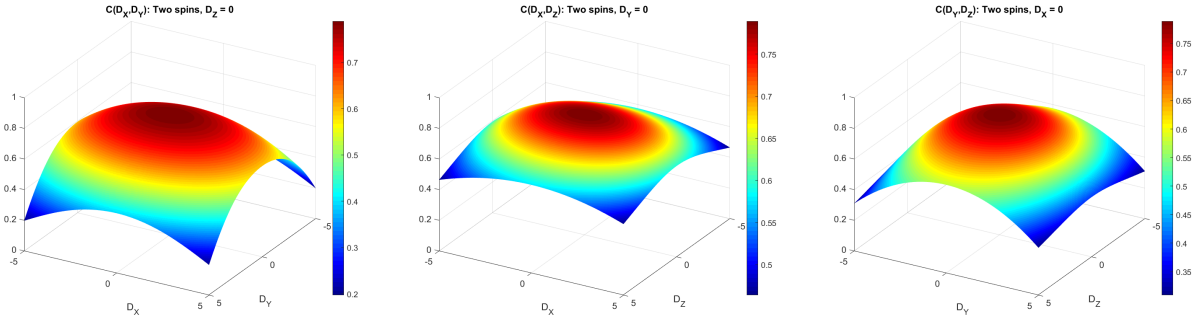

Figure 80: Entanglement as a function of two Dzyaloshinskii - Moriya interaction coefficients, while the third one remains equal to zero (from the left to the right: $D_Z = 0$, $D_Y = 0$, $D_X = 0$). System in consideration: two-spin chain.

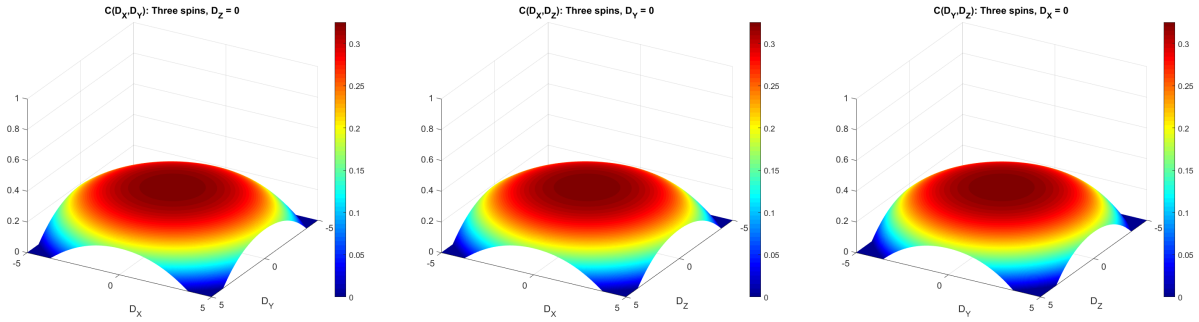

Figure 81: Entanglement as a function of two Dzyaloshinskii - Moriya interaction coefficients, while the third one remains equal to zero (as above). System in consideration: three-spin chain.

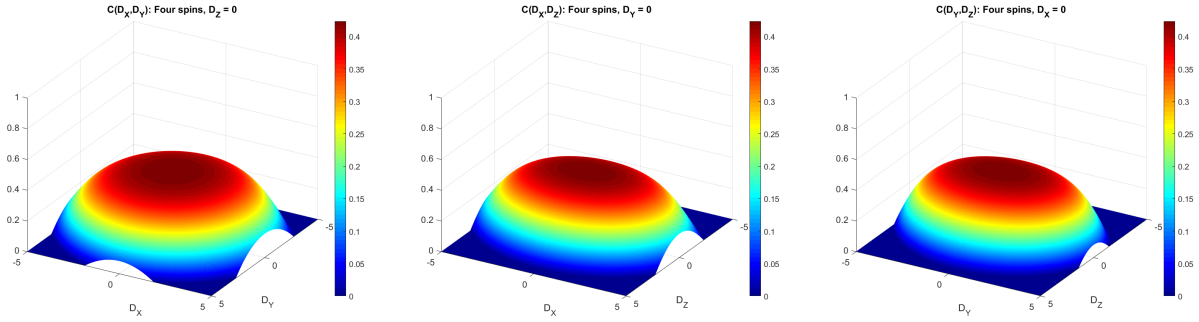

Figure 82: Entanglement as a function of two Dzyaloshinskii - Moriya interaction coefficients, while the third one remains equal to zero. System in consideration: four-spin chain.

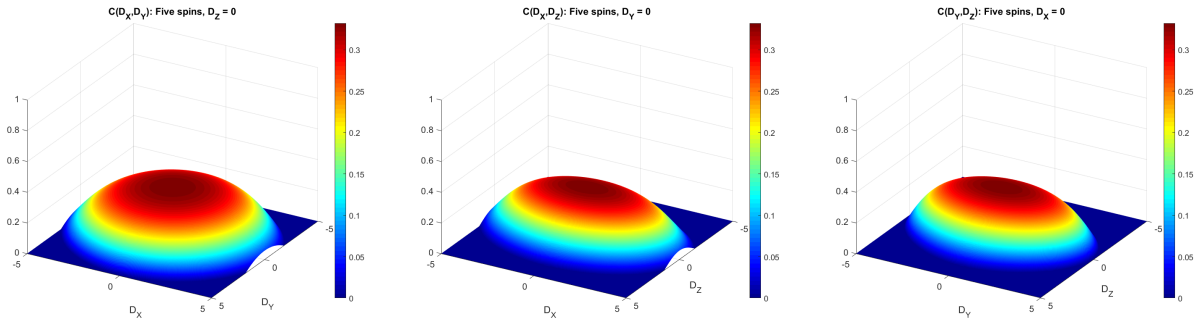

Figure 83: Entanglement as a function of two Dzyaloshinskii - Moriya interaction coefficients, while the third one remains equal to zero. System in consideration: five-spin chain.

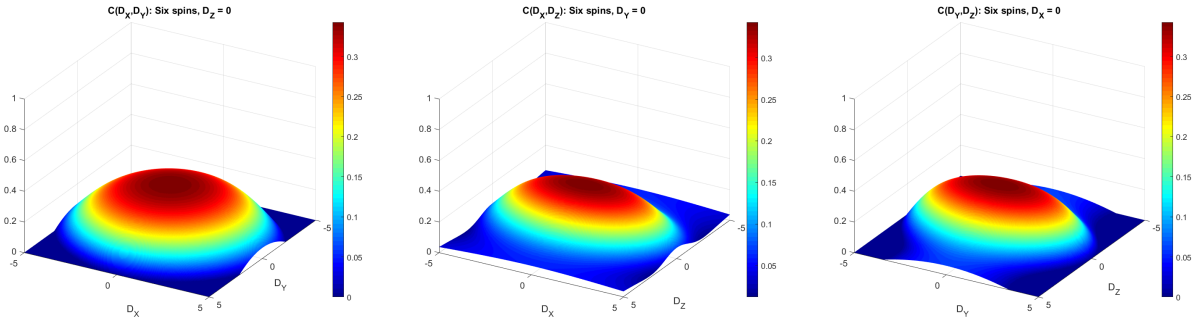

Figure 84: Entanglement as a function of two Dzyaloshinskii - Moriya interaction coefficients, while the third one remains equal to zero (from the left to the right: $D_Z = 0$, $D_Y = 0$, $D_X = 0$). System in consideration: six-spin chain.

CONCLUSION: Although some asymmetric properties can be seen in some plots, in general, neither the DM interaction component is a beneficial factor for entanglement in spin systems; the highest concurrence occurs clearly for all D_X, D_Y, D_Z equal to zero.

DYNAMICS OF ENTANGLEMENT IN THE DISSIPATIVE ENVIRONMENT:

In this section, the time evolution of entanglement is analyzed for systems with three-dimensional Dzyaloshinskii–Moriya antisymmetric exchange in a dissipative environment. Five Hamiltonians were taken into account, and their labelling is as follows:

$$H_0 : D_X = 0; D_Y = 0; D_Z = 0 \quad \text{(control case)}$$

$$H_A : D_X = 1; D_Y = 1; D_Z = 1 \quad \text{(isotropic case)}$$

$$H_B : D_X = 2; D_Y = 1; D_Z = 1 \quad \text{(X-direction factor higher than other)}$$

$$H_C : D_X = 2; D_Y = 2; D_Z = 1 \quad \text{(X- and Y-direction factor higher than Z)}$$

$$H_D : D_X = 1; D_Y = 1; D_Z = 2 \quad \text{(Z-direction factor higher than other)}$$

As their impact on the decoherence process is trivial, only one set of dissipation rates is analyzed, namely $\gamma_P = 0.01$ and $\gamma_N = 0.05$. The results of numerical simulations are presented in Figs. 85 - 88:

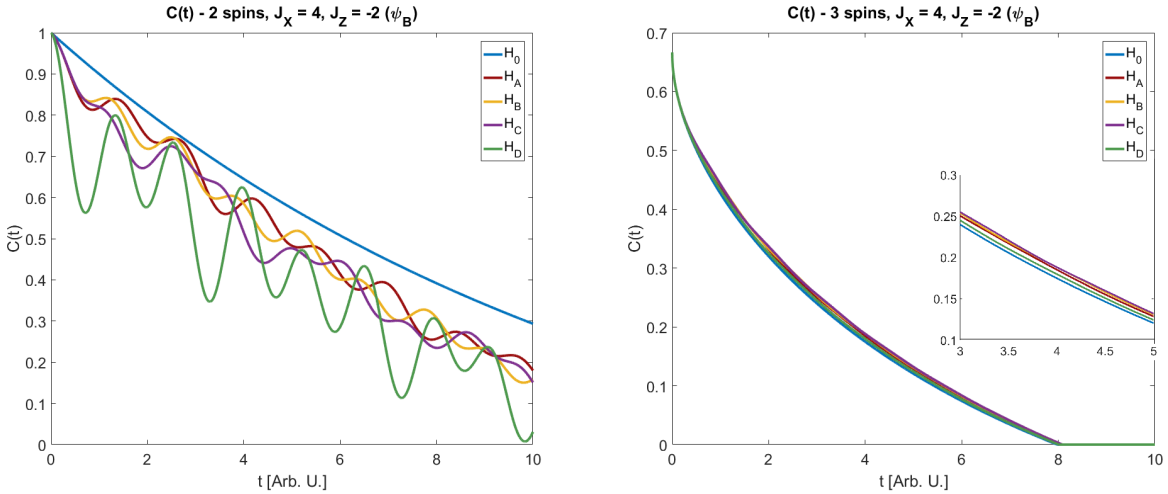

Figure 85: Time evolution of entanglement concurrence for two-spin (left) and three-spin chain (right) in the presence of three-dimensional DM interaction. Both initial states are characterized by single-flipped spin (ψ_B).

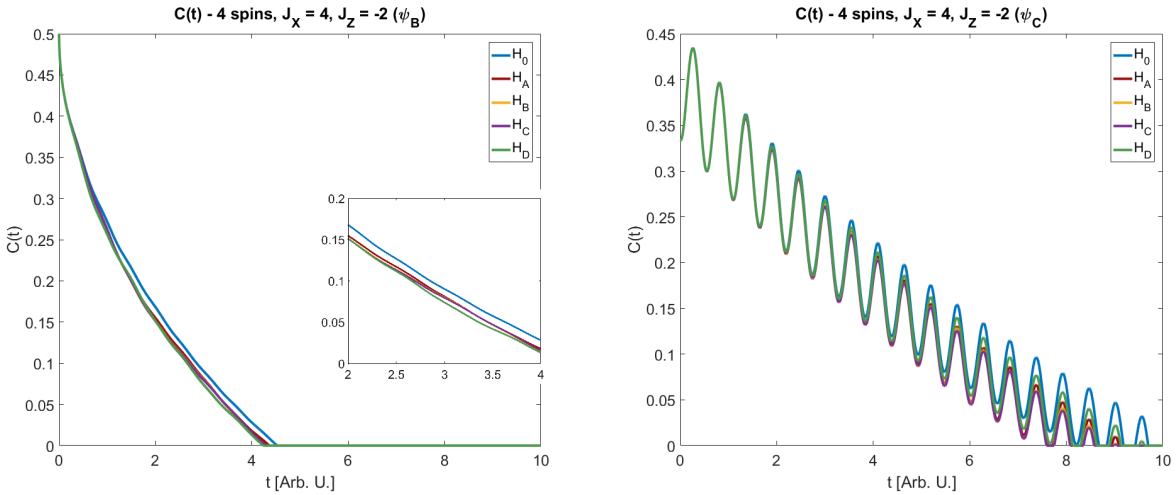

Figure 86: Time evolution of entanglement concurrence for a four-spin chain in the presence of three-dimensional DM interaction. The left plot presents this evolution for the initial state with one flipped spin (state ψ_B), the right one - for two flipped spins (state ψ_C).

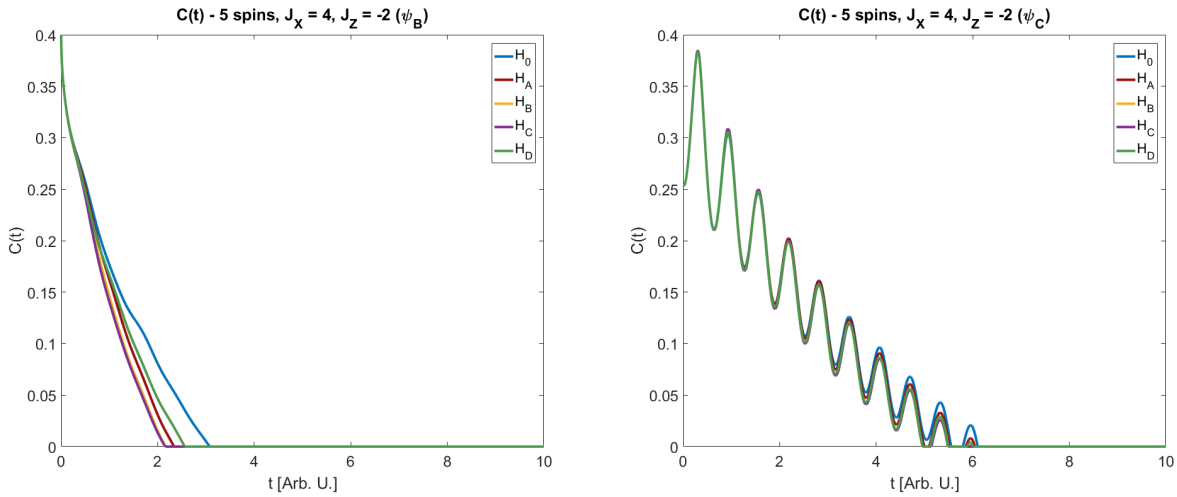

Figure 87: Time evolution of entanglement concurrence for a five-spin chain in the presence of three-dimensional DM interaction. The left plot presents this evolution for the initial state with one flipped spin (state ψ_B), the right one - for two flipped spins (state ψ_C).

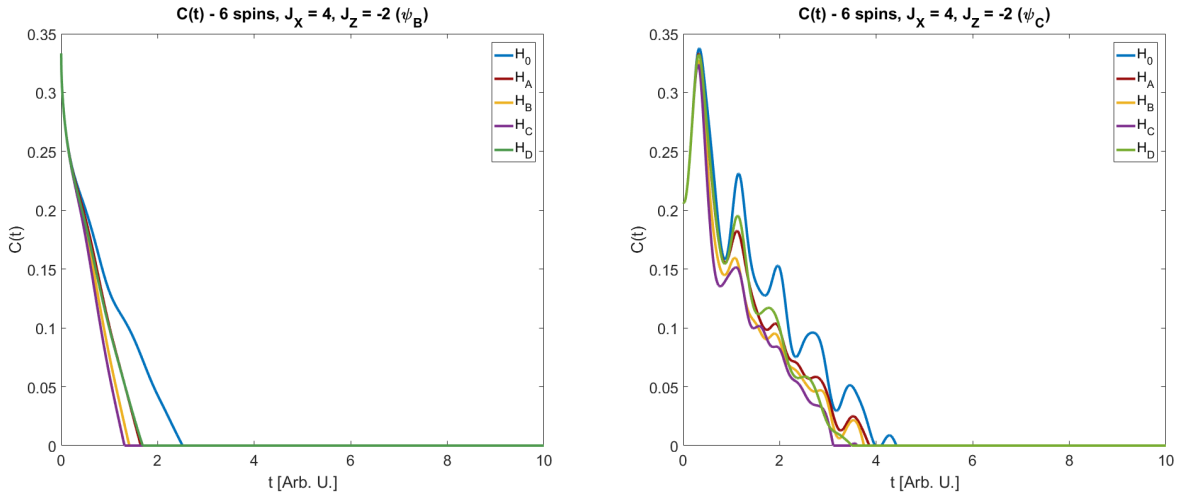

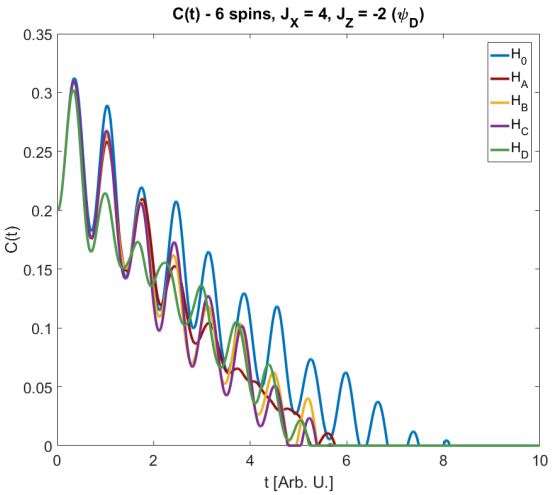

Figure 88: Time evolution of entanglement concurrence for a six-spin chain in the presence of three-dimensional DM interaction. Initial states are: state with one flipped spin (ψ_B, upper left plot), state with two flipped spins (ψ_C, right upper plot) and state with three flipped spins (ψ_D, lower plot).

CONCLUSION: With the sole exception of the three-spin case (Fig. 85, right plot), the most beneficial in maintaining entanglement in systems which undergo Markovian evolution are systems without Dzyaloshinskii - Moriya interaction, as all the figures above demonstrate the negative impact of DM antisymmetric exchange on entanglement. Excluding the blue plot, all others run similarly and no clear trend is showing; the greatest discrepancies between plots for selected Hamiltonians occur in the two-spin case and disappear for longer spin chains.

4.2.4 Kaplan - Shekhtman - Entin-Wohlman - Aharony interaction

Unidirectional KSEA interaction

The most commonly analysed case of KSEA interaction is the one restricted to K_{XY} component, described by the following Hamiltonian:

$$\hat{H} = \sum_{i=1}^{N} \left(-J_X (S_i^X S_{i+1}^X + S_i^Y S_{i+1}^Y) - J_Z S_i^Z S_{i+1}^Z + K_{XY} (S_i^X S_{i+1}^Y + S_i^Y S_{i+1}^X) \right).$$

The matrix form of this Hamiltonian for two spin chain reads:

$$\hat{H} = \begin{bmatrix} -J_Z & 0 & 0 & -2iK_{XY} \\ 0 & J_Z & -2J_X & 0 \\ 0 & -2J_X & J_Z & 0 \\ 2iK_{XY} & 0 & 0 & -J_Z \end{bmatrix}$$

and gives rise to following eigenvalues and eigenvectors:

$$E_1 = -2K_{XY} - J_Z \qquad |\alpha_1\rangle = \frac{1}{\sqrt{2}}\left(|\uparrow\uparrow\rangle + i|\downarrow\downarrow\rangle\right)$$

$$E_2 = J_Z - 2J_X \qquad |\alpha_2\rangle = \frac{1}{\sqrt{2}}\left(|\uparrow\downarrow\rangle + |\downarrow\uparrow\rangle\right)$$

$$E_3 = J_Z + 2J_X \qquad |\alpha_3\rangle = \frac{1}{\sqrt{2}}\left(|\uparrow\downarrow\rangle - |\downarrow\uparrow\rangle\right)$$

$$E_4 = 2K_{XY} - J_Z \qquad |\alpha_4\rangle = \frac{1}{\sqrt{2}}\left(|\uparrow\uparrow\rangle - i|\downarrow\downarrow\rangle\right)$$

This results, as well as their counterparts for longer chains were used to prepare the thermal states and the entanglement concurrence was calculated for particular sets of system parameters. The results of numerical simulations are shown in Figs. 89 - 93, whereby in the 89 and 92 the rotated reference frame is used to better visualize the entanglement:

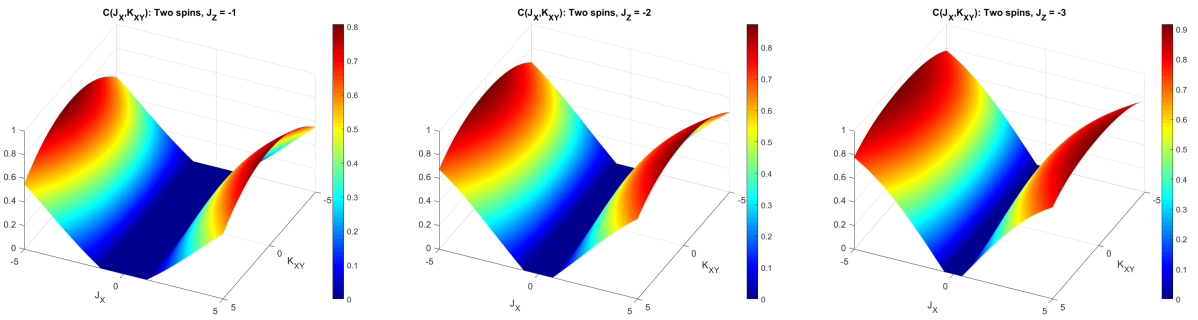

Figure 89: Entanglement as a function of J_X exchange integral and K_{XY} KSEA coefficient in two spin chain described by XXZ Heisenberg model with Kaplan - Shekhtman - Entin-Wohlman - Aharony interaction for thermal state.

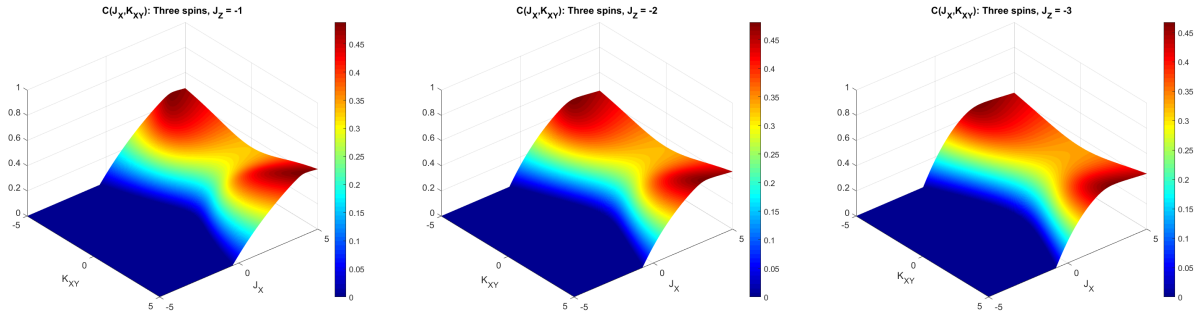

Figure 90: Entanglement as a function of J_X exchange integral and K_{XY} KSEA coefficient in three-spin chain described by XXZ Heisenberg model with KSEA interaction for thermal state.

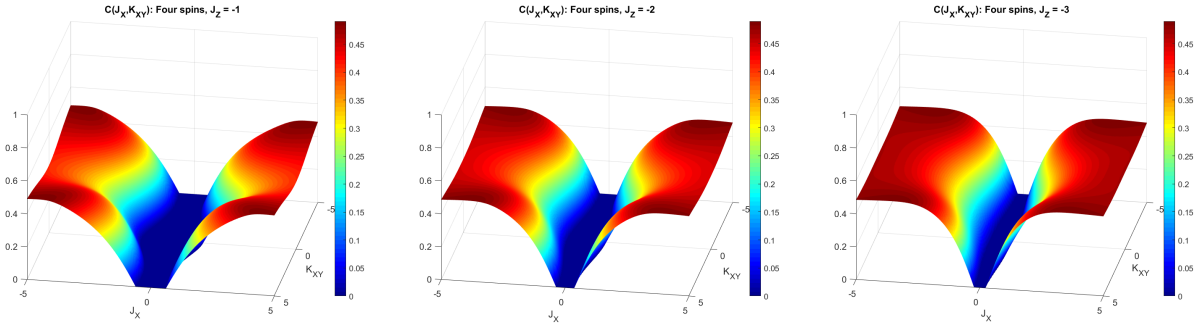

Figure 91: Entanglement as a function of J_X exchange integral and K_{XY} KSEA coefficient in four-spin chain described by XXZ Heisenberg model with KSEA interaction for thermal state.

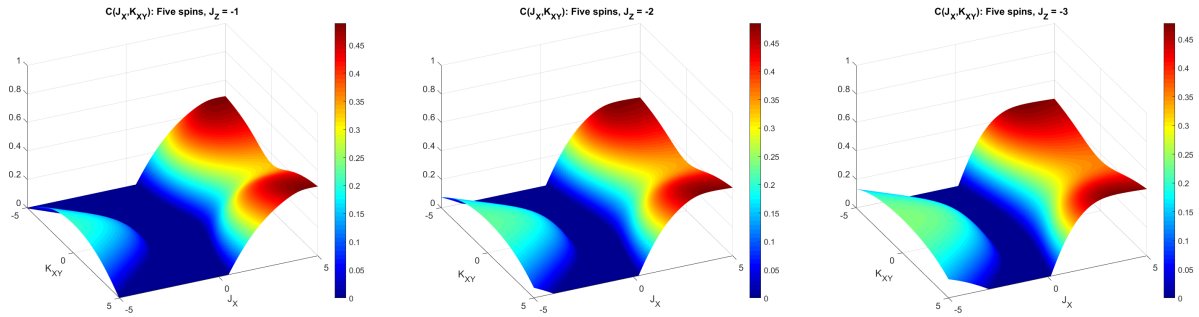

Figure 92: Entanglement as a function of J_X exchange integral and K_{XY} KSEA coefficient in five-spin chain described by XXZ Heisenberg model with KSEA interaction for thermal state.

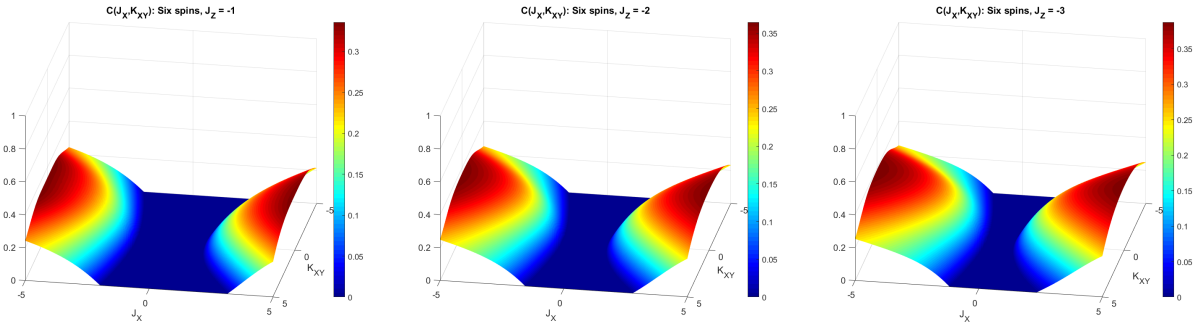

Figure 93: Entanglement as a function of J_X exchange integral and K_{XY} KSEA coefficient in six-spin chain described by XXZ Heisenberg model with KSEA interaction for thermal state.

CONCLUSION: From the point of view of entanglement in the thermal state, the impact of KSEA interactions is highly dependent on the number of spins in the chain. However, for two (Fig. 89) and six-spin chains (Fig. 93) it decreases the entanglement concurrence in the thermal state. For three, four and five spins in the chain (Figs. 90 - 92) the opposite effect can be observed. However, it is true only for systems for which the thermal state exhibits a high degree of entanglement. Comparing Fig. 24 and 92 one can notice that for the negative J_X exchange integral, which generally results in lower entanglement than its positive counterpart, the impact of the KSEA interaction is negative. The best result is obtained for $K_{XY} = 0$.

DYNAMICS OF ENTANGLEMENT IN THE DISSIPATIVE ENVIRONMENT:

In the following section, the results are presented for determining the evolution of entanglement for systems described by the XXZ Heisenberg Hamiltonian (the values of the $J_X = 4$, $J_Z = -2$ integrals are chosen following the results from the previous calculations). The results of numerical simulations for various spin chain lengths with KSEA interaction of different strengths put into Markovian dissipative environment are presented in Figs. 94 - 97:

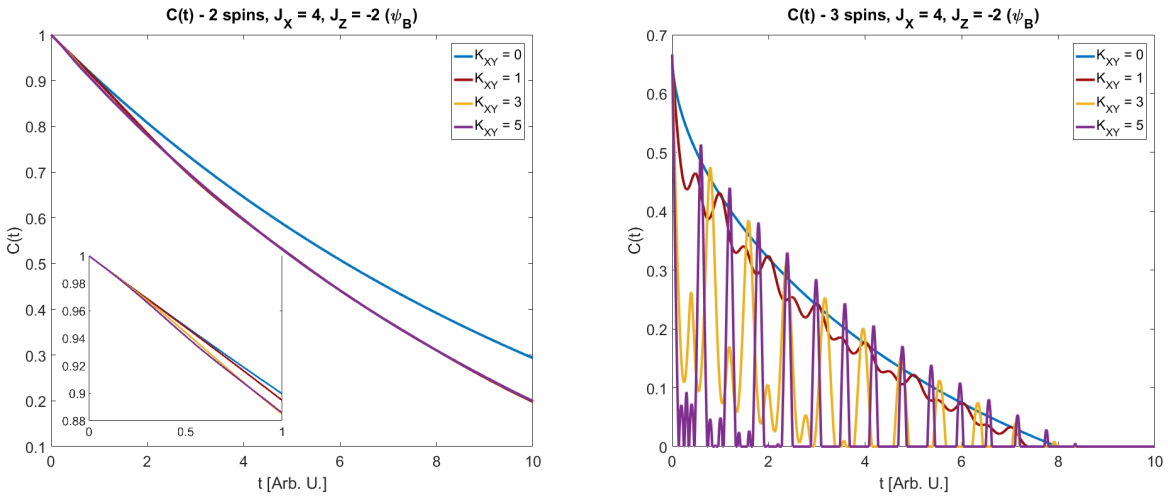

Figure 94: Time evolution of entanglement concurrence for two-spin (left) and three-spin chain (right) in the presence of unidirectional KSEA interaction of XY-type. Both initial states are characterized by single-flipped spin (ψ_B).

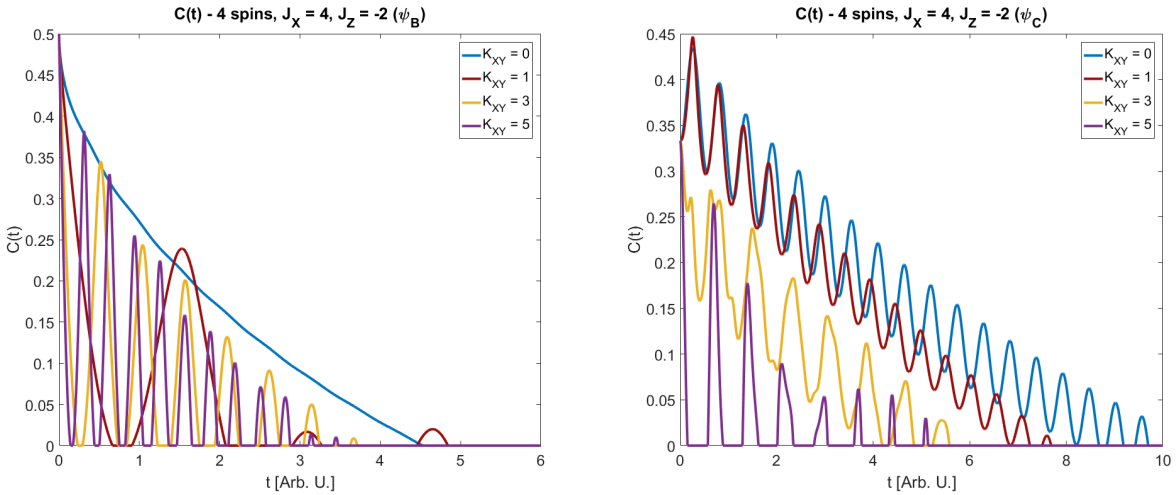

Figure 95: Time evolution of entanglement concurrence for a four-spin chain in the presence of unidirectional KSEA interaction of XY-type. The initial state was characterized by one (ψ_B, left) or two flipped spins (ψ_C, right).

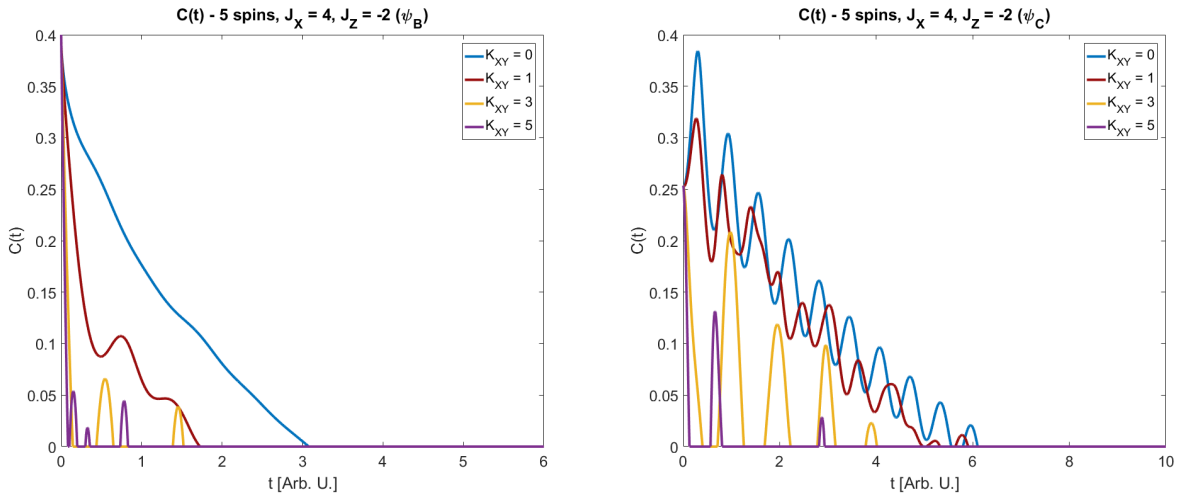

Figure 96: Time evolution of entanglement concurrence for a five-spin chain in presence of unidirectional KSEA interaction of XY-type. The initial state was characterized by one (ψ_B, left) or two flipped spins (ψ_C, right).

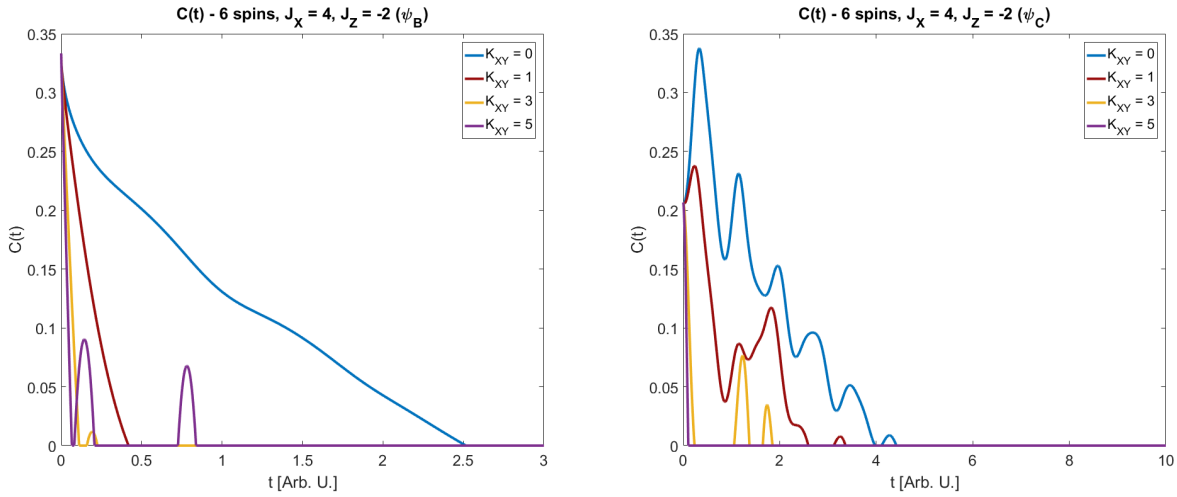

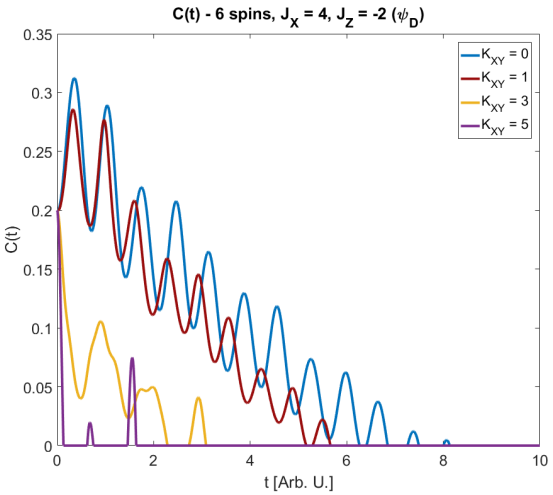

Figure 97: Time evolution of entanglement concurrence for a six-spin chain in the presence of one-dimensional KSEA interaction. Initial states are: state with one flipped spin (ψ_B, upper left plot), state with two flipped spins (ψ_C, right upper plot) and state with three flipped spins (ψ_D, lower plot).

CONCLUSION: With some exceptions, generally the XY-type KSEA interaction did not turn out to be beneficial in terms of preserving entanglement under the influence of the Markovian environment. The points of entanglement for the systems with non-zero KSEA coefficients overcome the entanglement for the systems without this interaction taken into account - for example, in a three-spin chain with one excitation from the ferromagnetic state (Fig. 94, right), where appropriately high KSEA interactions and adapted sampling allow the use of slightly higher entanglement, or in case of four spins and one excitation in initial state (Fig.95, left), where similar property can be utilized, here however for low KSEA interaction. In all other analyzed cases, the KSEA interaction shortens the decoherence time and leads to more rapid changes in entanglement - faster decreases and increases to low values. The more significant the interaction of the KSEA is, the greater the discrepancy between the total number of spins in the chain and the number of flipped spins in the initial state - if the number of spins "up" is close to the number of spins "down", the plots for small K_{XY} resemble the plots for systems without this effect (see, for example, Fig. 96, right or 97, the low one) - however, this is lost for higher number of spins.

Multidirectional KSEA interaction

The general Hamiltonian describing the XXZ Heisenberg chain with KSEA interaction reads:

$$\hat{H} = \sum_{i=1}^{N}(-J_X(S_i^X S_{i+1}^X + S_i^Y S_{i+1}^Y) - J_Z S_i^Z S_{i+1}^Z$$

$$+K_{XY}(S_i^X S_{i+1}^Y + S_i^Y S_{i+1}^X) + K_{YZ}(S_i^Y S_{i+1}^Z + S_i^Z S_{i+1}^Y) + K_{ZX}(S_i^Z S_{i+1}^X + S_i^X S_{i+1}^Z)).$$

which for two spin chains translates to the following matrix representation in the calculational basis:

$$\hat{H} = \begin{bmatrix} -J_Z & K_{ZX} - iK_{YZ} & K_{ZX} - iK_{YZ} & -2iK_{XY} \\ K_{ZX} + iK_{YZ} & J_Z & -2J_X & -K_{ZX} + iK_{YZ} \\ K_{ZX} + iK_{YZ} & -2J_X & J_Z & -K_{ZX} + iK_{YZ} \\ 2iK_{XY} & -K_{ZX} - iK_{YZ} & -K_{ZX} - iK_{YZ} & -J_Z \end{bmatrix}$$

Similarly as in the case of three-dimensional DM interaction, also here all the eigenvalues and components of eigenvectors are functions of all five parameters of Hamiltonian and therefore again the derivation of density matrix is entrusted to computational software. The results of numerical calculations of the entanglement concurrence are shown as color maps in Figs. 98 - 102:

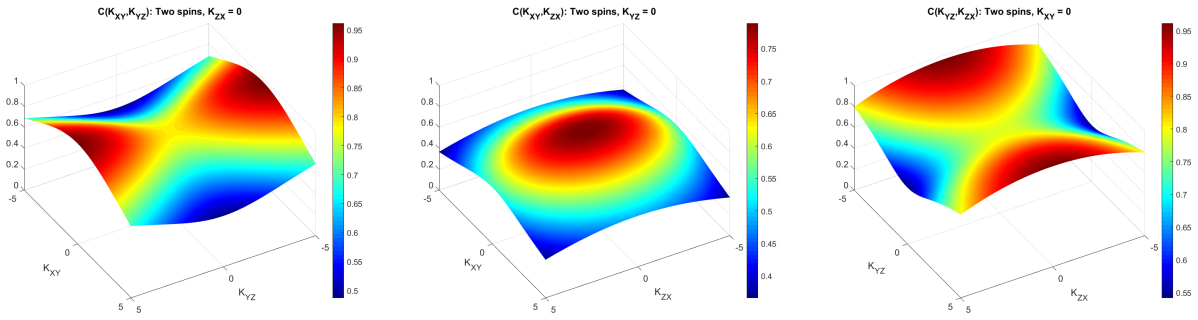

Figure 98: Entanglement concurrence in XXZ Heisenberg chain of two spins with KSEA interactions as a function of: K_{XY} and K_{YZ}(left), K_{XY} and K_{ZX} (centre) and K_{YZ} and K_{ZX} (right).

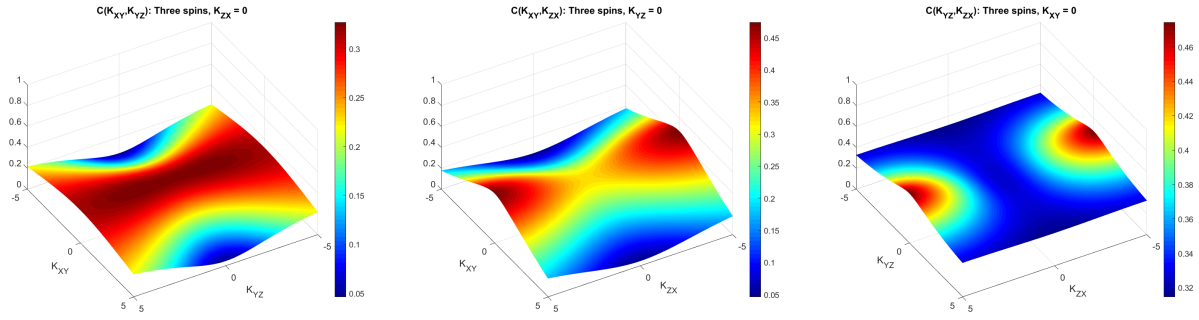

Figure 99: Entanglement concurrence in XXZ Heisenberg chain of three spins with KSEA interactions as a function of: K_{XY} and K_{YZ}(left), K_{XY} and K_{ZX} (centre) and K_{YZ} and K_{ZX} (right).

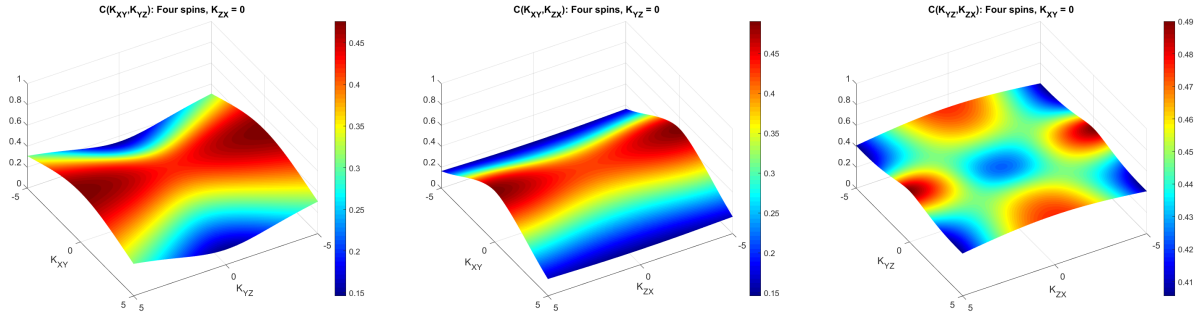

Figure 100: Entanglement concurrence in XXZ Heisenberg chain of four spins with KSEA interactions as a function of: K_{XY} and K_{YZ}(left), K_{XY} and K_{ZX} (centre) and K_{YZ} and K_{ZX} (right).

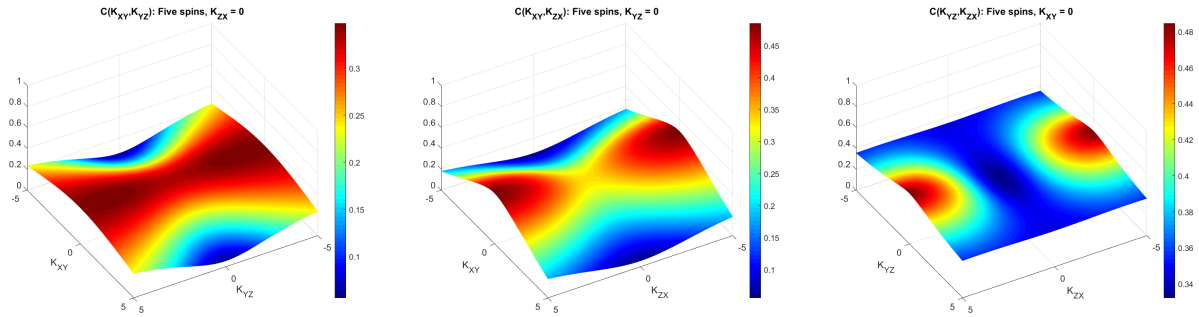

Figure 101: Entanglement concurrence in XXZ Heisenberg chain of four spins with KSEA interactions as a function of: K_{XY} and K_{YZ}(left), K_{XY} and K_{ZX} (centre) and K_{YZ} and K_{ZX} (right).

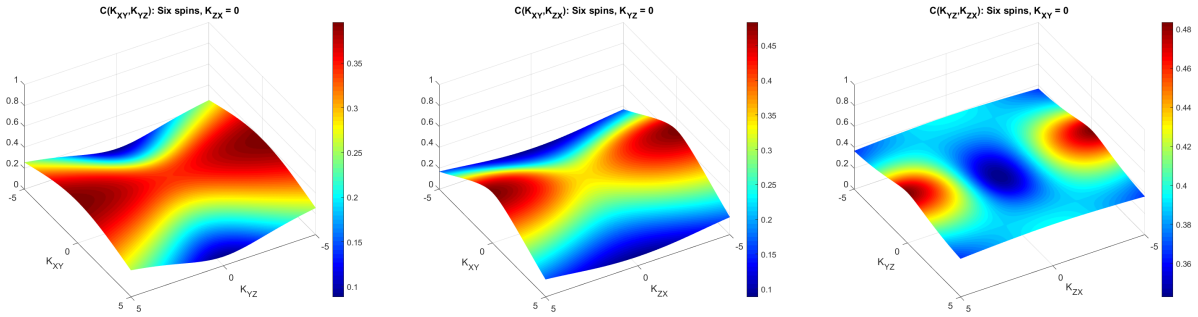

Figure 102: Entanglement concurrence in XXZ Heisenberg chain of six spins with KSEA interactions as a function of: K_{XY} and K_{YZ}(left), K_{XY} and K_{ZX} (centre) and K_{YZ} and K_{ZX} (right).

CONCLUSION: The results above show that each KSEA interaction component has a different impact on entanglement concurrence in the thermal state. Firstly, it is once again confirmed that with an increase in K_{XY}, the entanglement in the thermal state vanishes, which corresponds to the results of the previous section. High values of the K_{ZX} component are undesirable for two spin chains (Fig. 98) but may enhance entanglement in chains of odd number of spins (Figs. 99 and 101). In the case of two spins, the K_{YZ} component has a strictly positive impact (it enhances the entanglement when high enough); however, for longer chains, the behavior of the entanglement as a function of this particular parameter became more complex. For high values of K_{ZX}, it became a negative factor for entanglement. For values of K_{ZX} close to zero, this behaviour turns around and K_{YZ} enhances the entanglement with increasing. It is most visible in chains of even number of spins (see Figs. 100 or 102, the rightmost one). For the odd number of spins in the chain, the entanglement increase property of K_{ZX} reveals itself only for low values of K_{YZ}.

4.2.5 Three Spin Interaction

TSI interaction only

Hamiltonian describing the XXZ Heisenberg chain with three spin interaction is in general given by the following formula:

$$\hat{H} = \sum_{i=1}^{N}(-J_X(S_i^X S_{i+1}^X + S_i^Y S_{i+1}^Y) - J_Z S_i^Z S_{i+1}^Z)$$

$$+k\sum_{j=2}^{N-1}\left(\hat{S}_{j-1}^X \hat{S}_j^Z \hat{S}_{j+1}^X + \hat{S}_{j-1}^Y \hat{S}_j^Z \hat{S}_{j+1}^Y\right)$$

and the simplest chain in which this type of interaction is present is a three-spin chain. The matrix representation of such a Hamiltonian in a calculational basis is:

$$\begin{bmatrix} -3J_Z & 0 & 0 & 0 & 0 & 0 & 0 & 0 \\ 0 & J_Z & 2k-2J_X & 0 & 2k-2J_X & 0 & 0 & 0 \\ 0 & 2k-2J_X & J_Z & 0 & 2k-2J_X & 0 & 0 & 0 \\ 0 & 0 & 0 & J_Z & 0 & -2k-2J_X & -2k-2J_X & 0 \\ 0 & 2k-2J_X & 2k-2J_X & 0 & J_Z & 0 & 0 & 0 \\ 0 & 0 & 0 & -2k-2J_X & 0 & J_Z & -2k-2J_X & 0 \\ 0 & 0 & 0 & -2k-2J_X & 0 & -2k-2J_X & J_Z & 0 \\ 0 & 0 & 0 & 0 & 0 & 0 & 0 & -3J_Z \end{bmatrix}$$

and it can be diagonalised to obtain the following eigenenergies and eigenvectors:

$$E_1 = -3J_Z \qquad |\alpha_1\rangle = |\uparrow\uparrow\uparrow\rangle$$

$$E_2 = 2J_X + J_Z - 2k \qquad |\alpha_2\rangle = \frac{1}{\sqrt{2}}\left(|\uparrow\uparrow\downarrow\rangle - |\uparrow\downarrow\uparrow\rangle\right)$$

$$E_3 = 2J_X + J_Z - 2k \qquad |\alpha_3\rangle = \frac{1}{\sqrt{2}}\left(|\uparrow\uparrow\downarrow\rangle - |\downarrow\uparrow\uparrow\rangle\right)$$

$$E_4 = 2J_X + J_Z + 2k \qquad |\alpha_4\rangle = \frac{1}{\sqrt{2}}\left(|\uparrow\downarrow\downarrow\rangle - |\downarrow\uparrow\downarrow\rangle\right)$$

$$E_5 = 2J_X + J_Z + 2k \qquad |\alpha_5\rangle = \frac{1}{\sqrt{2}}\left(|\downarrow\uparrow\downarrow\rangle - |\downarrow\downarrow\uparrow\rangle\right)$$

$$E_6 = J_Z - 4J_X - 4k \qquad |\alpha_6\rangle = \frac{1}{\sqrt{3}}\left(|\downarrow\uparrow\downarrow\rangle + |\downarrow\downarrow\uparrow\rangle + |\uparrow\downarrow\downarrow\rangle\right)$$

$$E_7 = J_Z - 4J_X + 4k \qquad |\alpha_7\rangle = \frac{1}{\sqrt{3}}\left(|\downarrow\uparrow\uparrow\rangle + |\uparrow\downarrow\uparrow\rangle + |\uparrow\uparrow\downarrow\rangle\right)$$

$$E_8 - -3J_Z \qquad |\alpha_8\rangle = |\downarrow\downarrow\downarrow\rangle.$$

Using these eigenvalues and eigenvectors, the thermal state was constructed and the set temperature and the different values of J_X and k the concurrence was calculated. The results are presented in colormaps below (the reference frame in Fig. 103 is rotated to better visualize the function):

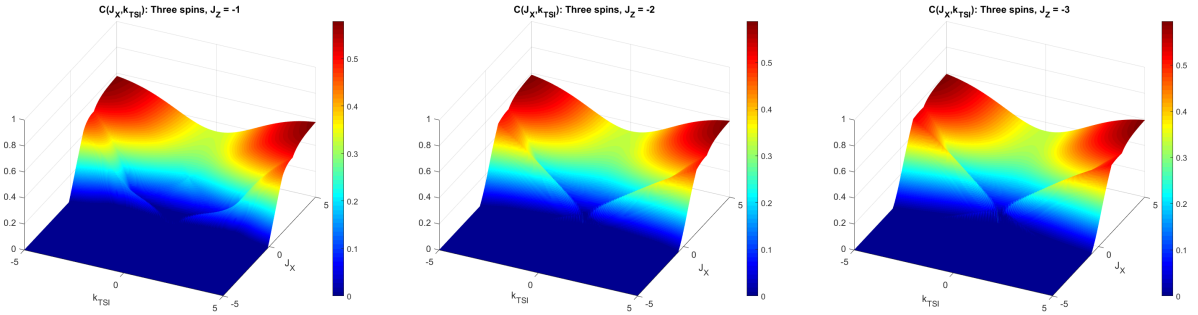

Figure 103: Entanglement concurrence in XXZ Heisenberg chain of three spins with TSI as a function of exchange integral J_X and k - three-spin interaction coefficient.

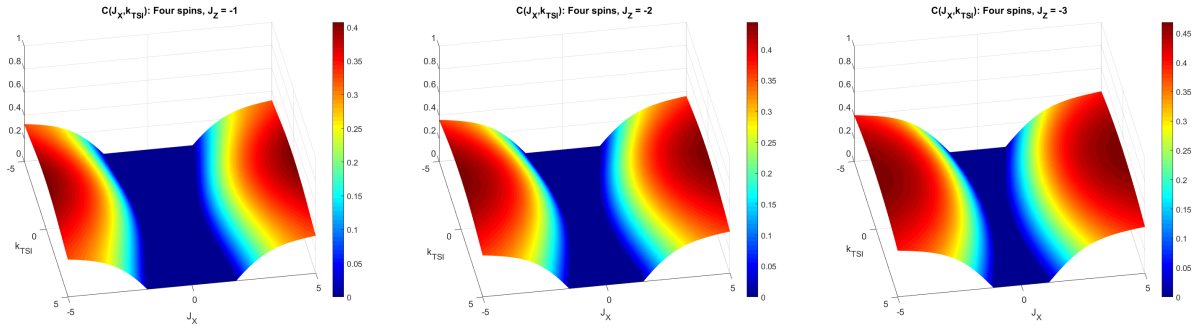

Figure 104: Entanglement concurrence in XXZ Heisenberg chain of four spins with TSI as a function of exchange integral J_X and k - three-spin interaction coefficient.

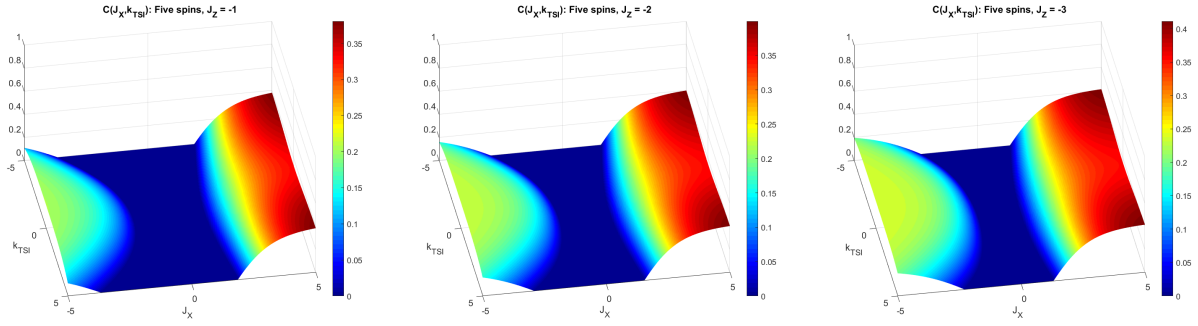

Figure 105: Entanglement concurrence in XXZ Heisenberg chain of five-spins with TSI as a function of exchange integral J_X and k - three-spin interaction coefficient.

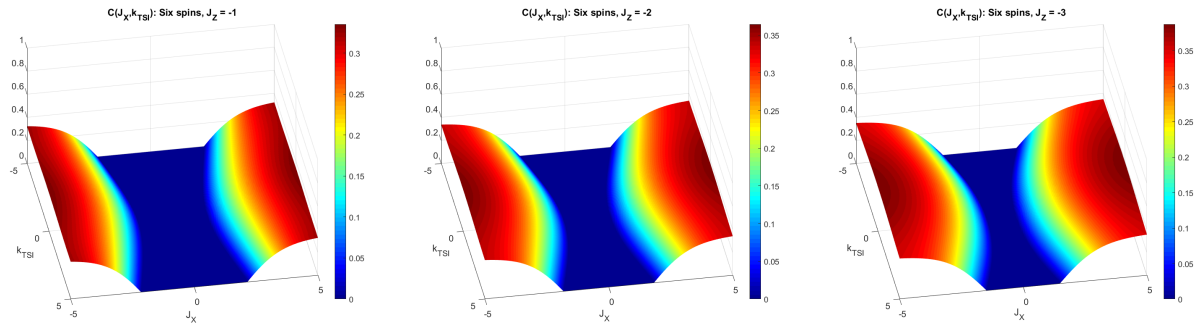

Figure 106: Entanglement concurrence in XXZ Heisenberg chain of six-spins with TSI as a function of exchange integral J_X and k - three-spin interaction coefficient.

CONCLUSION: As for several previously analyzed factors, Three Spin Interaction (TSI) impact on the entanglement depends on the parity of the chain. For four (Fig. 104) and six (Fig. 106) spins in the chain, this impact is clearly negative; the higher this interaction strength, the lower the entanglement in the state of thermal equilibrium. However, for an odd number of spins in the chain, this effect differs - paired with a positive J_X exchange integral, a high value TSI tends to increase the entanglement in the thermal state. It is clearly visible in Fig. 103 and to a lesser extent in Fig. 105, that for negative J_X TSI remains the factor that reduces the entanglement in the thermal state.

DYNAMICS OF ENTANGLEMENT IN THE DISSIPATIVE ENVIRONMENT:

In this section, the results of calculations of the entanglement time evolution for the systems described by the XXZ Heisenberg Hamiltonian with TSI effect are presented. The exchange integrals are set to $J_Z = -2$, $J_X = 4$, based on the results of the previous sections. Various chain lengths, as well as TSI of different strengths, together with the Markovian dissipative environment were taken into account:

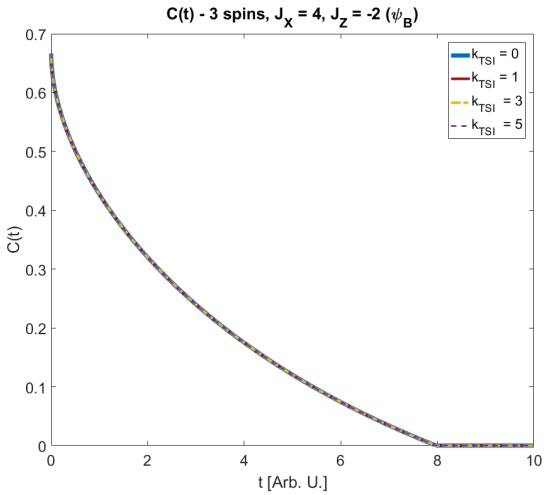

Figure 107: Time evolution of entanglement concurrence for three spin chain with Three Spin Interaction (TSI) for initial state with one flipped spin (ψ_B).

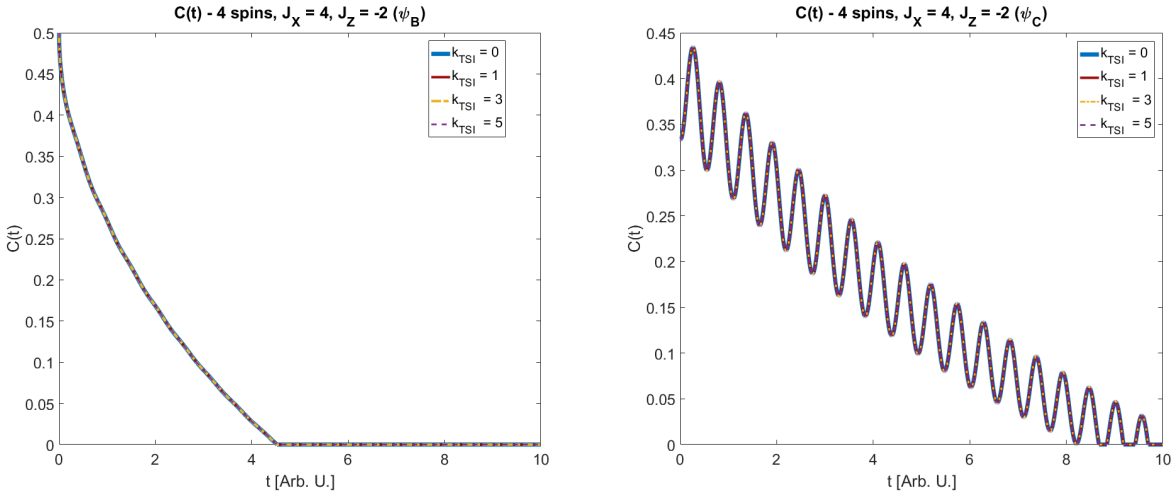

Figure 108: Time evolution of entanglement concurrence for four spin chain with Three Spin Interaction (TSI) for initial states: with one flipped spin (ψ_B, left) and two flipped spins (ψ_C, right).

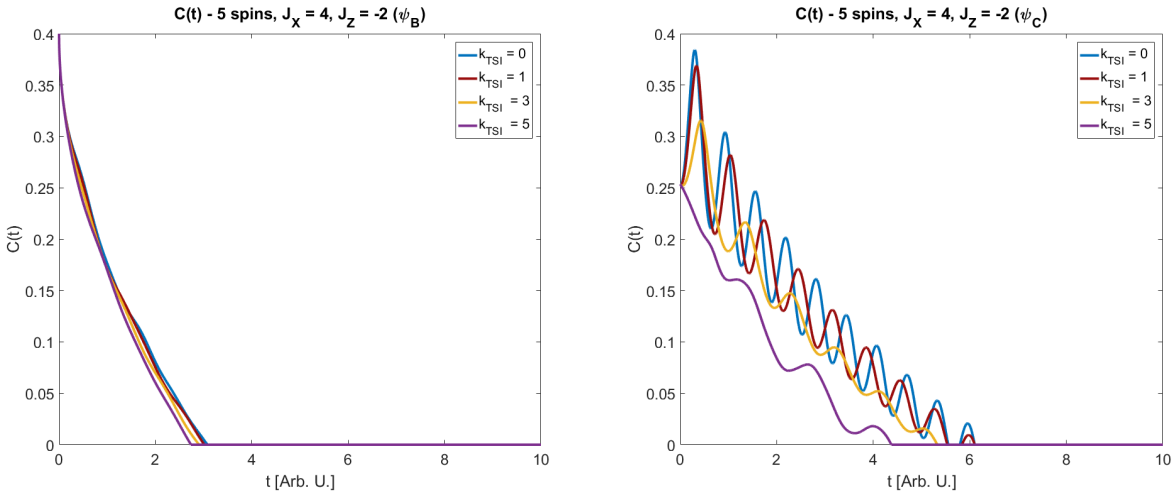

Figure 109: Time evolution of entanglement concurrence for five spin chain with Three Spin Interaction (TSI) for initial states: with one flipped spin (ψ_B, left) and two flipped spins (ψ_C, right).

CONCLUSION: For short spin chains, the presence of TSI is undetectable in terms of the time evolution of entanglement (Figs. 107 and 108, as well as the states with one flipped spin from Figs. 109 and 110) - the time evolution of entanglement does not differ for systems with this effect and systems without it. For longer spin chains and a low number of spin excitations in the initial state, only the high values of TSI become a negative factor for entanglement preservation. For five- and six-spin chains and two

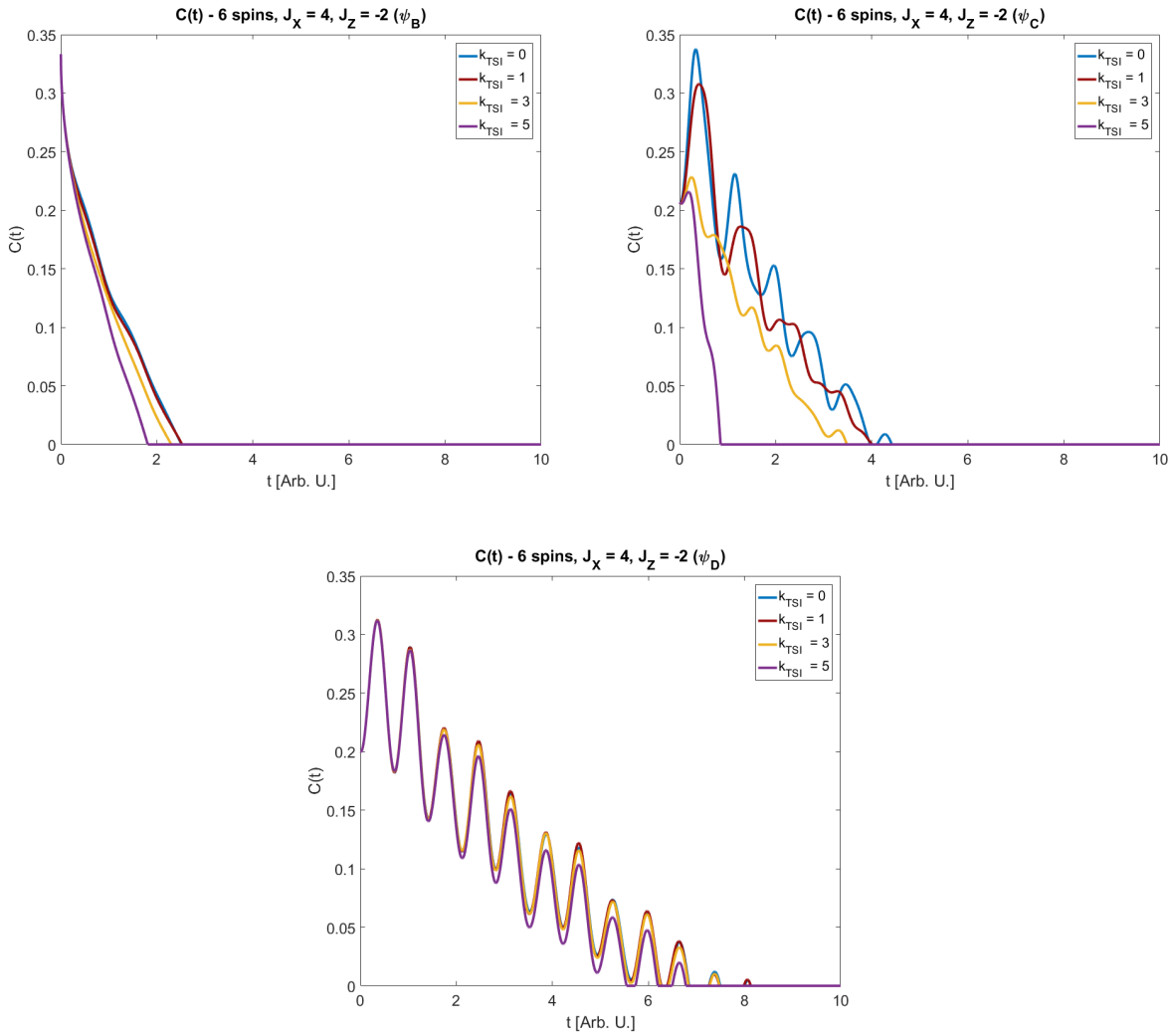

Figure 110: Time evolution of entanglement concurrence for six spin chain with Three Spin Interaction (TSI) for initial states: with one flipped spin (ψ_B, left upper one) and two flipped spins (ψ_C, right upper one) and with three flipped spins (ψ_D, lower one).

excitations in the initial state, TSI begins to play an important role; that is, the higher the magnitude of TSI is, the shorter the time of total decoherence, and the plot of entanglement concurrence as a function of time moves closer to the initial time. The most interesting result can be seen in Fig. 110 - namely, the $k_{TSI} = 1$ provides a better result than $k_{TSI} = 0$ - however, this discrepancy is negligible when compared to the entanglement concurrence of both plots.

Summary

This work has been written to determine the impact of system parameters on the entanglement between parts of spin chains. The study concerns isolated systems and their quantum correlations in thermal state and time evolution of the entanglement in chains coupled to the environment with a bosonic, Markovian nature. Chains of different lengths are considered, and various effects are taken into account: three types of Heisenberg exchange (XXX, XXZ, XYZ), uniform and non-uniform or constant and time-dependent magnetic field, Dzyaloshinskii - Moriya (DM) and Kaplan - Shekhtman - Entin Wohlmann - Aharony (KSEA) type of superexchange or Three-Spin Interaction (TSI). The analytical part of this thesis is based on original computational procedures created to determine and diagonalize the thermal density matrix and then calculate the entanglement in such a state. Also, the software tools were created to numerically solve the Lindblad equation, that governs the time evolution of an open system coupled to a Markovian environment, and to reduce the density matrix to indicate, between which spins the entanglement is investigated.

The study of the entanglement between spins of an isolated system in a thermal equilibrium state reveals the following conclusions: the systems described with the Heisenberg XXX model (isotropic exchange interaction) require the negative exchange integral to exhibit any degree of entanglement. With the temperature increase, the absolute value of the exchange integral necessary to provide a desired value of entanglement also grows. In the XXZ model, the most beneficial conditions for thermal entanglement occur for the negative value of J_Z exchange integral and the high value of J_X integral, regardless of the sign of the former. For the XYZ model, the most advantageous conditions for high entanglement are for specific combinations of exchange integral signs - for example, the chains consisting of an even number of spins benefit from the negative product of exchange integral in perpendicular directions. A conclusion true for all the analysed models is as follows: the longer the chain is, the smaller the bipartite entanglement is (which is a direct consequence of entanglement monogamy), however, for

shorter spin chains, the system with an even number of spins manifests higher entanglement for the same set of parameters than are shorter, odd-numbered counterparts. A uniform magnetic field turned out to have a negative impact on the entanglement in the thermal state for chains with an even number of spins, and for short chains with an odd number of spins, the maximal value of entanglement is reached for some non-zero magnetic field. This value is, however, small and decreases as the chains lengthen; therefore, this effect vanishes for longer chains. Introducing the non-uniformity in a magnetic field can have a slight entanglement-enhancing property; it appears, however, only for systems with low to medium entanglement in the uniform field - systems with high entanglement remain unaffected by this non-uniformity. Unidirectional DM interactions have an almost generally negative impact on the entanglement - in some analysed cases it slightly enhances the entanglement. Still, this phenomenon occurs rarely (is observed only in five spin chains) and with negligible intensity. Moreover, the analysis of three-dimensional DM interactions shows that no direction of this superexchange interaction is desired from the point of view of high entanglement. Unidirectional KSEA interaction impact depends on the length of the chain - short chains, from three to five spins in them, exhibit higher entanglement for a larger absolute value of the KSEA coefficient, regardless of its sign. For two- and six-spin chains, the opposite effect is observed: entanglement decreases with the growth of this parameter. A similar, more general result can be seen in three-dimensional KSEA interaction analysis: K_{XY} component, the one investigated in the section concerning only one component of this interaction, confirmed its negative impact on the two- and six-spin chain. Other components have a more complex impact: K_{YZ} enhances the entanglement in all the cases, but its positive effect diminishes for longer chains. K_{ZX} impact differs depending on whether the chain cardinality is odd or even - in the latter case it positively affects the entanglement, in the former - it negatively. Finally, the TSI effect also turns out to be dependent on chain parity - chains of odd cardinality benefit from it, while chains with an even number of spins lose the entanglement due to the presence of this interaction. Nevertheless, all these parity-dependent effects vanish for long spin chains.

Numerical simulations of open system behaviour in terms of entanglement provide other information about the investigated topic. In terms of system parameters' impact on the entanglement behaviour, the following conclusions are formulated: the general observation is that in all cases entanglement disappears exponentially, with an additional effect - wave-like behaviour of the entanglement in time - resulting from the transition between the eigenstates. This occurrence may cause temporary entanglement increases, and it is solely dependent on the system Hamiltonian (as it dictates the structure of energy

levels). The study of the change in entanglement during the evolution of the spin chain described only in terms of the Heisenberg exchange interactions reveals that the most resistant to the environmental influence are the systems in which the J_Z integral is negative and smaller in absolute value than the J_X integral. The sign of the latter does not affect in any way the decoherence of the system. A similar conclusion holds also for the XYZ Heisenberg model - when J_X and J_Y in the Hamiltonian are positive, the systems exhibit somehow shorter decoherence time than their counterparts with negative values of these integrals. In such systems, even when the chain loses the entanglement totally (sudden entanglement death), under the appropriate conditions, there may be a temporary entanglement re-establishment, called sudden entanglement rebirth. The time-independent magnetic field has no impact on the entanglement evolution; however, the field varying periodically in time may be a beneficial factor for shorter chains. Still, whether applying this field enhances the entanglement depends on the angular frequency of the field and its adjustment to the model parameters - initial states with an odd number of magnetic excitations (relative to the fully ferromagnetic state) benefit from the lower frequencies, states with an even number of excitations - from the higher. The presence of the DM and KSEA interaction almost universally turns out to be a negative factor in terms of preserving the entanglement, and TSI slightly increases the entanglement in longer chains; however, the discrepancies between the decoherence times in chains with and without this effect is negligible. In all the analysed chains, only the high values of this effect result in a more rapid entanglement decrease; for the chains in which the TSI coefficient is similar in value to the exchange integral its effect is non-detectable. As a summary, to create a chain with high resistance to loss of entanglement, one may resort to materials interacting under the XXZ Heisenberg model, with a positive J_X exchange integral, and a negative and lower in absolute value J_Z integral, with no additional factors. The particular time-dependent magnetic field may slightly and temporarily increase the entanglement concurrence, but the most important factor is still the influence of the environment.

At the end, the author expresses the hope that the results obtained for this dissertation will reach a wider group of readers, will be re-analysed, processed, and in some way contribute to Quantum Informatics development as guidelines for designing the devices for quantum computations settled on the spin systems.

Scientific activity of PhD candidate

During my education at the University of Rzeszow's Doctoral School, I participated in the preparation of the following articles:

1. P. Jakubczyk, A. Wal, **M. Kaczor**, D. Jakubczyk, M. Łabuz, J. Milewski, *A Maple package for combinatorial aspects of Bethe Ansatz*, Comput. Phys. Commun. **261**, 107720 (2021).

2. L. Gálisová, **M. Kaczor**, *Ground State, Magnetization Process and Bipartite Quantum Entanglement of a Spin-1/2 Ising–Heisenberg Model on Planar Lattices of Interconnected Trigonal Bipyramids*, Entropy **23**, 1671 (2021).

3. **M.Kaczor**, I. Tralle, P. Jakubczyk, S. Stagraczyński, L. Chotorlishvili, *Switching of the information backflow between a helical spin system and non-Markovian bath*, Ann. Phys. **442**, 168918 (2022).

4. **M. Kaczor**, P. Jakubczyk, *Numerical analysis of bipartite entanglement evolution in simple cubic 1/2-spin system with additional spin 1 dopant*, Quant. Inf. Process. **22**, 168 (2023).

5. **M. Kaczor**, A. Stasik, *Dissipative Time Evolution of Entanglement in the Tetrahedral Structure of Spins $s = \frac{1}{2}$ - a Numerical Analysis*, Int. J. Theor. Phys. **63**, 63 (2024).

and actively participated in the following conferences:

1. **XVIII Ogólnopolska Sesja Koł Naukowych Fizyków** (Kraków, 21 - 24 November 2019): *Własności dyspersyjne fal spinowych w strukturach BCC z frustracja magnetyczna* - oral presentation.

2. **Sympozjum Młodych Naukowców Wydziału Fizyki Uniwersytetu Warszawskiego** (Warszawa, 24 - 28 August 2020): *Wpływ otoczenia oraz oddziaływań wymiennych na wielkość splatania kwantowego w układzie spinów - sieci krystalicznej* - poster presentation.

3. **YOUNG MULTIS. Multiscale Phenomena in Condensed Matter** (Kraków, 5 - 7 July 2021): *Analysis of information dynamics in chiral spin chain coupled to boson reservoir* - short oral presentation (flash talk) supplemented with the poster.

4. **XIV Interdyscyplinarna Konferencja Naukowa TYGIEL 2022** (Lublin, 24 - 27 March 2022):*Określanie wpływu parametrów modelu na splatanie termalne w układach spinowych* - oral presentation.

5. **Multidyscyplinarna Konferencja Doktorantów Uniwersytetu Szczecińskiego 2.0** (Szczecin, 22 - 24 June 2022): *Analiza wpływu parametrów układu na splatanie termiczne w łańcuchach spinowych opisywanych modelem Heisenberga typu XXZ* - oral presentation.

6. **XV Interdyscyplinarna Konferencja Naukowa TYGIEL 2023** (Lublin, 23 - 26 March 2023):*Analiza numeryczna ewolucji czasowej splatania w układzie kubicznym spinów* $s = \frac{1}{2}$ *domieszkowanym spinem* $S = 1$ - oral presentation.

7. **XVI Rzeszowska Konferencja Młodych Fizyków** (2 June 2023), *Wpływ domieszkowania tetraedralnej struktury spinów s = 1/2 dodatkowym spinem na ewolucje czasowa splatania w otoczeniu o charakterze markowiańskim* - oral presentation.

8. **Gdańsk Workshop of Mathematical Physics: Mathematical Structures in Quantum Mechanics** (Gdańsk, 19 -23 June 2023): *Time evolution of entanglement in the tetrahedral structure of spins located in Markovian environment* - oral presentation.

9. **XVI Kopernikańskie Seminarium Doktoranckie** (Toruń, 29-30 June 2023): *Ewolucja czasowa splatania w tetraedralnej strukturze spinów* $s = \frac{1}{2}$ *w otoczeniu markowiańskim* - poster presentation.

10. **XVII Rzeszowska Konferencja Młodych Fizyków** (6 - 7 June 2024), *Hybrydowa dynamika splatania kwantowego w jedno- i dwuwymiarowych układach spinowych* - oral presentation.

Bibliography

[1] A. Peres, *Quantum Theory. Concepts and Methods*, Springer, Dordrecht 2002.

[2] J. L. Basdevant, J. Dalibard, *Quantum Mechanics*, Springer-Verlag, Berlin Heideberg (2002).

[3] D. J. Griffiths, *Introduction to Quantum Mechanics*, Prentice Hall, 2004.

[4] J. von Neumann, *Mathematische Grundlagen der Quantenmechanik*, Springer-Verlag, Berlin 1932. English Translation: R. T. Beyer, *Mathematical Foundations of Quantum Mechanics*, Princeton University Press, Princeton 1955.

[5] A. Einstein, N. Rosen, B. Podolsky, Phys. Rev. **47**, 777 (1935).

[6] E. Schrödinger, Naturwissenschaft, **23**, 807 (1935).

[7] J. S. Bell, Physics Physique Fizika, **1**, 195 (1964).

[8] D. Bohm, Phys. Rev., **85**, 166 (1952).

[9] E. S. Fry, Phys. Rev. A, **8**, 1219 (1973).

[10] A. Aspect, P. Grangier, G. Roger, Phys. Rev. Lett., **49**, 91 (1982).

[11] A. Aspect, J. Dalibard, G. Roger, Phys. Rev. Lett., **49**, 1804 (1982).

[12] M. A. Nielsen, I. L. Chuang, *Quantum Computation and Quantum Information*, Cambridge University Press (2000).

[13] A. Ekert, P. L. Knight, Am. J. Phys., **63**, 415-423 (1995).

[14] R. F. Werner, Phys. Rev. A, **40**, 4277 (1989).

[15] R. Horodecki *et al.*, Rev. Mod. Phys., **81**, 865 (2009).

[16] A. Peres, Phys. Rev. Lett. **77**, 1413 (1996).

[17] M. Horodecki, P. Horodecki, R. Horodecki, Phys. Lett. A **223**, 1-8 (1996).

[18] G. Vidal, J. Mod. Opt., **47**, 355-376 (2000).

[19] S. A. Hill, W. K. Wooters, Phys. Rev. Lett., **78**, 5022 (1997).

[20] W. K. Wooters, Phys. Rev. Lett., **80**, 2245 (1998).

[21] B. Schumacher, Phys. Rev. A, **51**, 2738 (1995).

[22] C. E. Shannon, Bell Labs Tech. J., **27**, 379 - 423 (1948).

[23] R. Horodecki, M. Horodecki, Phys. Rev. A, **54**, 1838 (1996).

[24] N. J. Cerf, C. Adami, Phys. Rev. Lett., **79**, 5194 (1997).

[25] E. Santos, Phys. Rev. A, **69**, 022305 (2004). *Erratum:* E. Santos, Phys. Rev. A, **70**, 059901 (2004).

[26] V. Vedral, M. B. Plenio, Phys. Rev. A, **57**, 1619 (1998).

[27] L. S. Lima, Eur. Phys. J. D, **73**, 6 (2019).

[28] B. M. Terhal, Phys. Lett. A, **271**, 319–326 (2000).

[29] D. Chruściński, G. Sarbicki, J. Phys. A: Math. Theor., **47**, 483001 (2014).

[30] D. Girolami, T. Tufaerelli, G. Adesso, Phys. Rev. Lett., **110**, 240402 (2013).

[31] E. P. Wigner, M. M. Yanase, Proc. Natl. Acad. Sci. USA, **49**, 910 (1963).

[32] S. L. Luo, Theor. Math. Phys., **143**, 681 (2005).

[33] E. H. Lieb, Adv. Math., **11**, 267-288 (1973).

[34] I. Marvian, R. W. Spekkens, Nat. Commun., **5**, 3821 (2014).

[35] S. L. Braunstein, C. M. Caves, Phys. Rev. Lett., **72**, 3439 (1994).

[36] S. L. Braunstein, C. M. Caves, G. J. Milburn, Ann. Phys., **247**, 135 - 173 (1996).

[37] S. Kim *et al.*, Phys. Rev. A, **97**, 032326 (2018).

[38] O. Gühne, G. Tóth, H. J. Briegel, New J. Phys., **7** 229 (2005).

[39] I. Bengtsson, K. Życzkowski, *Geometry of Quantum States. An introduction to Quantum Entanglement*, Cambridge Univ. Press, 2017.

[40] D. M. Greenberg *et al.*, Am. J. Phys., **58**, 1131 (1990).

[41] D. Bouwmeester *et al.*, Phys. Rev. Lett., **82**, 13407 (1999).

[42] M. Eibl *et al.*, Phys. Rev. Lett., **90**, 200403 (2003).

[43] Z. Zhao *et al.*, Phys. Rev. Lett., **91**, 180401 (2003).

[44] X.-C. Yao *et al.*, Nat. Photonics, **6**, 225-228 (2012).

[45] X.-L. Wang *et al.*, Phys. Rev. Lett., **117**, 210502 (2016).

[46] Y. Tsujimoto *et al.*, Sci. Rep., **8**, 1446 (2018).

[47] W. Dür, G. Vidal, J. I. Cirac, Phys. Rev. A, **62**, 062314 (2000).

[48] X. Wang, Phys. Rev. A, **64**, 012313 (2001).

[49] D. Bruß *et al.*, Phys. Rev. A, **72**, 014301 (2005).

[50] M. Freisen *et al.*, Phys. Rev. Lett., **98**, 230503 (2007).

[51] L. Zhou, Quant. Inf. Process., **12**, 2087 - 2101 (2013).

[52] B. Gu *et al.*, Int. J. Theor. Phys., **53**, 1337 - 1345 (2014).

[53] W. H. Żurek, Ann. Phys., **9**, 855-864 (2000).

[54] H. Ollivier, W. H. Żurek, Phys. Rev. Lett., **88**, 017901 (2001).

[55] L. Henderson, V. Vedral, J. Phys. A, **34**, 6899 (2001).

[56] B. Dakić, V. Vedral, Č. Brukner, Phys. Rev. Lett., **105**, 190502 (2010).

[57] M. Okrasa, Z. Walczak, Europhys. Lett., **96**, 60003 (2011).

[58] A. Bera *et al.*, Rep. Prog. Phys., **81**, 024001 (2018).

[59] B. Wang *et al.*, Phys. Rev. A, **81**, 014101 (2010).

[60] F. F. Fanchini *et al.*, Phys. Rev. A, **81**, 052107 (2010).

[61] T. Werlang, G. Rigolin, Phys. Rev. A, **81**, 044101 (2010).

[62] G. J. Milburn, Phys. Rev. A, **44**, 5401 - 5406 (1991).

[63] F. Haake, S. M. Tan, D. F. Wall, Phys. Rev. A, **40**, 7121 (1989).

[64] J.-H. Chen, H-Y. Fan, Commun. Theor. Phys., **52** 85-87 (2009).

[65] A. Kossakowski, Rep. Math. Phys., **3**, 247 - 274 (1972).

[66] H. P. Breuer, F. Petruccione, *The Theory of Open Quantum Systems*, Oxford Univ. Press, 2002.

[67] M. Asorey *et al.*, J. Phys.: Conf. Ser., **196**, 012023 (2009).

[68] E. T. Jaynes, F. W. Cummings, Proc. IEEE, **51**, 89-109 (1963).

[69] G. Lindblad, Comm. Math. Phys. **48** 119-130 (1976).

[70] C. A. Brasil, F. F. Fanchini, R. de J. Napolitano, Rev. Bras. Ensino Fís., **35** 1303 (2013).

[71] D. Manzano, P. I. Hurtado, Adv. Phys., **67**, 1 - 67 (2018).

[72] D. Manzano, AIP Advances **10**, 025106 (2020).

[73] D. Maldonado-Mundo *et al.*, Phys. Rev. A **86** 042107 (2012).

[74] B. M. Garraway, Phys. Rev. A, **55**, 2290 (1997).

[75] V. Weisskopf, E. Wigner, Z. Phys., **63**, 54-73 (1930).

[76] S. Lorenzo, F. Plastina, M. Paternostro, Phys. Rev. A, **87**, 022317 (2013).

[77] M. Kaczor *et al.*, Ann. Phys., **442**, 168918 (2022).

[78] W. H. Żurek, Phil. Trans. R. Soc. Lond., **A356**, 1793 - 1821 (1998).

[79] S. Bose, Phys. Rev. Lett., **91**, 207901 (2003).

[80] P. Karbach, J. Stolze, Phys. Rev. A, **72**, 030301(R), (2005).

[81] A. Kay, Phys. Rev. A, **73**, 032306 (2006).

[82] Y. Tserkovnyak, D. Loss, Phys. Rev. A, **84**, 032333 (2011).

[83] S. Bertaina *et al.*, Phys. Rev. B, **90**, 060404(R) (2014).

[84] D. Hong-Liang, F. Xi-Ming, Chinese Phys. Lett. **24** 3051 (2007).

[85] G. L. Kamta, A. F. Starace, Phys. Rev. Lett., **2002**, 107901 (2002).

[86] A. Abliz *et al.*, Phys. Rev. A, **74**, 052105 (2006).

[87] J.B. Parkinson, D.J.J. Farnell, Lect. Notes Phys., **816** (2010).

[88] P. Zeeman, Nature, **55**, 347 (1897).

[89] I. Dzyaloshinskii, J. Phys. Chem. Solids, **4**, 241 - 255 (1958).

[90] T. Moriya, Phys. Rev. Lett., **5**, 228-230 (1960).

[91] S.- H. Park *et al.*, Dalton Trans., **41**, 1237 (2012).

[92] N. S. Kiselev *et al.*, J. Phys. D, **44**, 392001 (2011).

[93] B. Göbel, I. Mertig, O. A. Tertiakov, Phys. Rep., **895**, 1 - 28 (2021).

[94] R. Ramesh, N. A. Spaldin, Nature Materials, **6**, 21-29 (2007).

[95] T. Moriya, Phys. Rev., **120**, 91 (1960).

[96] F. Keffer, Phys. Rev., **126**, 896 (1962).

[97] M. Elhajal *et al.*, Phys. Rev. B, **71**, 094420 (2005).

[98] T. A. Kaplan, Z. Phys. B, **49**, 313 - 317 (1983).

[99] L. Shetkhman, O. Entin - Wohlman, A. Aharony, Phys. Rev. Lett., **69**, 836 (1992).

[100] A. Zheludev *et al.*, Phys. Rev. Lett., **81**, 5410 (1998).

[101] I. Tsukada *et al.*, Phys. Rev. B, **67**, 224401 (2003).

[102] H. Shiba, K. Ueda, O. Sakai, J. Phys. Soc. Jpn., **69**, 1493 - 1497 (2000).

[103] H. A. Brown, J. Magn. Magn. Mater., **43**, L1-L2 (1984).

[104] U. Falk *et al.*, Phys. Rev. Lett., **58**, 1956-1959 (1986).

[105] E. Müller-Hartmann, U. Köbler, L. Smardz, J. Magn. Magn. Mater., **173**, 133-140 (1997).

[106] U. Köbler *et al.*, Eur. Phys. J. B, **8**, 217–224 (1999).

[107] J. Łuczak, B. R. Bułka, J. Phys.: Condens. Matter, **24**, 375303 (2012).

[108] G. B. Furman, V. M. Meerovich, V. L. Sokolovsky, Quant. Inf. Process., **11**, 1603 - 1617 (2012).

[109] G. Sadiek, S. Kais, J. Phys. B: At. Mol. Opt. Phys., **46**, 245501 (2013).

[110] O. M. Del Cima, D. H. T. Franco, S. L. L. Da Silva, Quantum Stud: Math Found., **3**, 57-63 (2016).

[111] G. Najarbashi, L. Balazadeh, A. Tavana, Int. J. Theor. Phys., **57**, 95 - 111 (2018).

[112] M. Milivojević, Quant. Inf. Process., **18**, 48 (2019).

[113] D. Park, Quant. Inf. Process., **18**, 172 (2019).

[114] A. Redwan *et al.*, Chaos, **29**, 013138 (2019).

[115] L. S. Lima, J. Low Temp. Phys., **198**, 241 - 251 (2020).

[116] A. Niezgoda, M. Panfil, J. Chwedeńczuk, Phys. Rev. A, **102**, 042206 (2020).

[117] L.-J. Li *et al.*, Physica E, **113**, 114802 (2021).

[118] A. V. Fedorova, M. A. Yurischev, Quant. Inf. Process., **20**, 169 (2021).

[119] L. Gálisová, M. Kaczor, Entropy, **23**, 1671 (2021).

[120] L.-Y. Huang, Int. J. Theor. Phys., **60**, 4023 - 4029 (2021).

[121] Y. Khedif, A. Errehymy, M. Daoud, Eur. Phys. J. Plus, **136**, 336 (2021).

[122] S. Elghaayda *et al.*, Quant. Inf. Process., **22**, 117 (2023).

[123] R. Tae-Hung *et al.*, Int. J. Theor. Phys., **62**, 1 (2023).

[124] Q. Xu, G. Sadiek, S. Kais, Phys. Rev. A, **83**, 062312 (2011).

[125] M. Mahmoudi *et al.*, Phys. Rev. A, **95**, 012336 (2017).

[126] I.N. Sivkov, D. I. Bazhanov, V. S. Stepanyuk, Sci. Rep. **7**, 2759 (2017).

[127] Y. Hama *et al.*, Phys. Rev. A, **98**, 052133 (2018).

[128] A. R. Kuzmak, J. Phys. A: Math. Theor., **51**, 175305 (2018).

[129] A. R. Kolovsky, Phys. Rev. E, **101**, 062116 (2020).

[130] M. Mahmoudi, Physica A, **545**, 123707 (2020).

[131] M. Tchoffo, A. G. Tene, Int. J. Theor. Phys., **59**, 2232 - 2248 (2020).

[132] M. Hashem *et al.*, Appl. Phys. B, **128**, 87 (2022).

[133] Z. Noorinejad *et al.*, JTAP, **16**, 162228 (2022).

[134] G. Sadiek, M. AlQasimi, Results Phys., **35**, 105403 (2022).

[135] M. Kaczor, P. Jakubczyk, Quant. Inf. Process., **22**, 168 (2023).

[136] Z. N. Hu *et al.*, J. Phys. A: Math. Gen., **39**, 10523 (2006).